UNIVERSIDAD PONTIFICIA COMILLAS

ESCUELA TÉCNICA SUPERIOR DE INGENIERIA (ICAI)

Instituto de Investigación Tecnológica (IIT)

Voltage Control Design of Wind Energy Harvesting Networks

Tesis para la obtención del grado de Doctor

Supervisors: Prof. Dr. D. Enrique Lobato Miguélez

Prof. Dr. D. Ignacio Egido Cortés

Author: Ing. Dña. Elena Sáiz Marín

Madrid 2015

CONSTANCIA REGISTRAL DEL TRIBUNAL DEL ACTO

DE LA DEFENSA DE TESIS DOCTORAL

TÍTULO: Wind Energy harvesting networks voltage control design

AUTOR: Elena Sáiz Marín

DIRECTOR: Enrique Lobato Miguélez, Ignacio Egido Cortés

TUTOR-PONENTE: Enrique Lobato Miguélez

DEPARTAMENTO: Instituto de Investigación Tecnológica

FACULTAD O ESCUELA: Escuela Técnica Superior de Ingeniería

Miembros del Tribunal Calificador:

PRESIDENTE: Firma:

VOCAL: Firma:

VOCAL: Firma:

VOCAL: Firma:

SECRETARIO: Firma:

Fecha de lectura:

Calificación:

En muchos momentos pensé que nunca llegaría a escribir esta página y si por fin lo estoy haciendo es gracias a todos vosotros. **MUCHÍSIMAS GRACIAS! – THANK YOU VERY MUCH!**

En primer lugar quería agradecerle a Luis Rouco la oportunidad que me brindó entrando al IIT, en pocos sitios se aprende tanto como aquí, y por su puesto a mis directores, Enrique Lobato e Ignacio Egido que confiaron en mi tesis hasta cuando yo no lo hacía. También a toda la gente con la que he trabajado a lo largo de estos años y de los que he aprendido un montón. Muy en especial a todos los miembros del proyecto TWENTIES el cuál representó el pistoletazo de salida de esta tesis. Juan Carlos Pérez Campión, Iñigo Azpiri, Clara Combarros, Roberto Veguillas, Juan Rivier, Placido Ostos, Miguel Lorenzo, Guillermo Juberias, Miguel Linares…. Y por supuesto a los de dentro del IIT Javier García, Pablo Frías, Camila Formoso y Mercedes VallesGracias a todos mis compañeros o mejor dicho amigos en todo este tiempo. A los que ya estaban cuando yo llegué y que siempre han estado dispuestos a ayudarme Lukas, Ale, Maria, Paco a los que han compartidos desayunos, comidas (con curso de lekue incluido), pachangas de baloncesto… Álvaro, Alessandro, Adela, Rafa, Carlos, Adrián, William y por su puestos a Inma y Luis que compartieron principio y fin de tesis siendo un soporte esencial durante la misma, qué hubiese hecho yo sin vosotros! Y como no a toda la gente que ha formado parte esencial en a mi vida. A los del Cole, la banda y por supuesto a los de la Universidad. Tampoco me quería olvidar de mi profesor de clarinete, Juan Luis, que me descubrió la melanina y me ha ayudado más de lo que él se puede llegar a imaginar.

I will never forget my time in Ireland, which also proved to be my most fruitful research period. Thanks to Andrej Gubina who suggested I make the move there and, of course, to Andrew Keane who embraced me into his research group. Thank you very much to all the ERC students who made my stay unforgettable – Álvaro, Killian (my jazz professor!), Peter (I now never miss any Ireland rugby match!), Connor, Alison, Mostofa, Mario, Padraig, James, Jonathan ... and a special and big thanks to Paul Cuffe. Thanks for all the discussions during my stay and all the Skype conversations when I was back in Spain. I have learned a world of new vocabulary and you always provided me with useful, distinctive points of view. I am certain I would not have finished my PhD without your help. Also, huge thanks to Ronald Besser and again to Killian Mc-Kenna and Paul Cuffe for proofreading the thesis and correcting my "Spanglish". You were my saviours and I am eternally grateful.

Y por supuestísimo a toda mi familia, no se podría haber tenido más suerte. Gracias a mi hermana la mejor reportera del mundo que siempre ha sido la alegría de la casa. A mi pronto cuñado Olly (Bienvenido a los Sáiz-Marín), gracias por corregir mi inglés aunque te sonase a chino lo que decía. A mi madre, el gran pilar de la familia, que dejo de lado su camino para dedicarse por entero a sus hijas y que no te lo agradecemos lo suficiente, tu me has enseñado el valor del esfuerzo y de la perseverancia. Como pasito a pasito se alcanza cualquier cosa que nos podamos proponer. A mi padre, yo ya de pequeña tenía claro que de mayor quería ser como tu (ni austronauta, ni veterinaria, ni médico…) así que cuando alguien me preguntaba que quería ser de mayor les decía "yo, como mi padre" ese deseo me ha llevado hasta aquí y ha sido el motor de mi vida. Mil gracias sois los mejores. Y como no, a Ángel (mi futura familia) no me hubiese imaginado una persona mejor con la que compartir mi vida, el más bueno que existe y al que más le he dado la murga con esta tesis.

ABSTRACT

Specific networks developed solely to harvest wind energy (HNet) are becoming a common scheme. Moreover, it is foreseen that in the near future, they will be the solution adopted for large integration of wind, commanding greater transmission system impact potential. However, despite the huge literature available related to wind farms and their integration, few works focus on these networks, a gap covered in depth by this thesis. These potentials are highly dependent on the HNet characteristics; hence its classification is essential. This is done by analyzing the influence of OLTC transformers based on three relevant indices: PQ chart, power losses, and voltage margins deriving three different HNets types (A, B and C). For each one, the most suitable control strategy is proposed considering simple control schemes which can nowadays be implemented without additional investments. Consequently their steady-state performance and temporal evolution analysis are required. In that sense a wide variety of techniques are used throughout the thesis: data-mining techniques (regressions, clustering, decision trees …), metaheuristic algorithms (genetic algorithms and multiple particle swarm optimization), quadratic programming or multi-period OPF.

Specifically, for type A, power loss minimization strategy based on control rules is suggested allowing the understanding of power flows performance within the grid and identifying those wind farms with negligible impact. For that purpose a novel variable, active power losses from wind farm *i* to the transmission network bus (P_{lossi}), was defined. In addition, to avoid online computations, the total HNet active power has been considered as an explanatory variable resembling the power factor concept (with respect a global magnitude instead of the individual wind farm active power). In that manner, simple regression rules are used to estimate wind farm reactive power, and a classification tree for each transformer is used to estimate their taps.

For type B, a minimum HNet impact on the transmission network strategy is suggested analyzing different possible control schemes: *reference control*, *power factor control*, *local voltage control* (representative of the current regulation direction) and *remote voltage control*. For each control scheme static fit-and-forget settings are obtained thanks to the AC-multi-period OPF and therefore autonomous control schemes are obtained. Comparing these control schemes it has been observed that the best option is a voltage control where wind farms control the voltage at a remote bus. Otherwise, of the localized control schemes that do not require telemetry, *power factor control* scheme has a better performance contrary to the widespread idea of *local voltage control* adequacy as many regulation proposals suggest.

Finally for type C, a pro-active voltage control (i.e., the whole HNet resembles a conventional power plant) is suggested demanding adaptive static parameters contrarily to what was proposed for the previous HNet types. Hence, a central controller distributes set-point depending on the operational and external conditions. This central controller has been developed following the guidelines of well-known TNet hierarchical voltage control and more specifically in its secondary loop performing and optimization by means of quadratic programming every 10 seconds. Nonetheless, several modifications

have been made in accordance with HNet characteristics and the nature of distributed generation such as its variability as are explained throughout the thesis.

In addition, any control scheme design should also consider the dynamic coordination of wind farms and cascade OLTC transformers to ensure that such set points redispatche can be harmoniously achieved. In that sense this thesis proposes tuning offline relevant dynamic settings (i.e., settings that affect the control scheme temporal time evolution) to be applied to Type B and C HNets. These settings are wind farms' controller time constants and for OLTC transformers the time delay and dead band. This last setting is not commonly used with coordination purpose although there is no barrier that impedes its use, as this thesis proposes. For that purpose two well-known metaheuristics algorithms (Genetic algorithm and MOPSO) have been used. On one hand the former provides the settings tendency whereas the latter one provides the whole Pareto frontier; allowing the settings categorization depending on the agents preferences (tap changes minimization, voltage breaches minimization and voltage deviation minimization). Concerning type B, this analysis reinforces the idea of inadequacy of *local voltage control* scheme owing to the necessity of slow controller action for avoiding oscillations. Finally, a demanding voltage control such as the *remote* one significantly increases the number of tap changes. Concerning type C, the same method has been employed focusing this time only on the MOPSO algorithm. The results obtained have been expanded clustering the Pareto front obtaining different dynamic settings patterns.

APPENDICES

ACRONYMS

Symbol	Description
ACD	Adaptive critic design
ANN	Artificial neural network
AVR	Automatic voltage regulator
CART	Classification and regression tree algorithm
CECRE	Renewable energy control center (operated by REE)
CORE	Renewable energy control center (operated by Iberdrola)
CSVC	Coordinated secondary voltage control
DFIG	Doubled fed induction generator
DG	Distributed generation
DSO	Distribution system operator
DNSGA-II	Dynamic multiple objective genetic algorithm
ENTSO-E	European network of transmission system operators for electricity
FACTS	Flexible alternative current transmission system
GA	Genetic algorithm
HNet	Harvesting network
MOPSO	Multiple objective particle swarm optimization
MPC	Model predictive control
MVMO	Mean-Variance Mapping Optimization
NSGA-II	multiple objective genetic algorithm
OLTC	On load tap changing
OPF	Optimal power flow
Pcc	Point of common coupling
Pf	Power factor
P.O.	Operation procedure (Spanish nomenclature)
PSO	Particle swarm optimization
RD	Royal decree
REE	Red eléctrica de España (Spanish transmission system operator)
REPORT	Microprocessor reactive and voltage regulator employed in the Italian secondary voltage control
SART	Sistema Automatico per la Regolazione di Tensione (Automatic system for voltage regulation)
SCADA	Supervisory Control and Data Acquisition
SONI	Independent electricity Transmission System Operator and Market Operator in Ireland
SVR	Step voltage regulator
TNet	Transmission network
TSO	Transmission system operator
TWENTIES	Transmission system operation with large penetration of Wind and other renewable Electricity sources in Networks by means of innovative Tools and Integrated Energy Solutions
Common symbols used throughout the thesis	
P	Active power (MW)
Pcc	Common coupling bus, connects the HNet to the TNet
Q	Reactive power (MVAR)
SCC	Short circuit capacity (MVA)

POWER LOSSES

Symbol	Description
c_0, c_1, c_2	Polynomial coefficients
f_{WF}	Active power losses factor assigned to a certain wind farm
$Pgross_{WF}$	Gross active power losses delivered by a certain wind farm (MWh)
$Pnet_{WF}$	Net active power losses delivered by a certain wind farm (MWh)
P_{WF}	Individual wind farm active power (MW, p.u.)
$Q_{WF}^{min}, Q_{WF}^{max}$	Maximum a minimum reactive power provided by wind farms (MVAR, p.u.)
R^2	Coefficient of determination
S_W^{min}, S_W^{max}	Maximum a minimum wind speed (m/s)
V_{WF}	Voltage at wind farm grid connection point (kV, p.u.)
WF	Wind farm
Explanatory variables selected	
$P_{loss\ ij}$	Active power losses from bus *i* to bus *j* (MW, p.u.)
$P_{loss\ WF}$	Active power losses from wind farm *WF* to the transmission network bus (MW, p.u.)
TQ_{losses}	Total wind energy HNet reactive power losses (MVAR, p.u.)
TP	Total wind energy HNet active power (MVAR, p.u.)
TP_{losses}	Total wind energy HNet active power losses (MVAR, p.u.)
V_{TNet}	Transmission network voltage (kV, p.u.)
Control variables	
Q_{ref}, Q_{WF}	Wind farms reactive power references (MVAR, p.u.)
t	Tap position

VOLTAGE CONTROLS SCHEMES

Symbol	Description
K	Proportional control scheme slope
R	Proportional control scheme droop (%)
$V_{measured}$	Measured voltage at a certain bus (kV/p.u.)
$V_{pcc,t}$	Measured voltage at Pcc for period t (kV/p.u.)
$V_{setpoint}$	Voltage set-point at a certain bus (kV/p.u.)

	Hierarchical voltage control schemes
Sets	
c	Controlled bus (corresponding to those buses in which a generator is located)
p	Pilot buses
s	Critical buses
Parameters	
a, b, c	Coefficients of straight lines used for modelling the reactive power limits
k	Sample time of the discrete controller
Q_c^{min}, Q_c^{max}	Minimum and maximum value of the reactive power that can be provided by the generators (MVAR, p.u.)
T_c	Time constant of the secondary voltage control (s)
w_v	Weight of the pilot buses voltage deviation term
w_q	Weight of the reactive power increment at the generator
w_g	Weight of the voltage increment at the generator

Symbol	Description
V_c^{min}, V_c^{max}	Minimum and maximum value of the voltage of the controlled buses
V_p^{max}	Maximum pilot bus reference
V_s^{min}, V_s^{max}	Minimum and maximum value of the voltage of the critical buses
α	Coefficient between zero and one that considers the dynamic performance. The time constant of the control fulfill the following formulas as demonstrated [Pagola 1993]. Hence, it can be elucidated that if $\alpha = 1$ a *dead beat* control is obtained. This means that the control action is achieved in just a sample time Δt (considering perfect modelling of the system and a lineal response) $T_c = \frac{-\Delta t}{\ln(1-\alpha)}$
γ	Gain
Input of the controllers	
$A_{cc}(k)$	Sensitivity matrix of the reactive power generated with respect to the voltage at the controlled buses both correspond to the generator buses $\frac{\partial Q_c}{\partial V_c}$ in sample *k* (MVAR/kV)
$Q_c(k)$	Reactive power vector of the controlled buses in sample *k* (MVAR, p.u.)
$S_{pc}(k)$	Sensitivity matrix of the pilot buses voltages with respect to the controlled voltages $\frac{\partial V_p}{\partial V_c}$ in sample *k.* In the specific case that is addressed in the thesis a single pilot bus is considered. Hence, a vector instead of a matrix is evaluated. To outline this distinction a different notation is used $vS_{pc}(k)$
$S_{sc}(k)$	Sensitivity matrix of the critical buses voltages with respect to the controlled voltages $\frac{\partial V_p}{\partial V_s}$ in sample *k*
$V_c(k)$	Voltage vector of the control buses in sample *k* (kV, p.u.)
$V_p(k)$	Voltage vector of the pilot buses (kV, p.u.)
V_p^{ref}	Voltage vector of the references of the pilot buses provided by the higher control loop (kV, p.u.)
$V_s(k)$	Voltage vector of the critical buses in sample *k* (kV, p.u.)
$\Delta V_c^{ref}(k)$	Voltage reference increment (kV, p.u.)
Output of the controllers	
$Q_c^{ref}(k+1)$	Reactive power references vectors of the control buses in sample *k* +1 (MVAR, p.u.)
$V_c^{ref}(k+1)$	Voltage references vectors of the control buses in sample *k* +1 (kV, p.u.)
$d(k)$	Vector of area reactive power level (%)
$\Delta T_{losses}(k)$	Active power losses component (MW)
$\Delta T_{Qmargins}(k)$	Reactive power margins components

List of figures

List of tables

CHAPTER 1

INTRODUCTION

Before explaining the thesis itself, this chapter presents the problem stament and the derived specific objectives. Specifically, it is structured as follows. The motivation and scope of the thesis is outlined in section 1.1. As the title states, the thesis focuses on wind energy harvesting networks possessing the characteristics and peculiaritites presented in section 1.2. Subsequently, the current situation of wind generation, from technical and regulatory perspectives is presented in section 1.3. Then, the objectives, which are the main questions that are answered in this thesis, are defined in section 1.4. Finally, the structure of the whole document is given in section 1.5.

1.1. MOTIVATION AND SCOPE

Recent years have seen a global significant growth in the use of wind power. For instance, Spain (which is used as a case example throughout the thesis) has the fourth highest installed capacity of wind power, with 22,959 MW at the end of year 2013 [Global Wind Energy Council 2013]. The level of penetration[1] can now exceed 60% on certain windy days; for example, on the 24th of September 2012 it was 64.2% at 03:00. In addition, the Spanish Ministry of Industry, Tourism and Trade regards as a probable scenario 34,318 MW of installed on-shore wind power capacity and 750 MW of off-

[1] Energy provided by wind generation with respect to the total energy supplied

shore wind power capacity by 2020 [Spanish government, 2011]. This wind penetration level could be reached in addition to other factors, because the wind generation is already contributing to the voltage control in a restricted way. As will be seen later, the Spanish operator currently requires a tight power factor range. Within that range, most wind farms are operated at a lagging power factor. The associate reactive consumption is essential during off-peak hours when the voltage raise is very significant due to the reactive generation of unloaded lines. Moreover, it should not be forgotten that is precisely during those hours when typically there is more wind available. In order to avoid this situation several reactors are connected. However, it has been seen that these elements sometimes are not enough and between 70 and 80 lines have been already disconnected from the grid in order to solve this situation.

Given these trends, increasing the controllability of these energy resources is becoming a necessity. In fact, the Spanish transmission system operator has already proposed a new grid code which demands voltage control functionality from wind farms, such that the reactive power delivered by the wind farm depends on the voltage deviation at its connection point [REE 2011]. It is clear that better harnessing of the reactive power from distributed generators has much to offer for the broader power system, both from the steady-state and dynamic perspectives. However, the various benefits that could be obtained with different control schemes should be analyzed in detail in order to understand the relative strength of each approach.

This thesis deals with this issue focusing on wind energy harvesting networks (HNets). These networks, which are explained in section 1.2, were developed solely to harvest energy and thus, no demand customers are accommodated. In such networks the internal voltage profile is principally established by the bulk supply tap-changing transformers that connect the HNet to the transmission system. Therefore, some questions arise: could the introduction of wind farm voltage control cause unwanted interactions with current transformer voltage control? How might both controller types be coordinated to avoid unnecessary tap changes and possible instabilities?

It should be noted that voltage control provision in the transmission network (TNet) by decentralized elements such as generators and OLTC transformers is not a new concept and, although the wind generation peculiarities should be undertaken, the philosophy behind the HNet control is equivalent to the existing one. In the TNet several hierarchical voltage controls are currently being operated or have been evaluated (e.g., France [Lefebvre, et al. 2000], Italy [Corsi et al. 2004a, Corsi et al. 2004b], Spain [de la Fuente 1997, Alonso 2001], South Africa [Corsi, et al. 2010]). In all these hierarchical schemes different control loops can be identified: primary, plant (not always), secondary and finally tertiary, having the settling times 1s-2s, 5s-10s, 1minute and 15 minutes respectively. Although these loops are explained in more detail in Chapter 2, a brief summary of the motivation for the implementation of these schemes follows. These loops allow the complex voltage control issue to be simplified by spatial and temporal decomposition. The fastest action corresponds to the primary loop in which the AVR of the synchronous generators compensate for local voltage deviations. Then, the plant control is in charge of coordinating the action of all generators allocated in the same plant

for maintaining a desired voltage set-point and reactive power balance between generators. Those voltage set-points are calculated by the secondary control in order to compensate the voltage deviation of selected pilot buses (controlled buses). Finally, the tertiary loop determines the voltage set-point of the pilot buses as well as the action of the discrete elements such as OLTC transformers, shunts and reactors. In this last loop is where traditionally the optimal operation (minimizing power losses, maximizing reactive margins) is carried out. If wind farms are to be integrated in the existing hierarchical voltage control of a TNet, the whole HNet should behave as closely as possible to a conventional plant.

However, as depicted in Figure 1-1, the equivalent plant control of a HNet in order to avoid interactions involves more loops than the traditional one. Indeed, the HNet itself can be seen as a TNet in miniature. Firstly, wind farms internal control which is equivalent to the TNet plant control of synchronous machines. Nevertheless, two more loops should be taken into account: the HNet wind farms coordination and finally the OLTC transformers and optimization control. Thus, a question arises at this point: Do the benefits obtained thanks to incorporating wind power HNets into the TNet hierarchical voltage control justify the increase of control complexity?

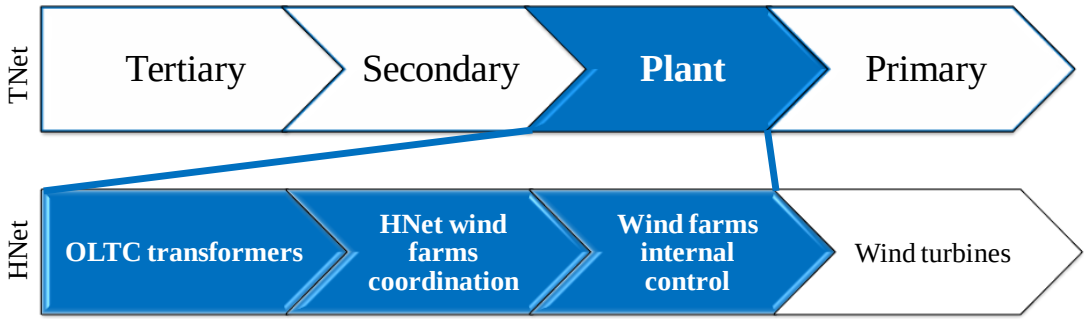

Figure 1-1 Current Voltage hierarchical voltage control on the TNet and the HNet integration

The answer to this question depends on the characteristics of the HNet which affect the impact that the HNet could have in the TNet. Thus, the features of the HNet must be known before any control is proposed. In this dissertation, these properties are evaluated in accordance with the maximum reactive power that can be consumed from or generated into the TNet, the maximum voltage increase or decrease that the reactive limits imposed and finally the power losses originated within the HNet. Thanks to that preliminary analysis it is possible to identify which HNets can play an important role in the TNet control. For others HNets different strategies are investigated and proposed in the context of this thesis.

1.2. WIND ENERGY HARVESTING NETWORKS

When the first wind farms were installed in various power systems, the usual scheme was that their power was harvested through existing distribution networks. However, those networks were not designed with that purpose. With the increment of distributed generation the power flows sometimes became bidirectional, increasing the complexity

of network operation. This fact motivated several research efforts, for example in [Borghetti 2012] the best radial configuration in order to minimize power loss is evaluated, or, in [Gao et al. 2011] how line drop compensation of the transformers should be configured depending on the direction of the power flow.

Nowadays, due to the significant increase of wind power, another scheme is that wind farms harvest their power through a dedicated network in which there are no demands. For instance, in Spain this scheme was incentivized by the previous regulations already abrogated RD 436/2004 [Spanish government 2004] and RD 661/2007 [Spanish government, 2007]. In these regulations it was indicated that in order to get the premium the maximum power of wind farms should be 50 MW. This fact fostered the creation of a network in which several small wind farms (less than 50 MW) were located instead of developing a large one. Moreover, a common scenario is that there are not distribution networks in the areas with good wind resources and hence, a dedicated network needs to be built. As a result, in Spain approximately 85% of wind generation is allocated in harvesting networks, representing a total capacity of 19,376 MW. In addition it is also becoming an important option in Ireland [Smith, et al. 2010, Cuffe et al. 2012a]. Nevertheless, this option is far from being the most common in other countries. Owing to this fact, there is little research literature that tackles wind energy harvesting networks.

Thanks to the existence of a dedicated harvesting network the performance of the whole network resembles a conventional plant, being this fact the principal reason of why this thesis focuses on harvesting networks. In Ireland, as a case example, the grid code imposes different requirements to wind farms located in the distribution networks that to the ones directly connected to the transmission network. In the latter ones, wind farms are required to provide a similar voltage control as the conventional plants do. However, it must be noted that the philosophy behind the voltage control design is independent of the existence of demands, a fact that is discussed throughout the thesis.

Next, in Figure 1-2 a simplified diagram of an invented HNet which compromises four different wind farms is presented depicting also the internal wind farms grid. It must be noted that wind farms grid typically is radial and could be formed of a single or several feeders being all wind turbines connected to the grid through a transformer (30-20kV/0.69 kV). Those transformers have not been depicted because they are not allowed to change their taps on load. In contrast, the harvesting network could be meshed. In addition, within the harvesting network several OLTC transformers are located controlling the low voltage side as is represented in the figure with a red dot. Within these transformers two different types can be identified. On one hand, the transmission transformer, (400kV/220kV-132kV). On the other hand, the transformers that connect wind farms to the HNet (220kV-132kV/30-20kV). Hence, it can be noted that in those networks there are already control elements which should be coordinated with the control provided by wind farms as had been said. In this simplified diagram the transmission network has been represented with the Thevenin equivalent in accordance with its short-circuit power and transmission network voltage. This simplification is used throughout the thesis.

Another important aspect is that usually different wind farm owners create a joint venture for building a harvesting network. Hence, the wind farm grid could belong to different wind farm owners, e.g., companies A, B and C. Nevertheless, who is responsible for managing the harvesting network itself? The answer is none of the aforementioned wind farm owners owing to the transmission system operator forces the existence of a single distribution operator. Hence, TSO, DSO and wind farm owners should cooperate in order to maximize the advantages (for all parties involved) of reactive power capabilities.

As will be seen in subsection 1.3.2 in Spain, wind farms' voltage set-points are sent to the meter point which varies in location: At the low voltage side if different wind farm owners share the transformers or at the high voltage side if all wind farms belong to the same owner. Hence, as can be seen in Figure 1-2 in accordance with the current grid code proposal several devices will control the same bus.

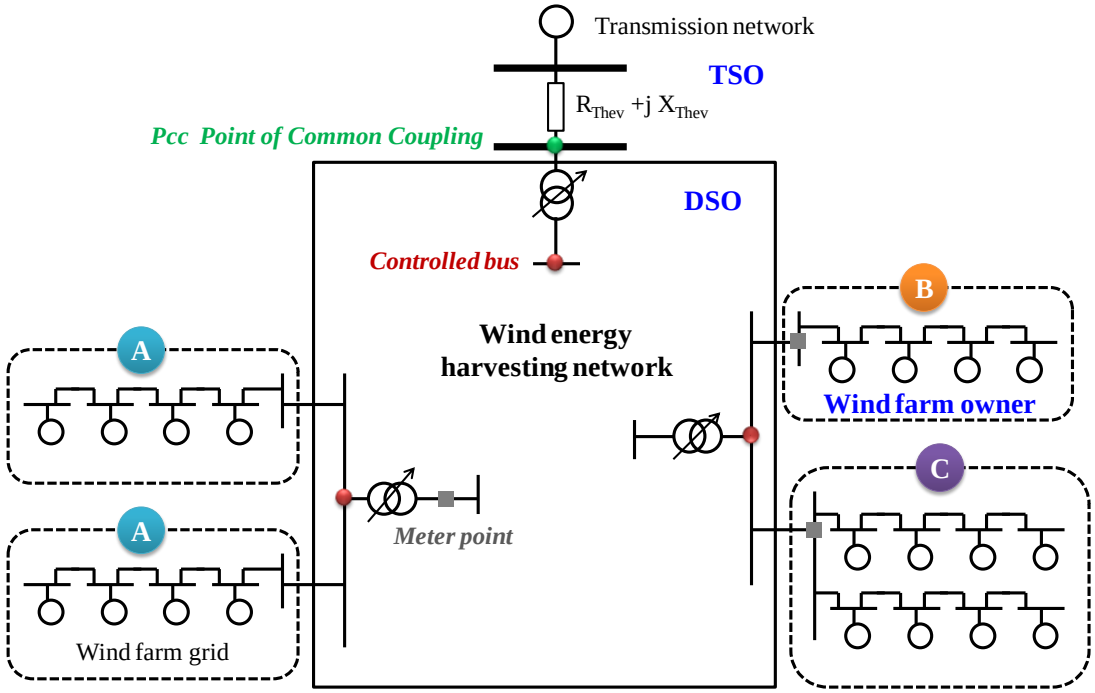

Figure 1-2 Wind Energy harvesting network diagram

Finally, it should be highlighted that this thesis focuses on onshore HNet. Offshore HNets will be commonly connected to the transmission network through a high voltage direct current (HVDC) link [Bresesti et al. 2007] and hence, appropiate analysis should be carried out. Nonetheless the philosophy of all control schemes proposed and their methodologies are totally applicable to these grids.

1.3. CURRENT SCENARIO OF WIND VOLTAGE CONTROL

Within this subsection the current technological development and regulatory framework are discussed in subsection 1.3.1 and 1.3.2 respectively.

1.3.1. TECHNOLOGICAL DEVELOPMENT

The HNets compromises two different control devices: wind turbines and transformers. The characteristics of these devices are as follows:

- **Wind turbines**: At the beginning of the development of wind energy technology, the wind turbines were of fixed speed. That means that the rotor wind turbine speed is determined by the supply grid frequency, the gear ratio and also the design of the machine. Consequently the rotor speed is independent on the wind speed [Ackermann 2005]. Normally, those wind turbines were equipped with an induction generator that was directly connected to the grid, and typically, a capacitor bank was added in order to reduce the reactive power consumption. Although this turbine has clear advantages such as its simplicity and robustness, it has important drawbacks. On one hand, it requires additional elements (capacitor banks) for providing reactive power. On the other hand, those machines are designed to achieve maximum efficiency at a certain wind speed.

  Thus, in order to enhance its controllability the variable speed turbines were introduced. In fact, in Spain at the end of year 2009 the variable speed turbines represented 74.07% of the total installed turbines and, more importantly, the new ones are of variable speed. As can be derived from its name, variable speed, the main characteristic of these turbines is that they are designed to achieve maximum efficiency over a wide speed range. This fact is achieved adapting the rotor speed to the wind speed, thanks to the incorporation of a power converter. Within the variable speed turbines there are different types [Ackermann 2005]. The most relevants are the full converter and the doubly fed induction machine (DFIG). Currently, DFIG is the most common one. In this type of turbine the stator is directly connected to the grid whereas the rotor is connected to the grid through a converter allowing the provision of frequency[2] and voltage control. [Ackermann 2005, Engelhardt et al. 2011, Martinez et al. 2011, Singh, et al. 2010, Xiangyu Zhang, et al. 2010, Konopinski et al. 2009, Ozturk, et al. 2009]. From the voltage control perspective (control under study in this thesis), this turbine is able to provide reactive power without adding any element. The side of the converter connected to the stator compensates the reactive power generated by the machine and consumes or generates the reactive power in accordance with the grid codes requirements. Hence, the reactive generation/consumption is limited by the power converter. Normally, owing to economic reasons, it is

[2] The rotor speed is principally determined by the supply grid frequency. In the event of an induction machine the rotor frequency (f_2) is related to the supply grid frequency (f_1) through the following equation $f_2 = (1 - w_r) \cdot f_1$ being w_r the machine speed. Since the system frequency is fixed (50 Hz), the machine speed depends on f_2.

sized at around 25–35% of the generator rating. This fact also means that the speed range is between ± 25-35% [AEMO 2013].

In a full converter machine, the power converter has the same rating (or greater) as the generator, which is not directly connected to the grid. As a result, the generator can be operated at any speed from zero to maximum, and provides an improved reactive power capability range (PQ chart) compared to the DFIG as can be seen in Figure 1-3. In this figure a generic full converter (considering the limitation factors: converter current limitation, converter voltage limitation and active power limitation [Valverde, et al. 2014]) is depicted jointly with the common *GAMESA* wind turbine G87 [Gamesa 2013]. The characteristics of *GAMESA* wind turbine have been employed throughout the whole thesis. In addition, the extended PQV charts of both machines are compared with the synchronous machine in [Valverde, et al. 2014]

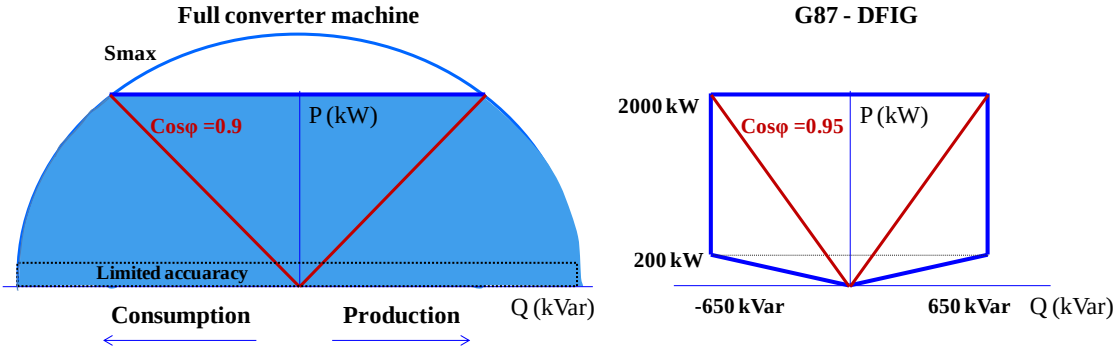

Figure 1-3 Reactive power capabilities

Finally, it must be outlined that new developments related to improving wind turbines and also wind farm controllability are being carried out. For example, *GENERAL ELECTRIC* in its 2.5 MW turbine specification [GE 2010] already offers the optimization of the wind power plant performance, which includes services such as, WindCONTROL* (Voltage and power regulation like a conventional plant) or WindFREE* (Provides reactive power even with no wind).

- **Transformers:** Thanks to a variable transformer ratio, i.e., the relation between the primary and the secondary, the voltage can be controlled. As an example, a 400/220 kV transformer commonly has 21 tap positions (central tap ± 10), changing the voltage ± 1% with each tap modification.

  In that sense, the tap position can be changed offline or online. This thesis focuses on the latter scheme, commonly known as OLTC transformer. In those cases a voltage set-point must be fixed. If the voltage measure differs from that set-point then the tap position is modified. That modification is not instantaneous; there is an intrinsic mechanical time delay which depends on two actions, the switching time and the motor drive. The former is around 50

ms for oil breaking transformers and 100 ms for vacuum transformers whereas the latter can be as high as 5 seconds. Nonetheless, some manufactures are trying to reduce this time as was seen at CIGRE bienal session [CIGRE. 2014] reaching mechanical time delays below 1 second. In addition, any OLTC transformer is defined by two additional settings, dead band and intentional time delay, which are used for coordination purposes. In this thesis as a relevant contribution those values are tuned for avoiding undesirable performance.

1.3.2. REGULATION FRAMEWORK OF THE WIND ENERGY VOLTAGE CONTROL PROVISION[3]

Since the technical viability of providing reactive control has been proven, several countries have recently developed new grid codes, where some of them take into account the actual wind farms' reactive power capabilities. The rise of wind farm requirements show a clear tendency: wind farm performance should be as similar as possible to the performance of a conventional power plant.

The grid codes of the European countries most representative from the wind share of total electricity perspective. Those countries are: Denmark, Spain, Portugal, Ireland and Germany [EWEA 2012] with 25.9%, 15.9%, 15.6%, 12% and 10.6%, penetration level respectively, being the mean value of the whole Europe 6.3%. Table 1-1 gathers the information indicating the TSO, the control mode specified, where the set-point is specified, the specifications, the time in which the set-point should be fulfilled, the voltage ranges and finally the corresponding reference. As can be seen in most countries, three different control modes are distinguished: reactive power, power factor, and voltage control. Currently the control mode that typically is used is the power factor. In fact, in countries like Spain or Portugal wind farms are operated at a unity power factor in order to reduce their impact on the TNet. Other countries such as Denmark or Ireland consider wider reactive ranges. Indeed, ENTSO-E wider range opens the doors of an enhanced utilization of the actual wind farm capabilities

System operators increasingly demand voltage control in the connection bus of the wind farm to the grid as is the case of Denmark, Ireland, Spain and also as has been proposed by ENTSO-E. In the event of considering this control model the system operator should define the droop (Voltage deviation / Reactive power increment). This concept, which is equivalent to the speed droop parameter *R*, is very well established in the primary control of active power (frequency control).

[3] The regulation is subject to continuous changes. The regulation that is summarized in this document corresponds to the existing one when the thesis was written.

Table 1-1. Reactive power technical requirements

Country	TSO	Control specified	Set points specified at	Specifications	Set point changes completed	Voltage margins	Reference
Denmark	Energinet	Reactive power control	Grid connection point (**)	0,1 lag - 0,1 lead Power output range 11 kW -25 kW	30s	0.9 -1.06	[Energinet, 2010]
				0,228 lag - 0,228 lead Power output range 25kW -25 MW	30s	0.9 -1.06	
				0,33 lag - 0,33 lead Power output range >25 MW	30s	0.9 -1.06 (step1 0.9 -1.1)	
		Power factor control		0.995 lag - 0.995 lead Power output range 11 kW -25 kW	30s	400 kV: 0,8 – 1,15 220 kV: - – 1,12 150 kV: 0,9 – 1,13 63 kV: 0,9 – 1,12 0.69 kV: 0,9 – 1,10 Typically +/- 10%	
				0.975 lag - 0.975 lead Power output range 25kW -25 MW	30s		
				0.95 lag - 0,95 lead Power output range >25 MW	30s		
		Voltage control (>25MW)		Required for wind plants higher than 25 MW	10s	0.9 -1.06 (step1 0.9 -1.1)	
Spain	REE	Reactive power control (*)	Meter point	0,3 lag - 0,3 lead	1 min	0.95 - 1.05	[REE, 1998], [REE, 2010], [REE, 2011] [Spanish government, 2010]
		Power factor control (Current scheme)		0.979 lag - 0.979 lead (mandatory)		Contingencies N-1 400 kV: 0,95 – 1,09 (P.O. 1.1)	
				0.995 lag - 0.995 lead (incentivized)			
		Voltage control (*)		0-25		0.95 - 1.05	
Portugal	REN	Power factor control	Grid connection point	0.980 lag - 0.958 lead peak hours (depends on the localization of the wind farms)	-	Contingencies N-1 400 kV: 0,93 – 1,05 220 kV: 0,93 – 1,11 150 kV: 0,93 – 1,10 63 kV: 0,95 – 1,05	[Ministério da economia,da inovação e do desenvolviento, 2010]
				1 valley hours	-		
Ireland	EIRGRID, SONI	Reactive power control	Grid connection point	0,33 lag - 0,33 lead	20s	Contingencies N-1 400 kV: 0,88 – 1,05 220 kV: 0,91 – 1,11 110 kV: 0,90 – 1,12	[EirGrid, 2011], [EirGrid, 2014]
		Power factor control		0,95 lag - 0,95 lead	20s		
		Voltage control		1%-10%	20s		
Germany	EON, EnBW, Vattenfall, RWE	Reactive power control. The TSO shall select one of the	Grid connection point	0,228 lag - 0,48 lead	1 min	380 kV: 0.92 – 1.16 220 kV: 0.88 – 1.15 110 kV: 0.87 – 1.15	[eon, 2006]
				0,33 lag - 0,41 lead			
				0,41 lag - 0,33 lead			
		Power factor control. The TSO shall select one of the variants		0,975 lag -0,887 lead			
				0,95 lag - 0,925 lead			
				0,925 lag - 0,95 lead			
		Voltage control		-			
Europe	ENTSO-E	Reactive power control	Grid connection point	0,5 lag - 0,65 lead	-	Inner envelope 0.9-1.075 Fixed outer envelope 0.875 -1.1	[ENTSO-E 2012] [ENTSO-E 2013]
		Power factor control		0,894 lag - 0,838 lead	-		
		Voltage control		2% -7%	-		

(*) Draft grid codes P.O. 12.2 & P.O. 7.5

(**) The electricity undertaking choose the location of the voltage reference point. Normally at the high voltage side of the plant transformer.

As can be seen in Figure 1-4 a 4% droop means that a 4% frequency deviation is caused by a 100% change in the output power. In the event of voltage control, some countries use the equivalent of this definition, i.e., a droop of 4% means that a 4% of voltage deviation is caused by a 100% change in reactive power (Q lagging + Q leading). In the case of Spain, the droop is defined slightly differently: $K = (\Delta V/Vrate) / (Q/Prate)$ where K goes from 0 to 25 corresponding to a droop of 4%. In all countries the system operator is the one in charge of fixing this value which is analyzed in this thesis from an optimal perspective.

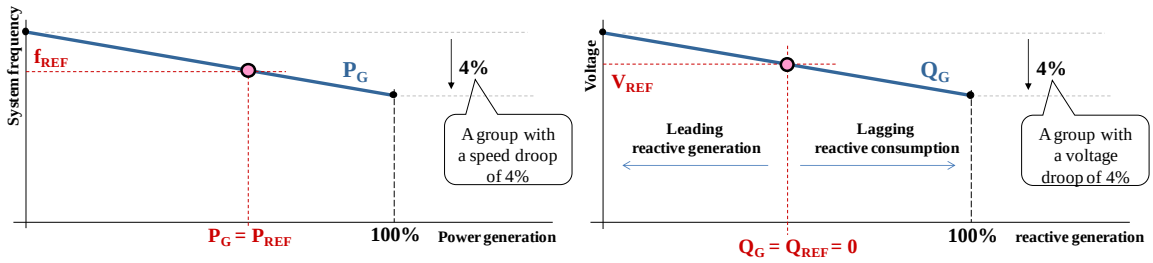

Figure 1-4 Droop controls

For each control mode a different settling time may be defined, for example Denmark demands a faster settling time in the event of voltage control mode. The result is that a significant variability exists among countries (from 10 s to 1 minute). All set-points are commonly given at the grid connection point which typically corresponds to the high voltage side of the transformer. Nonetheless, in Denmark is chosen by the *electricity supply undertaking* company. In this case this point could be the grid connection bus, the common coupling bus bus (commonly selected if there is a tap changer) or one in between.

In Spain the set-point is specified at the meter point which can vary in location. In the event that all wind farms sharing the transformer belong to the same owner, the meter is at the high voltage side whereas if wind farms belong to different owners the meter point is located at the low voltage side. Moreover, in order to implement wind voltage control, it is necessary to coordinate the droop controls of wind farms and the current OLTC transformers control. This fact is outlined by Eirgrid and SONI (Ireland Transmission system operators). In order to define guidelines for adequate coordination different demonstrations are being carried out within the project *"Delivering a Secure Sustainable Electricity System (DS3)",* [Eirgrid et al. 2012, Eirgrid et al. 2013].

In all cases analyzed, this service (reactive power/voltage control) is mandatory not contemplating any remuneration scheme. Nonetheless, some grid codes continue under review as the Spanish one. In this country, one of the main concerns of the Spanish wind association (AEE), is this issue.

1.4. OBJECTIVES

This thesis aims to design a voltage control scheme which takes the maximum advantage of wind farm reactive power capabilities. TSOs seek that the whole HNet resembles a conventional plant which could be integrated in a hierarchical voltage control scheme. This strategy, as will be discussed in this thesis, benefits both TSO and wind farm owners. Nonetheless, the HNets infrastructure could differ significantly. Hence, the control limits, i.e., the maximum reactive power that can be injected or absorbed could change sifnificantly varying also the voltage margins. These limits will be used for determining whether the HNet is suitable for providing this service or not. In the case that it is not suitable, other strategies should be considered. In addition, how the strategy should be implemented must be considered. In this thesis a special emphasis is placed on

simple control schemes which most of them do not require communication. In addition, in all cases additional investments are not necessary and hence, these strategies can directly be implemented.

In any case, the voltage control design does not end with its steady-state analysis requiring temporal evolution assessments (referred to in this thesis as dynamic analysis). Taking into account this temporal evolution the control performance can be optimized by paying special attention to OLTC transformers and the possible interactions among controllers that may appear. Consequently, two types of analysis are going to be carried out: steady-state and dynamic.

Once the global picture is clear, the concrete objectives are presented in the subsequent subsections.

1.4.1. STEADY-STATE ASSESMENT AND HNETS CLASSIFICATION

As has been mentioned, the first step is the evaluation of the HNet limits and potentials. On one hand, the limits are imposed by the maximum reactive power that the whole HNet is able to absorb from or inject to the transmission network. This maximum reactive power determines the maximum voltage variation that can be obtained. This variation highly depends on the strength of the bus, i.e., on its short circuit power. Hence both magnitudes: reactive power and voltage variation should be evaluated in detail. In that sense the well-known OPF will be used, being the reactive power at the HNet common coupling (- and +) maximization the objective function. This contrast with the common employment of the OPF for determining generator operational points in accordance with well-know objectives such as power losses or cost minimization. On the other hand, the potential that wind farms' reactive power capabilities represent for both TSO and the HNet itself are also evaluated. In that sense, in addition to the reactive power and the voltage variation of power losses are also included. Those potentials will be compared with the ones obtained by common control schemes evaluating the improvements required for taking maximal advantage of wind farm capabilities. For carrying this analysis a bespoke tool which evaluates any HNet considering any objective function and imposing a certain control scheme will be developed.

Subsequently, the HNets should be characterized in accordance with their limits and potentials. Anticipating the results, three different types of HNets will be identified proposing for each one a different control strategy:

- Power losses minimization
- HNet minimum impact on TNet
- Pro-active voltage control

Moreover a different way of implementing each strategy will be discussed trying to minimize communication requirements and even avoid them.

1.4.2. OPTIMAL STATIC SETTINGS DESIGN

For each control strategy the optimal static settings (i.e., settings that impose the steady-state) should be determined. It is clear that in all cases those setting can be optimally evaluated each period. This approach will be followed in the event of a pro-active voltage control. In this case the optimal wind farms and OLTC transformers set-points are calculated each period by means of quadratic programming as will be detailed explained in Chapter 6. Nonetheless, this approach demands communication which not always is justified. In that sense others approaches more suitable for the other control strategies are discussed: data mining techniques for the power losses minimization and fit-and-forget static setting for the HNet minimum impact on TNet strategy. The former contributes with simple control rules of easy interpretability and which in some circumstances and for some devices can be used in a decentralized manner, totally avoiding communication. The latter contributes evaluating the optimal fixed settings for all set of scenarios. In that sense, it is guarantee that the settings are feasible under all circumstance and hence communication can also be avoided.

1.4.3. TIME VARIANT AND OFFLINE TUNING OF DYNAMIC SETTINGS

In addition to the static settings each control scheme is defined by some relevant dynamic settings (i.e., settings that affect the temporal evolution as time delays, time constants or dead band). Those settings will be tuned offline guarantying an optimal control performance and not requiring online updating. In that sense a control scheme simulator (developed in this thesis) will be used jointly with different metaheuristic algorithms minimizing relevant objectives such as:

- Tap changes minimization
- Voltage breaches minimization
- Transformers voltage set-point deviation minimization
- Oscillations minimization

This contrast with other techniques proposed in the literature and which have been explained in the subsequent chapter such as model predictive control or multi-agents. Techniques used for an online application which could demand two-way communication not available yet in the HNet.

1.5. STRUCTURE OF THE DOCUMENT

This dissertation contains 7 chapters and 8 appendices. Chapter 2 presents the state-of-the-art of wind farms' reactive power capabilities utilization in order to enhance the power system operation. Moreover the solutions presented in the literature from both steady-state and dynamic perspectives are gathered. Subsequently, Chapter 3 first outlines the technical benefits of voltage control provision from a technical perspective. Then, this same chapter expounds the steady-state analysis of HNets determining their potential and limits. Moreover, those HNets will be classified as one of three different types of HNet (A, B and C) and for each one a preferred strategy is selected.

Subsequently, the next three chapters focus on a specific type of HNet. Specifically, Chapter 4 focuses on type A where the strategy selected is power losses minimization. Then, Chapter 5 analyzes type B HNets where a minimum HNet impact on TNet strategy has been chosen. Next, Chapter 6 evaluates the pro-active voltage control strategy. Finally conclusions and future research are drawn in Chapter 7.

Concerning the appendices, the first one (Appendix A) presents the HNets characteristic and wind farms requirements. Subsequently, a brief summary of the reactive power voltage relationship is provided in Appendix B showing the importance of reactive power control provision. Then, Appendix C presents the sensitivity matrixes that are used in pro-active voltage control. Next, Appendix D analyzes actual wind farm data obtaining correlation factors and time evolution patterns. After that, Appendix E presents the simulator developed within this thesis in order to carry out the dynamic analyses. Moreover, the metaheuristics algorithms employed are summarized in Appendix F. Appendix G collects the detailed dynamic analysis of all control schemes evaluated within Chapter 5 and Appendix H compares these schemes with the pro-active voltage control strategy. Finally, Appendix I provides a simple analysis of an internal wind farm network, which throughout the thesis has been neglected.

CHAPTER 2

STATE OF THE ART

This chapter presents research that has been carried out concerning wind farms voltage control, outlining the gaps which will be addressed by this thesis. At first the main research focus was evaluating the impact of wind generation on network voltages trying to minimize it at the planning stage. However, it was seen that the controllability of this generation was needed. Hence, great efforts have been done in this sense as will be seen. Recalling the title of this thesis, the focus is HNets (a typical scheme in countries with high wind penetration such as Ireland or Spain). Nonetheless, wind farms in many countries are commonly located in DNets and schemes such as the smart grids have been more investigated. Hence, those networks cannot be forgotten and a deep understanding of their operation should be acquired. In those networks special attention to the enhanced control schemes which consider reactive power capabilities of wind farms must be paid. Among all strategies the more suitable ones in accordance with the HNet potentials will be selected as is later explained in Chapter 3. One of these strategies is a pro-active voltage control. For that purpose a control of decentralized devices (OLTC transformers and wind farms) and its coordination should be carried out. Nonetheless, as has been outlined in the previous chapter, the control of decentralized elements is well understood in the TNet, where several hierarchical controls have been implemented. In addition, several alternatives are proposed focusing on DNet. This chapter classifies and studies the philosophy behind all controls for its later application to the HNets. It must be not forgotten that the final goal is integrating the HNet into an existing TNet hierarchical control.

In order to address all these issues the chapter has been structured as follows. Firstly, some important concepts that are used throughout the chapter are introduced in section 2.1. Section 2.2 introduce the solutions provided for DNet and smart grids taking into account both dimensions of the control, steady-state and temporal evolution performance. Subsequently the TNet solutions are described paying a special attention to hierarchical voltage control. Those schemes are emphasized because in the event of pro-active voltage control the whole HNet control resembles a conventional plant to be integrated in it. Then, the field experiences that have been conducted are summarized in section 2.4. Finally, the gaps identified in the state-of-the-art are outlined in section 2.5

2.1. CONTROL CONCEPTS

In recent years wind farms reactive power capabilities have been used for obtaining diverse objective functions: voltage rise mitigation [Liew et al. 2002, Kulmala, et al. 2007, Capitanescu et al. 2014, Masters 2002], power losses minimization [Ochoa et al. 2011, Meegahapola, et al. 2012, Hu et al. 2014], thermal constraints minimization [Sansawatt et al. 2012, Alnaser et al. 2015], active power shedding minimization [Siano et al. 2010, Ochoa et al. 2010], reactive power support maximization [Ochoa et al. 2011, Cuffe et al. 2014a, Bolognani et al. 2013, Yanhua Liu, et al. 2011] or voltage profile regulation [Capitanescu et al. 2014, Di Fazio et al. 2013] changing the typical passive paradigm of these resources to an active one. For that purpose different approaches have been employed. This section clarifies the most relevant concepts that will be later used throughout this chapter. It has been structured as follows. Firstly, subsection 2.1.1 presents the definition of distribution network and smart grid, identifying the role that wind farms play. The different communication schemes are described in subsection 2.1.2 outlining the selection performed in this thesis. Then the different control configurations that are used and the concepts related are explained in subsection 2.1.3. Next, the coordination of different control devices is explained in subsection 2.1.4. Subsequently, the control parameters are described in subsection 2.1.5. Finally the global picture of the different approaches followed is drawn in subsection 2.1.6.

2.1.1. CHANGING WIND FARMS PASSIVE PARADIGM

Passive distribution networks

Distribution networks were designed to accommodate only loads. In such networks the internal voltage profile is typically established by the tap-changing transformers or static compensation devices. Thus, the control capabilities of distribution generation are not exploited.

Active distribution networks

Active network management has been considered as an intermediate step towards the concept of *smart distribution grids* [Capitanescu et al. 2014]. In this case a real time monitoring of the grid is performed, taking advantage of the control capabilities of

distribution generators. Hence, important advantages can be obtained such as voltage rise mitigation or hosting capacity[4] increase.

Smart grids

As it is clearly defined in [Farhangi 2010], "The smart grid is the collection of all technologies, concepts, topologies and approaches that allow the silo hierarchies of generation, transmission, and distribution to be replaced with an end-to-end, organically intelligent, fully integrated environment where the business process, objectives, and needs of all stakeholders are supported by the efficient exchange of data service". This means that within a smart grid all devices involved, especially renewable generation, should be controlled. In this context, consumers are able to increase or reduce its consumption in accordance with cost signals. Moreover, those networks are self-organized, relying on the agent's technologies, and are able to take corrective actions in order to avoid possible failures. A HNet is not a smart grid. Nonetheless, owing to the massive literature review of voltage control and reactive power management in these networks, they cannot be forgotten and have been included in the literature review.

2.1.2. COMMUNICATION SCHEMES

The existing networks rely on one-way communication, i.e., set-points are only sent in one direction without receiving any feedback. However this system has evolved in order to respond to the increasing demand of smart grids where the communication is a key element. In that sense the two-way communication is gaining relevance (i.e., several agents interchange information implying feedback). Nonetheless, although both options have been reviewed, this thesis has focused on the one-way communication which represents the current status of communication. Another important fact that supports this decision is the existence of wind farms of different owners in the same HNet (a two-way communication between assets that act as competitors may not be desired). Moreover, the possibility of avoiding communication will be discussed throughout the thesis.

2.1.3. CONTROL CONFIGURATION

Centralized

This configuration considers the whole power system as a unique control area. As a result, it has global information of the whole system. Hence, in this case a central controller distributes set-point (one-way communication) among the control devices based on that global information. The main drawback of this configuration is the large amount of data, which could make computational time excessively slow and hence, not suitable for online applications. In addition, reliability is also an important drawback because in the event of a failure the whole control system is lost [de la Fuente 1997].

[4] Defined by [Etherden et al. 2011] as "the maximum amount of generation that can be connected to a power distribution system"

Moreover, this terminology is also employed when a single element (e.g., bulk transformers) is used for controlling the voltage of a certain grid.

Decentralized

This configuration splits the system in different control areas. Note that in the extreme situation each control area is composed by a single control device. As a result the amount of data decreases significantly and hence communication is also reduced. In contrast to the centralized approach, in the event of a failure, the whole control system is not lost. Nonetheless, in this case there is no global information. Moreover, it must be noted that the different areas or devices should be coordinated in order to avoid unwanted/undesirable interactions [de la Fuente 1997].

These drawbacks could be solved in the event of a distributed configuration, i.e., if two-way communication is considered. In this case global information can be inferred as is achieved by self-organized biological populations (e.g., hives, folks, shoals) as will be explained in this thesis.

Pilot buses

In large systems such as the transmission network, it is not affordable to control the voltage of all buses. Hence some relevant buses, which have been named "*pilot buses*" must be selected. Performing this selection has been widely discussed and many algorithms have been evaluated as was discussed in [de la Fuente 1997]. In the end, all of them seek a trade-off among two important concepts: controllability and observability. In this thesis a single pilot bus corresponding to the connection bus HNet-TNet has been considered. Hence, this thesis does not go in depth in this aspect.

- *Controllability*:
  This concept reflects, how easily a certain bus can be controlled, taking into account how far that bus is from the generators.
- *Observability*:
  This concept reflects how the voltage of a certain bus gives information of the system disturbances or other demand buses voltages.

Hierarchical

In a hierarchical configuration several control loops are defined, e.g., primary, secondary and tertiary allowing the simplification of the complex voltage control issue by the spatial and temporal decomposition. As has been explained in the introduction, the fastest action is carried out by the primary loop, which is in charge of controlling the local voltages. In contrast, the tertiary loop evaluates the system from a global point of view considering discrete elements. In this last loop is precisely where traditionally the optimization process has been carried out. In each control loop the required set-points for its downward loop are evaluated. Commonly, a one-way communication system is considered, e.g., the implemented transmission network hierarchical voltage control

schemes which will be later explained in section 2.3. Nonetheless, recent hierarchical schemes relying on two-way communication is also proposed.

2.1.4. COORDINATION

As has been already mentioned, coordination is essential when several control devices interact. Nonetheless, this term could be ambiguous owing to the fact that it is used for referring to two different problems: how to distribute control actions among devices? And how to prioritize control actions?

In both cases different alternatives can be employed as is next presented Nonetheless, all of them can be gathered in two groups: online or offline processes. The former evaluates the coordination each period of the control. Contrarily, the latter is carried out by an external study.

- **How distribute control actions among devices?**

  For avoiding interactions among controllers the set-point of one device should be computed taking into account the effect of neighbour devices. As an example of this coordination, the coordinated secondary voltage control implemented in France (CSVC) is introduced (control that is later described in detail in paragraph 2.3). In this control scheme the control actions of one area are computed online taking into account the voltage deviation at its pilot bus and also the effect of the neighbour areas pilot buses. In this thesis, this control dimension has been called *steady-state coordination*.

- **How prioritize control actions?**

  It should be noted that the same steady-state operation does not imply the same temporal evolution. Hence, another effect is the controller interactions that can arise as various devices in a network dynamically respond to the changing set points they receive from any controller. This thesis will analyze how to ensure that such set-points redispatch harmoniously. This is an important fact, especially when there are discrete controllers involved such as OLTC transformers. In this thesis, this control dimension has been called *dynamic coordination*. In that sense different techniques and concepts have been used: zone discrimination, control cycle determination, dynamic programming, model predictive control (MPC) and multi agents. The first two ones are offline processes constituting the first sensible way of approaching this problem. In contrast, more sophisticate control schemes evaluate online, the priority of each control devices. Those control schemes could be centralized, as MPC, or distributed as multi-agents. In addition, a technique widely used for both, online and offline processes is dynamic programming. This technique has widely evolved resulting in a large number of algorithms. In this thesis, this technique will be considered in its offline approach as will be explained in its corresponding paragraph.

In this first approach just the definitions are provided. How these concepts and techniques have been used for dealing with the voltage control provision will be explained later throughout the chapter.

- *Zone discrimination*:

  For avoiding these possible interactions some works propose determining the priority of each control device in the system based on the concept of zone discrimination, e.g., [Muttaqi, et al. 2013]. In that sense, the influence zone of each control device is identified. Hence the control device is responsible for controlling the voltage in that specific zone and only acts as a supporter in other zones when the actions of their responsible devices are not sufficient. Nevertheless, this approach has been dismissed within this thesis because all control devices are near from an electrical point of view.

- *Control cycle determination*:

  As is outlined in [Alnaser et al. 2015] the control cycle which normally corresponds to the sample time is "the time interval between two consecutive constraints checks". Hence, it seems undoubted that if the control cycle increases the possible control interactions will decrease. However that decrement is at the expense of undesirable performance such as voltage above its limits or congestions. Consequently, its evaluation is essential for obtaining and admissible trade-off among objectives (control action minimization vs over voltages …) as is later discussed in this chapter.

- *Dynamic programming*:

  This technique was first proposed in 1957 by R.E. Bellman which formulates its optimal principle "An optimal policy has the property that whatever the initial state and initial decision are, the remaining decision must constitute an optimal policy with regard to the state resulting from the first decision" [Bellman 1957]. Hence a complex problem can be decoupled in simpler ones which are successively solved. This technique has been widely used for diverse systems: "discrete-time or continuous-time systems, linear or non-linear systems, deterministic or stochastic systems" … In fact, it has been widely used for solving the Riccati equation [Lewis 1992] (when the system is modeled by linear dynamic and the cost function by a quadratic one) and the Hamillton-Jacobi-Belmman [Lewis et al. 1995] (when the system is non-linear or the cost function is non-quadratic). For solving this last equation the adaptive/approximate dynamic programming algorithm stands out as is explained in [Fei-Yue Wang et al. 2009]. Among them it is essential to outline the contribution of [Werbos 1977] originating the adaptive critic designs (ACD) the merit

of which relies on solving dynamic problems forward-in-time instead on the traditional backward approach. This new way of solving problems has been widely extended resulting in many different synonymous algorithms in the literature: Approximate/Adaptive Dynamic Programming (ADP), Asymptotic Dynamic Programming, Heuristic Dynamic Programming, Neuro-Dynamic Programming [Fei-Yue Wang et al. 2009]. In this thesis the dynamic programming term is employed assuming its backward approach, widely used for planning control actions such as tap changes as is later discussed. On the contrary, those algorithms that solve dynamic problems forward-in-time will be explained jointly with the model predictive control (MPC) which is next explained. This division has been made because as is stated in [Bertsekas. 2005] "the two methodologies [ADP and MPC] are closely connected, and the mathematical essence of their desirable properties (cost improvement and stability, respectively) is coached on the central dynamic idea of policy iteration". Moreover with this approach, the online control algorithms (forward-in-time approach) are distinguished from the planning analysis, typically solved considering a backward approach.

- *Model predictive control*:

  As is stated in [Moradzadeh et al. 2013] one of the most successful control schemes is MPC, which also is called receding/moving horizon control. The main advantage of this scheme is that the control actions of a certain period k are optimized taking into account the future periods $k+1$, $k+2$, ... $k+N$ although only the actions at that period k are implemented. Hence, for a possible control sequence $[u(k), u(k+1), u(k+2), \ldots u(k+N)]$ the system performance is predicted for a time horizon in accordance with an explicit *model*. The first element of the best control sequence according to the objective function is then implemented. Then all this process is repeated for the next period $k+1$ and so on.

- *Multi-agents system*:

  Many agent definitions have been provided as is surmised by the multi-agent IEEE working group [McArthur et al. 2007]. This fact shows the difficulty of defining this concept. Nonetheless all definitions share the basic concepts. Next the qualities that any agent should are explained in [McArthur et al. 2007] and are next enumerated.

  - **Autonomy** – Each agent can manage the behavior of a individual unit mostly autonomously in a cooperative or competitive environment

- **Reactivity** – agents can perceive environment, and respond adequately in accordance with the function it is designed to achieve.
- **Pro-activity –** In the Wooldridge definition [Wooldridge. 1996] this concept is explained as the agents ability to "take the initiative" meaning that an agent can dynamically change its behavior in order to achieve its goals.
- **Social ability –** Intelligent systems are able to interact with other agent systems. Nonetheless, it is important to note that a social ability is more than mere data exchanges, it implies the ability to negotiate and interact in a cooperative manner. This ability relies on a specific agent communication language which allows to *converse* instead of simply pass data

These qualities facilitate the appearance of multi-agent systems. In these systems many agents are grouped together and depend on each other to form a community, in which all agents cooperate to achieve the individual and system goals.

2.1.5. CONTROL PARAMETERS

Any control scheme has several parameters that should be adjusted. Those parameters could be fixed, also known also as fit-and-forget, or adaptive.

Fit-and-forget

In this case constant parameters independent of the operation conditions are considered (for instance in proportional control droop is a constant). The Italian secondary voltage control is a good example of fixed parameters as will be explained in paragraph 2.3.

Adaptive

In this case the parameters are adapted taking into account the operational conditions (in proportional control droop changes depending on the scenario). The French secondary voltage control, in which an optimization problem is solved each period, is a good example of adaptive parameters as will be explained in paragraph 2.3. Nevertheless, this is not the only method employed for adapting the parameters, other alternatives such as the self-adjusted and the predictive-corrective techniques are gaining importance

2.1.6. GLOBAL OVERVIEW

As can be derived from the previous subsections there are many concepts involved in voltage control design and a huge amount of literature available (more than 110 000 references can be found in the IEEE browser). Hence, a huge effort has been made for providing the global picture which will be expanded throughout the chapter. In Figure

2-1 the principal concepts are gathered. This figure will be used to establish the framework of this thesis. At the end of this chapter the same figure will be presented highlighting the areas to which this thesis contributes.

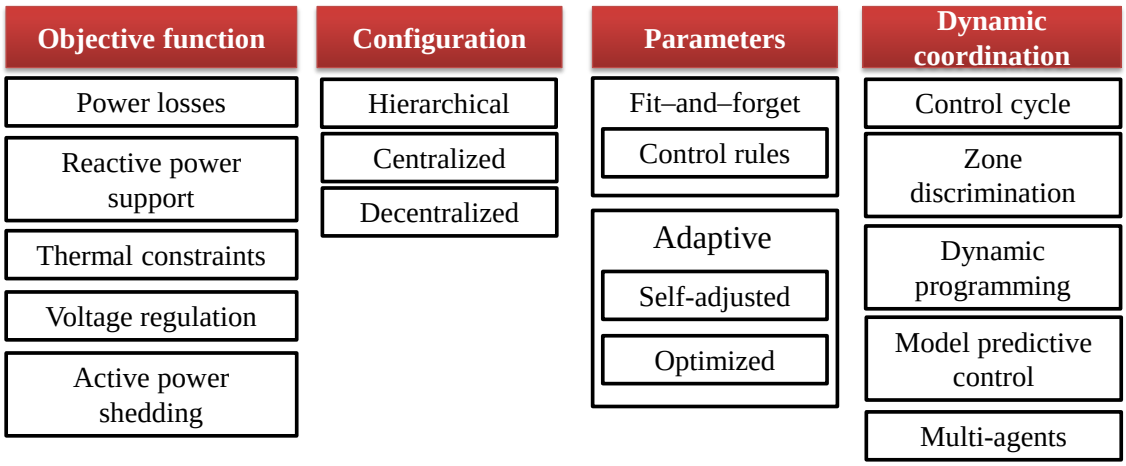

Figure 2-1 Control strategies and configuration

2.2. DNET AND SMART GRIDS SOLUTIONS

2.2.1. OLTC TRANSFORMERS COORDINATION

As is mentioned in [Van Cutsem et al. 1998], OLTC transformers coordination is being performed by means of an intentional time delay. In the example presented in this reference, it is explained how in order to avoid unnecessary tap changes the downstream transformer, and hence the nearest to the load, should be between 20 and 40 seconds slower than the upstream one. Moreover, in [Hashemi, et al. 2011] and [Ye Li, et al. 2010] control rules obtained using fuzzy logic are proposed, allowing an adequate coordination of both parallel and cascade elements. In addition alternative control schemes based on a few remote measurements have been proposed [Caldon, et al. 2013]

OLTC transformers coordination should be revised owing to the wind penetratuin increment, which an increment of control devices. Moreover how to deal with bidirectional power flows, (in the event of networks which accommodate loads) has been an important focus of research. This is a fact that directly affects the line drop compensation and its design. As an example in [Gao et al. 2011] a distribution network in which wind generation is allocated is analyzed. Nevertheless the wind generators do not provide any control. This author proposes changing the line drop compensation voltage threshold in accordance with the sense of the current of the transformer. Moreover, in the event that generation is higher than demand, the voltage threshold is fixed 5% below its maximum voltage, in order to avoid voltages over its admissible values. In this thesis the line drop compensation will not be analyzed because its design is not relevant in the event of unidirectional power flows, which is the case of HNets.

Transformers coordination should be done in both areas static and dynamic as has been already mentioned. In that sense several alternatives have been proposed throughout the literature considering a single OLTC transformer and a set of other control devices as is presented in the subsequent subsections. Nonetheless some analysis of cascade OLTC transformer coordination has been done [Alnaser et al. 2015] representing an important focus of this thesis. Moreover, different alternatives in both areas will be proposed within this thesis taking into account its online performance.

2.2.2. ENHANCED UTILIZATION OF REACTIVE POWER CAPABILITIES, STEADY-STATE COORDINATION

It is clear that wind farms' reactive power capabilities have much to offer the broader power system. In that sense, many contributions have evaluated how best to evolve passive distribution networks into active ones, which is an intermediate step towards the concept of *smart distribution grids* [Capitanescu et al. 2014]. Indeed [Liew et al. 2002] first evaluated how active management can play an important role for increasing the wind penetration in existing distribution networks where voltage rise effect was seen as the principal barrier. Subsequently, several works have extended and complemented this approach showing its potential using diverse techniques of increasing complexity (linear programming [Keane et al. 2007], OPF [Vovos et al. 2007] and multi-period OPF [Siano et al. 2010, Ochoa et al. 2010]). For such purpose, centralized [Liew et al. 2002, Capitanescu et al. 2014, Vovos et al. 2007, Pilo et al. 2011, Kulmala et al. 2014], decentralized [Sansawatt et al. 2012, Cuffe et al. 2014a, Di Fazio et al. 2013, Berizzi et al. 2012, Hamzeh et al. 2013, Calderaro et al. 2014] and hierarchical [Biserica, et al. 2011] reactive power control schemes have been evaluated. Notably, the focus of the existing research is primarily on the steady-state reactive power performance where several objectives have been evaluated: power losses [Ochoa et al. 2011, Bolognani et al. 2013, Kulmala et al. 2014, Calderaro et al. 2014, Madureira et al. 2009], thermal constraints [Sansawatt et al. 2012], active power shedding [Kulmala et al. 2014], reactive power support [Ochoa et al. 2011, Keane et al. 2012] or voltage network profile [Di Fazio et al. 2013]

As the references show power losses minimization has represented an important focus for researchers. In addition in countries such as England thermal constraints have become a relevant issue. In [Sansawatt, et al. 2010] a dual control mode was first proposed where wind farms are operated at a certain power factor for normal conditions and as a reactive power source if the voltage rise effect is inadmissible. Moreover as is done in many studies, wind energy curtailment is seen as a last resource for mitigating this effect. Nonetheless, in this thesis reactive power control will never compromise active power production. Hence, this objective will not be addressed within the thesis. The work presented in [Sansawatt, et al. 2010] was extended in [Sansawatt, et al. 2011] evaluating which power factors should be used in 5 different operational situations and [Sansawatt et al. 2012] incorporated sensitivity analysis. Moreover, its real time operation was tested in [Robertson, et al. 2012] using time domain simulation. These objectives are mainly related to distribution network or microgrid internal operation in which wind farms are located. However, a more demanding strategy in which wind farms offer reactive power

support to the TNet or at least reduce its demand has also been studied opening the doors for a pro-active voltage control strategy. All these objectives have been combined in diverse ways, e.g., reactive power support + power losses [Calderaro et al. 2014], thermal overload + network voltages [Alnaser, et al. 2013].

Nonetheless, these objectives may be opposite, as demonstrated [Keane et al. 2012], depending on factors such as the grid impedance or the wind penetration level. This thesis addresses this issue, identifying which HNet is more suitable for each objective, maximizing all its potential and, in the event of considering several objectives, the weighting factor between them. For this classification the best results (minimum/maximum objective function) will be obtained when a smart strategy is implemented (the best set-points are considered in each period). Moreover, these strategies can be evaluated in economic terms, a fact that is also evaluated in this thesis. Concerning the economic impact of the reactive power support by wind farms, most of the works studied the problem from a market and regulatory perspective e.g., [Rueda-Medina et al. 2013, Bignucolo, et al. 2009]. Moreover, there is a scarcity of works that directly face with the cost/benefits that this service could mean to the agents involved (wind owners, DSO) under a specific regulation scheme. A first approach was done in [Zechun Hu et al. 2012] where the economic impact is computed for a simple active network management scheme in which only the tap position and the wind power curtailment is considered as control variables, i.e., wind farms' reactive power capabilities are not contemplated.

Nonetheless, smart strategies although have been widely studied are not commonly implemented owing to reasons such as the increment of communication infrastructure and data requirements or the necessity of an adequate coordination among controllers. Due to these reasons an intermediate approach, which does not require additional communication, was suggested. This approach relies on the well-known concept of passive networks, 'fit-and-forget'. In the same way passive control schemes in which the bulk transformer tap position or the power factor are optimally determined have been analyzed. In [Keane et al. 2011] those settings are evaluated considering both, DSO and TSO requirements and objectives[5]. For that purpose a linear programming optimization is carried out with the objective function of maximizing the injected reactive power from all resources (note that this objective function is equal to minimizing the reactive power import from the transmission network) considering the DNet constraints. It should be noted that a DNet highly loaded is not able to export reactive power to the TNet. Hence, the aim of this objective function is to reduce the DNet impact on the TNet. The study has been conducted using an actual Irish DNet and the whole Irish system. The results show the potential of wind farms as a reactive power provider. In [Ochoa et al. 2011] the previous work is improved in order to handle the non-linearities. For this purpose the

[5] As is outlined by [Power, et al. 2014] a successful incorporation of wind farms to the voltage control service involve both DSO and TSO. That work stands out the future challenges in the control centre due to distributed generation and renewable. Moreover a CIGRE working group (C 2.16) directly faces these challenges.

OPF multi-period technique has been used. This technique has been proven as a reliable option for problems related to DG planning and optimization as was intimated in [Ochoa, et al. 2010]. The main advantage of this technique is the incorporation of several scenarios meaning that whereas the OPF gives the optimal control variables for a concrete scenario, the AC multi-period OPF gives simultaneous consideration to multiple scenarios, which could represent different load conditions. Moreover also different network configurations can be incorporated as has been done in [Al Kaabi et al. 2014] where a multi-configuration multi-period OPF is proposed.

In addition, the passive control presented in [Keane et al. 2011] (considering the same network and objective function) is compared with the possibility of changing the settings in real time. The results show that for this particular case (minimizing the reactive power import from the transmission network), passive control does not differ significantly from a smart strategy. However it must be noted that this analysis only considers the power factor control mode for wind farms and other control schemes may be more adequate.

Recently, this approach has been extended incorporating voltage control settings such as voltage set-point or droop [Cuffe et al. 2014a]. Hence the wind farm actively responds to voltage excursion in accordance with its parameters (voltage set-point or the droop) which are fixed. Thus, autonomous control schemes could be defined. Although, this approach (fit-and-forget settings) has been seen as an intermediate step it must be noted that under some situations it may be adequate, a fact that has already be mentioned and that is extended in this thesis. In addition this approach could be enhanced with self-adjustment control schemes, i.e., the fit-and-forget settings can be modified in accordance with local measurements, not requiring communication. These developments, provided by [Cuffe et al. 2014a], have been used in this thesis, where several autonomous control schemes have been compared.

As has been seen, most of these studies rely on optimization algorithms. However, sometimes simpler schemes based on control rules may obtain comparable results as is demonstrated in [Kulmala et al. 2014]. This scheme has been typically used in simple radial networks where only few control possibilities exists. This thesis will deeply analyze this possibility in a more complex network for the power losses minimization strategy in order to infer useful knowledge of the HNets.

2.2.3. DYNAMIC COORDINATION

Some recent work has indicated that dynamic coordination between control devices is essential for avoiding unwanted control actions [Ranamuka et al. 2014, Alobeidli et al. 2014]. In that research an online voltage control considering different voltage regulating devices is proposed. This work focuses on how the different devices, corresponding to one OLTC transformer, several step voltage regulator (SVR) and a DG unit, should be coordinated. This coordination is done with the time delays of the several devices. In addition the voltage and the dead band settings of the SVRs are selected based on the total number of taps and the percentage value of the voltage regulating range. Nonetheless, how those fixed parameters, used for coordinating the different controllers,

have been selected is not explained. This drawback is solved in this thesis where those settings are tuned in accordance with a multi-objective optimization.

Towards that end, other control alternatives which have been already described in section 2.1 are proposed. Those alternatives can be separated into two groups depending on the control configuration. Concerning the centralized approach the most relevant techniques are: knowledge based rules, model predictive control and dynamic programming. Concerning the decentralized approaches the multi agents systems represent the focus of current research. In the following paragraphs, all these alternatives are explained outlining their drawbacks that are solved with the methodology proposed in the thesis.

Control cycle determination

As has been already mentioned the control cycle determination can be used for reducing control actions as is demonstrated in [Sansawatt et al. 2012, Wei Zhang et al. 2014]. However, this is not without its own downsides, as it can result in [Alnaser et al. 2015]. Precisely, [Alnaser et al. 2015] analyze the effects of three different control cycle (1 min, 5 min and 15 min) for two control strategies (only distributed generation curtailment or curtailment +coordinated voltage control for the bulk OLTC transformer + power factor control in the event of the distributed generators). In both cases the control actions in each control cycle are evaluated by an OPF introducing the risk concept (crucially for handling wind generation uncertainties in a multi-cycle context). However a pro-active voltage control demands shorter control cycles. Moreover, other control schemes including voltage control of the distributed generators and all OLTC transformers are needed. This thesis also analyzes the impact of the control cycle also incorporating the impact of other relevant settings which directly affect the temporal evolution of the control scheme.

Dynamic programming

As [Young-Jin Kim et al. 2013] outlines, voltage control provision by wind generation will increase the number of tap changes. For reducing this increment dynamic programming, taking into account its backward approach (see subsection 2.1.4), has been seen as a suitable technique. In that respect, different devices (OLTC transformers, FACTS and distributed generators) are dispatched periodically (e.g., hourly) for a certain time horizon (e.g., one day) assuming perfect knowledge of generation and load forecast. As an example, [Young-Jin Kim et al. 2013] determines the tap position, number of unit capacitors and reactive level for one OLTC transformers, two shunt capacitors devices and a distributed generator respectively with the objective function of minimizing the number of switching device operations and power losses while maintaining grid voltages within admissible values. It should be noted that for the whole period, e.g., one hour, the tap position remains constant. This operation is not suitable in systems with high wind penetration which demands higher flexibility. Hence, alternatives methods are evaluated within this thesis.

Model predictive control and rolling algorithms

This approach has gained relevance owing to the increasing penetration of distributed generation, which implies relevant paradigms changes: generation variability and more demanding OLTC transformers actions.

In that sense in [Pappala, et al. 2010] the reactive power dispatch problem, taking into account the requirements imposed by the German grid code ([e-on, 2006]) is evaluated for a given time horizon considering two different approaches: deterministic and stochastic. In both cases the idea is to avoid short-term tap changes by adapting the control devices (wind farms and OLTC transformers) based on 15-30 minutes wind power expectation. That wind expectation is predicted thanks to a neural network which employs the past wind power as input data. Additionally, it is outlined that the wind velocity or direction can also be employed by augmenting the prediction accuracy, which is essential in the event of a deterministic model. Nonetheless, for those cases in which the prediction is not accurate enough this paper proposes a two stage stochastic programming formulation which relies on decision trees. In both cases the control actions sequence for the planning horizon (15 min) are evaluated assuming sampling times of 5 minutes. Hence four sets with the control actions (transformers tap position, wind farm reactive power, and reactive power of the compensator devices) are optimized using a PSO algorithm in order to minimize the operational cost of tap changes (assuming that each OLTC movement cost 10c€) jointly with power losses (which are estimated based on the wind power forecast and the power flow equality equations). This research is complemented in [Erlich, et al. 2011], where instead of employing the well know PSO algorithm a bespoke stochastic optimization called mean-variance-mapping-optimization (MVMO) is developed. The merit of this algorithm is that the new individuals, updated every iteration, are created with a mapping function that guarantees that they are always within limits. This control scheme is also explained in [Venayagamoorthy et al. 2012] where the importance of the prediction and the impact of wind uncertainty on the transmission network are also discussed. For mitigating this last effect the option of adding storage elements, which state-of-charge is optimized over a time window, is assessed taking into account an adaptive critic design (ACD) algorithm.

Moreover, in [Nakawiro. 2014] a predictive voltage control is proposed following the guidelines previously presented, considering an objective function of reference voltage deviation and tap changes minimization. However, the trade-off among objectives is not clearly defined. In this case the control variables considered are the transformer ratio and the voltage set-point of the solar and wind farms plant located in the test network evaluated. Nonetheless, whereas the voltage set-point may be updated every 5 minutes the optimal ratio is the same for an entire hour. In addition for estimating voltages of all distribution network buses for all 5 minutes sampling over the planning horizon (1 hour) three artificial neural networks (ANN) are required. The first two ANN are employed for estimating the active power of the wind farm and solar plant respectively. Thus, if an accurate forecast is available, they can be removed. The last one uses those estimations as inputs jointly with the apparent power of the whole distribution network to forecast the voltages.

Although the previous works can be seen as rolling algorithms (i.e., algorithms in which a control action policy is evaluated for a receding time horizon) which take into account active power predictions they are not pure model predictive controls (MPC). This fact is due to all the control sequence calculated is implemented and only is updated when other prediction is available. Contrarily, in [Valverde et al. 2013] a corrective control based on MPC, which uses a linear model (sensitivity matrix calculated offline) to predict the behaviour of the system and quadratic programming for performing the optimization is proposed. The aim of this control is to maintain voltages within admissible margins by applying optimal changes of the control variables (active and reactive power and OLTC transformers voltage set-point). Control actions changes that are minimized. Moreover, this controller distinguishes between cheap and expensive control actions. In that sense two limits are defined (normal and emergency). In the event that the voltages are outside normal limits but have not surpassed the emergency limits, only the cheapest control actions (reactive power and OLTC transformers actions) are allowed, since it is not economically justifiable to use expensive control actions (active power variation) for maintaining the voltage within narrow margins. On the contrary if the voltage surpasses the emergency limits all control action are allowed. In both situations the MPC does not change the local OLTC transformers control (if the voltage is out of a certain dead band the tap position increases/decreases after a certain time delay), but theirs voltage set-point may be modified. Hence, the prediction horizon should be higher than the control one and takes into account all possible tap changes.

This thesis will deeply study this alternative. Nonetheless, for obtaining better results the parameters that affect the dynamic performance of the control such as the time delay will be optimally determined.

Other area in which the MPC have gained relevance is the microgrids which are supposed to be operated in islanded mode. Hence, generation and consumption are tightly coupled. Also considering the variable nature of the renewable resources makes new voltage control schemes necessary as is suggested in [Falahi et al. 2013]. In this paper an MPC for which the objective is also minimizing the voltage deviation and the control actions is proposed. The control variables selected in this case are the voltage set-point of the master generator (selected owing to the lack of infinite bus), the reactive power of the others distributed generators and compensator elements. For all control elements and loads its dynamic models have been considered. Consequently, the prediction horizon and step size is chosen by the operator to cover the slowest dynamic of the microgrid under study. In that sense the dynamics models have been simplified for avoiding excessive computational time in the optimization process. In this thesis the dynamic models of wind farms will be neglected assuming an ideal response (Note that current grid codes imposed that wind farms should be able to deliver 90% of its reactive power capabilities in 1 second).

Finally, in [Moradzadeh et al. 2013] this approach is enriched with the multi-agents concept subsequently explained. Thus, a power system divided into several areas is evaluated. For each area a MPC is defined which is communicated with its neighbour areas. More precisely, distributed MPCs are conversed using two-way communication.

In that sense, each area sends to its neighbours available information, i.e., the state variables and the control sequence for the time horizon evaluated. Hence, the different areas avoid potential negative interactions although they do not cooperate.

Multi-agents

Recently multi-agent systems have gained relevance. In these systems several agents interoperate thanks to two-way communication allowing a decrement of interactions among controllers. In that sense many works can be found. As an example, [Yorino et al. 2014] focuses specifically in OLTC transformers coordination. In this case each transformer is seen as an agent for which the main functionalities are: interface, knowledge base and optimization. In addition an upper agent which monitors and manages the system is added. All these agents communicate with a common memory called blackboard memory. This means that the different local controllers are configured to react independently based on their local measurement and the common memory. Thus, unnecessary negotiating process among agents is eliminated while data communication is also minimized. Others works propose similar schemes [Zhao et al. 2005, Nasri, et al. 2012] incorporating renewable resources or capacity banks. Nonetheless in all of then an upper specialized agent is required for coordinating the operations of the other agents. This approach has derived in complex hierarchical system such as the proposed in [Chun-xia Dou et al. 2013] where a multi-agent based hierarchical control scheme is proposed for a microgrid considering both continuous and discrete dynamic performance. In this scheme three different levels of agents are distinguished. In the lower level the agents are in charge of the local control strategies mainly performed by the continuous control devices. Moreover other functionalities: recognition, learning and evaluation are incorporated. In the middle level discrete control strategies for mode switching are defined in a coordinated manner. Thus, the discrete control elements and the possibility of connect/disconnect of renewable resources or loads are evaluated for a region within the microgrid. Finally in the upper level the energy optimization and scheduling is performed for the whole microgrid. This scheme resembles the traditional TNet hierarchical schemes explained in the next section. Nonetheless, the incorporation of the agent concepts allows more flexibility thanks to the communication between the three levels in any direction. However, this means a complexity increase that may be not necessary and may be unaffordable as is identified in [Vaccaro et al. 2011]

In [Vaccaro et al. 2011] a totally decentralized architecture without the need of a central fusion centre (the upper specialized agent) is conceptualized. This means that the actual value of the objective function and its gradient (the objective function increment obtained when the control variables are increased) should be autonomously computed by several cooperative agents with the same functions. In short, this paper proposes that each local controller is composed of a set of sensors (needed for acquiring local measurements) and a dynamical system named oscillator which was first introduced in [Zhao et al. 2005] and [Barbarossa et al. 2007]. Thanks to this last component the nearby controllers are mutually coupled by proper local coupling strategies and it is possible to discover the global system information required for performing any optimization. This strategy resembles the self-organized biological population (e.g., hives, folks, shoals) that

is also behind some methauristics algortihms as will be later explained in this thesis. One difficulty of computing the gradients, is the time intervals identification between control updates $u(k)$ and $u(k+1)$ as is explained in [Wei Zhang et al. 2014] (whereas short time intervals may result in convergence problems larger time intervals could result in inaccuracies in the gradient calculation and are not admissible for systems with high renewable resources penetration). [Wei Zhang et al. 2014] proposes some simplifications in the gradient calculation allowing shorter time intervals for its online application in a smart grid. Specifically, the control settings are updated every 2 seconds. As it is outlined in this same paper "the information exchange between two agents takes less than 5ms and then the control update only takes a fraction of a millisecond". Hence, the major time consumption is done in the settings calculation, which this paper has drastically reduced. Moreover, further research has been done incorporating fuzzy logic [Loia et al. 2013] or analyzing specific configuration and its communication protocols [Farag, et al. 2013].

Despite the good performance of multi-agents systems this option has been discarded in this thesis. This is because all the solutions proposed in this thesis should be able to be implemented in an existing HNet with the current resources. In these networks several wind farms of different wind owners are located and hence, the communication between competitive assets may not be desired. In those cases the use of a blackboard memory could be a solution. Nonetheless, as the authors outlines that scheme requires additional investment. Contrarily, the TWENTIES project (later explained in detail) have shown that the one-way communication infrastructure involving TSO, DSO and wind farms is already available without significant investments.

2.3. TRANSMISSION NETWORK HIERACHICAL CONTROL SCHEMES

The reference countries in the TNet voltage control are Italy and France for being the first ones. In both cases a hierarchical voltage control of decentralized elements were implemented. This hierarchical control involves different loops which were first defined in the French system [Blanchon 1972] and the Italian one [Arcidiacono, et al. 1977] in the 1970s: Primary, secondary and tertiary. Thanks to these loops voltage control can be spatially and temporally decoupled. Both controls seek the "representative" buses, known as pilot buses, which by their control is also controlled the overall system. Next a brief summary of both hierarchical controls implemented are presented outlining the advantages and disadvantages that their operation has shown. Moreover, in both controls a special attention is paid to the secondary control, which is equivalent to the HNet control.

2.3.1. ITALIAN HIERARCHICAL CONTROL

In Italy, the power system was divided into three different regions. In addition each region was divided into several areas being each one characterized by a pilot bus (in total 18 pilot buses were defined [Corsi et al. 2004a]). The voltage control of these buses is

carried out by a hierarchical control formed by three loops which has been already described.

Concerning the secondary loops, two different regulators can be distinguished: the plant and the regional voltage regulators. Initially, the plant regulator was known as REPORT. This regulator determined the AVR set-points in order to reach the required reactive level in a certain area. That reactive level is distributed among the generators of that area in accordance with their limits. The philosophy of the REPORT has not changed. However, after 2005 code for transmission dispatching, the regulator was substituted by the *Sistema Automatico per la Regolazione di Tensione* (SART), which considers additional specifications for handling the regulated relations between TERNA (which is the Italian TSO) and the grid users. Moreover, recently in [Sulligoi, et al. 2011] several advantages were proposed.

The regional regulator evaluates what the reactive power level should be in each area in order to achieve the set-point of the pilot buses. Both regulators should be temporally decoupled in order to avoid instabilities. Hence the time constant of the SART is between 5-10 seconds whereas the time constant of the regional dispatcher ascend to 50 seconds. Both loops, jointly with the primary and tertiary, are depicted in Figure 2-2 taking into account the old REPORT. In this figure it can be seen how the regional dispatcher receives the pilot bus voltage measurement and its corresponding set-point (provided by the national dispatcher) and sends the reactive power level to the power plants. Those plants are in charge of computing the AVR signal as is also depicted in this figure.

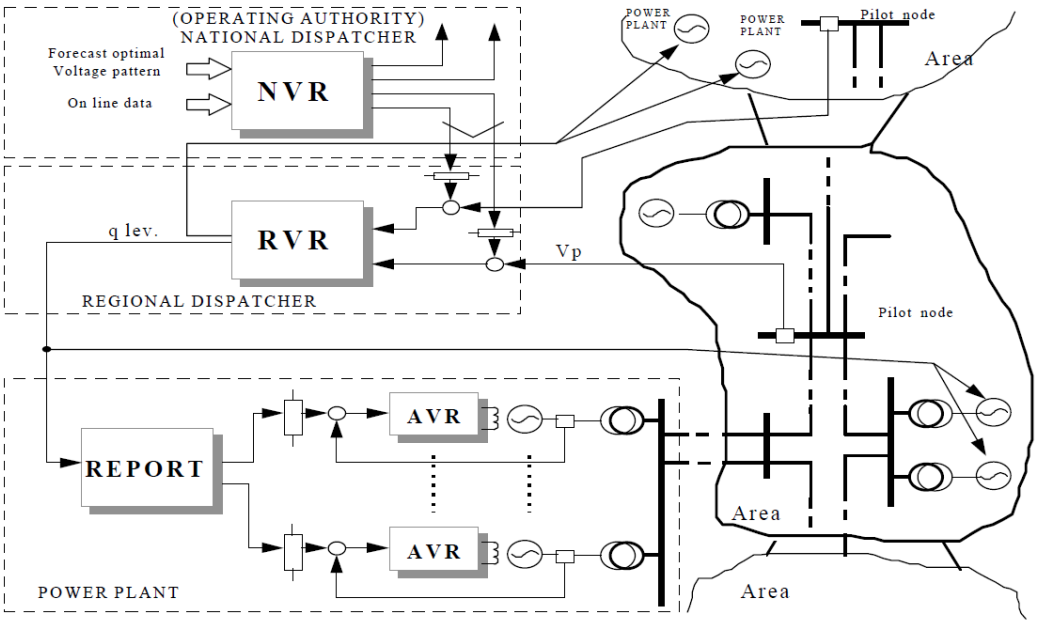

Figure 2-2 Italian hierarchical voltage control scheme. Source:[Corsi et al. 2004a]

The implementation of this control has clearly enriched the overall performance of the system. In fact, [Corsi et al. 2004b] outlines how useless reactive power misalignment has been avoided between the generating units of the same power plant as well as between

power plants in single regulating area. In addition, it also outlines that a rational exploitation of the reactive resources is achieved.

2.3.2. FRENCH HIERARCHICAL CONTROL

In France, the power system was first divided into 27 independent control regions. At the beginning a hierarchical control, known with the initials RST, with similar characteristics as the Italian one was implemented [Paul et al. 1987]. However, it was seen how this plant control was not adequate because it could originate instabilities (which do not appear in the Italian system because the transmission network is less meshed) as is explained in [Lefebvre, et al. 2000]. Moreover, the initial assumption of independent areas was not totally true and hence, an enhanced secondary control was proposed. In this second approach the number of regions was reduced and a coordinated secondary control, known by the initials (CSVC) was developed. In this case, the secondary loop is not a mere interface between the primary and the tertiary loops as was the case of the Italian control. This control carries out an optimization by quadratic programming with linear constraints each 10 seconds (which is the sample time of the monitoring) [Vialas et al. 1988]. Hence, the plant regulator proposed by the Italians is not necessary. Next the optimization problem solved each sample time is outlined.

$$\text{Minimize} \begin{Bmatrix} w \cdot \left\| \alpha \cdot \left(V_p^{ref} - V_p(k) \right) - S_{pc} \cdot \Delta V_c(k) \right\|^2 + \\ w_q \cdot \left\| \alpha \cdot \left(Q_c^{ref} - Q_c(k) \right) - A_{cc} \cdot \Delta V_c(k) \right\|^2 + \\ w_g \cdot \left\| \alpha \cdot \left(V_c^{ref} - V_c(k) \right) - \Delta V_c(k) \right\|^2 \end{Bmatrix}$$

$$subjet\ to:$$

$$V_c^{min} \leq V_c(k) + \Delta V_c(k) \leq V_c^{max}$$

$$V_s^{min} \leq V_s(k) + S_{sc} \cdot \Delta V_c(k) \leq V_s^{max}$$

$$a \cdot \left(Q_c(k) + A_{cc} \cdot \Delta V_c(k) \right) + b \cdot \Delta V_c(k) \leq c \qquad (2\text{-}1)$$

Where:

k	Sample time of the discrete controller
V_c, V_p, V_s	Voltage vectors of controlled, pilots and critical buses respectively
V_c^{min}, V_c^{max}	Controlled buses voltage vectors of minimum and maximum
V_s^{min}, V_s^{max}	Critical buses voltage vectors of minimum and maximum
Q_c	Reactive power vectors of controlled generators
$V_p^{ref}, Q_c^{ref}, V_c^{ref}$	Reference vectors of the magnitudes already mentioned

a, b, c	Coefficients of straight lines used for modeling the reactive power limits
A_{cc}	Sensitivity matrix of the reactive power generated with respect to the voltage at the controlled buses (both correspond to the generator buses)
S_{pc}, S_{sc}	Sensitivity matrixes of pilot buses and critical buses with respect to the controlled buses (buses where the generation is located) respectively
w, w_q, w_g	Weights of the different terms: pilot buses, reactive power and finally the voltages where the generators are located. Typically the first weight is much larger than the other two. However an accurate analysis is not provided, fact that will be overcome in this thesis
α	Coefficient between zero and one that considers the dynamic performance. The time constant is defined as follows: $T_c = \frac{-\Delta t}{\ln(1-\alpha)}$ as demonstrated in [Pagola 1993]. Hence, it can be elucidated that if $\alpha = 1$ a *dead beat* control is obtained. This means that the control action is achieved in just a sample time Δt (considering perfect modelling of the system and a linear response)

Focusing on the objective function the following terms can be distinguished:

- **Pilot buses voltage deviation compensation.**
  The aim of this term is the pilot buses voltage deviation minimization. Hence, the reference value V_p^{ref} should be compared with the measured one in the next period $V_p(k+1)$. Value that should be estimated in accordance with the generators voltage increments (output of the optimization) and their respective sensitivities

$$V_p^{ref} - V_p(k+1)$$
$$V_p(k+1) = V_p(k) + S_{pc} \cdot \Delta V_c(k) \quad (2\text{-}2)$$

  It should be reminded that for evaluating the generators voltage increments of a certain area, the voltages at the pilot buses of the neighbor areas are also taken into account for coordination purposes.

- **Reactive power provided by the controlled generators**
  In this case, the reactive power deviation between the optimal reference provided by the tertiary loop Q_c^{ref} and the reactive power measure in the next period $Q_c(k+1)$ is minimized. This value should be estimated in accordance with the generators voltage increments (output of the optimization) and their respective sensitivities , A_{cc}

$$Q_c^{ref} - Q_c(k+1)$$

$$Q_c(k+1) = Q_c(k) + A_{cc} \cdot \Delta V_c(k) \quad (2\text{-}3)$$

- **Voltages at the controlled generators**
  The aim of this term is the minimization of control actions. In this case those control actions are minimized with respect to the optimal voltage profile evaluated by the tertiary loop V_c^{ref}.
  $$\left(V_c^{ref} - V_c(k)\right) - \Delta V_c(k) \quad (2\text{-}4)$$

That objective function is subject to constraints which impose voltage limits at the controlled and critical buses. Moreover, reactive power limits are modelled in accordance with the following constraint, $a \cdot \left(Q_c(k) + A_{cc} \cdot \Delta V_c(k)\right) + b \cdot \Delta V_c(k) \leq c$.

This control was first operated in western France, an area with voltage problems. After two years of experience [Lefebvre, et al. 2000], published the EDF feedback, which reveals three mayor benefits for the TSO. Firstly, a more stable and precise voltage profile is obtained with less reactive power provided by the generators. Secondly, better use of reactive resources. This fact was achieved thanks to considering the proximity to the perturbation (thanks to the sensitivity matrixes incorporation) instead of simply aligning all units. Thirdly, a better dynamic response was seen thanks to the adequate tuning of α parameter.

2.3.3. HIERARCHICAL CONTROL NOT IMPLEMENTED

The hierarchical voltage control has been studied in many countries: Spain [de la Fuente 1997], Belgium [Piret et al. 1992, Janssens. 1993], Brazil [Taranto, et al. 2000], South Africa [Corsi, et al. 2010]. Nonetheless, those proposals have not always been translated into implementation. This is the case of Spain, where the current application of the operational procedure P.O. 7.4 cancels its implementation (the power plants have a voltage set-point which is fixed by REE in an hourly block framework (peak, off-peak) and with a seasonal adjustment). Nonetheless, all these proposals constitute an important knowledge. This section explains the most relevant ones focusing on the Spanish system.

One of the most detailed analyses of the hierarchical voltage control has been done in [de la Fuente 1997]. This analysis identifies the major deficiencies of the French and Italian hierarchical voltage controls. Concerning the secondary loop, one important drawback is that in both cases the dynamics are too slow. This fact guarantees the absence of dynamic interactions and the robustness of the controller. However in the event of an emergency it may not be rapid enough. In addition focusing on the French control scheme and important drawback was seen. In this case the secondary loop sends the voltage set-point to each generator, representing an inefficient performance. Owing to these reasons in [de la Fuente 1997] a hierarchical control formed by four loops were proposed: primary, plant, secondary and tertiary with dynamic response in 1-2 seconds, 5-10 seconds, 1 minute and 20 minutes respectively. This added a plant control; a priori may seem equal to the discarded reactive loop performed by the REPORT (see the Italian hierarchical control). However, significant difference among them can be seen.

- The REPORT is required for guaranteeing an equilibrated distribution of the reactive power reserves. Fact that can be avoided if this objective is included in the secondary loop (see French proposal). Moreover, this plant control can only be operated in the presence of a higher control loop. Hence its sole consideration has no sense.
- Contrarily, the plant control proposed by [de la Fuente 1997] can be solely applied for optimizing the internal assignment being totally compatible with a higher optimal control loop.

Next the optimization problem solved in the secondary loop each sample time (10 seconds as the French loop) is presented.

$$\text{Minimize} \begin{Bmatrix} \left\| \alpha \cdot \left(V_p^{ref} - V_p(k) \right) - S_{pc} \cdot \Delta {V_c}^{ref}(k) \right\|^2 + \\ w_q \cdot \left\| \alpha \cdot \left([Q_c^{ref} + S \cdot d(k)] - Q_c(k) \right) - A_{cc} \cdot \Delta {V_c}^{ref}(k) \right\|^2 \end{Bmatrix}$$

$$subjet\ to:$$

$$-\Delta V_c^{min} \leq \Delta {V_c}^{ref}(k) \leq -\Delta V_c^{max}$$

$$V_c^{min} \leq V_c(k) + \Delta {V_c}^{ref}(k) \leq V_c^{max}$$

$$Q_c^{min} \leq Q_c(k) + A_{cc} \cdot \Delta {V_c}^{ref}(k) \leq Q_c^{max}$$

$$-1 \leq d(k) \leq 1$$

$$V_s^{min} \leq V_s(k) + S_{sc} \cdot \Delta {V_c}^{ref}(k) \leq V_s^{max} \qquad (2\text{-}5)$$

In addition to the variables and parameters explained for the CSVC, two additional variables can be distinguished: d (vector which contains the reactive level of each area) and S, matrix which contains the slope of the controlled generators. In this matrix only the elements corresponding to the plants located in its generated control area are different from zero. As an example, the term corresponding to plant i and generation area j is next indicated $(i,j) = Q_c^{max}(i) - Q_c^{ref}(i)$. This fact is owing to the different treatment of the reactive power limits. Those limits are exemplified in Figure 2-3. Firstly, in subplot *a*, the common proportional scheme is depicted for two generators of different rated powers (note that both slopes coincide in the event of considering per units magnitudes). Then subplot *b* extends that approach in accordance with [de la Fuente 1997]. As can be appreciated, in that case although the reactive power level is the same for both generators they do not provide the same reactive power in per unit as in the previous case (subplot *a*). This fact is owing to the different initial point, optimally determined by the tertiary loop. In this thesis a different approach will be employed as is discussed in Chapter 6.

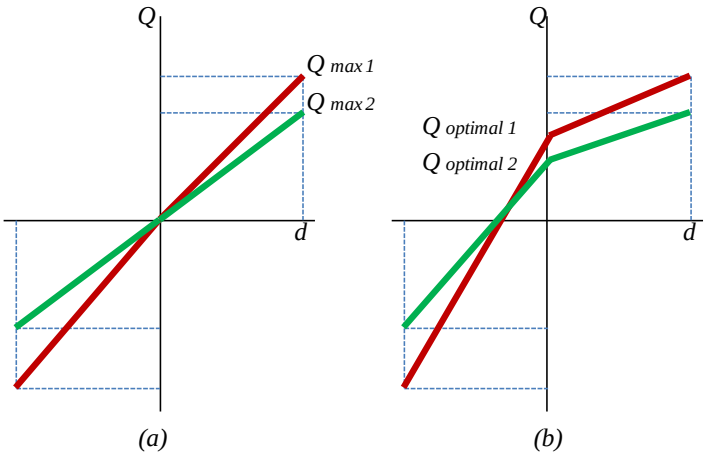

Figure 2-3 Reactive power limits consideration. Source [de la Fuente 1997]

In the formulation proposed by [de la Fuente 1997] two terms can be identified in the objective function.

- The first one, the pilot buses voltage deviation compensation, is equal to the corresponding French term.
- The second one, evaluates the reactive power (formulated in accordance with *d*) demanded for obtaining the controlled generators voltage increments required. As its equivalent French term, its aim is control actions minimization. The only difference between them is reactive power treatment. Next the equivalent among reactive power references is presented.

$$Q_c^{ref}(French) - Q_c^{ref} + S \cdot d(k) \qquad (2\text{-}6)$$

In addition, as in the French scheme, controlled and critical voltages limits are considered. Moreover, the maximum/minimum voltage increment/decrement is also determined. Finally, it can be noted that the reactive power limits are no longer defined with straight lines within the constraints $[Q_c(k) + A_{cc} \cdot \Delta V_c(k)] + b \cdot \Delta V_c(k) \leq c$. In contrast, those slopes are considered in the objective function by *S*.

In [Alonso 2001] a new optimization algorithm was developed. In this case a multi-objective function which minimizes power losses ($\Delta T_{losses}(k)$) and maximizes reactive margins ($\Delta T_{Qmargins}$) is considered in the secondary loop. This strategy contrasts with the previous ones where voltage deviation was the main driver. Nonetheless, the maximum pilot buses voltages are taken into account in the constraints (note that a power losses strategy tends to increase the voltages and hence, a minimum limit is not required). Consequently, the secondary control does not require any entrance from the tertiary control in order to perform the optimization. Indeed the tertiary loop could be eliminated determining the optimal tap position offline.

$$Minimize \quad \Delta T_{losses}(k) + w_q \cdot \Delta T_{Qmargins}(k)$$

$subject\ to$:

$$V_p(k) + \Delta V_p(k) \leq V_p^{max}$$

$$V_c^{min} \leq V_c(k) + \Delta V_c{}^{ref}(k) \leq V_c^{max}$$

$$Q_c^{min} \leq Q_c(k) + A_{cc} \cdot \Delta V_c{}^{ref}(k) \leq Q_c^{max} \quad (2\text{-}7)$$

Finally, [Frias 2008] goes further adding another loop for each agent involved, known as a rapid tertiary loop. In that sense, each agent could maximize its own profits.

In this thesis those formulations will be adapted taken into account the HNet characteristics as is explained in detail in Chapter 6.

2.3.4. INCORPORATION OF WIND FARMS IN TRANSMISSION NETWORKS, PQ CHART

Most wind farms control schemes proposed focuses on DNet. Recently special attention has been paid to TNet as is outlined in [Keane et al. 2013]. In fact in [Boamba, et al. 2013] a wind power plant control system is performed in the context of the Romanian Transmission grid, a country where the operational experiences have proven that wind farms have a significant impact on the TNet voltages, especially in those buses with a low short-circuit power. In this work two control levels have been considered (400 kV and 110 kV). The voltage threshold at 400kV is maintained by adjusting the 100kV voltage. For adjusting this voltage, the 110 kV controller modifies the reactive power settings of the wind turbines. In addition this hierarchical control also takes into account all OLTC transformers involved (transmission substation and wind farms transformers). Nevertheless an appropriate coordination of all transformers is not provided. Moreover, a proportional-integral control scheme, considering fit-and-forget parameters, has been used to compensate the voltage deviation without considering any optimal strategy.

Thus knowing the control limits of the whole plant is essential. Those limits are by its capability chart (i.e., PQ chart that contains all the possible operation points). This concept, well-known for a single element, has been extended as is next explained in order to incorporate the effect of several devices. In those cases the analytical method widely used for synchronous machines (each operating constraint define a line in the complex PQ plane) is no longer enough as it is outlined in [Chiodo et al. 1992] and optimization techniques are required. As a result the extended capability charts (considering the OLTC transformers impact [Frias 2008, Losi, et al. 1996, Losi et al. 1998], or for a whole combined cycle power plant [Gargiulo et al. 2002]) have been computed.

Recently, this concept has gained importance with the distributed generation incorporation [Delfino et al. 2010]. Indeed [Abdelkader et al. 2009] provides a graphical method for determining the capability of individual nodes to accommodate wind generation, representing a relevant information for transmission planning and operation. More specifically, [Cuffe et al. 2012a] tries to answer the following questions: Is the distribution generation able to provide effective reactive power support to the TNet? And, thanks to this support can synchronous generation be replaced by distributed generation without compromising the power system stability? In order to answer both questions a

simplified TNet (IEEE-30) has been evaluated. In this analysis the authors evaluate the capability chart at the common coupling bus of a small HNet to the TNet, in the event that wind farms provide a proportional control taking into account time series simulations. The results show how the power system could widely benefit from this support. However, this paper also outlines that some distribution generators provide less reactive power capabilities than the synchronous generator. Hence, for high distributed generation penetration levels, reactive power capabilities may not be enough for guaranteeing the power system stability. This analysis has been complemented with [Cuffe et al. 2014c] where instead of using time-series techniques to provide a proxy to this capability chart, an AC OPF is applied obtaining a more rigorous chart. In this new case a decentralized control scheme in which each generator maximizes its own reactive contribution has been assumed for resembling a decentralized control scheme performance.

In this thesis the extended capability charts of the HNet assuming a centralized control scheme (including OLTC transformers) are used as a classification index. In that way the potentials of each HNet are evaluated and the most suitable control strategy is implemented for each type of network.

2.4. FIELD EXPERIENCES AND INTERNATIONAL PROJECTS

As is outlined in [Kulmala, et al. 2012], although many theoretical works related to voltage control have been done it is not common that those works are translated into real implementations. In this paper a demonstration developed in a distribution network with a hydraulic power plant and the bulk transformer is explained. However, in this case wind resources are not incorporated into the control.

Concerning wind farms, the first demonstration, called SYSERWIND [Azpiri et al. 2013], was carried out within the TWENTIES project, which in fact was the starting point of this thesis. This project was carried out within the seventh framework program of the European Union and involved 26 participants of 11 different European countries (Denmark, France, Belgium, England, Nederland, Germany, Norway, Portugal, Ireland, Italy and finally Spain). Specifically, six different system operators including the Spanish one participated in this project showing its relevant impact [García-González, et al. 2010]. This demonstration proves the capacity of a cluster of wind farms, corresponding to one or several harvesting networks, of providing both frequency and voltage control and hence, being able to contribute to the overall controllability of the system. Specifically, three HNets located in the south of Spain (Hueneja 248 MW, Tajo de la Encantada 122 MW and Arcos de la Frontera 122 MW) were selected as is depicted in Figure 2-4. Focusing on voltage control, a proportional control scheme based on the Spanish grid proposal [REE 2011] was implemented. Nevertheless, whereas in P.O. 7.5. the control requeriments are measured at wind farms meter, typically located at the 20-30kV/132-220kV transformer (20-30kV in the event of different wind farm owners sharing the transformer or 132-220kV if all wind farms belong to the same wind farm owner), the demonstration fostered the control at the bus that connects the HNet to the

TNet, i.e., the common coupling bus. This decision was made for avoiding instabilities among controllers (wind farms and OLTC transformers). In addition, within this demonstration two control centers were involved as is depicted in Figure 2-5. REE in charge of CECRE (Control Center of Renewable Energies), determines the appropriate set-points for fulfilling a certain objective (in the event of the demonstration, minimizing the voltage difference among HNets). Those set-points are sent through the CORE (Iberdrola Network Control Center) to each cluster where the corresponding UCC (unit for communication and control) distributes the set-points among wind farms. Hence, in this test CORE acts as a mere interface. Finally, each wind farm distributes its set-point among the wind turbines. As can be seen in Figure 2-5, the configuration resembles the TNet hierarchical voltage control scheme, being the secondary loop the aim of this thesis. For that purpose the communication infrastructure needed to be updated [Azpiri et al. 2012]:

- New UCC units were included
- New version of the SGIPE wind farm SCADA system
- The transducers were changed for obtaining faster and more precise measurements. In that respect, the required intermediate communication application between traditional regulators and traducers was bypassed

Figure 2-4 HNets tested in the demonstration. Source [Azpiri et al. 2013]

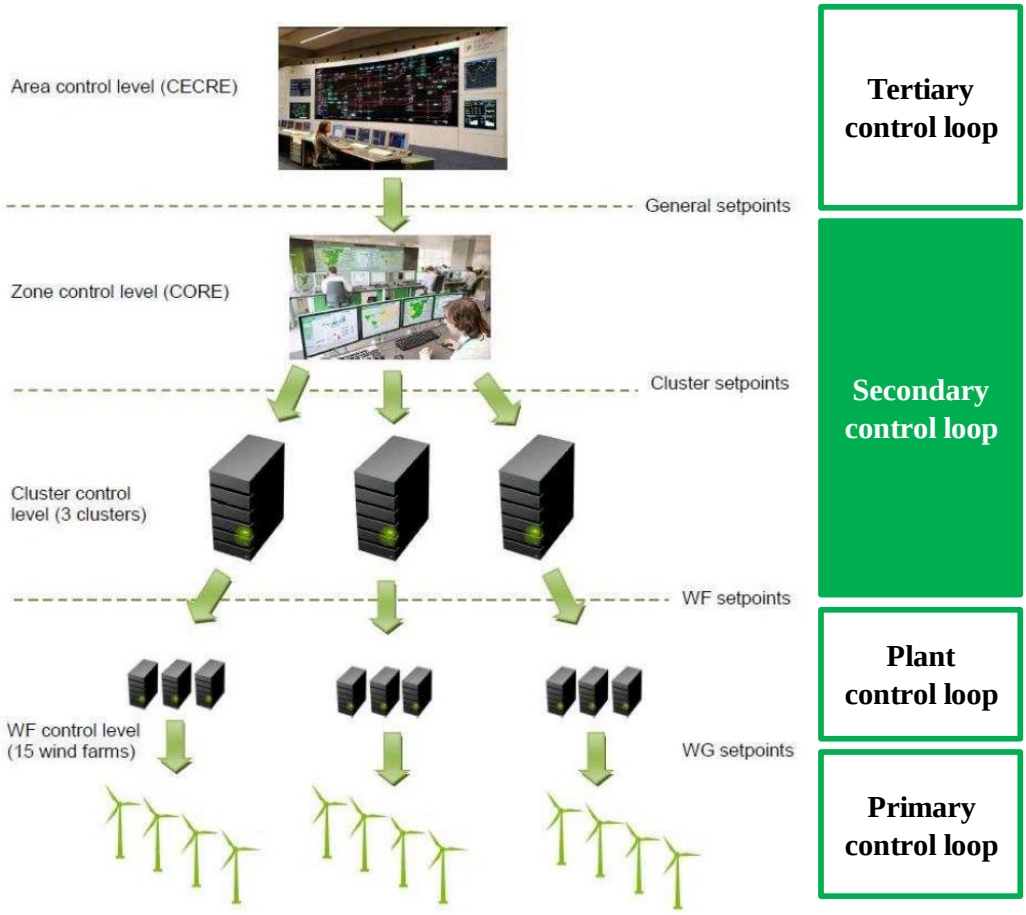

Figure 2-5 Communication infrastructure. Source [Azpiri et al. 2013]

Firstly, some tests were carried out in just one cluster [Azpiri et al. 2013]. At first, the control presented an oscillatory performance, describing among other aspects the importance of an adequate tuning of the control parameters. Those oscillations were eliminated acting in two different fronts. On one hand, increasing the control cycle; as a result a slower control was obtained. On the other hand, K (the slope of the proportional control) was reduced. Moreover, the importance of coordinating this control with the existing OLTC transformers was seen. In fact, this thesis emerges from the experience acquired thanks to the participation in this project.

Once that the drawbacks were solved a wide area voltage control test was done, which results are provided in Figure 2-6. In this figure the set-point are depicted with dotted lines whereas the measurement are depicted with continuous lines. As can be seen the performance obtained does not always correspond to the desired one. This fact can clearly be appreciated during the period 0.5-1h for Arcos where the measurement highly differs from the set-point. The aim of this thesis is to improve the voltage control scheme implemented in the TWENTIES demonstration.

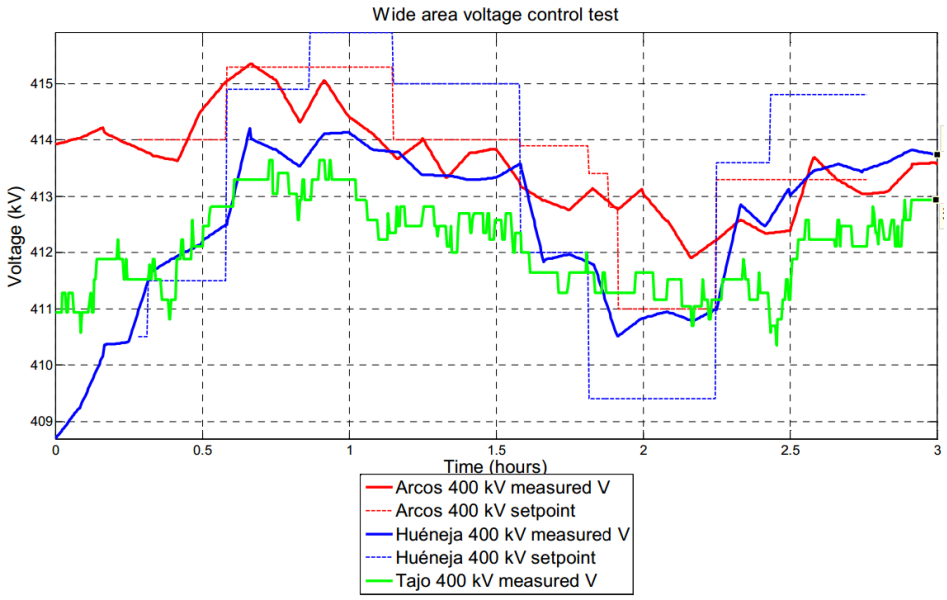

Figure 2-6 Performance of the demonstration. Source [Azpiri et al. 2013]

The demonstration has not been the only one performed in Spain. Acciona Wind energy has performed its own test [Arlaban, et al. 2012] in order to demonstrate that their wind farms are able to fulfill the requirements imposed by P.O. 7.5. This test has been conducted considering two different technologies showing that many installed wind farms could not provide this service without installing reactive compensation devices.

In addition other relevant international projects with similar characteristics should be outlined: ReServices, E-Highway2050, GridTech, Optimate [FP7, 2015]. All of them evaluated how the system can be operated in a more flexible way. Each of this projects analyze this problem from different perspectives: design of the operational requirements considering the participation of wind farms in the ancillary services, transmission network planning tackling the increasing level of wind penetration, design of pan-Europe markets facilitating wind integration, increasing the interchanges etc… All these projects show that the flexibility of the system is a relevant issue that must be studied from all the possible perspectives. This thesis focuses on a very specific one, what can be done from the voltage control perspective?

2.5. SUMMARY AND GAPS TO BE ADDRESSED

As the wide amount of recent references suggests wind farms reactive power/voltage control is a “hot topic”. Most of these papers focus on a specific control scheme which is implemented in a single simplified network, and few of them, focus on HNets as will be later detailed. Hence, two important gaps appear. Firstly, a deep analysis of HNets is demanded. Secondly, how the control schemes and their strategies are affected by the network characteristics. Ideally, a pro-active voltage control, in which the whole HNet resemble a conventional plant being able to be integrated in an existing TNet hierarchical voltage control, is the desired strategy. Nonetheless not all HNets offer a relevant impact

on the TNet which justifies the increase in control complexity. Consequently the following objectives, defined in the previous chapter, are addressed within this thesis:

- HNets capabilities should be evaluated assessing their potential and limitations. Moreover, other alternatives in the event that the HNet is not suitable for active voltage control must be found. Subsequently, each HNet can be classified in accordance with its suitable strategy.
- For each alternative, the best way of implementing it should be studied. Anticipating the results, this thesis, as will be presented in the next chapter, has defined three different types of HNets selecting a different strategy for each one:
    - **Type A:** Power losses minimization strategy, suitable for networks with significant power losses and with a restricted PQ chart
    - **Type B:** HNet minimum impact on TNet strategy, suitable for networks with not significant power losses and with a restricted PQ chart.
    - **Type C:** Pro-active voltage control strategy, suitable for networks with not significant power losses and with a broad PQ chart.

  For each type, a different technique has been employed. Data-mining and control rules for type A, multi-period OPF for type B and quadratic programming for type C.
- In addition a last essential objective is the coordination between all controllers involved, OLTC transformers and wind farms for each strategy selected.

For tackling the last objective two different ambits must be addressed, steady-state and dynamic coordination. This combined analysis is not common treatment in the literature. The steady-state coordination depends on the HNet control strategy selected depending on its type (A, B or C) as has been already outlined. On the other hand, dynamic coordination has been evaluated for type B and C considering for each one its associated strategy. For this second ambit of the coordination several alternatives as shown in the state-of-the-art have been suggested, e.g., multi-agents and MPC approaches. However, both alternatives present important drawbacks. The first one relies on two-way communication for which the infrastructure is not yet available in Spanish HNets and may be not desired between competitive assets. Concerning the MPC approach, the prediction horizon is dependent on parameters such as OLTC transformer time delay which is not adequately evaluated. In addition, the sensitivity matrixes used in the evaluation of the control action policy for a planning horizon may differ from the real values. Differences that increase when the time horizon also increases, especially when discrete elements such as OLTC transformers are considered. Consequently, another important gap related with the dynamic coordination has been identified. This thesis will contribute with an alternative and complementary approach where fit-and-forget dynamic settings (i.e., settings that affect how rapidly the central controller may respond) are determined offline. To clearly show the overall picture and framing the thesis contributions Figure 2-7 is incorporated, which as can be seen is equal to Figure 2-1 but outlining in a different colour where the thesis contributes for each type of network.

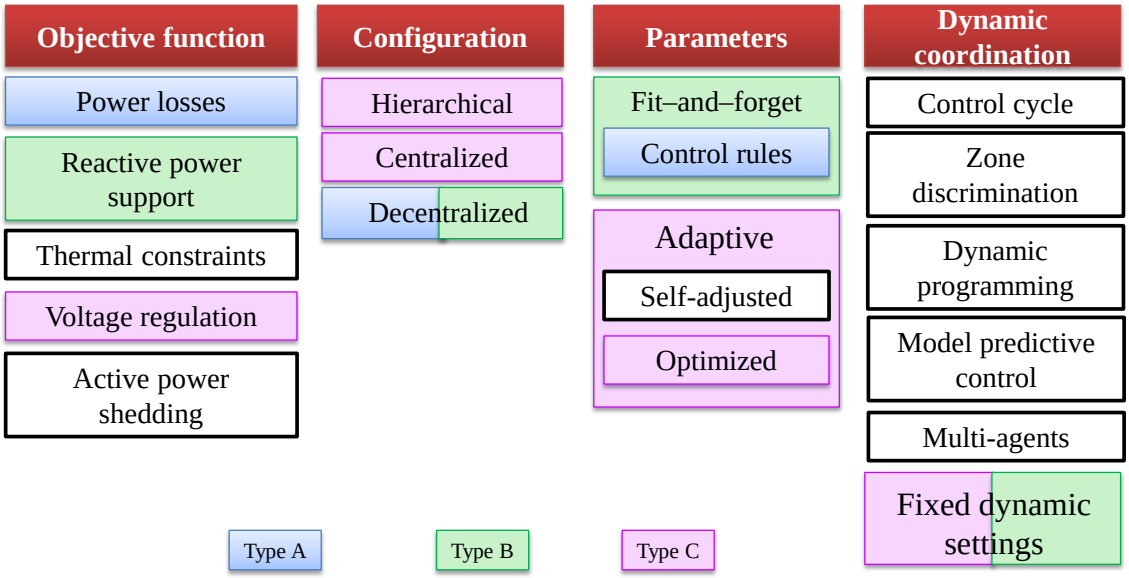

Figure 2-7 Strategies evaluated throughout the thesis

Finally, for contextualizing the thesis within the state-of-the-art Table 2-1 gathers and classifies the most relevant references shading the principal gaps previously described. In addition the last row of this table corresponds to this thesis where the type of network is also outlined. As can be seen DNets are the common platform of wind farms all around the world and only few works focus on HNets, all of them completed in Ireland [Keane et al. 2012, Cuffe et al. 2012b] or Spain [Arlaban, et al. 2012, TWENTIES 2013] the latter being the origin of this thesis. Moreover among these works only [Cuffe et al. 2014a] evaluates the possibility of enhanced control schemes in which autonomous (fit-and-forget parameters) and smart (adaptive parameter) strategies are compared. However, that paper only focuses on the steady-state perspective and avoids the practical issues related with the implementation, such as the discrete nature of communication required, especially for the smart strategy, and which is more important, for avoiding possible undesired interactions among controllers.

Thanks to these wind generation dedicated networks (HNets), the impact that wind farms could have on TNet could be very significant, representing an opportunity for improving TNet operation. For measuring this maximum impact the capability chart has been seen as an adequate index [Cuffe et al. 2012b, Cuffe et al. 2014b]. This index, essential for an appropriate classification and which has been improved incorporating OLTC transformers, is used within this thesis for evaluating the potential of different HNets considering also different control strategies (power loss minimization, HNet minimum impact on TNet and a pro-active voltage control).

As can be seen in Table 2-1 [Alnaser et al. 2015, Ochoa et al. 2011, Cuffe et al. 2014a, Di Fazio et al. 2013, Kulmala et al. 2014, Keane et al. 2012, Wei Zhang et al. 2014] compare different control strategies. Nonetheless, none of them compare the results for different HNets selecting the appropriate strategy for each one, this gap is fulfilled within this thesis.

Moreover, it can be noted that there are few references that deal with cascade OLTC transformers coordination in this context, and none of them, related to HNets. For addressing their coordination different online approaches have been suggested: rolling algorithm-MPC [Erlich, et al. 2011], or multi-agent [Yorino et al. 2014] or a combination of both approaches as is done by [Moradzadeh et al. 2013]. However these methods have been discounted because of their drawbacks already mentioned. An offline method based on the selection of the sample time is addressed by [Alnaser et al. 2015]. However the sample time may be imposed by communication requirements. Hence, this thesis proposes an alternative method based on tuning dynamic settings (i.e., those parameters that affect the temporal evolution). The importance of those parameters is mentioned in [Ranamuka et al. 2014]. However, its optimal determination is not addressed constituting an important contribution of this thesis.

Finally, it has been seen that many different techniques have been used for evaluating the steady-state coordination. In this thesis most of them are studied: OPF, quadratic programming, multi-period OPF, and data mining techniques for obtaining control rules. Concerning the last one, [Kulmala et al. 2014] state the adequacy of certain control rules in the event of radial network in which few control actions are available. This thesis goes in depth in this sense providing a methodology based on data mining techniques.

Table 2-1. References summary

	Configuration			*Parameters*			*Objective*							*Network*			*Methodology*										Dynamic coordination				
	Hierarchical (nº loops)	Centralized	Decentralized	Adaptative	fit-and-forget	fit-and forget (Optimal)	Power losses (-)	Thermal constraints (-)	Reactive power support (-) or (+/-)	Active power sheddings (-)	Voltage regulation	Tap changes (-)	OLTC transformers cascade coordination	implemented (Field experience)	Transmission network	Distributio/Smart grids	Harvesting network	Quadratic programming	Fuzzy lineal/Gradient programming	OPF	OPF multi-period	Risk based OPF	Control rules /data mining	Meta-heuristics algorithm	Time domain /series simulation	Networks comparison	Economic impact	Controls comparison	Dynamic programming	Rolling algorithm MPC	Multi- agents	Sample time	Fixed dynamic settings
[Vialas et al. 1988]	x(3)			x					x		x			x	x			x							x							
[de la Fuente 1997]	x(4)			x					x		x				x			x							x							
[Alonso 2001]	x(3)			x			x		x						x			x							x							
[Corsi et al. 2004]	x(3)				x						x			x	x										x							
[Ochoa et al. 2011b]		x	x	x		x			x							x					x						x					
[Erlich et al. 2011]		x		x			x					x	x			x								x	x				x			
[Keane et al. 2012]			x		x		x		x		x			x		x	x								x		x					
[Arlaban et al. 2012]			x		x						x			x			x								x							
[Sansawatt et al. 2012]			x	x				x		x	x					x									x						x	
[Di Fazio et al. 2013]			x	x							x					x									x		x					
[Loia et al. 2013]		x	x	x			x				x					x			x (F)											x		
[Dou et al. 2013]	x(3)			x			x (*)									x								x	x							
[Valverde et al. 2013]		x		x							x	x				x		x							x					x		
[Young-Jin Kim et al. 2013]		x		x			x					x				x									x				x			
[Moradzadeh et al. 2013]		x	x	x							x	x	x		x	x									x					x	x	
[Twenties project 2013]	x(4)				x						x			x			x									x	x					
[Cuffe et al. 2014 a.]			x	x		x			x							x					x							x				
[Cuffe et al. 2014 b.]			x	x					x								x			x												
[Kulmala et al. 2014]		x	x	x		x	x			x						x		x					x					x				
[Capitanescu et al. 2014]		x		x			x			x		x				x				x												
[Ranamuka et al. 2014]	x(2)				x						x	x				x									x							x
[Calderaro et al. 2014]			x	x			x		x							x								x								
[Kaempf E. et al 2014]		x		x							x				x	x								x								
[Zhang et al. 2014]			x	x			x				x					x			x(G)						x					x	x	
[Nakawiro et al. 2014]		x		x							x	x				x								x	x							
[Yorino et al. 2014]	x(2)			x							x	x	x			x		x	x(G)						x					x		
[Alnaser et al. 2015]		x		x				x		x	x	x	x			x						x			x			x			x	
THESIS	x (3) (C)	x (A)	x (B,C)	x (C)		x (A,B)	x (A)		x (B,C)		x (C)	x (B,C)	x (A,B,C)	x			x (A,B,C)	x (C)		x	x (B)		x (A)	x (B,C)	x (B,C)	x	x (A)	x					x

(*) Cost objective =cost function + pollutions emissions + power losses

(F) Fuzzy lineal / (G) Gradient programming

Once that the main thesis contributions have been clarified and framed within the state of the art, the document is structured around them as is next explained.

Chapter 3

- HNet potential has been classified in accordance with different indexes: capability chart, power losses and voltage margins. Identifying also the role of OLTC transformers and how those indexes improve when those control devices are incorporated. Categorization of HNets is done proposing the most suitable strategy for each one, taking advantage of wind farms capabilities.

After classifying HNets in this chapter, the next three ones focus on a specific type of HNet and the proposed voltage/reactive control strategy.

Chapter 4

- In the event of power loss objective function a control rule scheme has been proposed inferring useful knowledge for a DSO. Moreover, the control scheme proposed minimizes the needs of communication channels. This analysis has been carried out for a HNet of more complexity than the ones studied in the state-of-the-art

Chapter 5 and Chapter 6

- The dynamic coordination of all devices involved in the HNet is performed offline by tuning relevant dynamic settings in contrast to the online methods suggested in the state-of-the-art. This dynamic coordination highly depends on the control scheme evaluated. In that sense in Chapter 5 a detailed analysis of different control schemes considering fit-and-forget parameters is provided. On the contrary in Chapter 6 a central controller in which each sample time k the parameters are adapted is considered. Moreover, this central controller is integrated in a hierarchical control scheme in order to resemble the whole HNet to a conventional plant.
- In all control schemes cascade OLTC transformers are considered increasing the importance of an appropriate tuning of dynamic parameters.

CHAPTER 3

WIND ENERGY HARVESTING NETWORKS CLASSIFICATION BASED ON THEIR POTENTIAL

Before proposing any control scheme it is essential to know the possible limits of the whole wind energy HNet by means of reactive power support, voltage margins and power losses. In addition, this thesis not only evaluates the reactive control provision impact on the HNet itself, it also evaluates if it is worth from the TNet perspective. Thus, the benefits that voltage control provision represent for both, wind farm owners and TSOs is described in subsection 3.1. Subsequently, in subsection 3.2, a steady-state detailed analysis of two HNets is carried out showing the potential of those networks. Finally in subsection 3.3 those results are extrapolated to all HNets, and which is more relevant, a classification that will define the appropriate control strategy that should be applied in accordance with the features of each HNet.

3.1. VOLTAGE CONTROL PROVISION BENEFITS

In some countries with significant wind penetration levels, wind farms maintain a fixed power factor, which should be not far away from unity (e.g., Spain). Hence, they do not use all its reactive potential. Thus, one could ask why is it necessary to increase the wind energy reactive requirements if the system is already able to support high wind penetration. First of all, it is true that this strategy may be sufficient for countries with a

highly meshed TNet considering the current wind penetration levels. However, keeping a fixed power factor may be inadmissible for countries like Brazil, whose TNet is 800% less meshed than the Spanish one. This fact is owing to the local nature of the reactive control, which cannot be transported through long distances. In addition, for achieving these penetration levels an inefficient operation of the system may be carried out such as opening lines or allocating more capacitors banks (when wind farms already have reactive power capabilities). These actions can be drastically reduced in the event of considering wind farms' reactive power capabilities, representing a clear benefit for the TSO, and, justifying the increasing grid code requirements. Moreover, the system performance could be eroded if the wind penetration continues increasing and hence could be limited. Thus, it is clear that the wind farm owners could directly benefit from the voltage control provision moving away this limitation.

In Appendix B the reactive power-voltage relationship (QV) is analyzed by means of a simplified model, outlining the two possible reasons (from the voltage perspective) for hosting capacity limitation: over-voltage (the main barrier for wind penetration in distribution networks owing to the low reactance-resistance X/R ratios) or voltages under admissible values. Nevertheless, the local hosting capacity may differ significantly from the area capacity in poor meshed systems and hence, its conclusions cannot be scalable. This idea was expored considering the network depicted in Figure 3-1. In this case two areas (exporting and importing) can be distinguished. Consequently, the possible wind penetration limitations highly depend on where the wind farms are connected and where the synchronous generators are displaced as can be seen in Table 3-1.

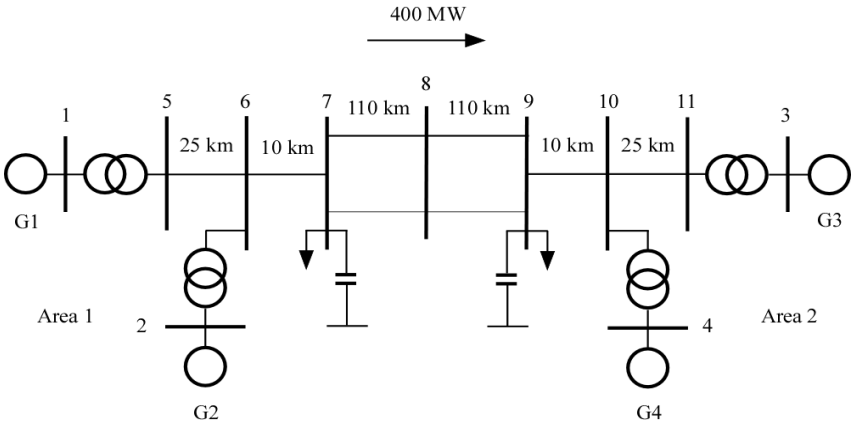

Figure 3-1 Power system with two areas. Source [Kundur 1994]

If wind generation is increased in bus 2 and synchronous generation is reduced in the other buses, the limitation (in the event that wind generation maintains a unity power factor) is reached at (130MW[6]). If wind generation provides reactive power support this limitation moves until (390MW). Both limitations (without and with reactive power support) move significantly when wind generation is increased in bus 4. In other words,

[6] Incremental values with respect the initial operational scenarios which could be found in [Sáiz-Marín et al.2014]

if the power transfer between areas decreases the limitation appears later. Finally, if these generator are jointly increased the limitation (740MW) will appear later than if they are increased separately (130 MW+550 MW). However, the contrary effect will be seen if the generation increment is only done in the export area.

Table 3-1. Hosting capacity increase by means of voltage control provision

Reduce	1,3,4	1,2,3	1&3
Increase	2	4	2&4
Unity power factor	130	550	740
Reactive power support	390	1450	1900
Increment	**260**	**600**	**1160**

Additionally, angle stability is enhanced thanks to an active voltage control. This issue was detailed analyzed in [Rouco et al. 2013] considering the same network. In this case the clearing time in the event of a fault in bus 8 were computed in two different situations: all generators are synchronous and two of them correspond to wind farms which fulfill all requirements specified in P.O. 12.2 [REE, 2010a]. In this last case the clearing time decreases. This decrease could be compensated by increasing reactive power support (adding FACTs devices or increasing wind farms requirements).

Moreover, recalling Chapter 2 wind farms' reactive power capabilities can be employed with other purposes such as: power loss minimization, curtailent minimization or avoiding thermal constraints.

3.2. DETAILED CHARACTERIZATION OF HNETS POTENTIAL

The potential that each HNet presents has been measured as follows. On one hand, the impact of the reactive power control on the HNet itself is characterised by means of the value of HNet losses. On the other hand, the impact on TNet is measured by the PQ capability chart and the voltage value at HNet common coupling bus. Within this section, those magnitudes are evaluated in detail for two HNets. Afterward, the next section will extend the results to all HNets presented in Table 3-2.

As can be derived from this table the HNets may differ significantly allocating few wind farms as HNet8 or a great number of them as HNet3 and HNet5. Moreover, in some cases other renewable plants could also be allocated. Those plants (wind farms and solar) could belong to several owners, the maximum number being 5, in the set of HNets examples analyzed within this thesis. Concerning the total amount of active power, HNet1 is the one with a higher output (516 MW) being also the network with more kilometres of lines (302.85 km). Regarding this last aspect, a great difference among HNet is seen being HNet2 and HNet3 the two networks with fewer kilometres of lines (39 and 41 km respectively). The next issue classified within Table 3-2 are the voltage levels, showing a wide range of alternatives. Finally, the short-circuit power at the HNet

common coupling bus is considered. This value is very significant because approximately gives the voltage deviation that can be achieved for a certain amount of reactive power absorbed or injected $\Delta V \sim \frac{\Delta Q}{S_{cc}}$. Consequently, two networks with a similar infrastructure and line length like HNet2 and HNet3 could have very different impact on the TNet regarding voltage.

Table 3-2. HNet characteristics summarize

HNet	Wind farms	Other plants	Owners	Total power [MW]	km of lines	Voltages [kV]	Mean SCC [MVA]
1	13	NO	4	516	302.85	0.69/20/132/400	8033
2	11	Solar	4	473.3	39	0.69/30/220/400	5065
3	15	NO	5	330	41	0.69/20-66/220/400	10686
4	9	NO	3	316	46.63	0.69/30/220	5842
5	15	NO	?	464	179.38	0.69/30/132/400	13738
6	13	NO	4	376	73.79	0.69/20/132/400	6824
7	11	NO	?	322.25	108	0.69/20/132/400	10179
8	3	NO	?	88	135.9	0.69/20/132	7749

Owing to the bureaucracy[7], HNet1 has dramatically more line distance than the rest of HNets, see Table 3-2. Consequently, the consumption of reactive power on this HNet is huge compared with the reactive capability of wind farms. Thus, it cannot be expected that the wind farms located in this network can contribute to the transmission controllability. In contrast, their reactive resources can be used in a smarter way reducing power losses.

This section has been structured as follows. Firstly, in subsection 3.2.1 the different control schemes analyzed and the PQ chart computation are presented outlining the modifications that should be introduced in the OPF model for their implementation. Subsequently, the characteristics of the two test networks (HNet1 and HNet2 from Table 3-2) are summarized in subsection 3.2.2. Then, the necessity of taking into account OLTC transformers in the optimization is discussed for the PQ chart and power loss minimization scheme in subsections 3.2.3 and 3.2.4 respectively. Next, non-optimal control schemes representative for the current and near future situation are evaluated and compared in subsection 3.2.5 with the previous ones.

3.2.1. PQ CHART AND CONTROL SCHEMES

For evaluating the maximum reactive power capabilities of the whole HNet, its PQ chart has been computed considering an optimal power flow for which the objective function is reactive power maximization provided by wind farms (generation and consumption) at the common coupling bus, i.e., the bus that connects the HNet to the

[7] Spain is organized in different autonomous communities, each one with their own renewable plan, in which the maximum wind power installed is fixed. Hence, sometimes a wind farm is connected to a further substation because the maximum installed capacity has been already reached in its autonomous community so it must be connected to another one.

TNet. Additionally, the minimum power losses are computed constituting a desired control scheme.

Others schemes representative of current and future alternatives should be also analyzed and compared with the maximum capabilities. One of them, currently extended in different countries, is maintaining a constant power factor; for instance in Spain [REE 2010b], the wind farms maintain a power factor close to unity, and the OLTC transformers perform all the voltage regulation functions within the HNet. This strategy, because it is used as a reference for evaluating how enhanced control schemes may offer enhanced performance, is named *reference control.* Under this scheme the wind farms do not compensate the HNet reactive power consumption. Hence, the reactive power consumed by the HNet lines should be provided through the transmission grid. However, several jurisdictions [REE 2011, Energinet 2010, Eirgrid et al. 2013] have considered the possibility of enabling voltage control functionality for wind farms (as is outlined Chapter 2), so that they inject or consume reactive power to control their voltage to a defined set-point. Thus, a *proportional control*, which means that a gain relates the reactive power injected/consumed by wind farms and the voltage deviation, is also studied. In this first approach of the proportional control the voltage deviation is considered at the common coupling HNet bus which may not coincide to what is proposed in some grid codes. Later, in Chapter 5 this last scheme is studied deeply from the steady-state and dynamic perspective analyzing the impact of where the voltage is measured (directly where the wind farm is located or at a remote bus).

In all cases explained, relevant magnitudes (reactive power, power losses and voltage margins) have been evaluated for different active power scenarios, ranging from no wind load to full wind production.

In all control schemes and PQ chart calculations an optimal power flow (OPF) is applied guaranteeing that all voltages are within limits. Thus, in addition to the power flow equality constraints, inequality constraints have been added which force all buses to be operated within their limits ($0.95 \leq V \leq 1.05$) and impose wind farms reactive power capability ($Q_{WF}^{min} \leq Q_{WF} \leq Q_{WF}^{max}$) specified at the grid code (using in this thesis the Spanish grid code proposal P.O. 7.5 which main requirements are indicated in Appendix A). In addition, for the *reference control* and the *proportional control* schemes additional constraints (one for each wind farm) are necessary in order to impose the required reactive power. In Figure 3-2 the flow chart of the different control schemes and the PQ chart calculation is presented, outlining the objective functions and the additional constraints imposed. Concerning PQ chart calculation, the objective function is doubled due to the requirement that both reactive power components (generation and consumption) should be maximized. In this thesis to avoid misunderstanding the reactive power generation is associated to reactive power maximization whereas the reactive power consumption is associated to reactive power minimization. First, the control variables only correspond to the reactive power delivered by wind farms. Then, the OLTC transformers' tap positions are incorporated. Both cases will be compared outlining the key role that OLTC transformers will play.

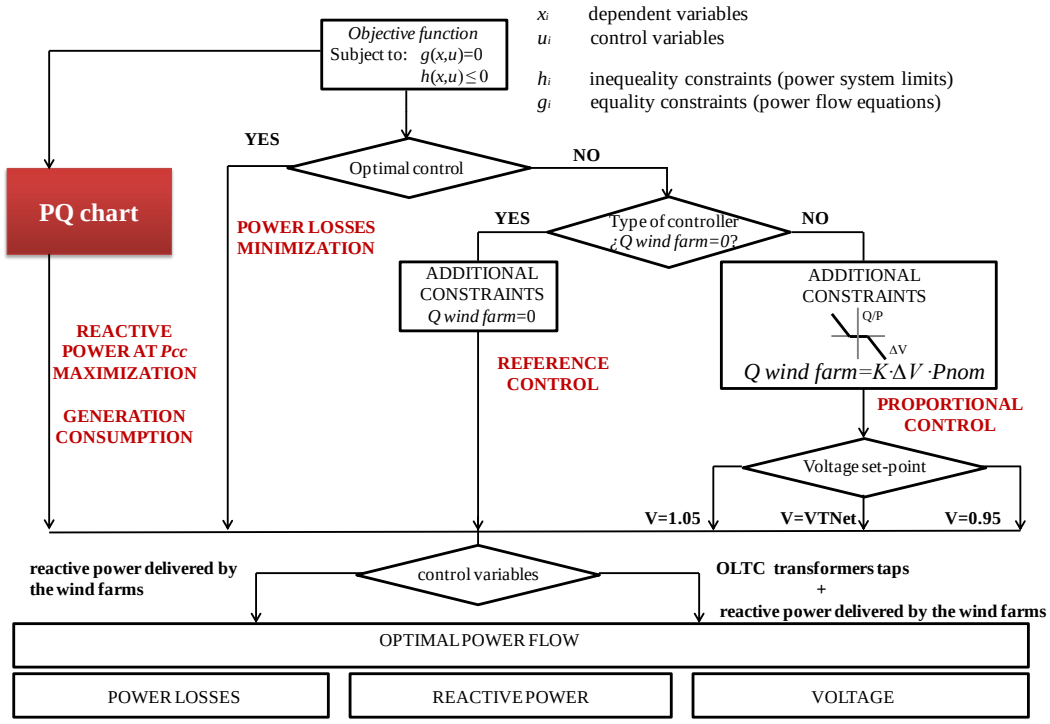

Figure 3-2 Flow-chart implementation of the different controls

The wind scenarios used in this study have been obtained considering that all wind farms on the HNet are close to each other (the geographical area where they are installed is small). Given this proximity, each wind farm is operated at the same active power scenario or in other words has the same active power production in p.u. In this section eleven scenarios (from 0 p.u. to 1p.u. taking into account steps of 0.1 p.u.) have been considered. Nevertheless, a discussion of the impact of a more realistic approach in which wind farms provide different active power outputs is also presented. These simplified scenarios are only valid for computing the limits. More sophisticated scenarios considering also their occurrence probability will be also employed throughout the thesis as is explained in Appendix E.

3.2.2. TEST NETWORKS

For the detailed analysis the first two HNets of Table 3-2 are deeply evaluated. These two networks, whose data are presented in Appendix A, are representative of most usual configurations. The first one, cannot provide active voltage control in a similar way than any conventional plant. Contrarily, the second network, which has significantly less lines kilometres may resemble its performance.

In order to compare both networks, results will be presented in percentage or in per unit. The active power is divided by the maximum active power which corresponds to the total installed power and the reactive power is divided by the potential maximum reactive power. The potential maximum reactive power has been evaluated neglecting the grid. Hence, the theoretical PQ chart at the HNet common coupling bus is equal to the sum of all wind farms PQ charts. This theoretical PQ chart will be also provided as a

reference. Power losses are presented in percentage of total active power delivered to TNet.

3.2.3. PQ CHART

In Figure 3-3 the maximum PQ chart, defined by minimum (reactive power consumption) and maximum (reactive power generation) limits, and voltage margin that these capabilities represent are presented for HNet1 (a) and HNet2 (b). All these magnitudes, active power, reactive power and voltage are computed at the HNet common coupling bus and are the result of the optimization. Evaluating the cases in which transformers' taps are fixed, it can be seen how the maximum PQ chart in both HNets are significantly lower than the theoretical one (presented in black). This fact is caused by the voltage inequality constraints imposed which force all buses to be operated within their limits ($0.95 \leq V \leq 1.05$). Figure 3-4 visualizes where these limitations came from for HNet2 (wind farms connection points are labelled with WF) considering two different scenarios of active power level (25% and 75%). In this case the buses with voltages higher than 1.0485 p.u are outlined over the one-line diagram (see Appendix A). In the event of high active power level, all these buses correspond to wind farm connection buses. Nevertheless, for lower active power level some of them are now located in the meshed part of the network.

Focusing again in Figure 3-3, it can be seen that because of the inductive performance of the HNet, the consumption capability is higher than the generation capability increasing this difference in high power scenarios. In the event of adding transformers' taps to the optimal control, the maximum PQ chart increases in both HNets, being more significant for the consumption part of the curve. Thus, from this figure it can be surmised that the OLTC transformers are essential for maximizing the reactive capability of the whole HNet. Despite their consideration, in HNets with a significant infrastructure the wind farms are not able to generate enough reactive power into the TNet for maintaining or increasing the voltage in high power scenarios.

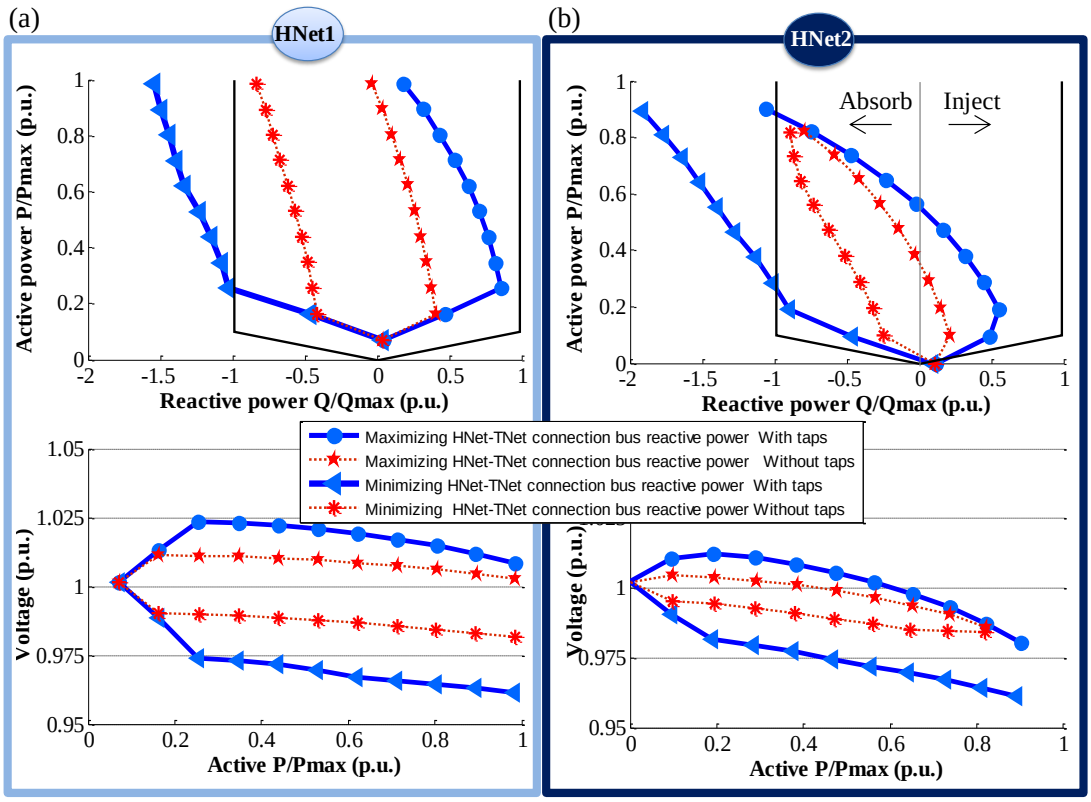

Figure 3-3 OLTC transformers impact on the PQ chart in HNet1 (a) and in HNet2 (b)

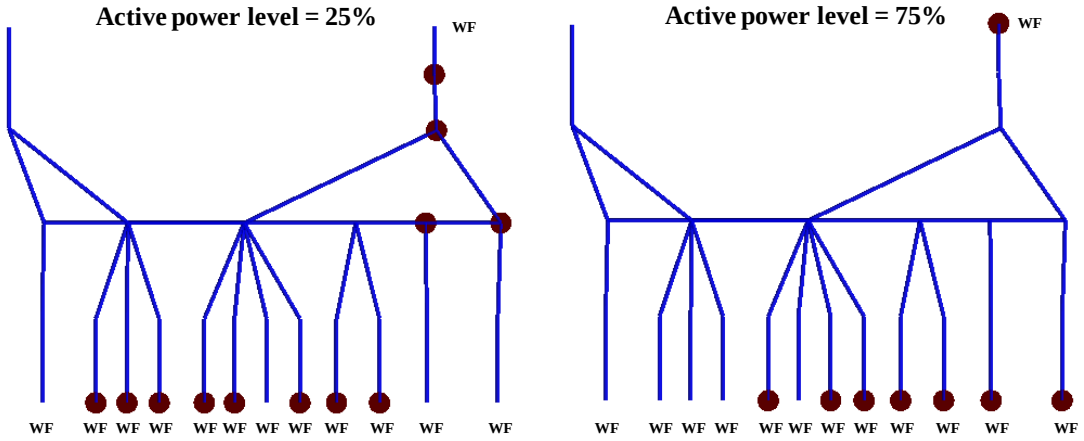

Figure 3-4 Voltage limitations

In order to discuss the impact of considering the same active power production in p.u. for all wind farms Figure 3-5 is shown. In this complementary analysis eleven global active power scenarios (from 0 p.u. to 1p.u .taking into account steps of 0.1 p.u.) have been considered. Within each global scenario, different levels of spread (0, 0.2, 0.4 and 0.6) among wind turbines have been assumed (e.g., if the global active level is 0.5 and the level of spread considered is 0.2 the wind turbines produce between 0.3 and 0.7 p.u.).

As can be surmised from this figure, the increment of the spread between the wind farms active power production in p.u. slightly reduces the PQ chart. At this stage of the

thesis the focus is on determining the maximum impact on the TNet (by measuring the PQ chart and the voltage at the HNet common coupling bus) and the HNet (by measuring power losses). Thus, same active power production in p.u. is considered throughout this chapter. Later, in Chapter 5, real active power data of two wind farms are analyzed evaluating the spread among them. Data that will be also used for develop more realistic scenarios as has been already mentioned.

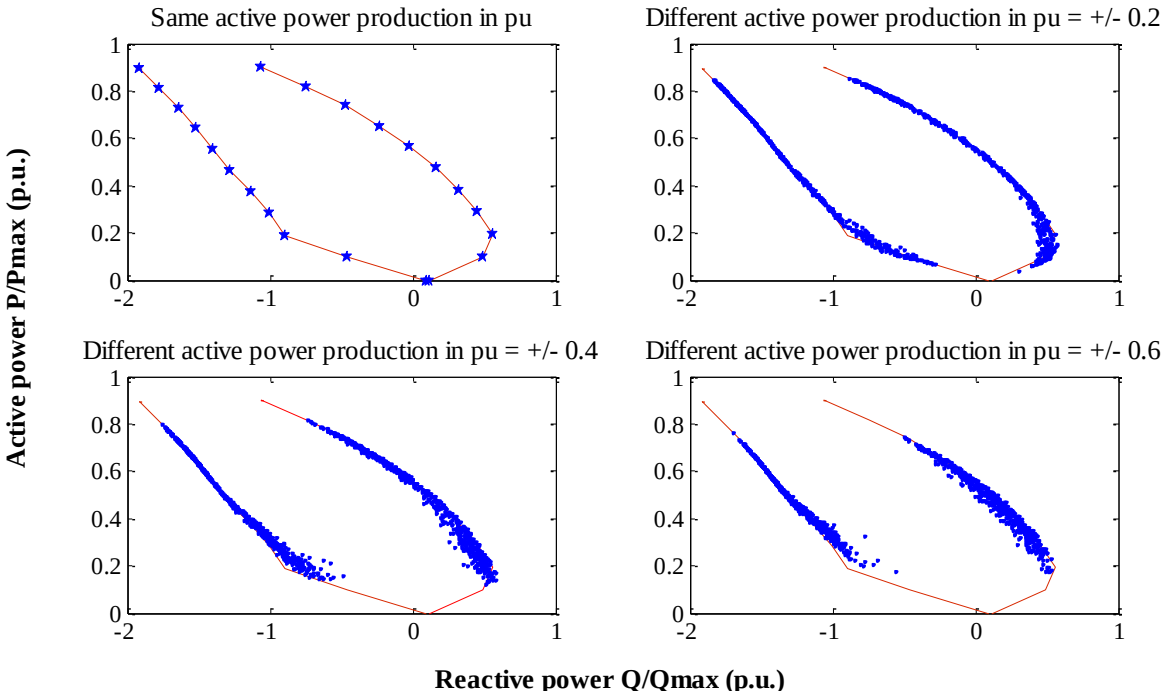

Figure 3-5 Impact of considering different wind farms active power productions. PQ chart in the event of taking into account transformers' taps as control variable

3.2.4. MINIMIZING POWER LOSSES

In the event of implementing an optimal voltage control for minimizing HNet power losses Figure 3-6 presents the reactive power capabilities and power losses for HNet1 (a) and HNet2 (b). In addition, the generation component of the PQ chart maintaining fixed the transformers' taps is depicted as a reference. The main goal of any voltage control scheme is increasing the controllability of both, HNet and TNet. The power losses minimization typically is an additional objective which may be the main one in the event of a HNet with a significant common infrastructure as HNet2. This network is not able to compensate its own consumption when active power level is higher than 0.5 as was seen in Figure 3-3.

Comparing both subplots (a and b) of Figure 3-6 it can be appreciated that the percentage that power losses represent depends a lot on the network evaluated (for the highest active scenario, 2% in HNet1 and 10% in HNet2). Thus, although in both cases power losses are reduced (next section for details), HNet2 will be more suitable for implementing an optimal voltage control whose objective function is minimizing power losses. A strategy not incentivized with the current regulation.

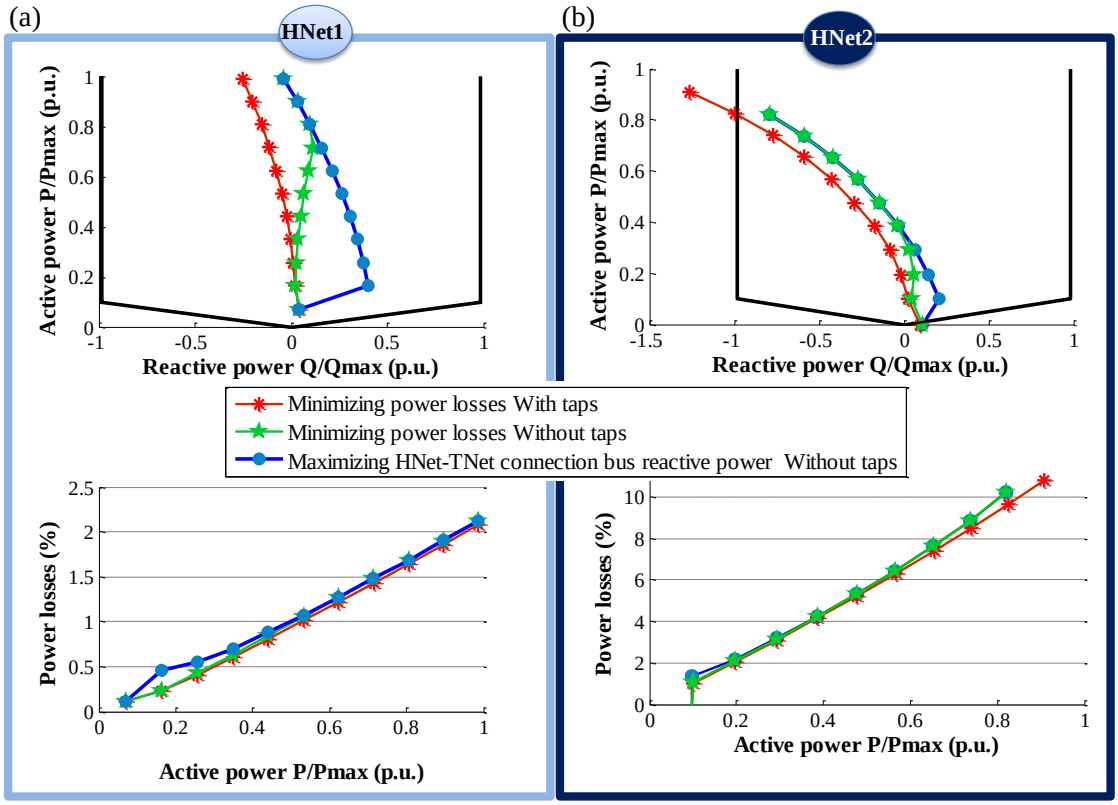

Figure 3-6 OLTC transformers impact on the optimal control (minimizing power losses) in HNet1 (a) and in HNet2 (b)

Secondly, if the transformers' taps are not control variables, in order to reduce power losses wind farms should generate reactive power. The problem is that reactive generation is very limited in that case strangling the power minimization potential. This fact can be seen in HNet1 when active power is higher than 0.7 p.u. whereas in HNet2 this limitation is achieved much earlier. Thus, it is essential to introduce transformers' taps to the optimization to remove this limitation. In addition, in HNet2 if the OLTC transformers are not considered in the optimization, power flow is not feasible for active power scenarios higher than 90%.

From both cases it can be noted that coordinated wind farms-OLTC transformers control is essential for developing an optimal voltage control scheme. Thus, from this point of the thesis on, all the analysis will consider transformers' taps as a control variable.

3.2.5. HNET LIMITS AND POTENTIAL AND COMPARION WITH CURRENT AND PROPOSED SCHEMES

Figure 3-7 shows the limits and potential for HNet1 (a) and HNet2 (b) presenting both the PQ chart and power losses minimization control scheme. For both HNets three subplots (reactive power, power losses and voltage) have been provided. Focusing on the third one it can be seen that a power losses minimization scheme maintains a voltage profile close to its nominal value. Nonetheless, in HNet2 voltage decreases until 0.98 owing to the significant common infrastructure. The maximum voltage variation is

obtained for the maximum PQ chart included in this figure (see first subplot). In the event of HNet1 voltage can be increased more than 2% (depending on the active power scenario) and decreased almost 4% when maximum active power is delivered. In the event of HNet2 the ability of reducing voltage is maintained. However, for scenarios with an active power level higher than 0.5 the ability of increasing voltage is lost. Hence, this network is not recommended for performing a pro-active voltage control. Concerning the second subplot, the minimum power losses are provided by the optimal control scheme. These losses are compared with the ones obtained with the PQ chart, which are quite similar for the generation component, especially for high loaded scenarios. This fact is owing to the reactive power injection required for compensating as much as possible the inductive performance of the network. Contrarily, power losses differ significantly for the consumption component. In fact for HNet2 a difference higher than 2% of the total active power delivered is seen.

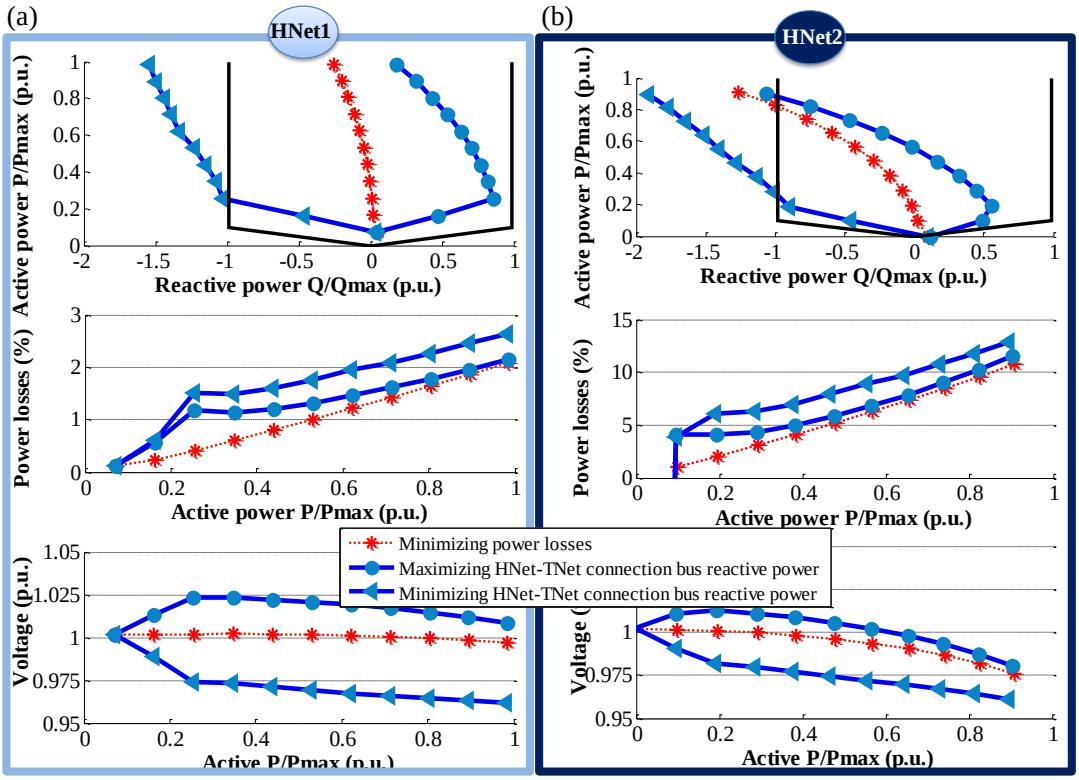

Figure 3-7 Optimal voltage control comparison for HNet1 (a) and for HNet2 (b)

In Figure 3-8 power losses in absolute value (MW) are presented for both networks. As can be seen, power losses are significantly higher for HNet2, making this control very suitable for this network (which is meshed).

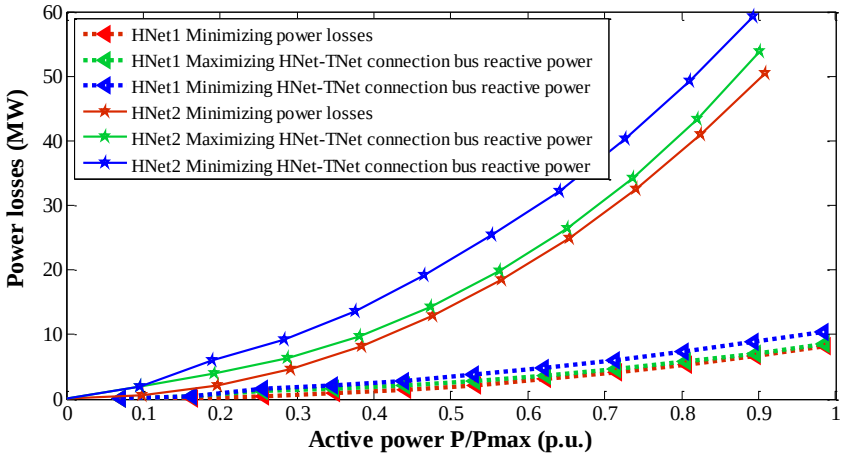

Figure 3-8 Absolute value of power losses for HNet1 and HNet2

Reference control scheme

The comparison between the *reference control* scheme (wind farm power factor equal to one) and the optimal control scheme (minimizing power losses) is presented in Figure 3-9 for HNet1 (a) and HNet2 (b). In both cases power losses are reduced when an optimal scheme is considered (second subplot). This reduction increases with the scenario, representing for the last one a 7.07% for HNet1 and a 10.97% for HNet2. For achieving this reduction, the wind farms generate reactive power in order to compensate as much as possible the inductive performance of the network and hence reduce the reactive power flows. Comparing both HNets it can be seen that the difference from the reactive power prespective is more significant for HNet1.

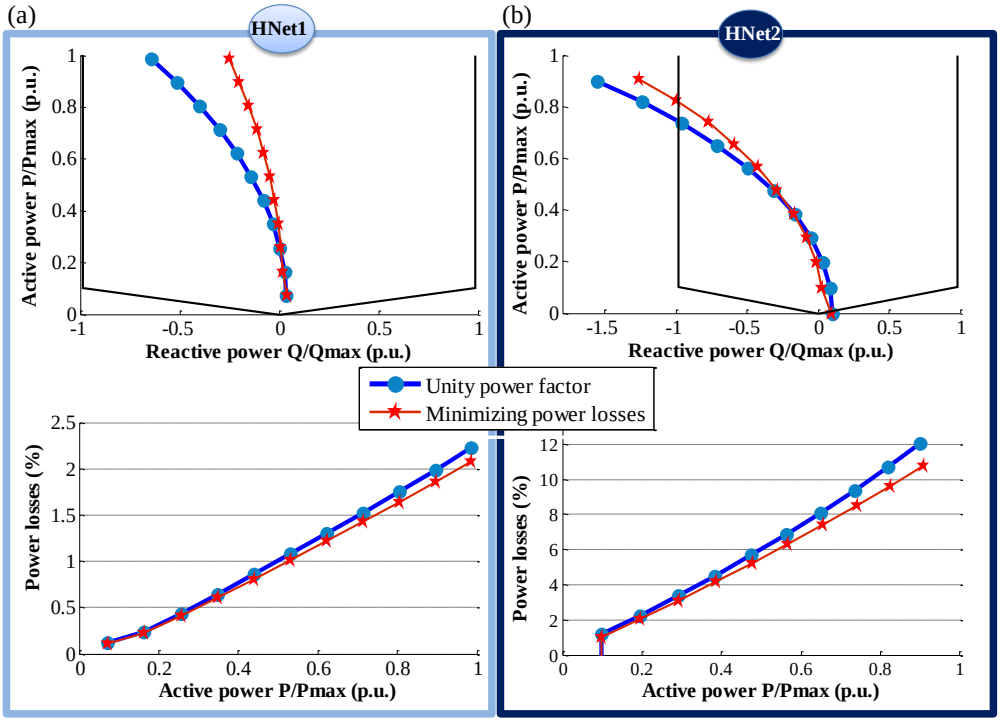

Figure 3-9 Current situation versus optimal voltage control (minimizing power losses) HNet1(a) and HNet2 (b)

Proportional control scheme

If *proportional control* scheme is implemented, reactive power support provided by the HNet to the TNet increase significantly, fostering all wind farms within the network to collaborate injecting reactive power as the following formulas indicate. These formulas are outlined in the grid codes slightly varying depending on the country. In this thesis both formulas are used.

$$\frac{Q}{Pnom} = K(Vmeasured - Vsetpoint) \quad or \quad Q = (Vmeasured - Vsetpoint)/R \tag{3-1}$$

Where at this stage of the thesis $V_{setpoint}$ and $V_{measured}$ are provided/measured voltages at the HNet common coupling bus. Thus, the wind farms control the voltage of a remote bus instead of controlling the voltage at each wind farm. Thanks to this strategy all wind farms see the same voltage deviation ($V_{measured} - V_{setpoint}$). Consequently, considering the same slope (K) or droop (R) for all wind farms it is guaranteed that all of them collaborate in the same proportion. Both parameters, K and R are used indistinctively throughout the thesis. A *remote voltage control* implies augmenting communication requirements (the wind farms must receive the voltage deviation measured at the HNet common coupling bus). Moreover, in networks partially meshed a *remote voltage control* scheme may not be adequate. For example, if $V_{measured}$ is lower than $V_{setpoint}$ all wind farms located in the HNet will generate reactive power. Depending on the grid topology, voltage in the mesh could increase without representing any improvement at the connection bus. The adequacy of a *remote control* scheme or a *local control* scheme is studied in detail in Chapter 5. Nevertheless, this subsection introduces some key aspects such as: the strategy adequacy, the appropriate value of the slope K (alternative droop R) and the necessity of adapting them depending on active power scenarios.

In that sense Figure 3-10 has been included for HNet1 (a) and HNet2 (b). For each HNet three subplots have been provided. The first one presents the maximum reactive injection/absorption of proportional control scheme (which has been obtained by changing K in different active power scenarios until convergence is lost meaning that no more reactive power is admissible). This means that all wind farms are operated at the same percentage of their maximum reactive capability. In addition, in this subplot the maximum PQ chart obtained with the optimal voltage control scheme (maximizing/minimizing reactive power) is also depicted. Comparing both curves, the loss of reactive capability due to proportional strategy is assessed. As can be seen the loss of reactive capability is more significant for HNet2 (the meshed network). The second subplot depicts the reactive level ($|Q/Q_{max}|$) equal to all wind farms since K and $V_{measured} - V_{setpoint}$ is the same for all wind farms. Finally, in the last subplot the value of K is provided, which should be between 0 and 25 as it is indicated in the Spanish grid code draft. For instance, the point outlined in Figure 3-10 means that all wind farms cannot provide their maximum capabilities; they can only be increased to 90% before some limit is reached. In both cases the reactive power level is higher for the consumption than for

the generation component. These levels are much smaller for HNet2. This fact is due to WF13 (wind farm with a higher installed power (150 MW)) which is located far from the common coupling point as can be seen in Appendix A in its diagram. This wind farm, for the same voltage deviation, injects/absorbs great amounts of reactive power increasing/reducing the voltage out of its limits. In these cases, where the loss of reactive power capabilities owing to the proportional strategy is significant, a different *K* for each wind farm can be considered. Other possibility, is the consideration of a *local control* scheme in which the wind farms control the buses where they are connected. Both, $V_{setpoint}$ and *K* could be optimally determined and hence the same results as the ones obtained with the optimal control scheme could be achieved.

If the *proportional control* scheme is implemented with the intention of providing active voltage support two extreme situations can appear if a fixed *K* independently of the active power scenario is considered. For a small *K* the increase or decrease of the voltage that can be achieved is also small. In the event of a large *K*, the problem that can appear is that all wind farms could reach their reactive power limits. However, as has been evaluated in the right subplot of Figure 3-10, it is not feasible that all wind farms provide the maximum reactive power (100% reactive level) in most of the scenarios (either inductive or capacitive). As a result, it seems more sensible to modify the *K* of the proportional control depending on the active power scenario. Only if *K* is modified depending on the active power scenario (*K*=*f* (P)), the PQ chart can be approximated to the maximum PQ chart obtained with the optimal control.

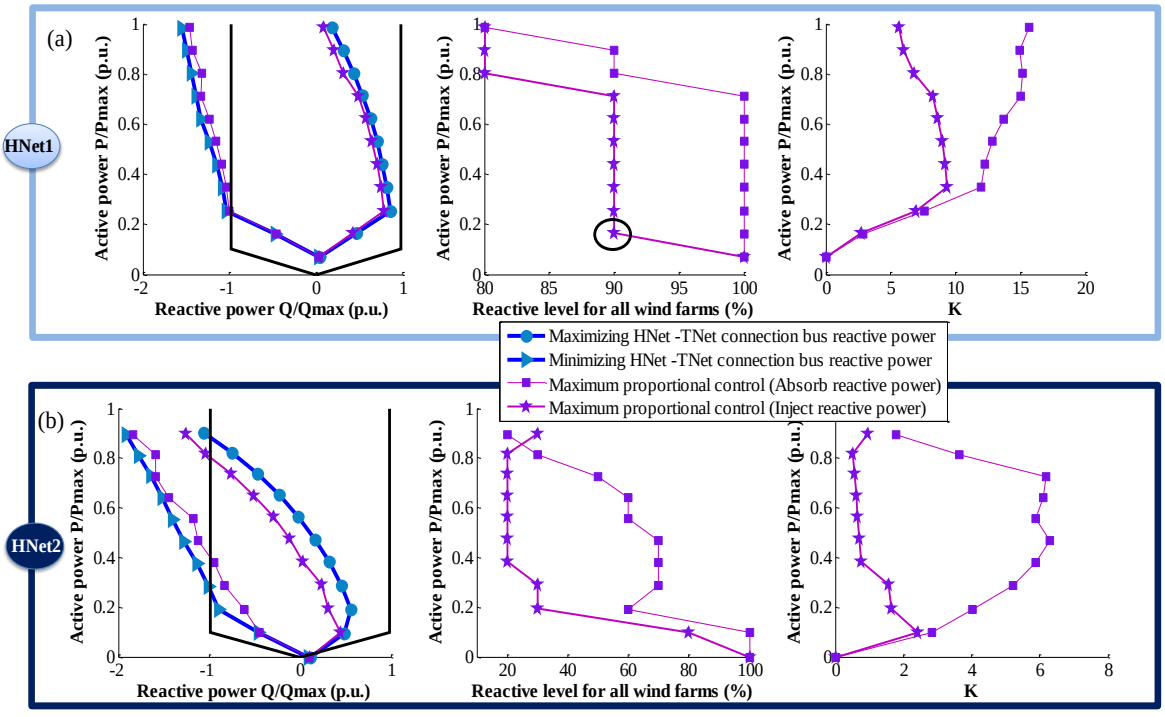

Figure 3-10 Maximum proportional control for HNet1and HNet2

3.3. STRATEGY SELECTION

The detailed analysis, based on two HNets, has shown that the maximum voltage variation that could be obtained at the common coupling bus, highly depend on the HNet characteristics. In fact, it has been seen how HNet2 cannot compensate its own reactive power consumption and hence increase the voltage when the total active power surpassed 0.5 p.u., not recommending this network for a pro-active voltage control strategy. Hence, other control strategies should be considered. This section extends this analysis to all HNets presented in this chapter. In Figure 3-11 all three magnitudes, reactive power, voltage margins and power losses, are depicted for all HNets, showing the variety of limits obtained for the different configurations. Based on those limits, the HNets can be gathered in three distinct groups for which representatives HNets have been also outlined in this figure, subplot (b). Firstly, networks with significant power losses (type A); meaning that its reactive support to the TNet is very limited from the generation point of view. Hence, a power losses minimization strategy is selected as has been already explained for HNet2. This strategy can be directly implemented running an OPF each period or by quadratic programming as suggested by [Alonso 2001], techniques well-known in the literature. Hence, this thesis tackles the problem in Chapter 4 in a different way facing some drawbacks. On one hand, the interpretability of the OPF control variables outputs. On the other hand, the possibility to infer simple control schemes which do not demand online optimizations and hence, communication requirements could be diminished and even avoided.

Contrarily, in most networks power losses are not significant. However, their PQ chart and voltage margins differ significantly. In fact, in some cases reactive power capability is not enough for compensating grid reactive power consumption in all active power scenarios (type B). Consequently, a pro-active voltage control scheme will not have the desired effect, and minimizing power losses is not relevant. Thus, for these types of HNets a strategy which will minimize the HNet impact on the TNet (for the most probable transmission voltage, otherwise a slight reactive power support is made) may be more appropriate as is deeply studied in Chapter 5. In those cases, fit-and-forget settings are sought avoiding communications as is explained in that chapter.

There are HNets with a great potential for implementing a pro-active voltage control scheme (type C), e.g., HNet1 (depicted in pink in Figure 3-11). These HNets could support the TNet as any conventional plant does. However, this strategy demands updating the settings online and hence communication is essential. Hence, a first sensible step can be done with the previous strategy. This means that the selection of one strategy is not trivial and highly depends on the communications available or desired. Consequently a fuzzy division among these two last strategies may be considered. In fact, in this thesis the same HNet will be employed for assessing both strategies. Identifying the improvements obtained thanks to optimally update the settings each period.

One question that arises at this point is who makes the control strategy selection? Recalling section 1.2, DSOs are in charge of HNet operation. Thus, they are responsible for implementing any of these control strategies. Consequently, DSOs should play a

relevant role in their selection. Nonetheless, it cannot be done without considering the TSO and wind farm owners. In that respect, a transparent regulation, in which the responsibility of each party and proper incentivizes are defined, is needed. This thesis only focuses on the technical aspects leaving this issue as a future work (see section 7.4). For facilitating its definition, specific indexes and ranges (for each HNet type) are next suggested based on the HNets set evaluated.

Precisely, the following specific assumptions have been considered in the network types identification:

- **Type A:** In the event that power losses represent more than 5% when the active power level, i.e., total wind farms active power/total rated active power, is higher than 0.5 (see second subplot of Figure 3-11).
- **Type B:** In the event that the whole HNet reactive power injection is negative in any active power scenario (see first subplot of Figure 3-11), or in the event that the voltage margin at the common coupling bus is less than ±2.5% (see last subplot of Figure 3-11).
- **Type C:** In the event that none of the previous conditions are reached.

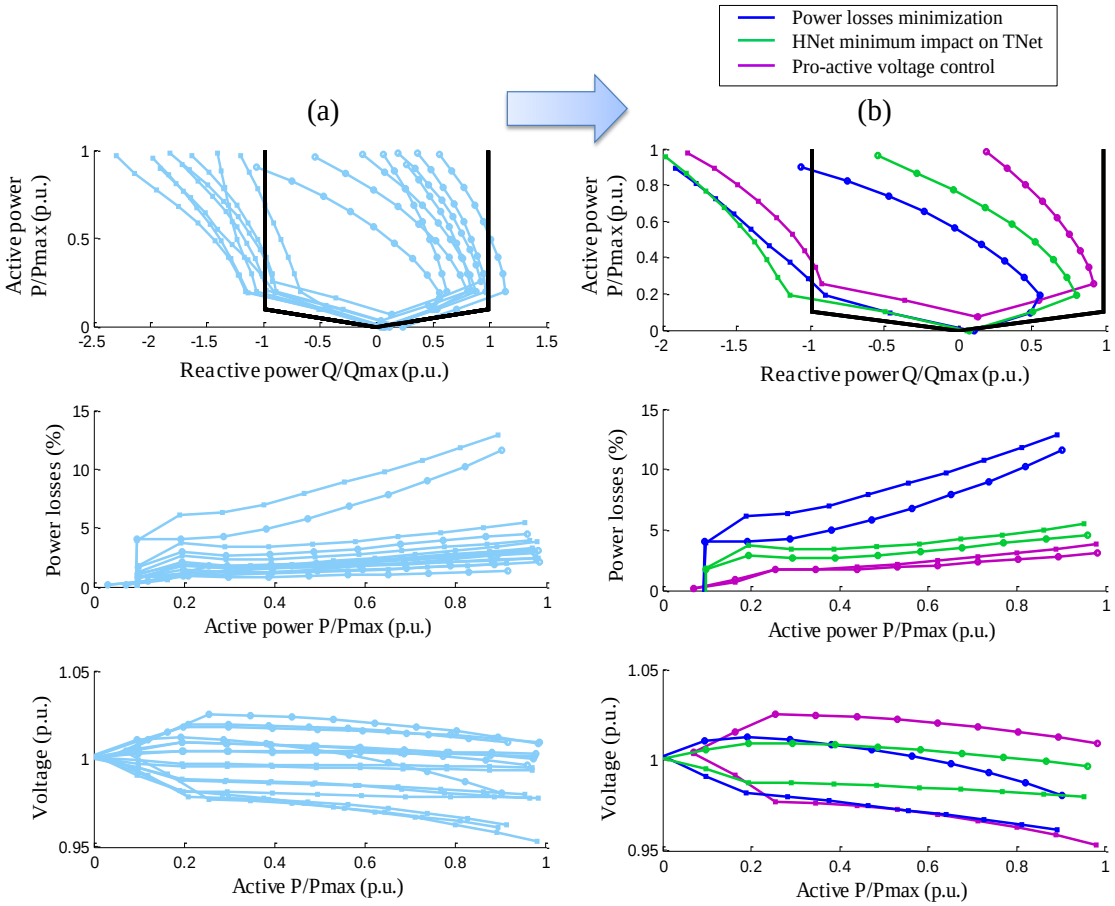

Figure 3-11 Limit performance of several HNet

Based on these specific considerations, Figure 3-12 indicates the characteristics of HNets suitable for each strategy: power losses minimization, HNet minimum impact on

TNet and pro-active voltage control. As could be imagined the kilometres of lines (KML) are a determinant factor which indeed could be used with regulation purposes.

- KML $\geq$ 250 km → Type A
- 250 km < KML $\geq$ 100 km → Type B
- KML < 100 km → Type C

Each strategy will be analyzed in a different chapter using a different technique: data-mining, AC multi-period OPF and quadratic programming. In addition, as has been explained in the previous chapter, voltage control design does not end with its steady-state assessment requiring dynamic coordination evaluation. This final analysis will be carried out for type B and C, where more variables are involved.

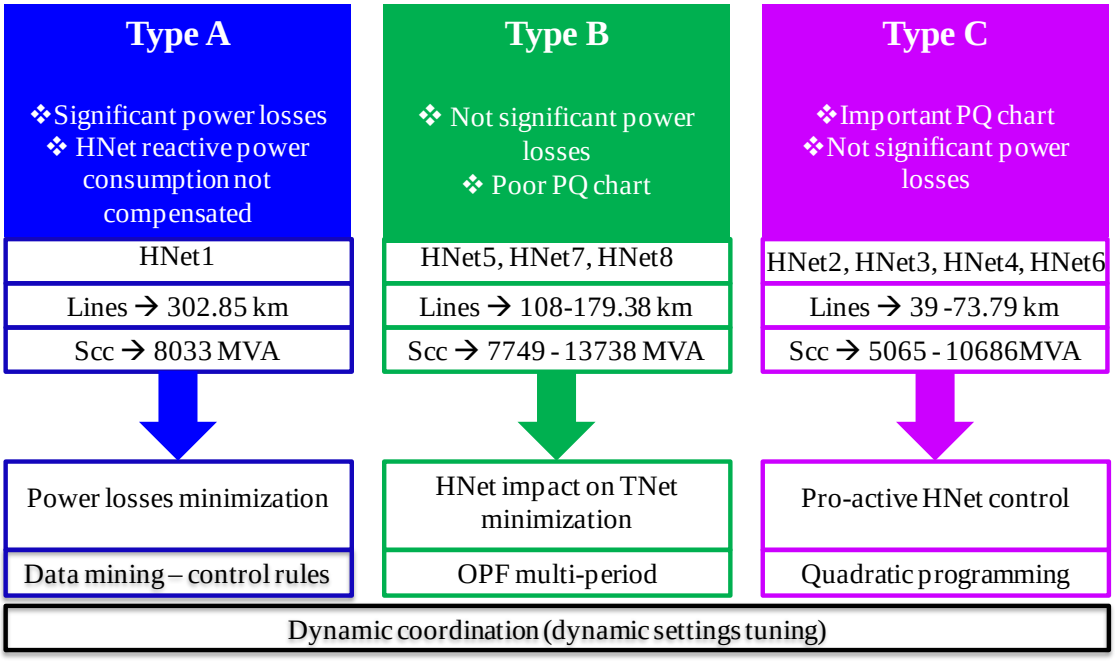

Figure 3-12 HNet characterization

3.4. SUMMARY AND CONCLUSIONS

This chapter has analyzed the necessity of wind farm reactive power provision and the potential and opportunities considering the HNets features. Firstly, the hosting capacity limitations and their increases thanks to the provision of this service have been assessed identifying the importance of where synchronous generators are displaced. This simple analysis shows how the local nature of reactive power makes indispensable the provision of this service by wind farms if their penetration is to be increased. Wind farms' reactive power capabilities are also essential from the TSO perspective avoiding technical constraints which increase the operational cost of the system.

Subsequently, the opportunities that these capabilities offer have been measured by means of the maximum PQ chart and the power losses minimization control scheme. In both cases it has been seen that the OLTC transformers play a key role and should be

considered in any control strategy. These schemes have been compared with the current and proportional control strategies (the latter being proposed by several grid codes) in order to measure how far they are from the control limits. This comparison suggests that there is margin for power loss reduction with respect to the simple current strategy (*reference control*). Moreover, if a pro-active voltage control wants to be implemented having a real impact on TNet an adaptive slope is essential.

This detailed analysis has been provided for two HNets with opposite characteristics clearly showing a dependence on the results. Hence, the strategy selection should consider the HNet feature. That analysis has been extrapolated to a set of eight actual HNets for identifying common characteristics and performance. For that purpose, as has been done in the detailed analysis, three relevant indices are employed: capability chart, power losses and voltage margins identifying three different HNet types.

- **Type A:** Power losses minimization strategy presented in Chapter 4, suitable for networks with significant power losses and with a restricted PQ chart.
- **Type B:** HNet minimum impact on TNet strategy presented in Chapter 5, suitable for networks with insignificant power losses and with a restricted PQ chart.
- **Type C:** Pro-active voltage control strategy presented in Chapter 6, suitable for networks with insignificant power losses and with a broad PQ chart.

For each one, different techniques will be employed for taking the maximum advantage of reactive power capabilities without unnecessarily increasing the control complexity and communication requirements as will be explained in the subsequent chapters.

CHAPTER 4

MINIMIZATION OF POWER LOSSES BY ONLINE CONTROL RULES

As has been seen in the previous chapter, HNets with significantly long lines are no suitable for a pro-active voltage control scheme. On the contrary, they are very appropriate for reducing power losses. This chapter focuses precisely on this type of HNets suggesting simple control rules computed offline for both, wind farms and OLTC transformers. In that sense, communication requirements can be diminished (not requiring online optimization process) and even avoided, in the event of OLTC transformers as is discussed throughout this chapter. This method contrasts with the well-known quadratic programming used for minimizing power losses each period as is suggested by [Alonso 2001]. Although it is undoubted that this last method derives more accurate results, providing the optimal value of all control variables each period, this chapter aims to demonstrate that simple control schemes can resemble its performance with less control complexities. As will be presented in Chapter 5, the AC multi-period OPF can be also employed in this sense obtaining fit-and-forget settings. Nonetheless, in this chapter an alternative method which additionally provides insight of the control variables assignment, evaluating their dependence with some relevant variables, is suggested. For this purpose the chapter has been structured as follows. Firstly, the holistic methodology, replicable to any other network including distribution ones, is explained in

section 4.1 outlining the explanatory variables and their relationship with the control ones. Subsequently, in section 4.2 the methodology is applied to HNet1, network representative of type A (power losses minimization strategy). Finally, conclusions are drawn in section 4.4.

4.1. METHODOLOGY

For the control rules achievement and later implementation, several steps must be followed. First of all, a data base of optimal power system scenarios should be built, taking into account the corresponding training and testing sets as will be explained. Subsequently, it is necessary to evaluate which are the variables that better explain the optimal control variables assignment, reactive power output and transformers' taps, and which relations can be found. Those relationships have been assessed in several HNets allowing to identify the main driver and hence, facilitating its later replicability and scalability. Finally, how this information can be used in an online implemented should be addressed, evaluating the advantages and disadvantages of the explanatory variables previously selected.

Each one of the steps identified: building the data base, identified the explanatory variables, extracting control rules and evaluating their online performance, are explained in depth in the subsequently subsections.

4.1.1. OPTIMAL OPERATIONAL SCENARIOS BUILDING

In order to define the relationship between input and control variables, many scenarios have to be studied. The proper way of evaluating representative wind farms' scenarios is explained in Appendix E, where the correlation factor among wind farms is derived from real data and a certain occurrence probability is assigned to each one. In this chapter, in order to derive general conclusions independent of real data or wind farms proximity most unfavourable scenarios have been created. In that sense, totally random values of active power have been assigned to each wind farm, obtained by multiplying a random number between zero and one by its rated active power. For each scenario a set of different TNet voltage set-points should be considered, which range should properly be selected in accordance with historical values of the transmission network bus in each case. In this chapter, as is done with active power scenarios, a wide range has been considered generalizing the assessment.

Each scenario, considering the active power of each wind farm and the TNet voltage set-point, is optimized using a commercial OPF [Siemens 2015] to register the optimal value of the control variables and some relevant explanatory variables as is explained in the subsequent section. Moreover, a power flow in which all wind farms provide unity power factor is also run; note that the proposed methodology needs an OPF to create the data base used. However, once control rules are established, an OPF is no longer required avoiding online optimization. These control variables correspond to the wind farms' reactive power capabilities and the OLTC transformers' taps, the latter being essential for power losses minimization as has been already emphasized in Chapter 3. Nonetheless,

a first attempt considering just the wind farms' reactive power capabilities is made for evaluating the OLTC transformers impact on the control rules obtained. Hence, two separate data bases are built. Anticipating the results, the wind farms reactive powers are estimated using regression rules, where their coefficients of determination (R^2) are used for measuring their adequacy. This coefficient is equal to the square of Pearson's product-moment correlation coefficient [DeVore 2004]. Contrarily, for each OLTC transformer a decision tree is employed. In the learning process of a decision tree, the data base must be divided into two different sets: training and testing [Yu et al. 2010]. The former is used for building the tree. The latter is used for measuring its accuracy. As is stated in [Tan et al. 2005] the training set typically correspond to two thirds of the data set whereas the testing set amount to one third.

Finally, the accuracy of the whole methodology should be also evaluated. This is achieved by contrasting the total power losses (objective function) obtained with the OPF with the ones obtained running a power flow taking into account the control variables output forecasted, i.e., wind farms reactive power and OLTC transformers tap position. This process must be done with a distinct data base. For clarifying this process Figure 4-4 has been included taking into account all possible control variables. The first data base is employed for obtaining the control rules (regression rules and decision trees) measuring their adequacy. Then, a different set of scenarios is considered taking into account the optimal value of the control variables (OPF output) and the forecasted one, based on the control rules previously obtained. This last step guarantee that the control scheme proposed is robust and valid for the long term.

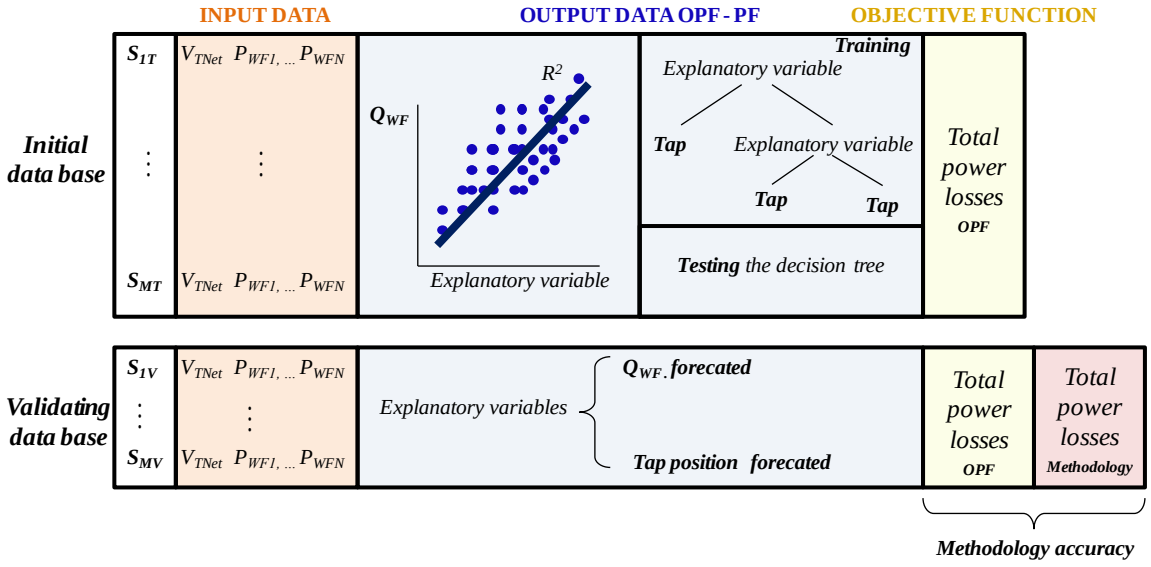

Figure 4-1 Data base building process

4.1.2. EXPLANATORY VARIABLES

For explaining the optimal assignment some relevant variables are needed. Those variables have been divided into two groups. Firstly, variables useful for explanation purposes but which require a previous power flow, assuming that all wind farms are operated at a unity power factor. Secondly, variables of easy implementation, i.e., do not

require calculations or/and communications, representing a clear advantage with respect to an OPF. However, as can be imagined their accuracy, i.e., their coefficient of determination is eroded compared to the other variables (first group). This erosion highly depends on the HNet characteristics and condition as is discussed at the end of this subsection. Hence, these last variables cannot always be employed.

Concerning the first group this thesis contributes with a novel explanatory variable whose accuracy is augmented significantly with respect to other common ones such as the total active and reactive power losses. This new variable corresponds to the specific power losses of a certain wind farm. The active power losses from wind farm *i* to the transmission network bus (P_{lossi}) are computed by adding the losses of all the lines that connect the wind farm *i* to the TNet bus. This variable takes into account both power flows and impedance also giving an estimation of wind farms' sensitivities (i.e., the wind farm relevance on the power losses minimization goal). As an example, Figure 4-2 shows a radial HNet that connects three different wind farms to the TNet. Taking into account this simple diagram P_{lossi} is computed for the wind farm 2 (outlined in Figure 4-2):

$$P_{loss2}= P_{loss01} +P_{loss12}+P_{loss23}+P_{loss35}= r_{01}i_{01}^2+ r_{12}i_{12}^2+r_{23}i_{23}^2+ r_{35}i_{35}^2 \quad (4\text{-}1)$$

Note that the term P_{loss35} is generated only by wind farm *2*, but the other terms are affected by other wind farms (P_{loss23} and P_{loss12} are also affected by wind farm 1 and wind farm 2 whereas P_{loss01} is affected by all wind farms in the network). Therefore, the value of P_{lossi} depends on the specific wind power generation profile. Within meshed HNets, as the one under study, P_{lossi} of all lines involved should be taken into account[8].

[8] Note that the active power losses of each (e.g., P_{loss01}) line are the result of a power flow

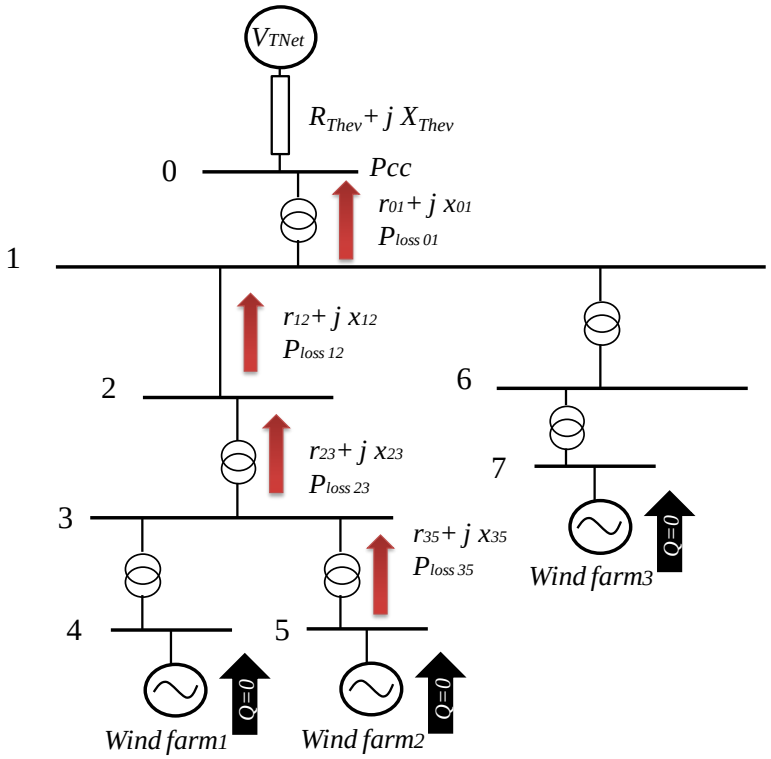

Figure 4-2 Diagram of a radial HNet that connects three different wind farms to the transmission network bus (TNet)

Concerning the second group, variables that can be measured by each control device avoiding communication requeriments have been studied. In that sense, voltage at wind farm grid connection point and their individual active power are assessed. However, these variables are not enough for a proper estimation as is discussed throughout the chapter. Thus, the global active power, i.e., the active power measured at the HNet common coupling bus is also considered. Note that this last variable implies communications. However no computations are required, power flows or OPF. In fact, a simple relationship could be established, a power factor with respect to the global active power instead of the common individual one.

In order to asses under which circumstances this last variable cannot be used and hence, a previous computation is required, Figure 4-3 has been included. In this figure the total HNet active power (*TP*) adequacy, measured with its coefficient of determination, is compared with the one obtained with $P_{lossi.}$ In addition other possible variables which finally have been discarded: total active power losses (*TPLosses*) and total reactive power losses (*TQLosses*) have been also included; both of them computed assuming that the wind farms are operated at a unity factor. All these variables have been computed for three wind farms located in different networks. Firstly, a wind farm of HNet1, network which will be deeply evaluated in this chapter. Secondly, a wind farm of HNet2 and finally, a wind farm located in a distribution network, i.e., in the presence of loads being also representative of a situation in which not all wind farms contribute to power losses minimization. As can be derived from this figure P_{lossi} is the best explanatory variable. However, for HNet1 the coefficient of determination erosion obtained for *TP* is negligible. This fact is owing to the long lines of this HNet.

Consequently, the variable that will be considered throughout this chapter will be *TP*. This variable is not suitable in the event of uncontrollable loads or generators. In those cases P_{lossi} is essential for understanding the optimal reactive power distribution among wind farms.

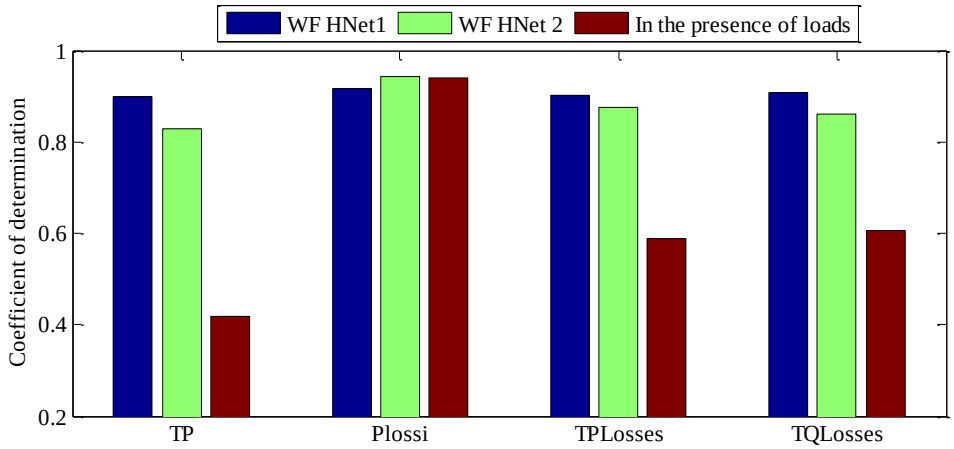

Figure 4-3 Adequacy of the explanatory variable

4.1.3. DEVELOPMENT OF CONTROL RULES

As has been anticipated, the reactive power provided by each wind farm is going to be estimated in accordance with regression rules, whereas the tap position of each transformer is going to be determined with a decision tree. Both, regression rules and decision trees, are defined based on an offline analysis of the data base.

In the event of not considering the OLTC transformers, a different regression rule ($Q_{refi} = f\,(TP)$ for different values of the transmission network bus (V_{TNet}) must be considered. When these devices are included that dependence is avoided and thus, only one regression function ($Q_{refi} = f\,(TP)$) independently of V_{TNet} is needed. However, now a decision tree for each transformer is required. The regression functions were obtained approximating the reactive production Q_i with a second grade polynomial depending on the explanatory variable owing to the high non linear performance of power losses.

$$Q_i = c_0 + c_1 TP + c_2\, TP^2 \qquad (4\text{-}2)$$

where c_0, c_1, and c_2 are the polynomial coefficients. The main strengths of this technique are [Li, et al. 2010, Wehenkel 1997]: i) its ability of selecting the most relevant variables ii) its interpretability, being one of the aims of this chapter and iii) its computational efficiency, critical for online applications as is the case of voltage control. Other alternatives may be employed such as neural networks. Which is a technique that better handles OPF non-linearities. However, it has been discarded owing to its obscure interpretation. The algorithm that will be used for the decision tree is the CART (Classification And Regression Tree) [Timofeev 2004, Ruggeri et al. 2008], which

classifies data in accordance with binary conditions. In this case, these conditions are V_{TNet}, the total active and reactive power that reaches the transmission network and the power losses of the whole HNet. Other algorithms apart from CART may be used to build the tree, such as the ID3 [Quinlan 1986] and the C4.5 decision tree generation algorithms [Quinlan 1993]. A detail survey of the possible algorithms is presented in [Barros et al. 2012].

4.1.4. OUTPUT OBTAINED AND IMPLEMENTATION

This subsection deals with the implementation issues that may arise when the relationship between the control variables and the explanatory ones are considered. Note, that those relationships must be evaluated in each network. Indeed, network particularities (topology and operation conditions) influence the explanatory variables adequacy, measured by R^2, increasing the difference between P_{lossi} and TP as has been discussed. This analysis also reveals the relevance of each wind farm on the common goal, power losses minimization. In fact, it will be seen that certain wind farms have a negligible impact whereas others present a great potential for power losses minimization. For the former, unity power factor is recommended whereas the latter is prone to saturate, fact that should be taken into account in the control rules evaluation process. Furthermore, the OLTC transformers, of which the tap position is evaluated with a decision tree, should be taken into account as has been seen.

Figure 4-4 summarizes the control scheme implemented outlining the difference between the two principal variables selected for explaining reactive power assignment. Moreover, the main differences with an OPF are also incorporated. In the event of considering this option the central controller, i.e., the OPF, should receive the V_{TNet} and the active power delivered by each wind farm (which can be, the measure of the previous period or the forecasted one) and sends the tap position and reactive power to OLTC transformers and wind farms respectively.

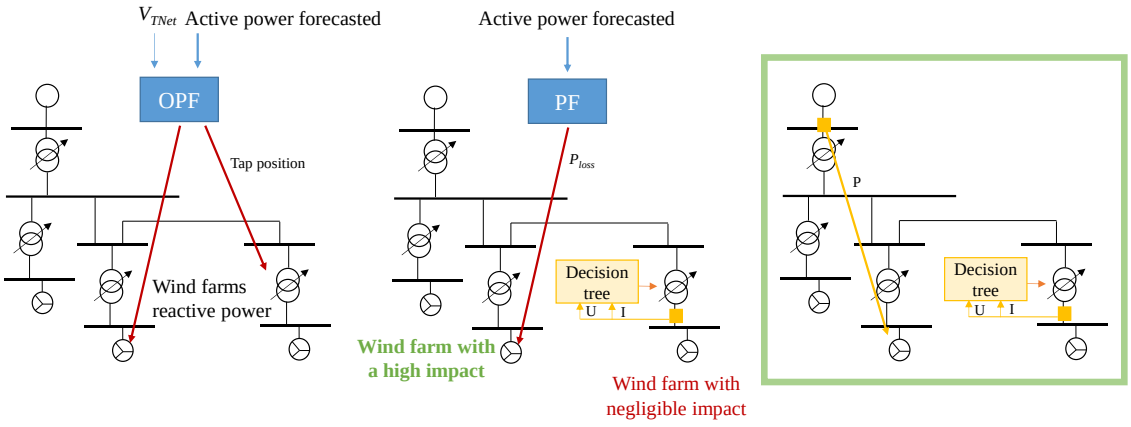

Figure 4-4 Control proposed using quadratic regression functions for each wind farm, in the event that only the reactive power capabilities of wind farms are used as control variables.

For the solution proposed in this thesis and if P_{lossi} is used as explanatory variable, computations are simplified requiring only a power flow. Computations are totally avoided when *TP* is considered. This magnitude, measured at the HNet common coupling bus, is sent to all wind farms. In both cases the OLTC transformers can be operated in a decentralized manner representing a clear advantage with respect to the OPF.

4.2. EXAMPLE CASE

This section explains the process followed to develop the optimal voltage control rules focusing on HNet1, network with a significant potential for power losses minimization. The first subsection 4.2.1 particularizes the data base building process for HNet1 (described in Appendix A). Subsequently, a first attempt in which the OLTC transformers are not evaluated is presented in subsection 4.2.2. Finally, the definitive control rules considering all control devices are included in subsection 4.2.3.

4.2.1. DATA BASE BUILDING

Focusing on HNet1, a total number of 100 cases of wind power production, each one with 9 different voltage set-points (0.97-1.05) of the TNet bus have been analyzed. These scenarios are created considering a random active power distribution among wind farms. In addition, scenarios in which all wind farms have the same active power level have been also incorporated for taking into account situations of high load. This great number of scenarios can be diminished if the correlation factors among wind farms are known.

Recalling the previous section, these scenarios have been divided into two sets: 600 scenarios have been used in the training process whereas 300 are used in the testing one. Finally, another set of 300 scenarios have been built for validating the optimal voltage control proposed.

4.2.2. REGRESSION RULES IN THE EVENT OF NOT CONSIDERING OLTC TRANSFORMERS

This subsection analyzes the optimal voltage control scheme in those cases where transformers do not cooperate in the power losses minimization goal. Thus, the data base has been created within each scenario only optimizing the reactive power output of wind farms. Moreover, the Lagrange multipliers which correspond to the equality constraint of the reactive power demand in each generator have been computed. These multipliers represent the sensitivity of HNet losses to the increase of wind farm reactive power and provide valuable information. In fact, wind farms with a low multiplier do not affect the total power losses and hence, their incorporation in the optimal voltage control is not necessary.

In Figure 4-5 the mean Lagrange multipliers for all the scenarios considered are presented. It should be noted that the absolute value of WF1 (6.48E-2) is drastically higher compared to the other wind farms. Hence, in this figure lower limits have been considered for their proper evaluation. The reason behind the high value of the WF1

Lagrange multiplier is that this wind farm saturates at the maximum reactive power limit. Thus, in this case a quadratic function could be adjusted only for values under the maximum reactive injection. Contrarily, wind farms can be identified that have a nengligible impact (WF11, 12 and 13 which have been outlined in the figure) which also will present with poor R^2. This means that the adequacy of the relationship between control and explanatory variables also gives some insight in the sensitivity of each wind farm to the common goal; relationships that are next evaluated.

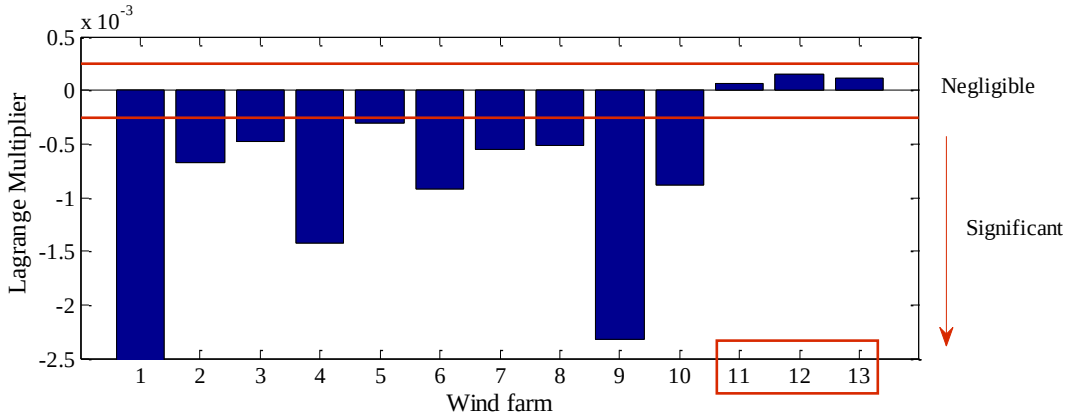

Figure 4-5 Lagrange multipliers of the equality constraint on the reactive power demand in each wind farm.

Firstly, the possibility of employing totally decentralized variables was studied. Specifically, wind farms individual active power (P_{WF}) and the voltage measured at wind farms connection point (V_{WF}). In Figure 4-6 the relationship between the reactive power and P_{WF} is provided for three different wind farms whose Lagrange multipliers diverge significantly, also meaning that their behaviour will diverge: WF1, prone to saturate, WF13, with a negligible impact and finally an intermediate one, WF5. In addition three different V_{TNet} values have been considered, 0.97, 1 and 1.03 p.u. In all cases all magnitudes have been normalized with respect to the maximum reactive injection for comparison purposes. Concerning WF1 a lack of any relationship can be seen. Focusing on WF5 a certain relationship can be found although it presents a high spread, fact that clearly undermines the selection of this variable as an explanatory one. This spread is reduced in the event of WF13; note its rated power is drastically higher compared to the other wind farms.

In Figure 4-7 the relationship between reactive power and V_{WF} is depicted for the same three wind farms. Focusing on WF5 (second subplot), a clear dependence can be seen between both variables which significantly augments when a different regression rule is considered for each V_{TNet}. Concerning, WF13 (third subplot) it can be seen how their reactive resources are not exploited. In fact, only when the voltage reaches a value of 1.05 can a certain variation of reactive power be seen. Finally, as was expected WF1 saturates. Moreover, a great reactive power variation can be seen for the same V_{WF}, especially when V_{TNet} increases, representing a drawback for its implementation.

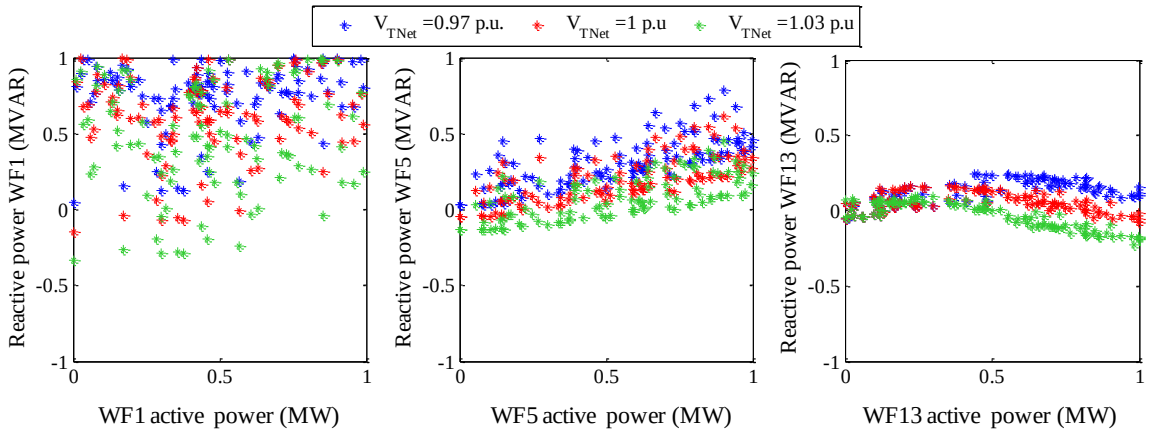

Figure 4-6 Relation between the reactive power and the individual active power of each wind farm

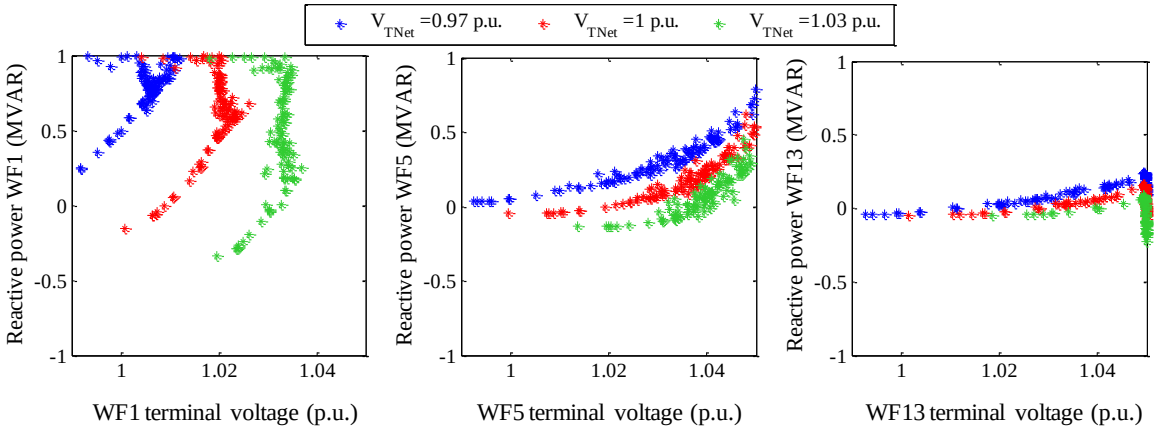

Figure 4-7 Relation between the reactive power and its voltages

Secondly, the possibility of employing a global variable was examined. Concretely, the total active power *TP*, which as has been mentioned presents promising results, i.e., a high coefficient of determination. This relationship is presented in Figure 4-8 for WF1, 5 and 13 as in the previous case, obtaining similar results: WF1 saturates, WF13 has a negligible impact, hence dependence between both variables cannot be seen, and finally an ideal performance can be seen in WF5. Nonetheless, a significant difference can be noted with respect to the previous case focusing on WF1. In this case a clear dependence between control and explanatory variables can be seen before the saturation is reached which is not eroded with V_{TNet} increment. For all wind farms a regression rule independent of V_{TNet} could be obtained. This regression rule has an adequate overall shape but it has a high spread. Therefore, the regression rules should be dependent on the voltage of the TNet bus.

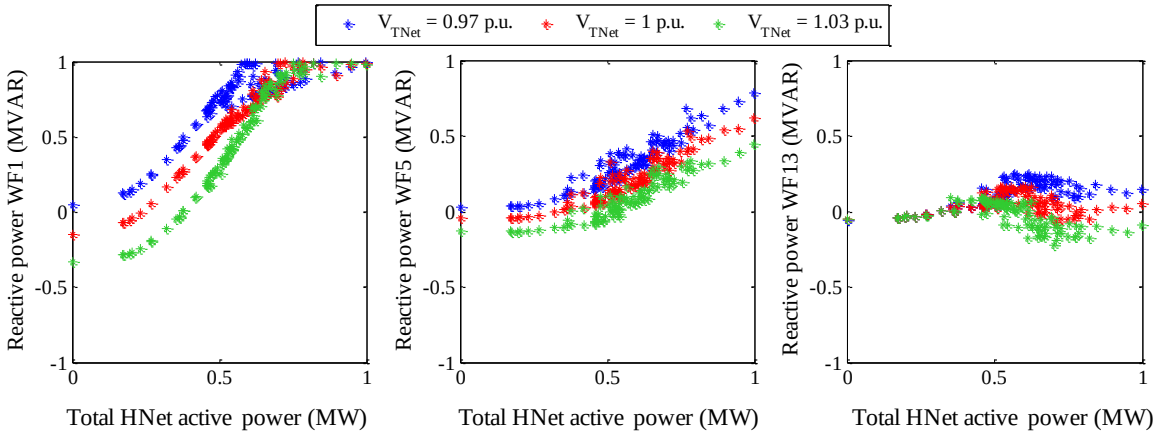

Figure 4-8 Relation between the reactive power and the total active power

Next, Table 4-1 presents R^2 in the event of considering *TP* as explanatory variable where coefficients higher than 0.8 in all cases except for WF11, WF12 and WF13 can be seen. These wind farms were precisely the ones with a negligible impact, identified with the Lagrange multipliers.

Table 4-1. R^2 of wind farms without transformers' taps

	WF1	WF2	WF3	WF4	WF5	WF6	WF7	WF8	WF9	WF10	WF11	WF12	WF13
V_{TNet} =0.97 p.u.	0.87	0.96	0.94	0.98	0.90	0.90	0.96	0.94	0.94	0.94	**0.24**	**0.54**	**0.58**
V_{TNet} =1 p.u.	0.95	0.95	0.93	0.97	0.89	0.92	0.96	0.95	0.93	0.93	**0.33**	**0.60**	**0.29**
V_{TNet} =1.03 p.u.	0.93	0.94	0.91	0.96	0.88	0.91	0.95	0.95	0.93	0.90	**0.29**	**0.60**	**0.43**

4.2.3. OPTIMAL VOLTAGE CONTROL WITH TRANSFORMERS' TAPS

Once that some preliminary control rules have been seen, this subsection analyzes the impact of incorporating OLTC transformers in the optimal control scheme. For this purposes the dependence of the wind farms reactive power with respect to the same explanatory variables have been included. In Figure 4-9 the explanatory variable considered is V_{WF} whereas in Figure 4-10 the global variable *TP* have been evaluated. In both cases it has been seen that the dependence of the regression rule on V_{TNet} is avoided. This can be explained by the optimal adjustment of transformers' taps depending on the TNet voltage. Moreover, focusing on V_{WF} (see Figure 4-9) it can be seen how the adequacy of this variable deteriorates due to its discrete behaviour. Contrarily, the adequacy of *TP* increases when the OLTC transformers are introduced as can especially be seen for WF13. Those increases have been measured with R^2 and are gathered in Table 4-2. As in the previous case, most wind farms R^2 are above 0.8 indicating a high relationship.

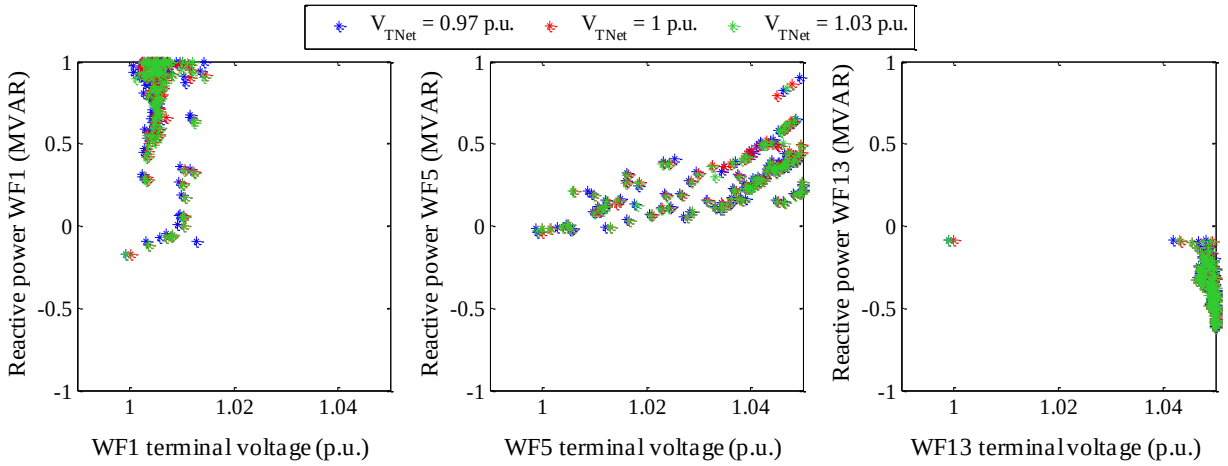

Figure 4-9 Wind farm reactive power vs voltage measured at its terminals

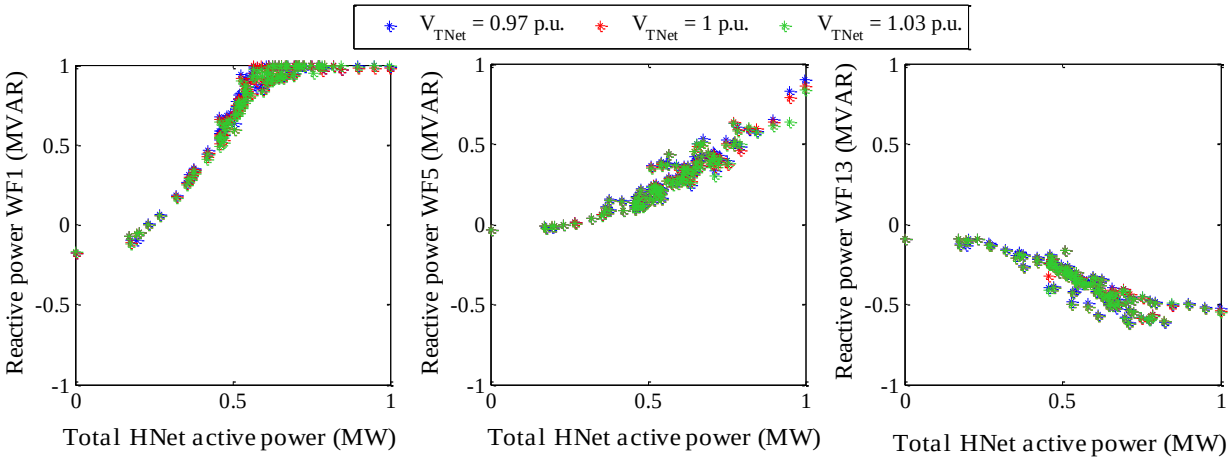

Figure 4-10 Wind farm reactive power vs total active power.

Table 4-2. R^2 of wind farms in the event of considering OLTC transformers

WF1	WF2	WF3	WF4	WF5	WF6	WF7	WF8	WF9	WF10	WF11	WF12	WF13
0.91	0.93	0.93	0.95	0.90	0.95	0.94	0.93	0.83	0.81	**0.64**	**0.79**	**0.26**

The tap position of each transformer is estimated with a decision tree, which uses the CART algorithm. This algorithm uses a set of historical data (optimized scenarios) which is splitted in a binary way. This algorithm searches within all possible variables, splitting the data with the maximum homogeneity. Figure 4-11 presents a simple decision tree obtained for a 132/20kV transformer where a single explanatory variable is used (wind farm voltage). This means that simple control rules of easy interpretability can be obtained. Nonetheless, the incorporation of other explanatory variables is required for other transformers especially for the 400/132kV one as is next discussed.

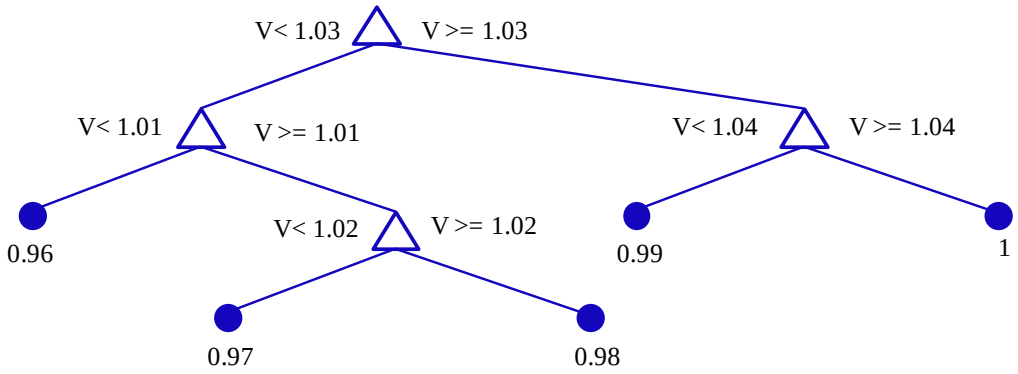

Figure 4-11 Example of a decision tree obtained for estimating the tap position of a specific OLTC transformer

For measuring the adequacy of the trees obtained a testing set is essential. Considering this set, the tap position is predicted with the decision tree (built with the training set) and contrasted with the optimal value provided by the OPF. Its performance is then evaluated thanks to the confusion matrix. In this matrix the rows correspond to the optimal value whereas the columns correspond to the predicted values. If there are only values in the diagonal matrix a perfect match has been achieved. Contrarily, the values not located in the diagonal are decision tree errors originated by the confusion of two different classes, being the origin of the name of this matrix. Figure 4-12 depicts this matrix for two OLTC transformers: (a) 132kV/20kV and (b) 400kV/132kV. As can be derived from this figure, in the case of 132kV/20kV the initial explanatory variables V and I are enough to obtain good results. In contrast, these variables are not sufficient to adequately predict the tap position of the 400kV/132kV where many confusion values can be seen. In that sense V_{TNet} has been incorporated clearly improving the results as is depicted in Figure 4-13. This incorporation does not necessary increase the communication requirements as is also mentioned in Chapter 5. This fact is owing to V_{TNet} is highly predicted base on the season and hour of the day. Hence, continuous communications are not demanded. Taking into account these variables the percentage of bad classified is gathered in Table 4-3, where the great potential of decision trees can be seen.

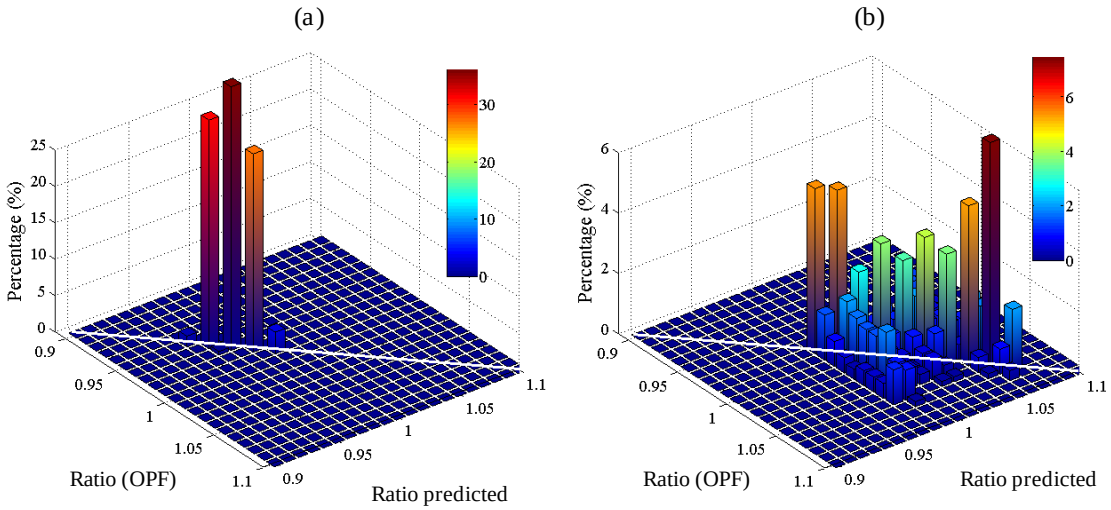

Figure 4-12 Confusion matrix. (a) 132kV/20kV transformer (b) 400kV/132kV transformer

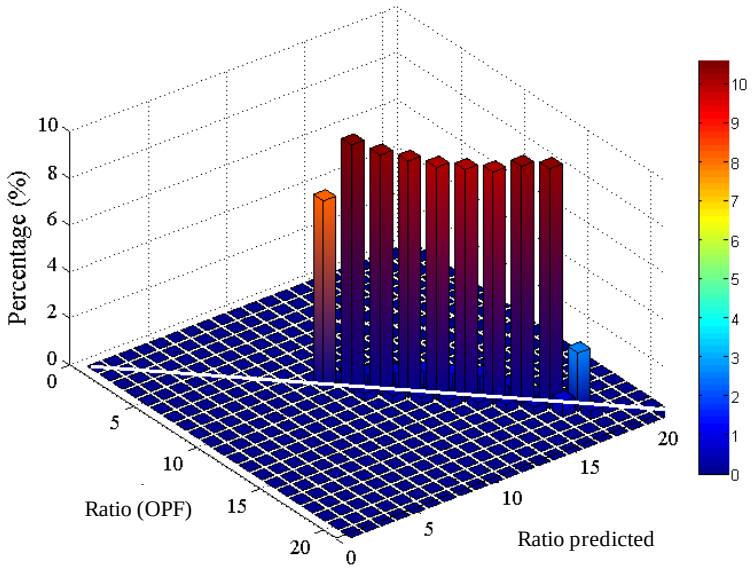

Figure 4-13 Confusion matrix 400kV/132kV transformer incorporating the transmission network voltage as explanatory variable

Table 4-3. Decision tree performance. Percentage bad classified

Bad classified percentage (%)											
132kV/20kV											400kV/132kV
11.11	28.62	9.09	26.94	7.74	3.03	24.24	26.94	29.97	9.09	20.88	12.46

Once that the control rules of all control devices involved are obtained the adequacy of the whole methodology is assessed. For that purpose, the global losses obtained with the OPF are compared with the ones obtained when the tap position is estimated with a decision tree and the wind farms reactive power with a regression rule. Moreover, in order to see the benefits that this simple online control scheme represents with respect to the *reference control*, i.e., the wind farms are operated at a unity power factor (in addition in this chapter nominal OLTC transformers' ratios has been assumed), the difference

between this scheme and an OPF is also included. Those differences (proposed methodology – OPF and *reference control* – OPF) are jointly depicted in Figure 4-14 where the zero line is incorporated as a reference. Considering a *reference control* scheme, voltages out of limits, i.e., above 1.05 p.u. can be obtained, which result in less power losses (note negative values in Figure 4-14). In the event of implementing the simple control scheme here proposed, these violations are drastically reduced. In fact the higher deviation is 0.48 MW. In this case voltage out of limits due to decision tree forecast errors can also be seen. These errors can be mitigated by computing the control rules considering narrow limits. Nonetheless, in the worst case the voltage breaches never surpassed the ones obtained with the current operation.

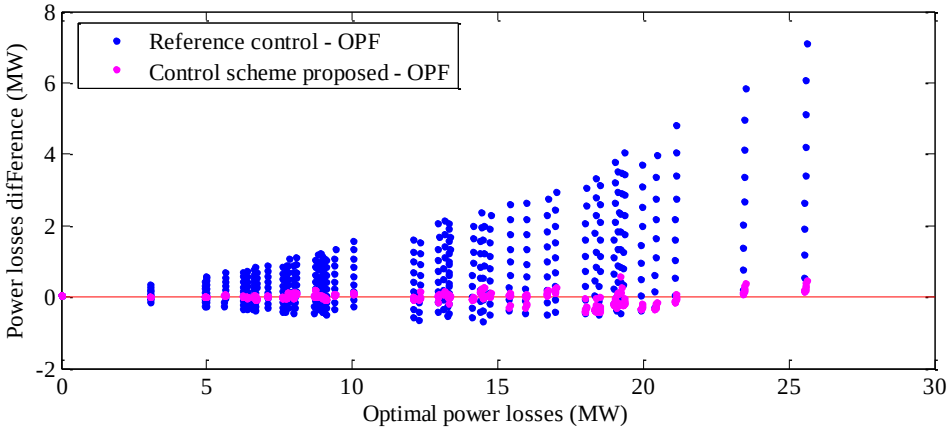

Figure 4-14 Validation of the online control scheme proposed

4.3. DETAIL POWER LOSSES IMPACT

This analysis has been extended also taking into account the internal wind farm grid. Hence two power losses components are distinguished as indicated by Figure 4-15. Firstly, the internal wind farm power losses which are directly computed as $Pgross_{0WF} - Pgross_{WF}$, i.e., the power delivered by all wind turbines within the wind farm minus the total active power at its meter point as can be identified in Figure 4-15. Secondly, the HNet power losses which should be allocated to the wind farms, considering the Spanish regulation. These losses, do not correspond to the real ones and are estimated in accordance with a fixed parameter (f_{WF}). As a result the net power that it is recognized is $Pnet_{WF} = Pgross_{WF}\ (1 - f_{WF}\ )$. Thus, although the HNet losses could be reduced, this reduction is not allocated to the wind farm owners representing a relevant drawback for implementing a power losses minimization control scheme.

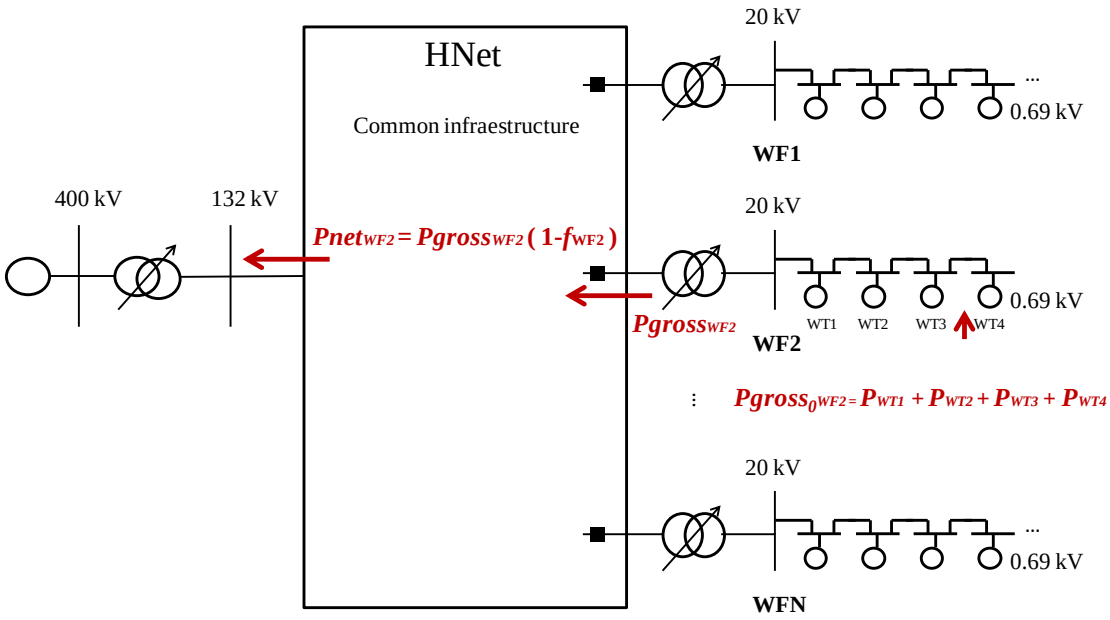

Figure 4-15 Gross and net power, HNet and wind farms power losses

A comparison between the *reference control* and the full network optimization schemes indicates the impact on the losses profile of using wind turbines' reactive power capabilities in an optimal way to contribute to both wind farm and HNet power loss reduction. In Figure 4-16 this comparison is presented in MWh for twenty scenarios. These scenarios have been created considering the wind turbine Weibull probability density function. Each scenario represents an interval of wind speed [S_W^{min}, S_W^{max}] in which the average value is considered. The first scenario will be the same for the first 438 hours of the Weibull probability density function; the second scenario will be the same for the next 438 hours and so on. Using as an example the power curve provided by the wind turbine manufacturer (Wind turbines correspond to 2MW, 0.69kV Gamesa G87 DFIG [Gamesa 2013]), the power scenarios are obtained for each turbine. These scenarios represent an estimation of the hourly power production of a wind turbine that occurs 438 hours a year. For the sake of simplicity the same scenario for all wind farms is considered. However, the same scenario does not mean the same wind speed because of the different wind farm Weibull probability density function parameters.

Considering these scenarios, in Figure 4-16 a positive loss increase means that the power losses in the *reference control* scheme are higher than in the event of implementing a full network optimization control scheme. It can be observed that when wind farms provide reactive power in an optimal way, active power losses in the wind farm grid increase whereas in the HNet, losses decrease significantly. Due to the fact that the decrease in the HNet is significantly higher than the increase in the wind farm grid, total losses fall sharply. Nevertheless, with the current regulation in Spain there is no incentive to provide a control which optimizes the whole network since the loss reduction in the HNet is not allocated to wind farm owners.

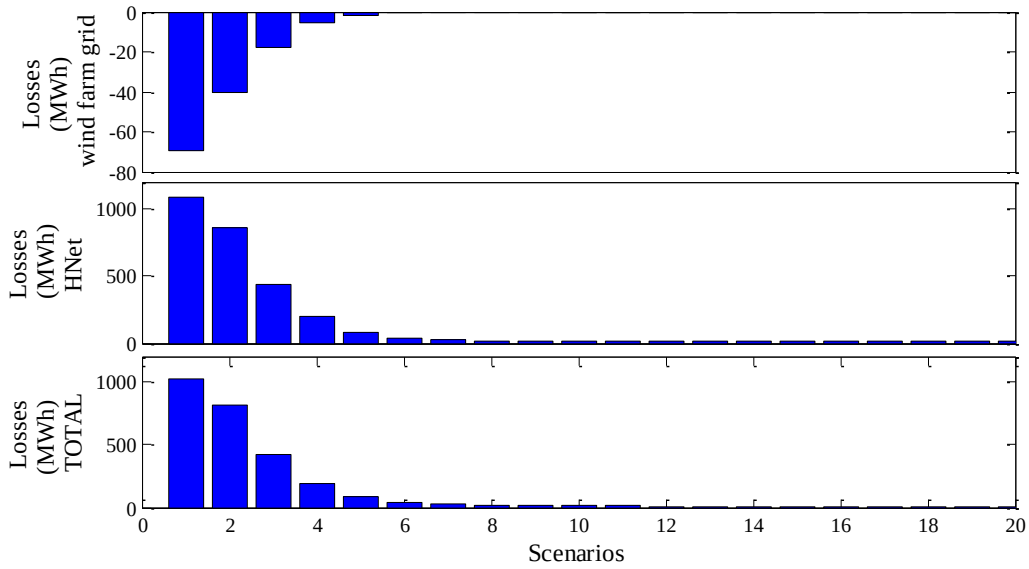

Figure 4-16 power losses in reference control scheme — power losses in power losses minimization control scheme in megawatt-hour.

In addition, for assessing the impact of implementing the Spanish grid code draft Figure 4-17 has been included. In this case the previous comparison is presented along with the (*reference control* scheme – *proportional control* scheme) comparison. As can be noted, in this case the internal wind farm power losses drastically increase without obtaining any benefit in the HNet. In fact, in the first three scenarios power losses also increase in this network.

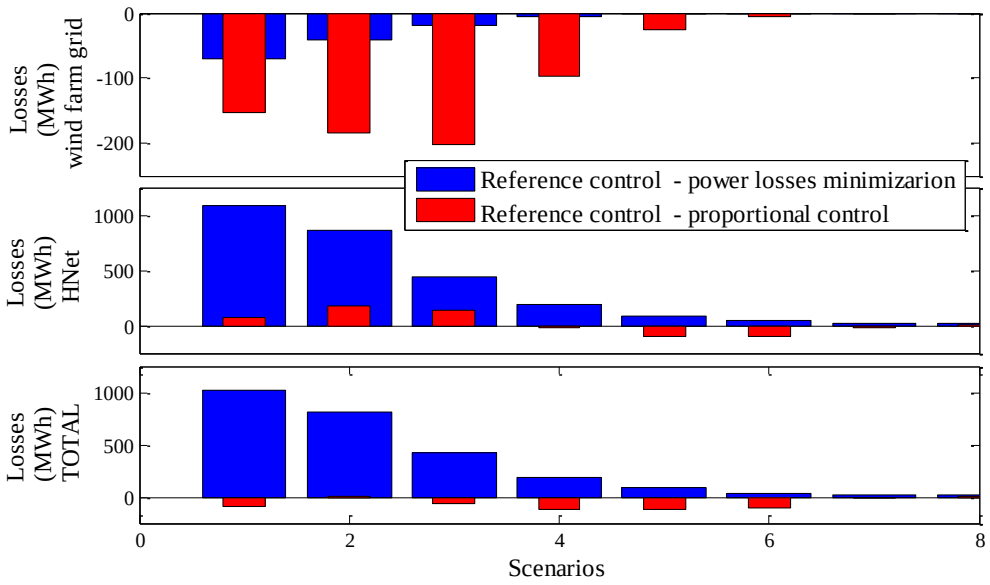

Figure 4-17 Power losses minimization scheme vs proportional control scheme

For understanding the impact of the different control schemes on each wind turbine Figure 4-18 is illustrated. This figure presents the reactive power delivered by each wind turbine of WF1 in the first scenario for all controls schemes. As expected, in the full

network optimization case, the wind turbines that are closer to the wind farm connection point generate more reactive power in order to diminish the losses. In addition, the reactive power generated is less than in the proportional control in all windmills as is depicted in Figure 4-18.

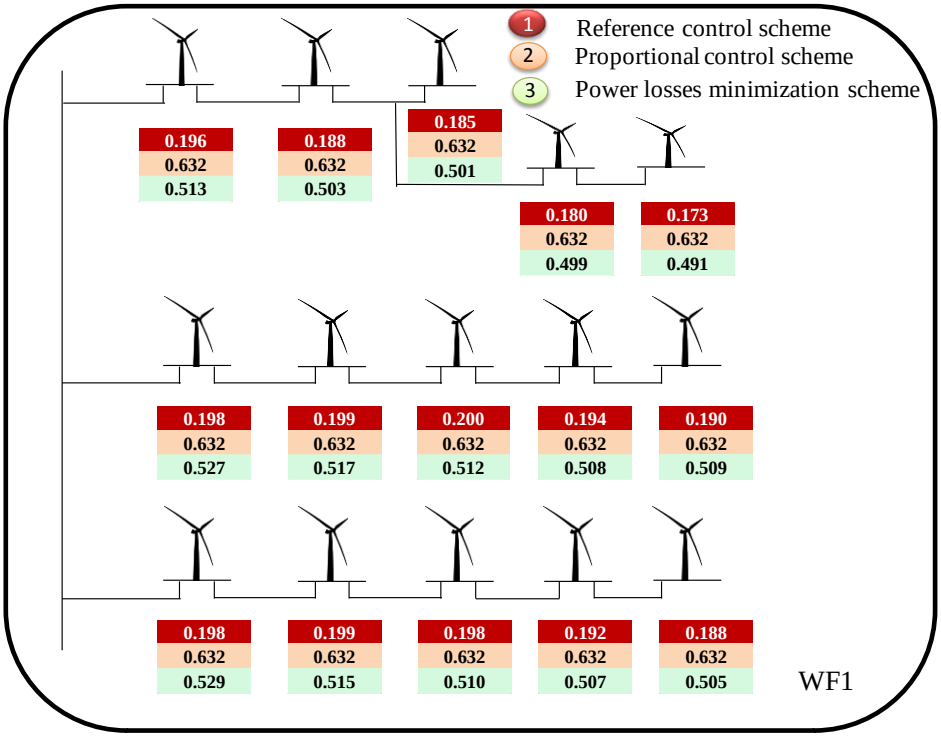

Figure 4-18 Reactive power provided by each wind turbine located in WF1.

4.4. SUMMARY AND CONCLUSIONS

This chapter has proposed an alternative method based on simple control rules which were obtained by inferring knowledge from an optimal scenarios data base. This simple approach avoids the necessity of solving an optimization problem in each time step. Moreover, a decentralized operation of the OLTC transformers can be made avoiding communication requirements constituting an important benefit with respect to an OPF.

For this purpose, two different types of variables have been assessed. Firstly, variables useful for explanation purposes but which require a previous power flow, assuming that all wind farms are operated at a unity power factor. Secondly, variables of easy implementation which do not rely in any previous computation. Concerning the first type this thesis has contributed with a novel variable, the active power losses from wind farm i to the transmission network bus (P_{lossi}). Concerning the second type the total HNet active power has been selected resembling the power factor concept. This factor is considered with respect to a global magnitude instead of the individual wind farm active power. In the particular case under study this last variable presents a high coefficient of determination, used for evaluating the adequacy of the regression rules. However, for other HNets its performance can deteriorate as has been seen, especially in the presence of loads or other wind farms that do not contribute to the global goal.

In addition to the regression rules employed for estimating the reactive power assignment, decision trees have been used for estimating the tap position of OLTC transformers. In these cases the explanatory variables considered are their voltage and current for 132kV/20kV transformers. Nonetheless, for the 400kV/132kV the V_{TNet} was also incorporated to enrich its performance. Hence, a totally decentralized operation of the OLTC transformers can be made avoiding communications. Both regression rules and decision trees are computed offline by simulation of multiple optimal scenarios of the power system. This simple control scheme clearly improves the current common operation obtaining negligible differences with respect to an OPF.

Summarizing, the methodology presented in this chapter is of value in a number of respects:

- Allows understanding the performance of the power flows in the grid under the different scenarios.
- Identifies which wind farms have a negligible effect on HNet losses. In those cases the reactive power set-point is fixed to zero independent of the scenario.
- May be of use in providing an initial point in the event of considering an OPF for each sample time.

CHAPTER 5

MINIMIZATION OF HARVESTING NETWORK IMPACT ON THE TRANSMISSION NETWORK

For various HNets it has been shown that some of them do not cause significant power losses, and also, that many do not have enough reactive capability to provide an effective voltage control function. For such cases, this thesis proposes a strategy that seeks to cause the minimum impact on the TNet, in which the settings of the control scheme are fixed independently of the operation scenario, meaning that no real time communications are required. For this purpose different control approaches, such as using power factor or voltage control, are analyzed in detail, from both the steady state and the dynamic perspective. In order to address these issues this chapter has been structured as follows. In section 5.1 the global methodology is presented outlining the incorporation of several controls schemes within the study. The global methodology is divided into two distinct studies in other to address both the steady state and dynamic perspectives. These analyses are presented subsequently in section 5.2 and 5.3 respectively.

5.1. METHOD OVERVIEW

A schematic summary of the methodology is given in Figure 5-1, with the first input being the wind farms' historic data. The holistic methodology can be spitted into two distinct studies one for obtaining the settings that affect the steady state performance and

another for obtaining the settings that affect the dynamic[9] performance of the control. For the steady state analysis an AC multi-period OPF is used, which provides an optimal solution for a whole set of scenarios. The settings considered depend on the control scheme selected. For the OLTC transformers, the voltage set-point or the ratio have been evaluated. On the other hand, for wind farms two possible alternatives have been studied. The first control possibility is a proportional control scheme. For this, the settings are: voltage set-point and droop. The second option is a power factor control scheme, in this case the settings correspond to the power factor of each wind farm.

The output of this optimization is used as an input for the dynamic analysis, which seeks to tune controller dynamic settings to best implement the desired steady-state regime. The dynamic settings tuned in this way are the time delay and dead band for the OLTC transformers, and, for wind farms, their controller time constant, which has been defined by a first order lag. All of the settings considered for each control scheme (dynamic and static) are summarized at the end of the section. In order to determine how the dynamic settings affect the performance of each control scheme a time domain simulation is needed. Dynamic settings should be tuned for avoiding undesirable performance such as unnecessary tap changes or voltage breaches. For this purpose metaheuristic algorithms have been identified as a good choice owing to their easy integration with simulators.

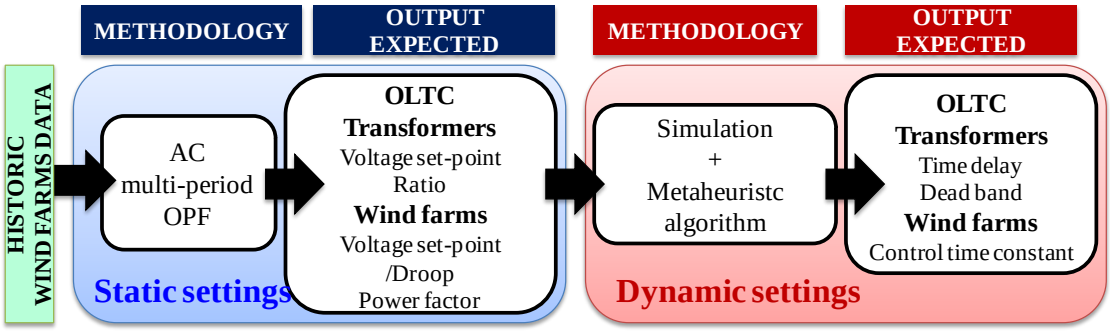

Figure 5-1 A schematic view of the complete proposed approach applied. Type B

There are various modelling differences between the two distinct analyses that must be noted. For instance, a fixed transmission-side voltage is stipulated for the steady state analysis. This value should correspond to the most probable one that may be encountered on the transmission system under study. In this chapter a nominal value has been selected for expository purposes. In order to evaluate possible controller interactions, voltage step-changes are modelled as part of the dynamic analysis. In both cases, varying wind outputs are considered whose temporal evolution is essential for the dynamic analysis.

[9] It should be noted that in this context the dynamic performance is closely dependant on the OLTC transformers. Hence, the time frame considered (a few minutes) is higher than what is normally considered (e.g. a short-circuit is cleared in milliseconds)

In subsection 3.2.1 some control scheme possibilities were already discussed. Those control schemes are classified into two types. The ones employed for computing the control limits (power losses minimization control scheme and PQ chart) and the controls representative of the current (*reference control*) and near future situation (*proportional control*). In all cases the most appropriate settings for each operational scenario and objective function were considered. In this chapter a detailed analysis of different control schemes is carried out, assuming that the settings are fixed in all scenarios. Recalling subsection 3.2.1, in the *reference control scheme* wind farms maintain a unity power factor, and the transformers perform all voltage regulation functions within the HNet. Hence, the network's performance can be easily enhanced by allowing wind farms to provide a different power factor, which can be optimally determined with the AC multi-period OPF. The same power factor (Pf) for all wind farms located in the same bus has been assumed, thus guaranteeing that all of them contribute reactive power in the same proportion. This control scheme is named *power factor* throughout this thesis. Both control schemes are depicted in Figure 5-2, which also shows where the OLTC transformers control the voltage.

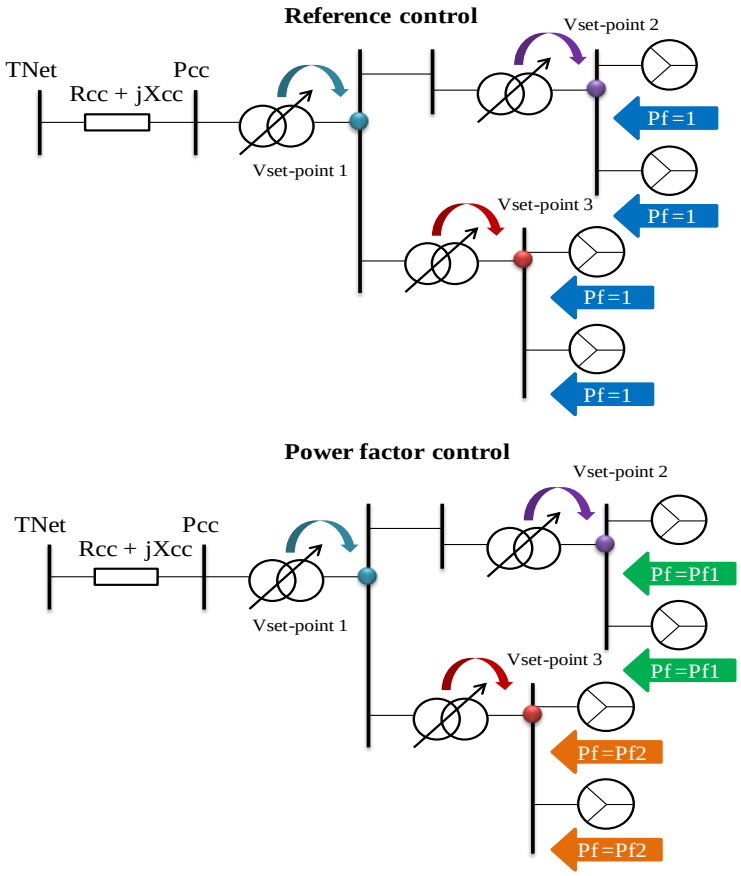

Figure 5-2 Reference and power factor control

The voltage set-point of each transformer is optimally determined individually (it is not necessary for all OLTC transformers to have the same voltage set-point). The power factor of each wind farm is equal to one for the *reference control* and is optimally determined under *power factor control scheme*.

The possibility of enabling voltage control functionality for wind farms was first analyzed in Chapter 3 with the proportional control. In this chapter this control scheme is extended by considering different alternatives. One possibility is that each wind farm maintains a set-point at its own connection bus: the set-point of different wind farms located at the same bus must thus be equal to avoid reactive power loop flows. This configuration is named *local voltage control* throughout this thesis. Under this scheme, the current operation of those transformers that directly connect wind farms cannot be maintained, because they would control the same bus that wind farms are now controlling. Although other transformers may maintain conventional tap-changing operation, for clarity's sake this chapter considers the same strategy for all transformers located in the HNet. Thus, a constant, optimally-selected tap position for all transformers is considered. If the current operation of the transformers is to be maintained wind farms must control a separate bus. One possibility is having each wind farm directly controlling the remote bus that connects the HNet to the transmission network; this scheme is here named *remote voltage control*. Both control schemes are shown in Figure 5-3.

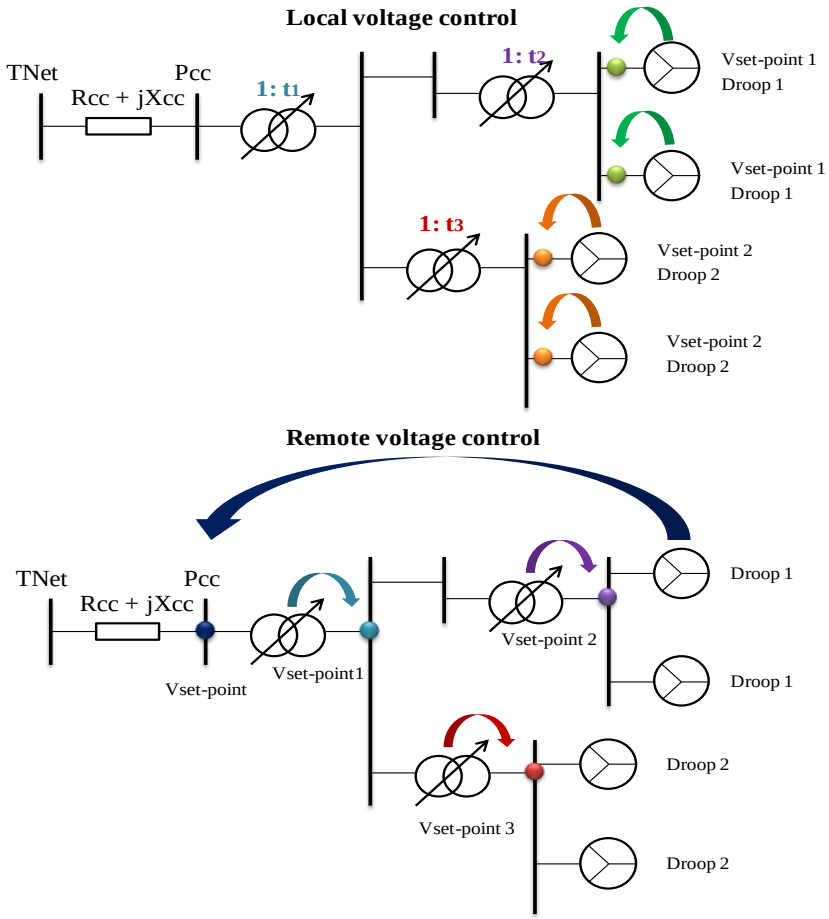

Figure 5-3 Local and remote voltage control

Four distinct paradigms of reactive power control are considered in this work, such that meaningful comparisons of their dynamic performance can be made. For each control scheme, the objective in view is a consistent voltage at the point where the HNet interfaces with the transmission system, such that the export of active power does not perturb the voltage magnitude there. As will be seen in the dynamic analysis wind farms

can contribute to reduce the transmission level voltage deviation. However, that contribution is not necessarily the optimal one: as will be seen, by comparing these results with the results obtained in the subsequent chapter, a better pro-active voltage control strategy can also be evaluated. These four reactive power control paradigms are classified into two different approaches: power factor or voltage control schemes. The settings that will be calculated trough this chapter are summarized in Table 5-1.

Table 5-1. Variables optimized in the different controls schemes

	OLTC Transformers				Wind farms control			
	Ratio	**Voltage set-point**	**Time delay**	**Dead band**	**Power factor**	**Voltage set-point**	**Droop**	**Time constant**
Reference control	-	static setting	dynamic setting	dynamic setting	-	-	-	-
Power factor control	-	static setting	dynamic setting	dynamic setting	static setting	-	-	-
Local voltage control	static setting	-	-	-	-	static setting	static setting	dynamic setting
Remote voltage control	-	static setting	dynamic setting	dynamic setting	-	static setting	static setting	dynamic setting

5.2. STEADY STATE ANALYSIS

For this assessment the AC multi-period OPF has been used, which is explained in subsection 5.2.1. This method requires different representative scenarios of active power production and transmission network voltage, considering their occurrence probability. Wind farm power outputs correlations should be evaluated to provide this (see Appendix E). For this analysis, recalling Chapter 3, a HNet of type B should be considered. HNet2 (from type C) has been selected for comparison purposes as was already indicated in Chapter 3. Subsection 5.2.2 discusses the results for this network.

5.2.1. AC MULTI-PERIOD OPF

The main difference between the well-known OPF and the AC multi-period OPF is the incorporation of several scenarios. This means, that whereas the OPF gives the optimal control variables for just one, concrete, scenario, the AC multi-period OPF gives simultaneous consideration to multiple network conditions. As such, any derived control settings will be feasible, and optimal, across the full set of scenarios considered. Ideally, these scenarios should consider all operational conditions (i.e., wind outputs of all wind farms and various transmission voltages). Focusing on active power scenarios, it must be noted that the same total active power production can be obtained from various different individual wind farms contributions as is shown in Figure 5-4 and Figure 5-5. For instance, Figure 5-4 depicts the active power delivered by three wind farms in three different scenarios, all of them sum up to the same total active power production. However, focusing on a certain wind farm (WF1), quite different active power scenarios can be appreciated. This means that active power scenarios form a plane, as is also depicted in this figure (the total active power x wind farms scenarios considered).

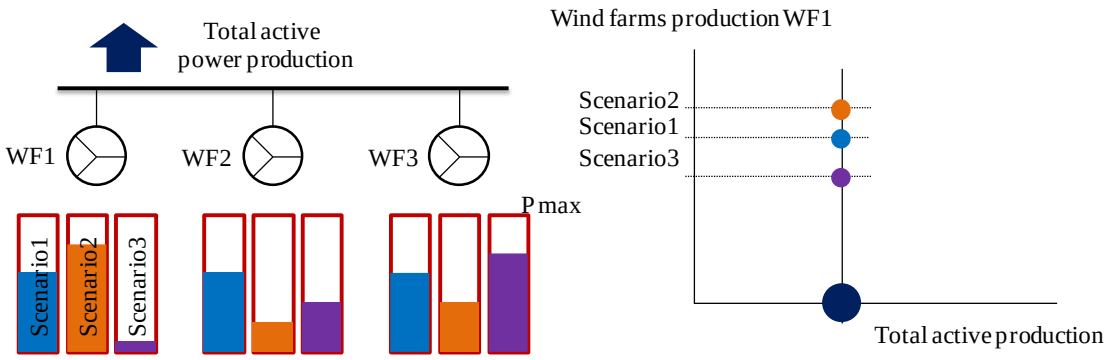

Figure 5-4 Active power scenarios

In addition, the voltage at the transmission voltage (V_{TNet}) must be also considered. Therefore, the set of all scenarios form a cube. Too wide a range of scenarios would incur in the impossibility of achieving a feasible solution. In that sense active power scenarios (the plane formed by the total active power and the specific wind farms scenarios) and the transmission network voltage are decoupled, as is depicted in Figure 5-5. In the event of considering just one voltage this cube is reduced to a plane (depicted in green). Thus, an optimal control scheme could be implemented with low communication requirements. Those requirements depend on V_{TNet} variation and the possibility of estimated it. As an example, several possibilities arise:

- There are unpredictable large voltage variations
- V_{TNet} variation depends on the seasons
- V_{TNet} variation depends on the hours (e.g. the voltages increase during the night whereas they decrease during the day)

It is clear that if those variations are unpredictable communications cannot be avoided, being necessary to telemeter V_{TNet} so settings can be updated in realtime. In this case, as has been already propose in [Di Fazio et al. 2013], the optimal settings for a specific transmission network voltage are fixed for all wind production scenarios (green plane Figure 5-5). However, these settings change when a large voltage excursion is identified.

For the other two options, the settings modifications can be scheduled in advance do not relying on the communications.

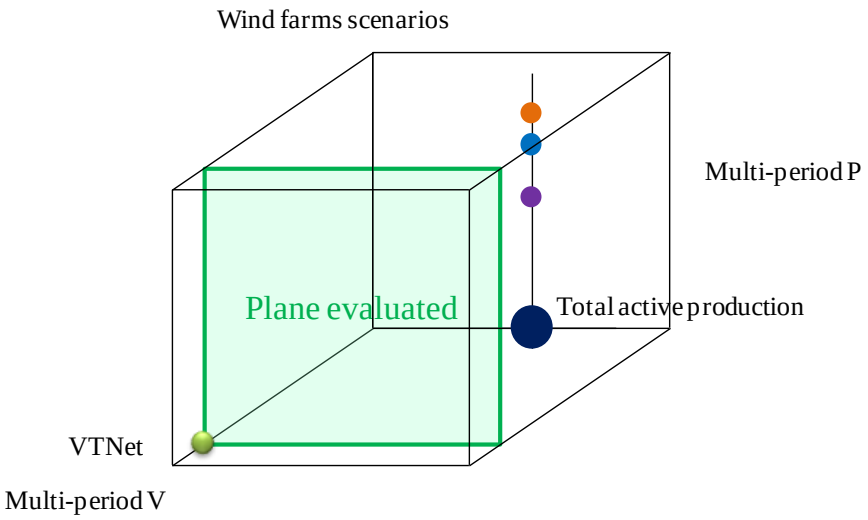

Figure 5-5 Multi-period scenarios evaluated

Considering these scenarios, the objective function used is the minimization of voltage deviations at the HNet common coupling bus formulated as follow:

$$Minimize \sum_{t} (V_{setpoint} - V_{Pcc,t})^2 \tag{5-1}$$

Where $V_{setpoint}$ is the desired set-point at the common coupling bus and $V_{Pcc,t}$ is the actual voltage at this bus for period *t*. In this thesis it has been assumed that $V_{setpoint}$ is equal to the most probable V_{TNet}, value, which has been assumed as 1 p.u.. In the dynamic analysis V_{TNet} voltage excursions of +/- 3% are evaluated considering the same settings in order to assess their robustness. It is important to outline that this objective function is equal to minimizing the HNet's impact on the TNet in the event that $V_{setpoint}$ is equal to V_{TNet}, otherwise the wind farms provide reactive power support to compensate the voltage deviation ($V_{setpoint} - V_{Pcc,t}$).

It must be noted that achieving an approximately consistent voltage profile at a connection bus simply requires the appropriate P/Q relationship through the line that connects the common coupling bus to the wider transmission system [Bollen, et al. 2011]. Hence, the aim of this thesis is evaluate how this relationship can be established using different control approaches.

5.2.2. RESULTS AND DISCUSSION

The steady state settings for all control schemes presented in section 5.1 are summarized in Table 5-2, considering a constant transmission voltage equal to 1 p.u. and a set-point also equal to 1 p.u. It can be seen that the best scheme from the transmission point of view is the *remote voltage control*, which achieves the minimal objective function. It is interesting to note that the *power factor* case has a slightly better performance than the *local voltage control* scheme This result may at first surprise, however it must be noted that in the event of a network with a non-negligible resistance

(as is the case of the HNets) the *local voltage control* introduces a broadly linear P/Q relationship which resembles *power factor control*, and which may in fact offer less desirable performance. Each of the various control schemes establishes a certain relationship between three key variables – the aggregate active and reactive power flows, and the external voltage at the transmission level. Exploring these relationships graphically, as done throughout this subsection, offer some insight on the differing values achieved for the objective function.

Table 5-2. Steady state settings considering HNet2

		Power factor approach		**Voltage control approach**			
		Reference control	**Power factor control**	**Local voltage control**		**Remote voltage control**	
		Voltage Setting	Voltage Setting	**Ratio**		**Voltage Setting**	
TRANSFORMERS	T1	1.048	1.046	**0.955**		**1.042**	
	T2	1.050	1.050	**1.007**		**1.050**	
	T3	1.050	1.050	**1.002**		**1.050**	
	T4	1.050	1.050	**1.008**		**1.050**	
	T5	1.050	1.050	**1.006**		**1.050**	
		Power factor	Power factor	**Voltage Setting**	**Droop**	**Voltage Setting**	**Droop**
WIND FARMS	WF 1-3	1.00	1.00	**1.050**	**2.39**	**Vset-point**	**2.39**
	WF 4-7	1.00	1.00	**1.050**	**2.39**		**2.39**
	WF 8-9	1.00	0.97	**1.050**	**2.91**		**2.91**
	WF 10-11	1.00	1.00	**1.050**	**2.91**		**2.91**
	WF 12	1.00	0.95	**1.046**	**1.00**		**1.00**
OBJECTIVE FUNCTION		2429.50	305.36	**343.57**		**5.23**	

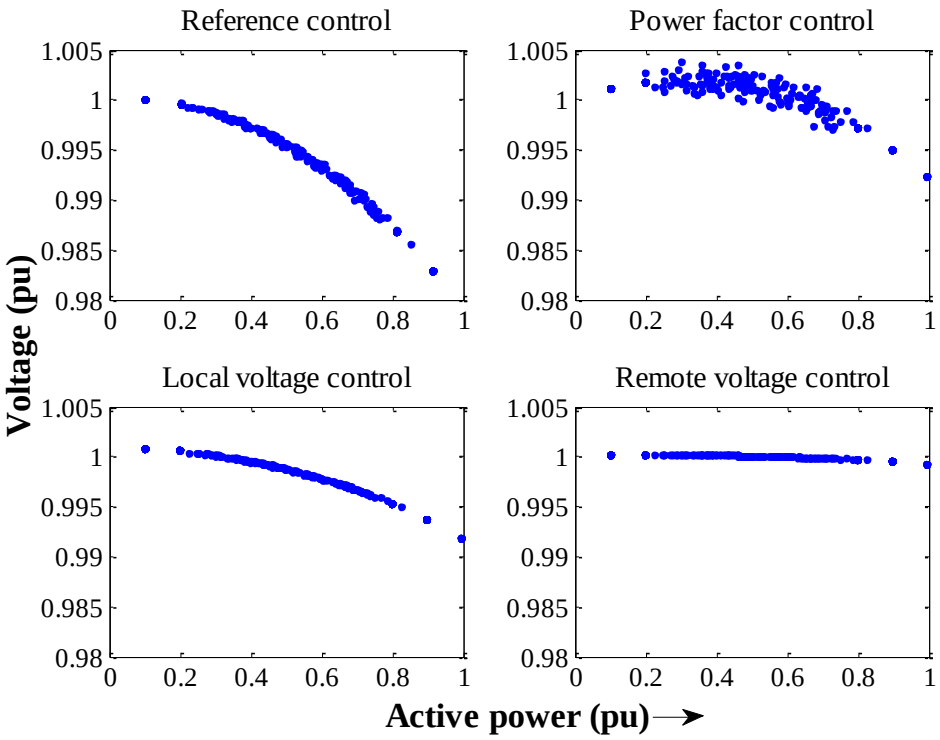

Figure 5-6 PV characteristic of the HNet

As has been previously mentioned, the enhanced *power factor control scheme* (where the power factor is a free variable not fixed to unity as in the *reference control*) achieves a better performance than the *local voltage control*, meaning that increasing the complexity of the control may not be necessary. The relation between P, V and Q is next presented. All magnitudes are measured at the HNet common coupling bus (Pcc)

Figure 5-7 and Figure 5-8 present PV and QV characteristics, respectively, for all control schemes, confirming this fact. In all cases a constant V_{TNet} equal to 1 p.u. has been assumed (i.e. the green plane depicted in Figure 5-5 has been evaluated). From Figure 5-7 it can be surmised that all the control schemes improve the connection point voltage compared to the existing scheme, with less deviation evident in the vertical dimension. Nonetheless, a significant spread appears in the event of implementing a *power factor control* scheme. It should be noted that in this scheme the power factor remains fixed, regardless of the wind farm voltage. Hence, the voltage is subject to the active power variability (note that the same total active power production can be obtained for different individual wind farms production) as can be appreciated in this figure. Whereas for a voltage control scheme the reactive power injection depends exclusively on the voltage, for a power factor scheme it should also complain with PQ relationship. Also Figure 5-7 shows that the reactive power consumption at the common coupling bus in the worst scenario is reduced 54.4%, 50.6% and 98.4% for the *power factor control*, the *local voltage control*, and the *remote voltage control* cases, respectively.

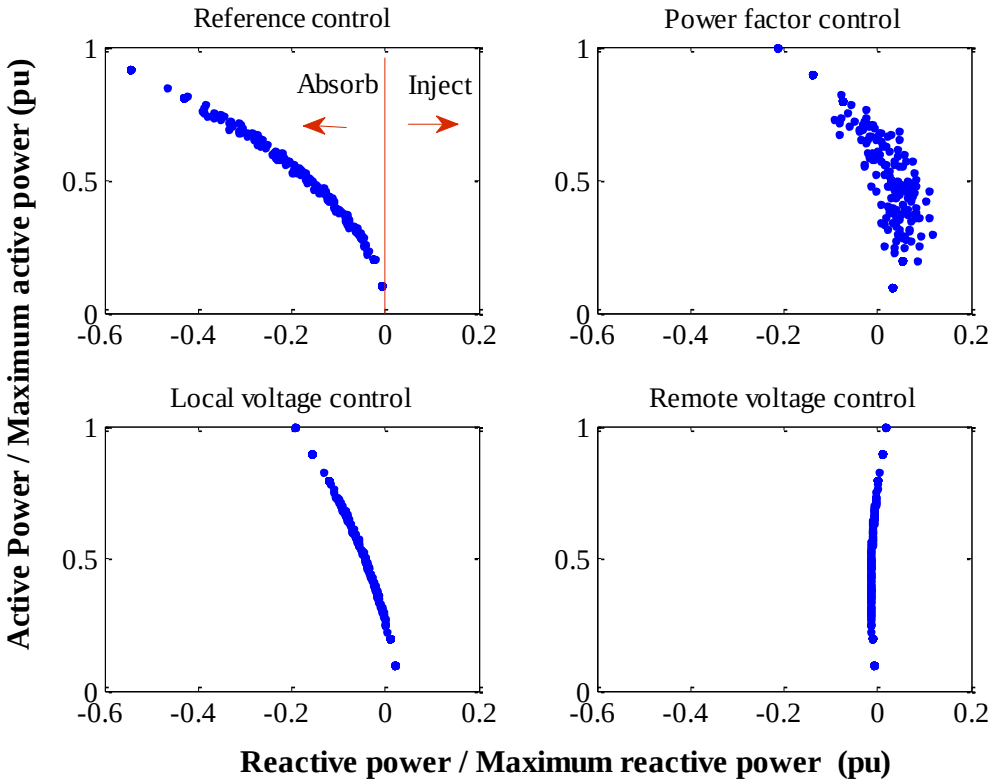

Figure 5-7 PQ characteristic of the HNet at the Pcc

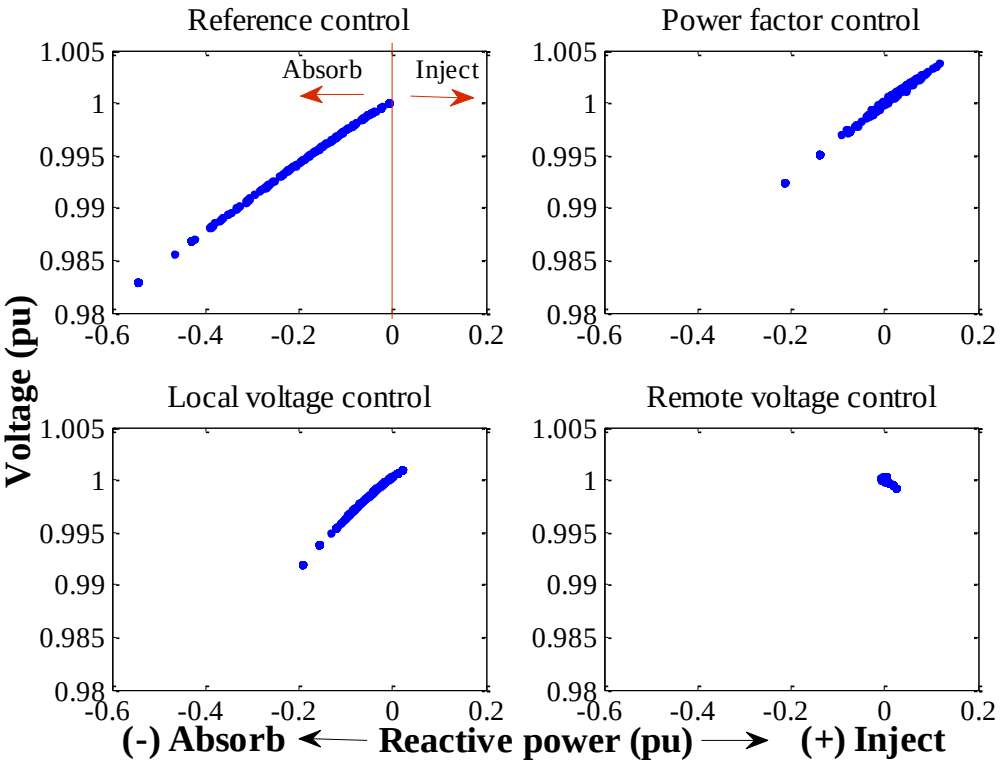

Figure 5-8 QV characteristic of the HNet at the Pcc

The PQ characteristics of the control schemes also differ significantly as can be seen in Figure 5-8. It can be noted that whereas the *power factor* and the *local voltage control* have a similar performance from the reactive power point of view the *remote voltage control* has a different performance. This last control scheme maintains a near-zero reactive power exchange level at all times.

In order to determine the implications that the voltage control schemes (*local* and *remote*) have for wind farms, Figure 5-9 and Figure 5-10 are presented. In these figures the PQ characteristic of four wind farms located in different buses are depicted for the *local voltage control* and the *remote voltage control* respectively. Control schemes in which the reactive power assignment depends on the voltages. In these figures it can be seen that whereas in the *remote voltage control* all wind farms generate reactive power, in the *local voltage control* WF12 is absorbing reactive power in many scenarios. This fact is due to the voltage set-point of WF12 is below its nominal value although is the nearest wind farm to the transmission network.

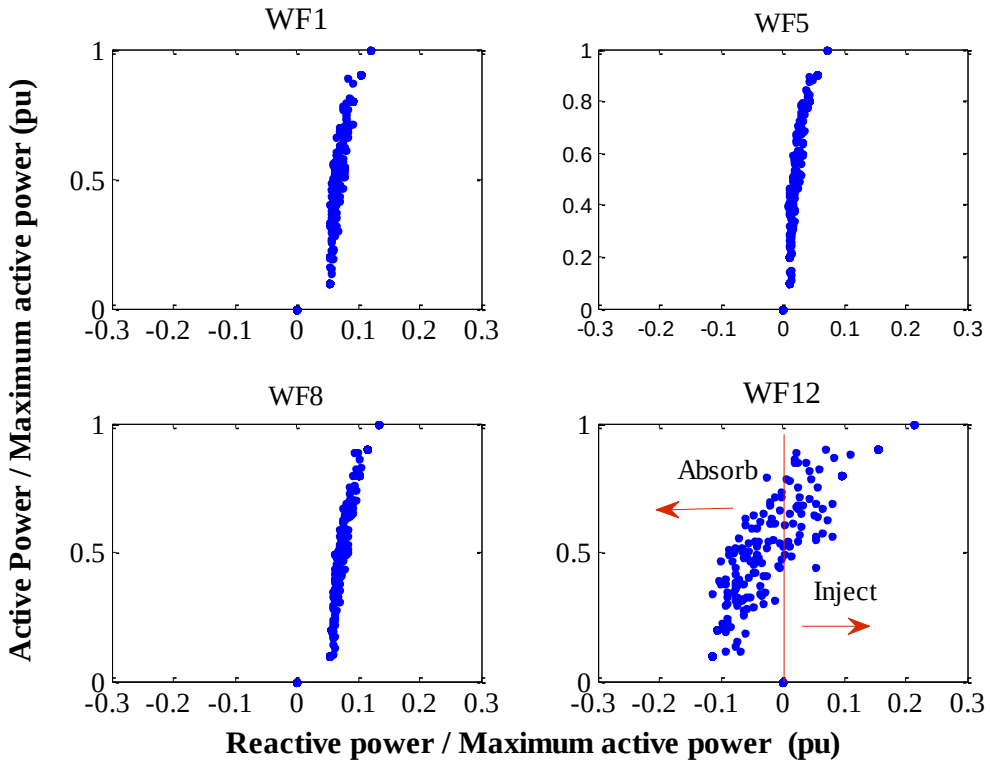

Figure 5-9 PQ characteristic of the local voltage control

To explore this fact, a sensitivity analysis, which is summarized in Table 5-3, has been undertaken. In this table it can be seen that if the voltage setting of WF12 is its maximum value, the voltage in bus 3 is the highest. However, it can be noted that the ratio of T1 is the smallest; hence the voltage at bus 2 is lower than in the optimal case. On the other hand, if the ratio of T1 is increased, then the voltage in bus 3 decreased. Consequently, the final objective function value, over all periods, decreases.

Table 5-3. Sensitivity analysis of the local voltage control

	Optimal solution	Maximum voltage setting	Increasing the ratio setting
Voltage 1	1	1	1
Voltage 2	0.9929	0.9926	0.9929
Voltage 3	1.0393	1.0399	1.0374
Ratio T1	0.9554	0.9543	**0.9570**
Voltage set-point WF12	1.0459	**1.05**	1.0439
Objective function	343.57	363.24	344.63

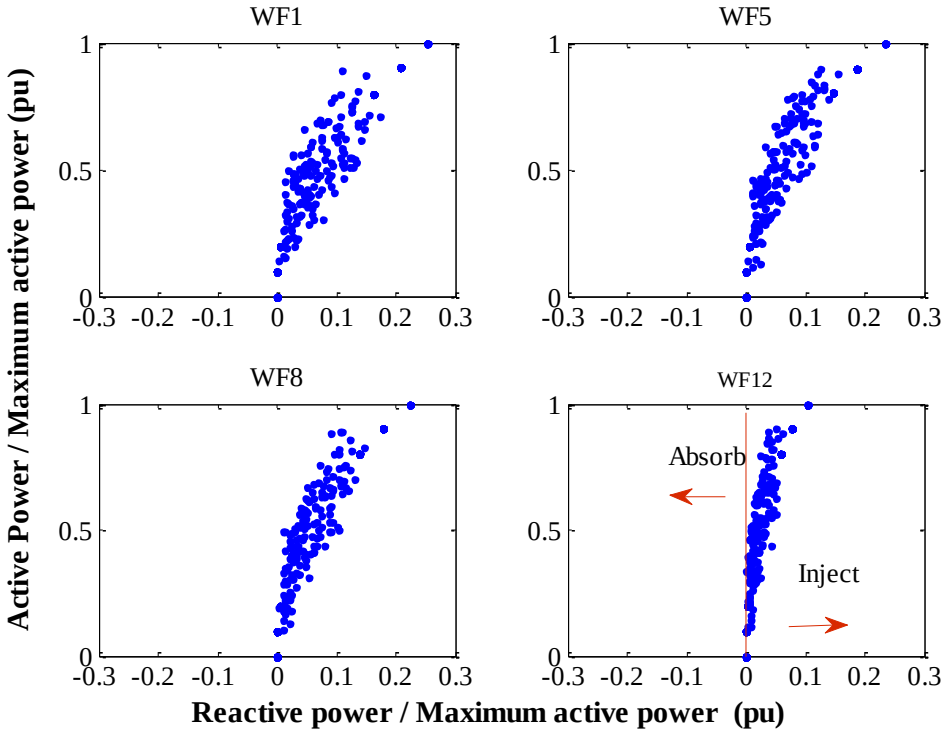

Figure 5-10 PQ characteristic of the remote voltage control

5.3. DYNAMIC ANALYSIS

Once these static settings are known the dynamic analysis should be carried out to tune the dynamic parameters: dead band, time delay for OLTC transformers and time constant for wind farms. For this, wind farms' active power temporal patterns are required (see Appendix E[10]).

[10] The control scheme performance considering the final tuned dynamic settings has been also analyzed for other less demanding active power patterns. In those cases less control activity is seen checking the adequacy of the settings selected.

In order to explain this analysis the section has been structured as follows. Firstly, in subsection 5.3.1, the control schemes' performance is presented, considering the different objectives to be minimized. For clarity this chapter only presents the *remote voltage control* scheme (the best one from the steady state perspective). The other schemes can be found in Appendix G. Next, the tuned dynamic settings obtained with methauristics algorithms are summarized in subsection 5.3.2. Finally, focusing again on the *remote voltage control* scheme, the initial and tuned settings are compared in subsection 5.3.3.

5.3.1. OBJECTIVE TO BE MINIMIZED

In Figure 5-11 the dynamic performance of the *remote voltage control* scheme, considering transmission voltage step excursions of +/- 3%, and the representative active power patterns (see Appendix E), can be seen. In this case the dynamic settings have been selected based on [Van Cutsem, et al. 1998]. This book mentions that the usual practice in coordinating two cascade transformers is to make the higher voltage one operate faster (normally between 20-40s). This book suggest 20s for the EHV/HV transformer (in our case 400kV/220kV) and 50s for HV/MV transformers (in our case 220/30kV). Moreover a dead band of 1.35% for all transformers and a time constant of 65s for all wind farm controllers have been considered.

In this scheme wind farms provide reactive power proportional to the voltage deviation at the common coupling bus, and the current OLTC transformers control strategy is maintained (i.e., they control their low voltage side). This means that in those periods where the voltage differs from its nominal value, reactive power support is contributed. Note that the optimal strategy (where the HNet has minimum impact on TNet) has been designed for the nominal transmission voltage. However, that reactive power support will be enhanced in the pro-active voltage strategy as will be seen in the next chapter.

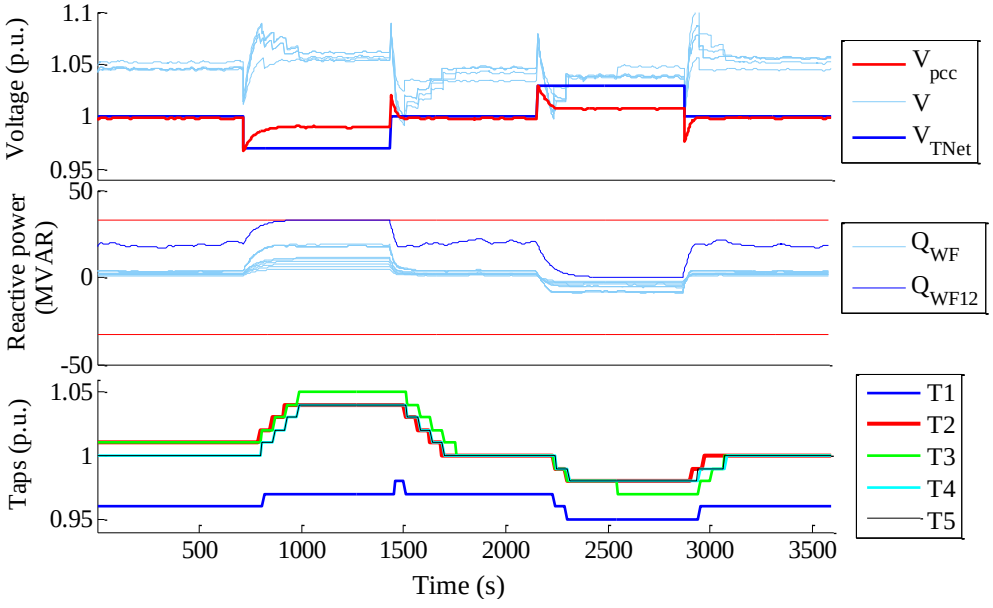

Figure 5-11 Remote voltage control dynamic performance

As a result, the number of tap changes and the time in which voltages exceeds the limits increases dramatically. This fact can be seen by considering the period that goes from 500s to 1500s. In this period the transmission network voltage drops to 0.97 p.u., consequently, to mitigate this deviation the wind farms inject reactive power, so increasing their voltage. Those voltage increase, are, in turn, compensated by the OLTC transformers, which maintain those voltages near their set-points.

In spite of considering sensible settings which aim to avoid unnecessary taps changes, it can be seen that not all excess tapping has been avoided (see t=1500s), significant voltage breaches can be seen which should be mitigated. Hence, there is a substantial margin for improving the network's performance. This margin is visualized in Appendix G for all control schemes. In the worst case (*reference control*) 4 taps are eschewed in one hour. To reduce the number of tap changes, the OLTC transformers' time delays and dead bands could be increased. However, this entails a cost. Increasing the dead band implies more deviations from the optimal operational point defined by the AC multi-period OPF. If the time delay is increased the time for which the voltage breaches persist is also increased. Thus, a compromise between these three objectives, total tap changes, transformers voltage deviation and voltage breaches, must be found.

This scheme has a clear advantage with respect to the one proposed in most grid codes (*local voltage control*); the lack of oscillations. These oscillations could be significant and although they can be damped, this is at the expense of slowing the control response, as is discussed in Appendix E. The formulation of each objective, including the oscillations (only applicable in the *local voltage control* scheme), is presented next.

Total tap changes =

$$\sum_{t=0}^{t=t_f} \sum_{TF=1}^{TF=N_{TF}} TC_{TF}$$

Transformers voltage deviation =

$$\sum_{t=t_{oSS}}^{t=t_{fSS}} \sum_{TF=1}^{TF=N_{TF}} \left(V_{ct\,TF}{}^{ref} - V_{ct\,TF}(t)\right)^2$$

Voltage breaches =

(5-2)

In the event that the voltage surpasses the dynamic limits

$$W3 \cdot \sum_{t=0}^{t=t_f} \sum_{bus=1}^{bus=N} t \cdot (V_{lim} - V_{bus}(t))^2$$

Oscillations =

$$\sum_{t=t_{oSS}}^{t=t_{fSS}} \sum_{WF=1}^{WF=N_{WF}} abs(Q_{WF}(t) - meanQ_{WF})$$

Where TC represents the tap changes of a specific transformer (TF) over a specific time period ($0 - t_f$). The transformer voltage deviation objective is only evaluated when the steady state has been reached ($t_{0SS} - t_{fSS}$). In the second and third terms the square of the voltage differences are considered, penalizing high deviations. By contrast, in the fourth term this consideration has not been made because the oscillations should be always totally damped independently of their size.

5.3.2. TUNED SETTINGS

The dynamic settings for each control scheme (see Table 5-1) have been tuned using two different metaheuristic algorithms: genetic and MOPSO. Both of them are explained in detail in Appendix F. The first one, the genetic algorithm, seeks a unique solution. This fact does not mean that multi objective problems cannot be solved. However the trade–off among the different objectives must be defined in advance, by assigning each a different weight factor. However defining those weights is not always easy. On the other hand, the MOPSO algorithm is well suited to multi-objective functions. As a result, the non-dominated solutions (which correspond to the Pareto frontier in the event of two objectives) are obtained. Based on this, the genetic algorithm seems unnecessary. Nonetheless, in this thesis it has been used to obtain an important insight on the dynamic setting's tendency, the analysis of which is presented in Appendix G. Table 5-4 gathers the tuned settings obtained in all schemes by this algorithm (considering the weights mentioned in Appendix G).

In each control scheme, the T1 transformer (400/220kV) has a lower time delay than the rest of transformers, as was expected. In fact it reaches the minimum value permitted, 10 seconds. Considering the others transformers, the higher time delay is obtained for the *power factor control* for coping with the active power variability. Contrarily, the lowest values are obtained for the *remote voltage control*, to reduce voltage breaches. Similar conclusions can be drawn for the dead band settings. In this case almost the same results are achieved for the *reference* and *remote voltage control* schemes, whereas for the *power factor* scheme higher values are seen, to avoid unnecessary tap changes. Finally, a wide range of wind farms controllers' time constant is seen, implying a slower response for the *local voltage control* scheme, to avoid oscillations.

Table 5-4. Final dynamic settings optimized for the different control schemes

	T1 (400/220kV)		**220/30kV transformers**		**Wind farms**
	Time delay (s)	**Dead band (%)**	**Time delay (s)**	**Dead band (%)**	**Time constant (s)**
Reference control	**10**	**1.1**	**35-55**	**1.3-1.5**	-
Power factor control	**10**	**1.4**	**60-75**	**1.45-1.6**	-
Local voltage control	-	-	-	-	**55-80**
Remote voltage control	**10**	**1.1**	**15-25**	**1.3-1.6**	**25-80**

This information is extended for the *reference*, *power factor* and *remote voltage control* schemes[11] with the MOPSO algorithm. The whole set of non-dominated solutions (solutions in which none of the objectives can be improved without degrading the others) are depicted in Figure 5-12. It can be seen that *reference* and *power factor control* have a similar performance. However a significant increase of tap changes and voltage breaches is seen for the *remote voltage control* scheme revealing the cost of improving the steady state performance.

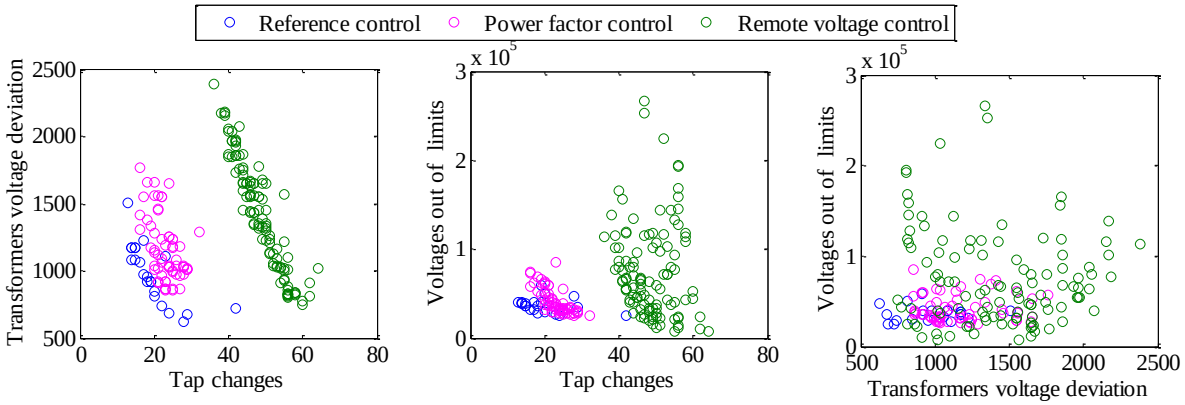

Figure 5-12 Comparison of non-dominated solutions: Reference, power factor and remote voltage control schemes

5.3.3. INITIAL VS TUNED SETTINGS

In order to better see the improvements obtained by tuning the dynamic settings, Figure 5-13 is included for the *remote voltage control* scheme. The other schemes are presented in Appendix G. In this figure the control scheme performance with the tuned settings (the mean dynamic settings obtained with the genetic algorithm) are compared with an initial sensible solution intended to avoid unnecessary tap changes. Both solutions have been located within the search space in Figure G-17, showing the quality of the initial solution considered and the margin for the improvement available.

In the first subplot, the voltage at one bus, where a wind farm is connected, is depicted. In addition, V_{TNet} is included, showing how the fast action of OLTC transformers is essential for mitigating voltage breaches. For the sake of simplicity, the reactive power delivered by one wind farm and the ratio of one transformer are depicted in second and third subplot respectively. It should be emphasized that all these magnitudes do not correspond to the same bus. Hence, a transformer tap movement may not directly correspond to any depicted voltage variation. With this figure it is clear that the dynamic settings can be tuned to improve the three aforementioned objectives. Moreover, the non-dominated solutions set allows the identification of the trade-offs between them.

[11] note that in the *local voltage control* only the oscillations are minimized

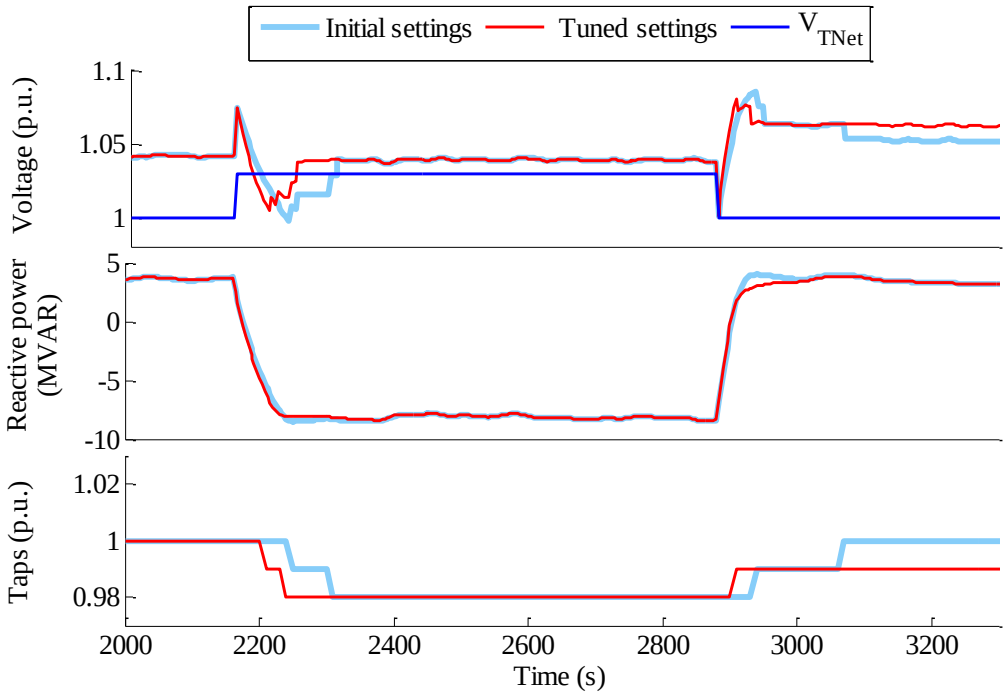

Figure 5-13 The remote voltage control scheme. Initial settings vs final settings

5.4. SUMMARY AND CONCLUSIONS

This chapter has provided a holistic analysis of four different control schemes: *reference control*, *power factor control*, *local voltage control* and *remote voltage control.* These schemes can be classified into two distinct groups, those control schemes that maintain a certain power factor and those who perform voltage control. For each control scheme, fixed parameters, of both static and dynamic settings, have been obtained. The static settings have been optimally determined by using an AC-multi-period OPF, whereas for tuning the dynamic settings two different meta-heuristic algorithms have been used.

From the steady state analysis it can be surmised that the best option is a voltage control where wind farms control the voltage at a remote bus. Otherwise, of the localized control schemes that do not require telemetry, *power factor control* has a better performance: this is a key result. In fact, a recent Spanish proposal (P.O. 7.5) [REE 2011] aligns with the *local voltage control* approach, which has not been seen to be the best option (It achieves a worse objective function than a power factor scheme). Moreover, the dynamic analysis reinforces this conclusion (see Appendix G). In the event of implementing a *local voltage control* scheme, to avoid oscillations, very slow controller actions are necessary.

Finally, it should be noted that an ambitious voltage control scheme like the *remote* one is not entirely desirable, as tap changes and voltage breaches are significantly increased

CHAPTER 6

PRO-ACTIVE VOLTAGE CONTROL

In the previous chapter, by using the AC multi-period OPF, optimal control schemes in which all settings, both static and dynamic, remain fixed were evaluated. Hence, additional communication requirements are avoided (only in the *remote voltage control* scheme, a remote measure must be sent to wind farms). In those control schemes a minimization of the HNet's impact on the TNet strategy was pursued. That approach, as explained in Chapter 3, is selected for those HNets with a "poor" PQ chart at the common coupling bus, which also do not suffer significant power losses. Nonetheless, for HNets with a substantial PQ chart (Type C) a more ambitious strategy, in which the whole HNet resembles a conventional plant that could be integrated in an existing TNet hierarchical voltage control, can be followed. In such cases the control performance could be enhanced if the static settings change in accordance with the operational conditions (see Appendix H). For that purpose a central controller for the HNet is proposed that operates in a way similar to the secondary loop of the current TNet hierarchical voltage controller.

In order to tackle these issues the chapter is organized as follows. In section 6.1 the mthod overview is performed. Then, section 6.2 presents the central controller components: wind farms and OLTC transformers. Each one is explained in section 6.3 and 6.4, respectively. Subsequently, section 6.5 presents the results, including the central controller performance and its dynamic coordination. Finally, a summary and the conclusions are provided in section 6.6.

6.1. METHOD OVERVIEW

A schematic summary of the methodology is given in Figure 6-1. Comparing this figure with the analogous one presented in the previous chapter (Figure 5-1) it can be seen that the offline process required for determining the static settings is not needed. Instead, a central controller (explained in detail in section 6.5) is used online in real time, by using quadratic programming techniques (this resembles the well-known secondary voltage control loop). As a result optimal settings for each period (sample time) are obtained. These settings are adaptive, thus, not always determine the steady state. Nevertheless, have been also termed *static;* using previous chapter terminology. The static settings correspond to the reactive power set-points of each wind farm and the voltage set-points of the OLTC transformers.

The existence of a central controller does not avoid the need for determining the dynamic settings. As in the previous chapter, these settings correspond to the time delay and dead band for the OLTC transformers and, for wind farms, the time constant of their internal reactive power controllers. For tuning those parameters the MOPSO algorithm, as explained in Appendix F, is used jointly with simulations in which the online central controller is considered.

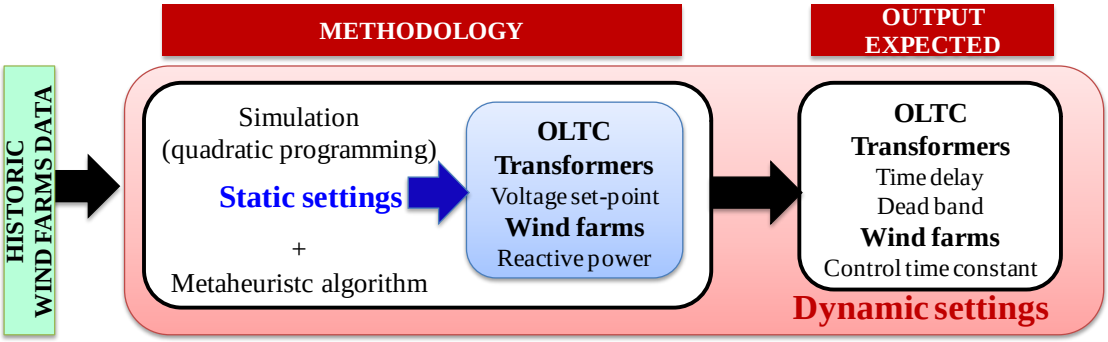

Figure 6-1 A schematic view of the complete proposed approach applied. Type C

This information is summarized in Table 6-1, where the settings and the method employed in their determination are indicated. In this table, in addition to the central controller, the *remote voltage control* scheme, as presented in the previous chapter, has been also included for comparison purposes. The same offline process followed for evaluating the dynamic settings is used. Contrarily, important differences can be seen in the static settings, now calculated online in real time. In this chapter the reactive power set-points are directly calculated by the central controller. Hence, a constant relationship, i.e., the droop, between the voltage deviation at the common coupling bus and the reactive power provided by each wind farm is not considered.

Table 6-1. Settings to be optimized

	OLTC transformers			Wind farms control			
	Voltage set-point	**Time delay**	**Dead band**	**Reactive power**	**Voltage set-point**	**Droop**	**Time constant**
Chapter 5 Remote voltage control	**static setting**	**dynamic setting**	**dynamic setting**	-	**static setting**	**static setting**	**dynamic setting**
	multi-period OPF	Simulation + Metaheuristic algorithm	Simulation + Metaheuristic algorithm	-	multi-period OPF	multi-period OPF	Simulation + Metaheuristic algorithm
	Offline	Offline	Offline	-	Offline	Offline	Offline
Chapter 6 Central controller	**static setting**	**dynamic setting**	**dynamic setting**	**static setting**	-	-	**dynamic setting**
	quadratic programming	Simulation + Metaheuristic algorithm	Simulation + Metaheuristic algorithm	quadratic programming	-	-	Simulation + Metaheuristic algorithm
	Online	Offline	Offline	Online	-	-	Offline

In order to assess the adequacy of this strategy with respect to the previous one Appendix H has been included. In addition, the essential differences of the central controller developed with respect to the well-known TNet hierarchical voltage control schemes, have been explained.

6.2. CENTRAL CONTROLLER COMPONENTS

A central controller which use HNet global information, has been evaluated. This controller dispatches wind farm reactive power to regulate the voltage at its *Pcc* (pilot bus) to some reference value ${V_p}^{ref}$. This value could be provided by a higher control loop or directly by the transmission system operator. Hence, wind farms' reactive power is taken as a control variable, whose setting is optimally calculated each period (10 seconds is taken as the control period in this work, as is done in some well-known secondary voltage control schemes). Those settings are dispatched after a first-order lag is imposed (one for each wind farms) to the wind farms, which time constant is tuned using a metaheuristic algorithm as has been done in the previous chapter. Note that these lags belong to the controller and should not be confused with the plant response. In addition, given their importance in establishing voltage profiles within distribution systems, voltage set-points for OLTC transformers are also optimized, albeit on a different time scale than that considered for the fast-acting reactive power resources. This last optimization will be only carried out when a significant change of the external conditions (pilot bus voltage magnitude or set-point change) is seen. Parameters related to this control scheme's temporal performance (the dead band and time delays) are subsequently tuned in an offline process. This strategy contrasts with the common OLTC transformers treatment in the TNet hierarchical voltage control schemes, where their tap positions were only evaluated in the tertiary loop (settle time ~ 15 minutes).

Consequently, two optimal control loops are proposed for determining ${Q_c}^{ref}$ and ${V_{ct}}^{ref}$ respectively by quadratic programming. Both of these are explained in the subsequent sections. Next, Table 6-2 summarizes the main characteristic of the central controller indicating the actions it can perform, what other control actions have been

included and finally the settings that correspond to these actions. Settings have been depicted in red or blue in to denote their nature, static or dynamic, respectively

Table 6-2. Characteristics of the central controller proposed

	OLTC transformers	**Wind farms**
Central controller action	Voltage set-point (V_{ct}^{ref}) Updated	Reactive power set-point (Q_c^{ref}) updated
Sample time	When a significant pilot bus voltage is seen	10 seconds
Additional control actions	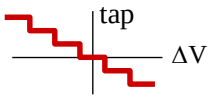	$\frac{1}{T \cdot s + 1}$
Control settings	• Voltage set-point V_{ct}^{ref} • Time delay • Dead band	• Reactive power set-point Q_c^{ref} • First order lag time constant

6.3. HNET SECONDARY CONTROL LOOP

This section explains the characteristics of HNet secondary control loop, i.e., the central controller component which determines wind farm reactive power operating points. This component adapts some well-known secondary control loop formulations. Nonetheless, some important differences can be observed (see Appendix H). This subsection has been structured as follows: firstly, in subsection 6.3.1, the formulation selected is explained, following the guidelines of some relevant ones already presented in Chapter 2. Subsequently, the trade-off among both objectives is evaluated in subsection 6.3.2. Finally, the value of the first order lag is discussed in subsection 6.3.3, where the control performance is analyzed from a theoretical point of view.

6.3.1. PROPOSED FORMULATION

To optimally evaluate the reactive power set-points (Q_c^{ref}) different approaches can be taken for example by using the pseudo-inverse law, by employing an optimization process, or by considering a proportional scheme as in the previous chapter. This subsection justifies the selected approach and formulation, as it differs from the ones already implemented in some TNet systems. It should be emphasized that the assumptions made about the central controller do not change the dynamic setting tuning process.

One simple approach, as was also employed in [de la Fuente 1997] employs the pseudo-inverse matrix. This matrix provides the minimum lest square error solution. This

fact can be easily seen for a system $A{\cdot}x{=}b$ (where A is a matrix 3x2 and b is a vector 3x1) as is presented in [Strang 1988]. In the event that the vector b is not a combination of the A matrix columns, the system has no solution and hence, it must be estimated→ $\bar{x}$. In this case the minimum error ($b - A\bar{x}$) is obtained when the vector b is projected in the plane formed by the column vectors of matrix A as can be seen in Figure 6-2. Hence, the error is perpendicular to A space, which means that this vector must be in the null space of A^T. Consequently the next relation must be accomplished $A^T A\bar{x} = A^T b$, where $A^+ = A^T[AA^T]^{-1}$ (considering that the rows are linearly independent) is the pseudo-inverse matrix. Matrix that fulfils two basic properties as the inverse matrix: $A^{+^2} = A^+$ and $A^{+^T} = A^+$

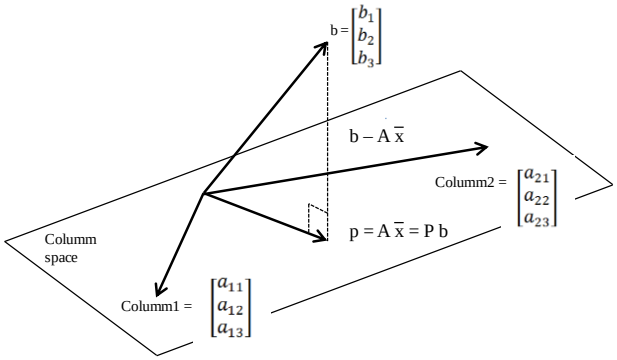

Figure 6-2 Projection onto the columns space of a 3 by 2 matrix [Strang 1988]

In our case study, for central voltage control, what needs to be obtained is the reactive power that should be delivered by wind farms (ΔQ_c) in order to correct a certain voltage deviation at the pilot bus (ΔV_p). These magnitudes can be related by the sensitivity vector $vS_{pc} = \frac{\partial V_p}{\partial Q_c}$. Hence, the system that needs to be solved is the following one: ${vS_{pc}}^{-1}\Delta Q_c = \Delta V_p$. In that system, considering its pseudo-inverse matrix (${vS_{pc}}^{+} = {vS_{pc}}^{T}\left[vS_{pc}{vS_{pc}}^{T}\right]^{-1}$), the reactive power increments can be minimized as the solution of the minimum squares problem, which seems to be a fair strategy to follow:

$$\min\left\{{\Delta Q_{c1}}^2 + {\Delta Q_{c2}}^2 + \cdots + {\Delta Q_{cn}}^2\right\} \tag{6-1}$$

The main drawback of this approach is that no reactive power limits are considered, as has been discussed in [de la Fuente 1997]. Nevertheless, this scheme can be used as a first approach which may be legitimate while the system is far away from its limits.

While the pseudo-inverse law is a useful starting point, it is not a good control method when units are near their limits. Hence, other alternatives have been studied and implemented. Among the schemes implemented, the secondary loop of the French hierarchical control scheme stands out, which solves an optimization problem each 10 seconds by means of quadratic programming with linear constraints. This approach was also adopted by [de la Fuente 1997] and is the approach adopted in this thesis taken into account wind energy nature such as its variability.

A different approach, in which the voltage deviation was seen as a constraint and not as an objective to be minimized, was suggested in [Alonso 2001]. This approach has been also evaluated here. Nevertheless, it has been discarded due to its drawbacks, as will be explained subsequently. Each of these approaches will be compared in Table H-3.

$$min \ \underbrace{\left\| \gamma \cdot \left({V_p}^{ref} - V_p(k) \right) - vS_{pc}(k)(\Delta {Q_c}^{ref}(k)) \right\|^2}_{\text{Voltage deviation minimization}} + W \underbrace{\frac{{Q_c}^{ref^2}(k+1)}{Q_{max}}}_{\text{Reactive margins maximization}}$$

Subject to.

$$ {Q_c}^{min} - \ Q_0 \leq \ \Delta {Q_c}^{ref}(k) \leq {Q_c}^{max} - Q_0 \tag{6-2}$$

As can be seen in the formulation selected, when the control variables are solely the reactive power outputs, the problem is significantly simplified. It can be seen that the objective function consists of two distinct terms:

- The first term is in charge of minimizing the voltage deviation at the pilot bus.
- The second term tries to maximize the reactive power reserves, essential for being able to cope with future perturbations.

It should be noted that both objectives are opposed to each other. Hence, typically a small weight (W) for the reactive power margins objective is assigned, a value that has been determined in the thesis by considering time domain simulations. In addition to the objective function, the optimization problem is also defined by the constraints imposed, whose number has also diminished. This fact is because the OLTC transformers are now in charge of maintaining voltages within admissible values. Hence, voltage constraints of both critical and generator buses are no longer required. Moreover, contrarily to what was proposed in [de la Fuente 1997], the reactive power references should not follow any guidelines. These guidelines were updated by the tertiary loop obtaining theirs optimal references. If they are avoided, the tertiary loop can be eschewed. Next, Figure 6-3 presents the reactive power assignment proposed by [de la Fuente 1997], taking into account the tertiary control loop action. As can be seen in this figure the tertiary loop action modifies the slopes, changing also the reactive power needed for the same reactive power level (d), equal for all generators within the same control area. Contrarily, in this thesis guidelines are not longer employed and the reactive power set-points can move freely within all their search space, i.e., their reactive capabilities. Hence, there is not any variable that constrains wind farms reactive power set-points, and they remain free to be dispatched within their bounds

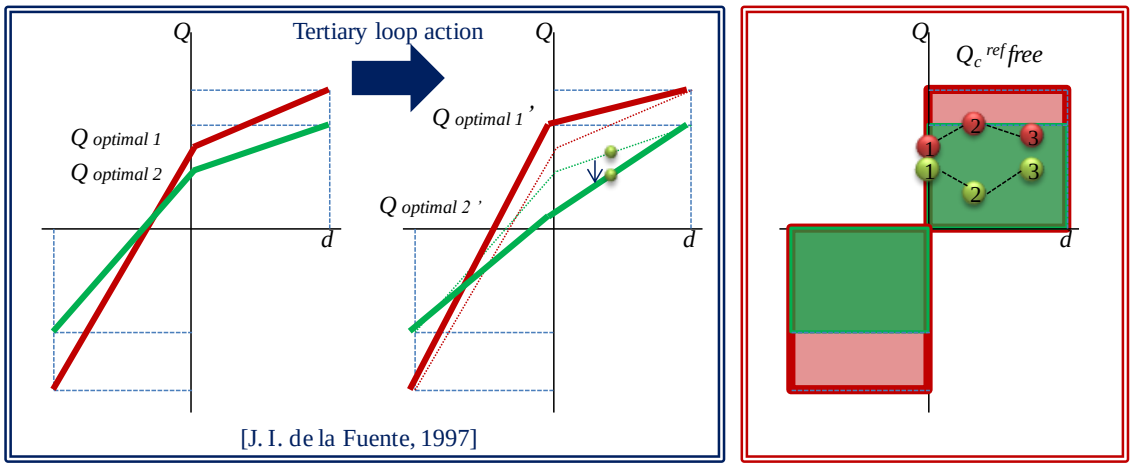

Figure 6-3 Reactive power assignment

Consequently, a single constraint which imposes the reactive power machine limits is included. According to this constraint, increments are computed with respect to their initial value Q_0 instead of its previous value $Q_c(k)$ as it is normally done. This means that a proportional response and not an integral one is obtained. Note that this integral response is not achieved, despite considering $Q_c(k)$, when the reactive power margins are incorporated into the optimization owing to both objectives are opposite. This fact jointly with the necessity of a robust and simple control has motivated this selection.

For ease of implementation in real time, the optimization problem is solved by quadratic programming, as is implemented in TNet hierarchical voltage control schemes. Thus, the problem should be expressed as follows, which is the canonical form for quadratic programming problems:

$$\frac{1}{2} \cdot x^T \cdot H \cdot x + f^T \cdot x \tag{6-3}$$

Where x corresponds to the control action $\Delta {Q_c}^{ref}(k)$

Including the voltage deviation term, the following expression is obtained:

$$\left\| \gamma \cdot \left({V_p}^{ref} - V_p(k) \right) - vS_{pc}(k) \cdot \Delta {Q_c}^{ref}(k) \right\|^T \left\| \gamma \cdot \left({V_p}^{ref} - V_p(k) \right) - vS_{pc}(k) \cdot \Delta {Q_c}^{ref}(k) \right\|$$

$$\begin{aligned} = \quad & \gamma^T \cdot \left({V_p}^{ref} - V_p(k) \right)^T \cdot \gamma \cdot \left({V_p}^{ref} - V_p(k) \right) - \\ & vS_{pc}(k) \cdot \Delta {Q_c}^{ref}(k) \cdot \gamma^T \cdot \left({V_p}^{ref} - V_p(k) \right)^T - \\ & vS_{pc}(k)^T \cdot \Delta {Q_c}^{ref}(k)^T \cdot \gamma \cdot \left({V_p}^{ref} - V_p(k) \right) + \\ & vS_{pc}(k)^T \cdot \Delta {Q_c}^{ref}(k)^T \cdot vS_{pc}(k) \cdot \Delta {Q_c}^{ref}(k) \end{aligned} \tag{6-4}$$

These four distinct terms have been reduced to just two. On one hand, the first term $[\gamma^T \cdot \left({V_p}^{ref} - V_p(k) \right)^T \cdot \gamma \cdot \left({V_p}^{ref} - V_p(k) \right)]$ is neglected because it is a fixed value

(note that γ , ${V_p}^{ref}$, and $V_p(k)$ are not optimization outputs) and hence, does not affect the optimization. On the other hand, the second and third terms have been grouped to obtain the following simplified expression:

$$-2\, vS_{pc}(k) \cdot \Delta {Q_c}^{ref}(k) \cdot \gamma^T \cdot \left({V_p}^{ref} - V_p(k)\right)^T + \\ vS_{pc}(k)^T \cdot \Delta {Q_c}^{ref}(k)^T \cdot vS_{pc}(k) \cdot \Delta {Q_c}^{ref}(k) \quad (6\text{-}5)$$

Extending the second term the following expression is obtained:

$$\frac{{Q_c}^{ref}(k+1)^2}{Q_{max}} =$$

$$\left({Q_c}^{ref}(k+1) - Q_c(k)\right)^T \cdot D \cdot \left({Q_c}^{ref}(k+1) - Q_c(k)\right) + \\ 2 \cdot \left({Q_c}^{ref}(k+1) - Q_c(k)\right)^T \cdot D \cdot \left({Q_c}^{ref}(k+1) - Q_c(k)\right) \quad (6\text{-}6)$$

Hence the final formulation is expressed as follows:

$$\frac{1}{2} \cdot \Delta {Q_c}^{ref}(k)^T \cdot \left(vS_{pc}(k)^T \cdot vS_{pc}(k) + W \cdot D\right) \cdot \Delta {Q_c}^{ref}(k) - \\ \left(vS_{pc}(k) \cdot \gamma^T \cdot \left({V_p}^{ref} - V_p(k)\right)^T - D\right) \cdot \Delta {Q_c}^{ref}(k) \quad (6\text{-}7)$$

In addition, other alternatives have been suggested, such as the one advocated by J. Alonso, where the maximum voltage deviation is defined by a constraint, which gives the following formulation (the power losses term presented in [Alonso 2001] has been eliminated because in the HNet under study in this chapter they are not relevant):

$$\min \qquad \Delta {Q_c}^{ref}(k)^T \cdot D \cdot \Delta {Q_c}^{ref}(k) + 2 \cdot {Q_c}^T \cdot D \cdot \Delta {Q_c}^{ref}(k)$$

Subject to.

$$vS_{pc}(k) \Delta {Q_c}^{ref}(k) \leq V_p^{max} - V_p(k)$$

$${Q_c}^{min} - Q_0 \leq \Delta {Q_c}^{ref}(k) \leq {Q_c}^{max} - Q_0 \quad (6\text{-}8)$$

This alternative way of formulating the same problem can be very effective. Nonetheless, it has been seen that its resolution may be very slow when the voltage deviation is close to its limit. Moreover, it may be infeasible.

6.3.2. TRADE-OFF AMONG OBJECTIVES DETERMINATION

As has been discussed, the trade-off among the objectives, the pilot bus voltage deviation and reactive power margins, is set by the value of *W*, which weights the importance of the latter. In order to determine a suitable value for *W*, several simulations have been undertaken, to measure each objective separately. The results of these

simulations are summarized in Figure 6-4, taking into account two voltage steps (V_{TNet} +/- 0 and V_{TNet} +/- 0.05). In this figure, for each voltage step change considered, two subplots are shown. In both cases, the relationship between the reactive power margins and the voltage deviation is presented. In the first subplot both magnitudes are integrated over the simulation's duration, whereas in the second subplot the maximum, mean, and minimum values are shown. In addition, it is important to note that each circle represents the actual objective values obtained by the simulation when a certain value of *W* is considered. This factor is changed constantly in steps of 0.005. Thus a good indicator for selecting *W* is the relationship between its change and the objectives change. Note that in both cases, for a low *W* the reactive margins increase drastically whereas the voltage deviation increment is admissible. For this reason a value of 0.005 for *W* is proposed. To clearly see the impact of *W*, three different time domain simulations, corresponding to the points labelled in Figure 6-4, are presented in Figure 6-5. As can be seen, when the reactive margins are not considered, wind farms are operated close to their limits, especially WF12, whose limits are the ones depicted in this figure. Nonetheless, those margins can be greatly increased, without any substantial erosion of the voltage deviation objective, when *W* is slightly increased. However, in the event of high *W* this erosion is inadmissible as it is outlined in the third simulation. Based on these results the weight factor finally selected is 0.005.

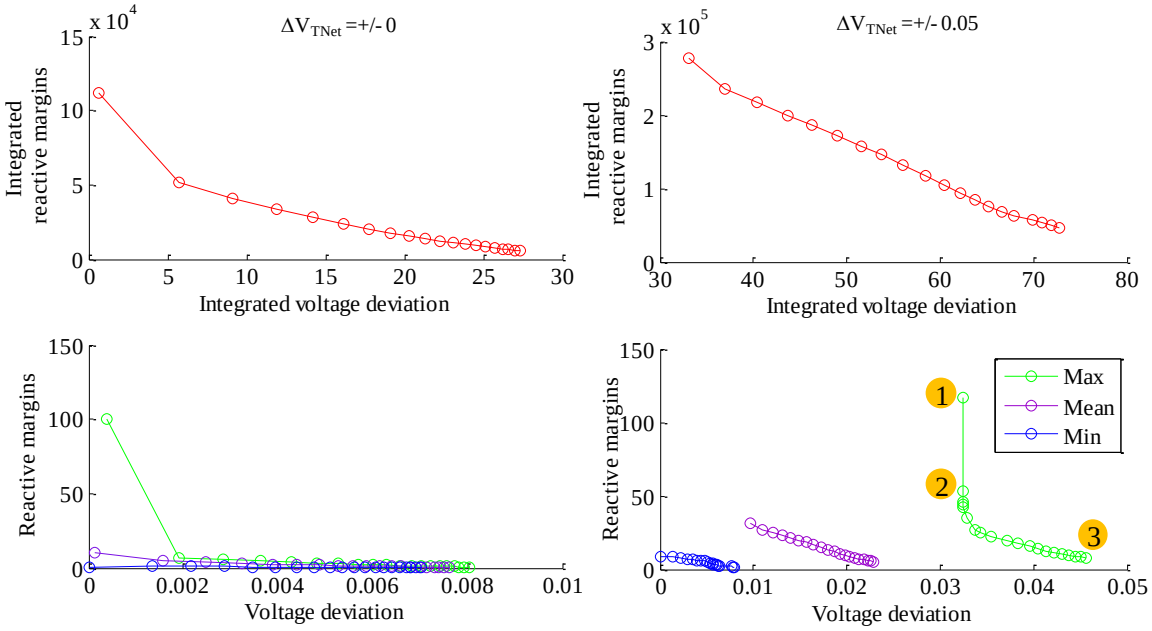

Figure 6-4 Determination of reactive power maximization weight

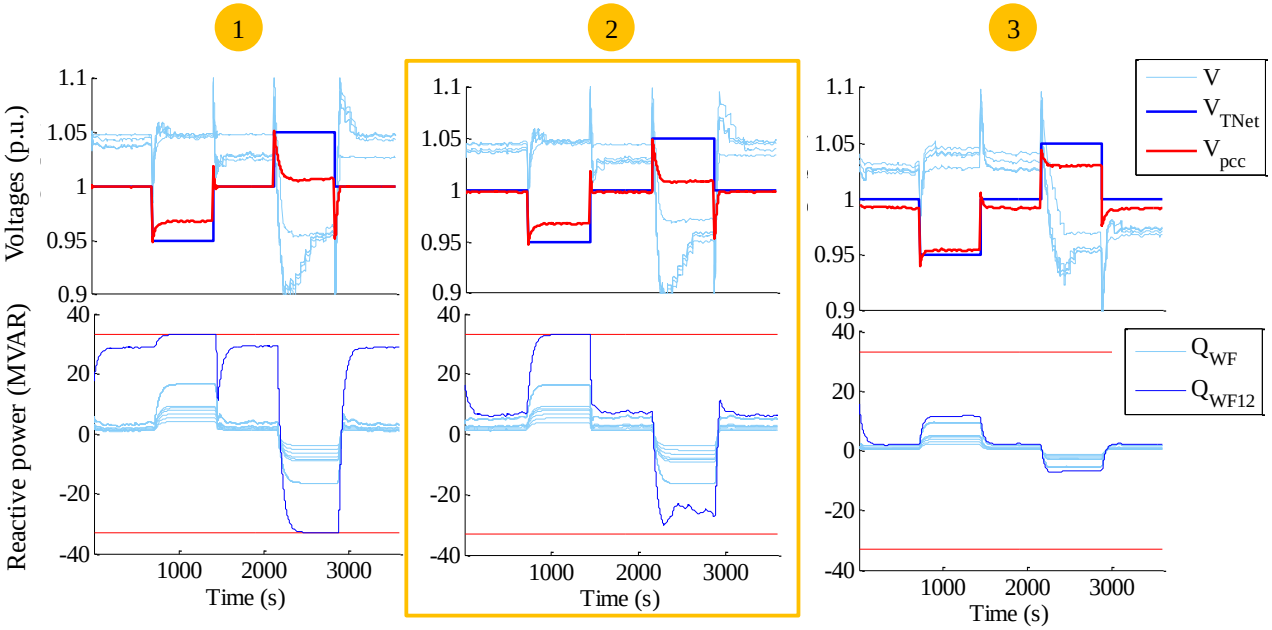

Figure 6-5 Time domain simulations considering different *W* values

6.3.3. FIRST ORDER LAG INCORPORATION AND CONTROL ADEQUACY

When evaluating the dynamic coordination within the HNet, the wind farms' controller time constants are very important. To impose a specific time constant different approaches can be followed. The most common option which has been widely studied, is simply imposing it in accordance with a gain, as was done in the secondary loop of the TNet hierarchical voltage control schemes presented. Hence, as was demonstrated by Pagola [Pagola 1993] the resulting time constant, which depends on the discrete sample time (Δt), is expressed as follows $T_c = \frac{-\Delta t}{\ln(1-\alpha)}$. If $\alpha = 1$ a *dead beat* control is obtained. This means that the control action is achieved in just a sample time Δt (considering perfect modelling of the system and a linear response). In the formulation selected for this thesis, the pilot bus voltage deviation is calculated in accordance with a gain γ, whose value has been fixed to 0.2. This gain has a role similar to a dead band and has been incorporated for avoiding oscillations. However, contrarily to other schemes, γ does not impose the reactive power response as was done with α in the [de la Fuente 1997]. Consequently different symbols have been employed.

In this thesis a different approach is proposed, which explicitly adds a first order lag. This allows a smother performance as different sample times can be considered. One sample time is used for the optimization process, which has been fixed to 10 seconds, and a smaller one is used for the first order lag. This second sample time has been fixed at 1 second, as it has been assumed that a wind farm can provide 90% of its reactive power capability within 1 second. Note that this distinction i.e. considering two different sample times, has no impact in the event of considering just a gain (as is done in the traditional TNet hierarchical control schemes). This consideration allows improving the control performance over three different objectives using the same dynamic settings. This is shown in Figure 6-6, where the voltage, the reactive power and the tap position are

depicted in different subplots. As in previous figures all these magnitudes do not correspond to the same bus. Consequently, tap changes may not correspond with voltage variations. In addition, a zoom is also provided where clearly can be seen that unnecessary tap changes are avoided.

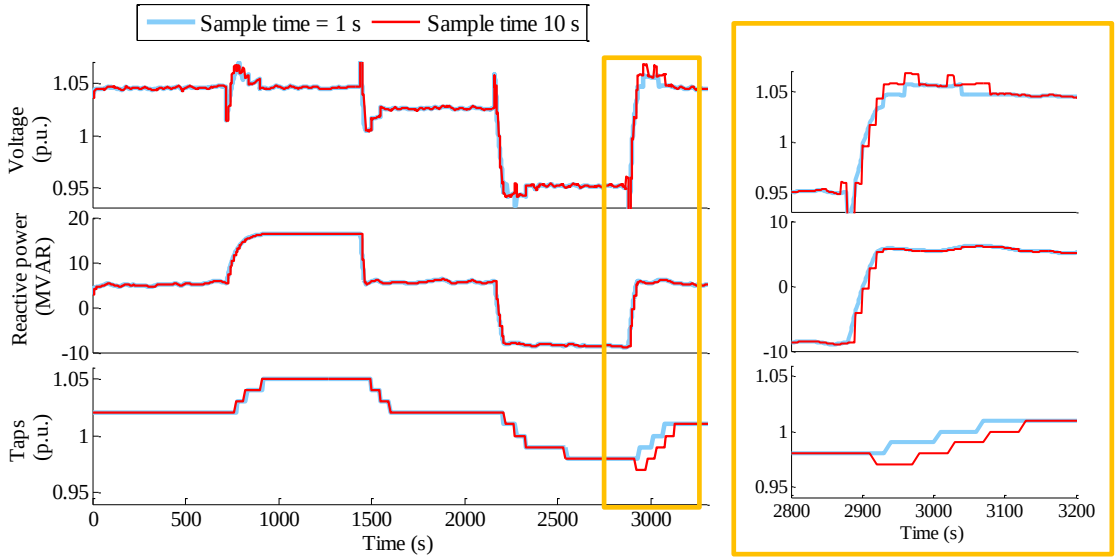

Figure 6-6 Sample time impact

Although the control scheme performance is analyzed by means of time domain simulations a first theoretical approach is done for understanding the influence of other control approaches. Hence, its stability is measured by the eigenvalue. This analysis was neglected in Chapter 5, due to the simplicity of the control schemes studied. The more accurate model is depicted in Figure 6-7. This model is built assuming a perfect match between the continuous and discrete control systems in the event of staircase inputs. Several simplifications have been made, obtaining the diagram presented in Figure 6-7:

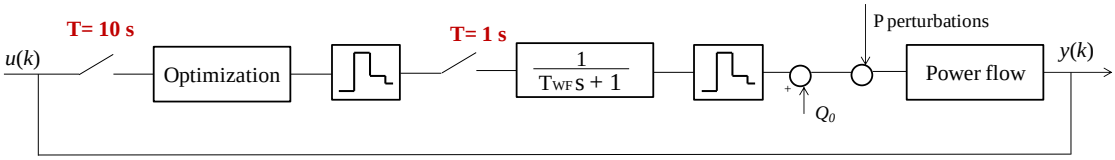

Figure 6-7 Discrete control system

In Figure 6-8 the model is particularized by disregarding the reactive power margins objective and the active power perturbations. Moreover, it assumes a single sample time for clarity. Finally, it should be noted that despite the model comprising a single input and output there is one state for each wind farm. This is shown in the figure with a double line.

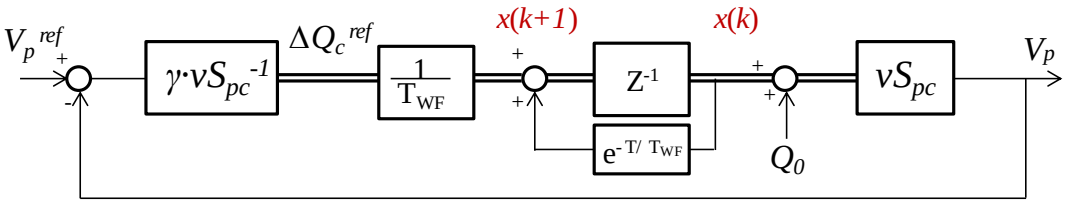

Figure 6-8 Simplified system analyzed

Assuming this simplified model the control scheme is defined by the following equation[12]:

$$x((k+1)T_d) = G(T_d)(x(kT_d) + H(T_d)u(kT_d) \tag{6-9}$$

$$x(k+1) = \begin{pmatrix} e^{-\frac{T}{T_{WF1}}} - \frac{\gamma}{T_{WF1}} & \cdots & 0 \\ \vdots & \ddots & \vdots \\ 0 & \cdots & e^{-\frac{T}{T_{WFn}}} - \frac{\gamma}{T_{WFn}} \end{pmatrix} x(k) + \begin{matrix} \frac{V_p^{ref} \cdot \gamma \cdot vS_{pc}^{-1}}{T_{WF}} \\ \frac{Q_0 \cdot \gamma}{T_{WF}} \end{matrix} \tag{6-10}$$

Obtaining one eigenvalue for each wind farm, which are equal when considering the same wind farms' controller time constants. If all of these eigenvalues are within the unit circle for the wind farms' controller time constant gamut (10s-100s), this proves its stability[13]. Another important concept that can be studied qualitatively is the robustness of the control schemes. For this purpose the sensitivity vector variation $vS_{pc} = vS_{pc_0} + \Delta vS_{pc}$ has been incorporated. The following equation is obtained:

$$x(k+1) = \begin{pmatrix} e^{-\frac{T}{T_{WF1}}} - \frac{\gamma}{T_{WF1}} - \frac{\gamma}{T_{WF1}}\Delta vS_{pc} & \cdots & 0 \\ \vdots & \ddots & \vdots \\ 0 & \cdots & e^{-\frac{T}{T_{WFn}}} - \frac{\gamma}{T_{WFn}} - \frac{\gamma}{T_{WFn}}\Delta vS_{pc} \end{pmatrix} x(k) + \begin{matrix} \frac{V_p^{ref} \cdot \gamma \cdot (vS_{pc_0} + \Delta vS_{pc})^{-1}}{T_{WF}} \\ \frac{Q_0 \cdot \gamma}{T_{WF}} + \frac{Q_0 \cdot \gamma \cdot \Delta vS_{pc}}{T_{WF}} \end{matrix} \tag{6-11}$$

[12] A common notation of this formula is $x(k+1) = Gx(k) + Bu(k)$ where the dependence of the discrete sample time is not included. This thesis includes the general expression for clarity purposes

[13] It must be noted that for simple control schemes (considering a single order) the stability analysis may derive unreal conclusions. Hence, the parametric analysis considering extreme values makes no sense.

Comparing both equations 6-10 and 6-11 it can be seen that an additional term is incorporated $\frac{\gamma}{T_{WFn}}\Delta vS_{pc}$ which represents a perturbation whose effects should be minimized, as is done when wind farms' controller time constants are increased. Hence, from the robustness point of view slow voltage control schemes are desired, suggesting that an appropriate trade-off must be sought.

6.4. OLTC TRANSFORMERS

In addition to the wind farms' reactive power capabilities, OLTC transformers can also help to maintain the desired ${V_p}^{ref}$. For this purpose a different optimization is carried out when a significant voltage deviation is seen. In the meantime the local control function of the OLTC will be maintained allowing a fast action and hence avoiding voltage breaches. This fast action is essential as most OLTC transformers are located at the same buses in which wind farms are connected. Hence, these buses are most sensitive to the fluctuations of reactive power.

Consequently the optimization problem is augmented to take into account also the OLTC transformers' effect. To this end, the voltage variation at the pilot bus originated by the OLTC transformers voltage set-points increments ($\Delta {V_{ct}}^{ref}(k)$) should be taken into account. This is done by considering their sensitivities $vS'_{pt}(k)$. It should be emphasized that all control variables are evaluated, i.e., $\Delta {Q_c}^{ref}(k)$ and $\Delta {V_{ct}}^{ref}(k)$, however only the latter is applied. This is done to avoid unwanted interactions among controllers.

$$min \quad \left\| \gamma \left({V_p}^{ref} - V_p(k) \right) - vS_{pc}(k)\left(\Delta {Q_c}^{ref}(k)\right) - vS'_{pt}(k)\left(\Delta {V_{ct}}^{ref}(k)\right) \right\|^2 + W\frac{{Q_c}^{ref\,2}(k+1)}{Q_{max}}$$

$$Q_0 - {Q_c}^{min} \leq \Delta {Q_c}^{ref}(k) \leq {Q_c}^{max} - Q_0$$

$$V_{ct\,0} - \left({V_{ct}}^{min} + Dead\ band\right) \leq \Delta {V_{ct}}^{ref}(k) \leq \left({V_{ct}}^{max} - Dead\ band\right) - V_{ct\,0} \quad (6\text{-}12)$$

In this case, an additional constraint emerges. This constraint takes into account the tapping limits of the OLTC transformers. As can be seen, a major difference with respect to the previous chapter is the incorporation of the dead band in the online optimization process. Thus, the voltage breaches are reduced as Appendix H shows.

Finally, it must be noted that throughout the thesis the OLTC transformers have been used for the benefit of the HNet, assuming an ideal performance of the wind farms (i.e. assuming the reactive power capabilities imposed by the operational procedures [REE 2011]). Nonetheless, as has been discussed in Chapter 2, currently not all wind farms are able to fulfil these requirements without retrofitting additional devices. Thus, in these cases the OLTC transformers could play an important role for maximizing the reactive

power contribution of the wind turbines. This possibility is briefly discussed in Appendix I, however its proper evaluation is out of the scope of the thesis.

6.5. CENTRAL CONTROLLER COORDINATION

Once the central controller has been defined its dynamic coordination should be addressed, and this challenger is the central research theme of Chapters 5 and 6 of the present thesis. Recalling the previous chapter, this coordination is performed by tuning the relevant settings using a metaheuristic algorithm, wherein each individual embodies a whole simulation of the central controller over one hour. In subsection 6.5.1 an initial approach is performed for the initial sensible dynamic settings set, which is used to justify the necessity of the objectives to be minimized. Then, subsection 6.5.2 presents the dynamic coordination assessment, which is complemented in subsection 6.5.3 with a detailed analysis of the non-dominated solutions, allowing the identification of patterns within the settings choices. Finally, 6.5.4 compares the initial dynamic settings with the tuned ones.

6.5.1. SCHEME PERFORMACE

The central controller dispatches new set-points (i.e reactive power set-points for wind farms and OLTC transformers voltage set-points when a transmission network change is detected) from period to period in order to minimize the voltage deviation at the common coupling bus (*Pcc*), while preserving reactive power machine limits. Figure 6-9 depicts the performance of the central controller when exposed to voltage step excursions of +/- 3%. As in the previous chapter, the sensible initial settings indicated in [Van Cutsem, et al. 1998] have been employed.

In the first subplot, at the top of the figure, voltages at various buses are depicted. The voltage at the common coupling bus is presented in red, and the transmission network voltage is presented in dark blue (both buses are explicitly shown in Figure 1-2, where the Thevenin equivalent is used for modelling the TNet). The second subplot presents the wind farms' reactive power. In the third subplot, transformer winding ratios (i.e. tap setting) are depicted. Finally, the last subplot presents OLTC transformer voltage set-points. This figure is also used to justify the necessity of the different objectives minimized with the MOPSO, which recalling the previous chapter, correspond to the tap changes, transformers voltage deviation and voltage breaches. This subplot shows that there is margin for minimizing all these objectives.

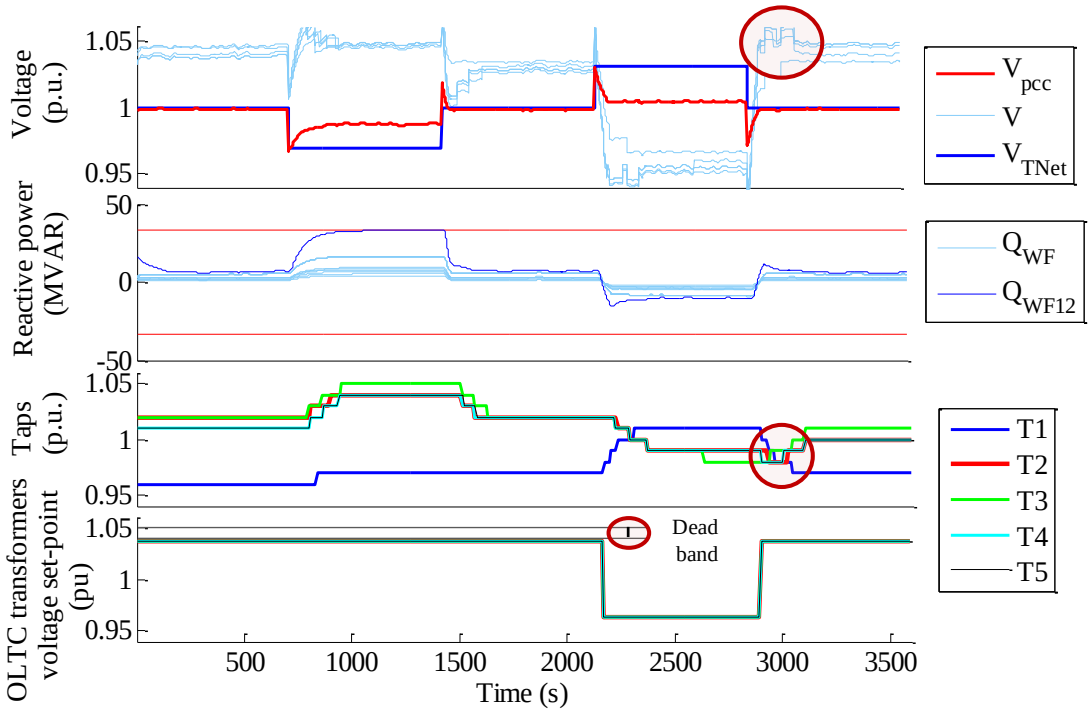

Figure 6-9 Central controller performance for a random set of non optimal dynamic settings

From the first subplot it can be seen that the voltage deviation at the common coupling bus is compensated when there is sufficient reactive power available. Reactive power margins are exhausted in the event of a significant decrease in the transmission voltage, as it is depicted in the second subplot. In this case all wind farms are at their maximum value, although for clarity's sake only the limits of WF12 have been included.

Concerning the transformers' settings, it can be noted that there are several unnecessary tap changes (as are circled). This behaviour could be avoided by better tuning of the dynamic settings. For that purpose a single objective, the minimization of tap changes, is not enough, as has been already mentioned, because it can cause unwanted performance in other areas (transformers voltage deviations and limit breaches). Both effects can also be seen in this figure. The transformers' voltage deviation effect can be seen by focusing on the period between 700s and 1400s. In this period the wind farms' reactive power saturates, causing a significant voltage deviation at the pilot bus. This deviation can be reduced by increasing $V_{ct}{}^{ref}$. However, its value is limited by the dead band as can be seen in the last subplot. Both effects are also circled. The three objectives are computed for this first case and in the following section will be compared with the non-dominated solutions obtained after tuning the dynamic settings. Finally, from the last subplot it can be seen how a high voltage set-point for wind farm transformers is desired when the transmission voltage is equal or lower than the set-point. A low voltage is desired in the opposite situation.

6.5.2. DYNAMIC COORDINATION

Thanks to the MOPSO algorithm the non-dominated solutions corresponding to the dynamic settings are obtained. Figure 6-10 presents the objectives (in each subplot a pair

of objectives is represented) for all candidate dynamic settings evaluated with the MOPSO iterations. In light blue are outlined the dominated solution, whereas the Pareto set, corresponding to the non-dominated solutions, is depicted with red circles. In addition a blue square represents the objectives calculated for the simulation with the initial selection whose time domain simulation was presented in Figure 6-9. As can be seen all objectives can be significantly improved.

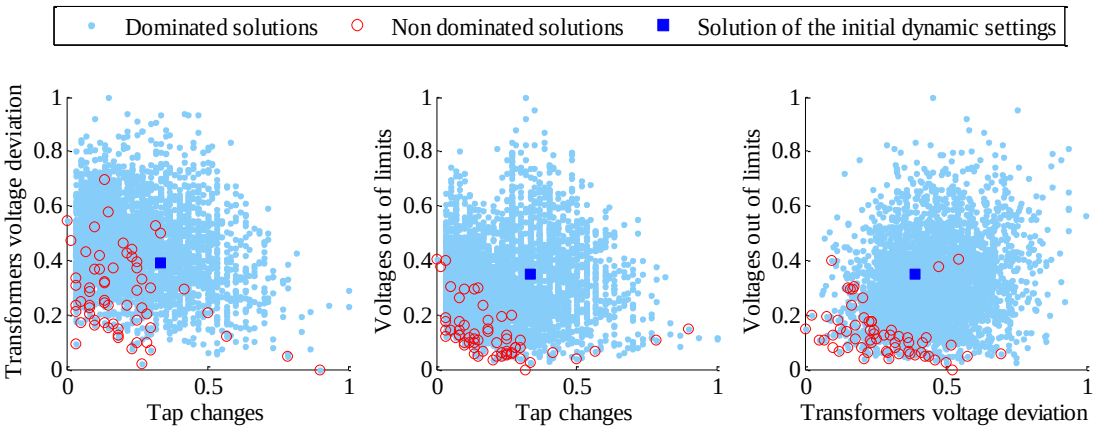

Figure 6-10 Search space (indicating the solution corresponding to the initial set of dynamic settings) and non-dominated solutions

6.5.3. NON DOMINATED SOLUTIONS ANALYSIS

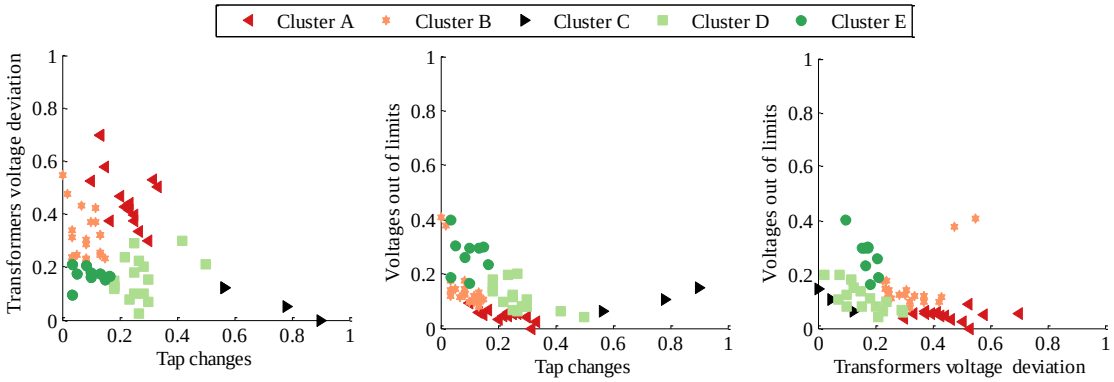

Figure 6-11 Non-dominated solutions characterized in different clusters

In order to categorize those non-dominated solutions a clustering analysis is performed. Thanks to this analysis different subsets or clusters which share some common characteristics, and also differ from the other clusters, are identified. The algorithm used is the fuzzy c-means [Windham 1982]. This categorization has been done based on the objective values achieved.

To select the optimal number of clusters, the cluster objective function (corresponding to the sum of distances from the data centre assigned to each value) is computed as a function of the number of clusters. As can be imagined, the cluster objective function decreases as the number of cluster increases. This chapter has selected the number that corresponds to the knee point of this relationship (5 clusters). In Figure 6-11 the Pareto

sets already presented in Figure 6-10 are depicted considering the 5 different clusters (each cluster is presented with a different symbol and colour). From this figure the dynamic setting patterns can be graphically selected in accordance with wind farm owners' trade-off among objectives. This information is numerically summarized in Table 6-3, were the mean dynamic settings corresponding to each cluster are presented, considering also their spread. The most relevant settings within each cluster, identified according to their membership grade, are also included. As can be seen in this table, in all clusters except cluster 3, the T1 time delay is significantly lower than the time delay of the other transformers, as was expected for minimizing the tap changes (recalling Chapter 2, the downstream OLTC transformers should be slower than the upstream one). Contrarily, the dead band for T1 is always higher than for the other transformers. This is because transformers T2-T5 are directly connected to the wind farms and hence are more vulnerable to their reactive power changes causing the voltage breaches. Finally, it can be seen that a considerably high mean wind farm controller time constants is demanded for avoiding both voltage breaches and unnecessary tap changes. It should be noted that for avoiding unnecessary tap changes the downstream transformers, which control the most sensitive buses from the voltage perspective, should be slower than the upstream transformers. Consequently, in the event of a fast wind farm reactive power response, the time in which the voltages are out of limits increases. This can be mitigated by reducing the transformers' time delay. However, this action may cause unnecessary tap changes.

Table 6-3. Dynamic settings patterns

		Cluster A			***Cluster B***			***Cluster C***			***Cluster D***			***Cluster E***			Units
Time delay	*T1*	11	1.0%	10	12	2.0%	10	70	3.3%	100	12	1.7%	10	17	2.9%	30	(s)
	T2	31	4.0%	16	52	1.9%	47	11	0.9%	14	48	3.5%	52	64	2.1%	77	(s)
	T3	21	2.3%	32	44	2.7%	48	20	4.0%	10	17	3.0%	10	34	3.1%	40	(s)
	T4	14	2.0%	26	31	1.7%	41	10	0.0%	10	40	3.2%	48	54	1.8%	26	(s)
	T5	15	2.3%	10	42	2.7%	27	10	0.0%	10	15	3.4%	10	75	1.6%	83	(s)
Dead band	*T1*	0.0170	0.3%	0.014	0.0171	0.3%	0.017	0.0150	1.1%	0.016	0.0177	0.2%	0.018	0.0174	0.2%	0.018	(pu)
	T2	0.0147	0.9%	0.012	0.0129	0.8%	0.013	0.0110	0.0%	0.011	0.0112	0.2%	0.011	0.0112	0.3%	0.011	(pu)
	T3	0.0144	0.8%	0.013	0.0147	0.4%	0.015	0.0110	0.0%	0.011	0.0136	0.6%	0.011	0.0127	0.5%	0.013	(pu)
	T4	0.0146	0.9%	0.011	0.0145	0.7%	0.015	0.0110	0.0%	0.011	0.0136	1.0%	0.016	0.0116	0.7%	0.011	(pu)
	T5	0.0144	0.9%	0.018	0.0123	0.7%	0.012	0.0117	0.4%	0.013	0.0111	0.1%	0.011	0.0136	0.8%	0.015	(pu)
Mean wind farms controller time constant		61	1.8%	54	64	1.6%	60	72	1.7%	45	68	1.9%	47	63	1.8%	51	(s)
Objectives	**Total tap changes**	**0.226**			**0.099**			**0.805**			**0.262**			**0.106**			
	Transformers voltage	**0.441**			**0.312**			**0.040**			**0.156**			**0.183**			
	Voltages out of limits	**0.054**			**0.124**			**0.119**			**0.110**			**0.267**			

6.5.4. COMPARISON

Finally the initial simulation presented in Figure 6-9 is compared with the one in which the dynamic settings have been tuned using the MOPSO algorithm. For this last assessment, the relevant dynamic setting of cluster 2 has been selected assuming that the tap changes objective has been prioritized. This comparison is presented in Figure 6-12, showing the voltage breaches (first subplot) and the tap changes (second subplot). As can be seen the number of tap changes is reduced, decreasing also the time in which the voltages are out of their limits.

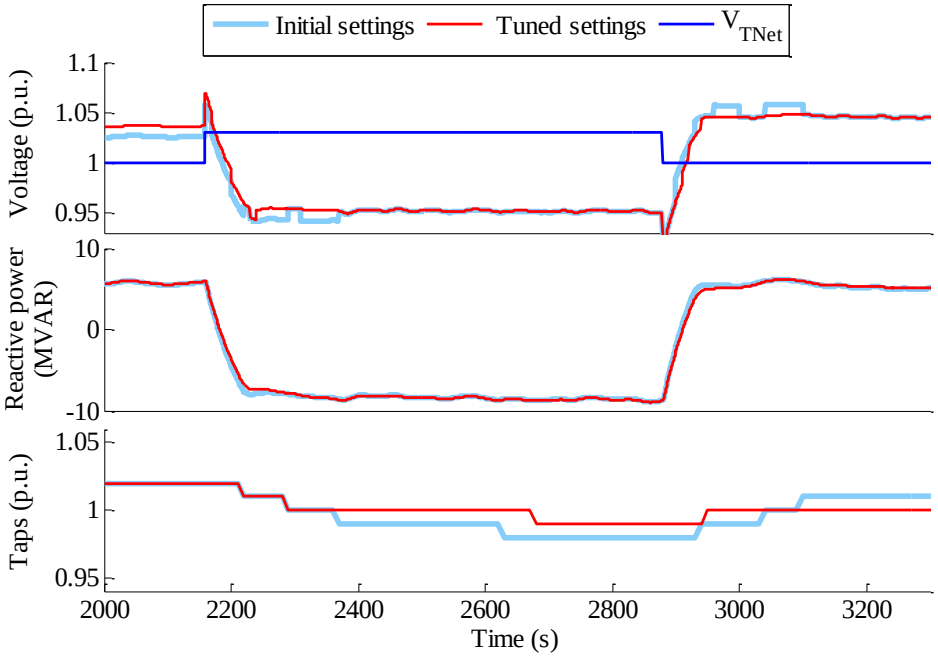

Figure 6-12 Temporal evolution simulation. Improvements due to dynamic settings tuning

6.6. SUMMARY AND CONCLUSIONS

This chapter has considered HNets of type C in which a pro-active voltage control strategy was proposed. Recalling Chapter 3, to take advantage of the whole PQ chart available, adaptive settings are required. To this end, the AC multi-period OPF employed in the previous chapter has been replaced by an online central controller which adapts the well-known secondary loop of the TNet hierarchical voltage control scheme. However, important modifications have been made. Firstly, the reactive power settings for each wind farm instead of voltage set-points have been considered. These reactive power set-points are controlled to minimize the pilot voltage bus deviation, taking into account reactive margins maximization also. For this last objective, linear constraints such as the ones imposed by [de la Fuente 1997, Paul et al. 1987] have been avoided, eliminating also the important role that the tertiary loop played in those schemes for reactive power management. A first-order lag has been added within the central controller allowing the usage of two different sample times: one for the optimization computation and other for the set-point updating. Hence a smooth response is obtained which also avoids unnecessary tap changes as has been already seen. Concerning OLTC transformers, a supervised decentralized operation has been suggested, which guarantees fast and optimal operations.

For the dynamic coordination the same method (based on fixed dynamic setting calculated offline) presented in the previous chapter has been employed, focusing this time only on the MOPSO algorithm. The results obtained have been expanded by clustering the Pareto set to show the different dynamic settings patterns.

CHAPTER 7

CONCLUSIONS AND FUTURE RESEARCH

This chapter provides a summary of this thesis paying special attention to the contributions. In addition, it contains the list of publications derived from the work of this thesis. Moreover several future research tasks that arise from this thesis are also outlined.

7.1. CONCLUSIONS

Wind voltage control is implemented in the most representative countries from the wind penetration perspective by means of a tight compulsory power factor range that wind farms should comply with. However, as wind installed power and penetration is increasing throughout the world, most system operators are moving toward a scheme that implies that wind farms should contribute to voltage control in a similar fashion as conventional generation. The technological state of the art of actual wind turbines show that they are able to provide a wide margin of reactive power (both consumed and absorbed) to the net. However, taking into consideration the wind power variability, and also the special networks into which the energy is delivered, it is not clear if wind farms are able to behave as conventional plants sustaining TNet voltages.

This thesis focuses on voltage control of wind energy that is integrated into harvesting networks (HNets). These networks are developed solely to harvest energy and thus, no demand customers are accommodated. HNets are becoming more common in countries

with high wind energy penetration levels, being the preferred option in Spain (85% of wind energy is located in HNets) and it is also very significant in Ireland. Moreover, it is foreseen that in the near future, it will be the solution adopted for large integration of wind. Nevertheless, there is very little research of HNets, a gap that this research covers in depth. Relevant characteristics of HNets, such as the presence of different wind owners, and the dynamic coordination among wind farms and cascade OLTC transformers makes the problem complex, and are the core of the analysis and one of the main contributions of this thesis.

As the literature review shows, there is significant work related to wind voltage control (mostly related to the integration of wind in DNets), but in general the algorithms, studies or solutions apply to specific case studies, so that the conclusions cannot be generalized. In this thesis, HNets are analyzed and classified depending on their characteristics (number of wind farms, number of wind owners, total wind installed power, total line kilometers and short-circuit power of the TNet connection bus). For this purpose, a set of 8 actual HNets embedded within the Spanish power system has been selected, that are representative of the types of harvesting networks that may be found, in order to propose an appropriate wind voltage control solution for each type of network. An optimal individual solution of wind voltage control for each HNet is proposed, taking into account both the steady-state and dynamic perspectives.

From the steady-state perspective different controls are tackled and compared (*reference control*, *power factor control*, *local voltage control* and *remote voltage control*) taking into account different objectives such as minimizing power losses, obtaining the reactive contribution limits of the HNet to the TNet (PQ chart) and minimizing the voltage deviation of the TNet. For this purpose, a **W**ind **E**nergy **H**arvesting Network **S**teady-state **A**ssessment (WEHSA) tool has been developed, which allows the steady-state analysis of any control scheme of any HNet pursuing any of the relevant objective functions previously mentioned.

From the dynamic perspective, a novel method for offline tuning the dynamic settings of wind farms and OLTC transformers has been developed that ensures an optimal and feasible dynamic behaviour of the solutions proposed by this thesis. For this purpose, a **W**ind **E**nergy **H**arvesting **Sim**ulation (WEHSIM) tool has been developed which tests and validates the solutions proposed.

In this thesis, a wide variety of techniques have been exploited in order to search for the best wind voltage control alternative that suits each type of HNet. Among the ones used in the thesis are data-mining techniques (regression, clustering, decision trees …), methauristic algorithms (genetic algorithms and multiple particle swarm optimization), quadratic programming or multi-period OPF.

7.2. CONTRIBUTIONS

This thesis establishes the best way of implementing voltage control of wind farms within HNets in a holistic way, proposing and testing a feasible solution for each type of

HNet. This general objective has been accomplished in several subsequent tasks, each of them representing thesis contributions: (a) comprehensive steady-state assessment, (b) classification of HNets and proposal of a suitable wind voltage control solution for each one, (c) development of an algorithm based on control rules to minimize HNet losses, (d) development of a simulator for evaluating any control scheme temporal evolution and validate the solutions proposed for certain types of HNets (B and C). In fact, this simulator has been tested for both fixed static settings obtained thanks to an AC multi-period OPF and adaptive settings distributed by a central controller. And finally (e), the simulator is integrated with different metaheuristic algorithms for tuning the dynamic settings.

The following subsections highlight the main contributions of this thesis within the aforementioned steps.

7.2.1. STEADY-STATE ASSESSMENT

First, the hosting capacity limitations and their increments (thanks to the provision of wind voltage control) have been assessed, identifying the importance of where the synchronous generators are displaced. The reactive power local nature makes the provision of this service by wind farms indispensable if their penetration is to be increased. In addition, the qualitative study of Apendix B indicates how voltage control of wind farms can mitigate voltage increases and decreases when the penetration is increased, thus allowing an increment of the hosting capacity of HNets. Moreover, the role of TNet decisive variables such as the short circuit power and the ratio X/R of the connection point of the HNet to the TNet is discussed. These values decisively affect the HNet PQ chart.

A complete steady-state analysis is done in Chapter 3 using the developed WEHSA tool to measure the behaviour that different control schemes offer. Two different optimal control schemes have been tested: *power losses minimization* and maximum *PQ chart*. In both cases it has been seen that OLTC transformers play a key role and should be considered in any control strategy. Then these schemes have been compared with the current control scheme: wind farms are operated at a unity power factor (*reference control*) and the *proportional control* proposed by some TSO (as P.O. 7.5 proposal of the Spanish TSO) in order to measure how far they are from the optimal ones. The steady-state analysis shows that if a pro-active voltage control by means of a proportional control is to be implemented having a real impact on TNet, an adaptive slope is essential. This comparison suggests that there is margin for power loss reduction with respect to the simple current strategy (*reference control*). Nonetheless, with current regulations, wind farm owners do not have any incentives for minimizing HNet power losses.

7.2.2. CLASSIFICATION OF HARVESTING NETWORKS

The comprehensive detailed steady-state analysis of wind voltage control provided for two HNets with opposite characteristics show a clear dependence on the type of network. Hence, this thesis concludes that the strategy selection should consider the HNet particular features. A key contribution of this thesis is the novel classification of HNets

into three types. This classification is unique in the literature, providing an overall picture of the voltage control problem of HNets, and enabling the proposal of suited strategies for each type of HNet. This classification has been done based on three relevant indexes: PQ chart, power losses and voltage margins. The three identified clusters, and the associated proposed strategies are:

- **Type A:** Power loss minimization strategy presented in Chapter 4; suitable for networks with significant power losses and with a restricted PQ chart.
- **Type B:** HNet minimum impact on TNet strategy presented in Chapter 5; suitable for networks without significant power losses and with a restricted PQ chart.
- **Type C:** Pro-active voltage control strategy presented in Chapter 6; suitable for networks without significant power losses and with a broad PQ chart.

7.2.3. CONTROL RULES ALGORITHM TO MINIMIZE POWER LOSSES

Focusing on type A HNets, an alternative method to the well-known OPF based on simple control rules is proposed in this thesis. This method infers knowledge from an optimal scenarios data base. This simple approach avoids the necessity of solving an optimization problem for each sample, also reducing communication requirements. For this purpose, two different types of variables have been assessed. The variables belonging to the first group are useful for explanation purposes. Nonetheless they require a previous power flow, assuming that all wind farms are operated at a unity power factor. In the second group, variables do not require any previous computation facilitating their implementation. Concerning the first type, this thesis has contributed with a novel variable, the active power losses from wind farm *i* to the transmission network bus (P_{lossi}), which takes into account both the electric distance and the load of the HNet lines. Concerning the second type, the total active power has been selected resembling the power factor concept. This factor is considered with respect to global magnitude instead of the individual wind farm active power. In the particular case under study, it has been seen that this last variable presents a high coefficient of determination, used for evaluating the adequacy of the regression rules obtained. However, its performance can deteriorate especially in the presence of loads or other wind farms that do not contribute to the global goal.

In addition to the regression rules employed for estimating the reactive power assignment, decision trees have been used for estimating the tap position of OLTC transformers. In those cases the explanatory variables considered are the voltage and current for 132kV/20kV transformers. Nonetheless, for the 400kV/132kV the V_{TNet} was also incorporated enriching its performance. Hence, a totally decentralized operation of OLTC transformers can be made avoiding communication, representing a clear advantage with respect to OPF. Both regression rules and decision trees are computed offline by simulation of multiple optimal scenarios.

Finally, it should be noted that the methodology presented in Chapter 4 is of value in a number of respects. Firstly, it allows understanding the performance of the power flows

in the grid under the different scenarios. Secondly, it identifies which wind farms have a negligible effect on HNet losses. In those cases a fixed reactive power set-point equal to zero is sufficient, independent of the scenario. And thirdly, it may be of use in providing an initial point in the event of considering an OPF for each sample time.

7.2.4. CONTROL SCHEME STATIC SETTINGS AND TEMPORAL PERFORMANCE

In order to analyze any control scheme dynamic performance, a simulator is required. In that sense a new tool, **W**ind **E**nergy **H**arvesting **Sim**ulation (WEHSIM), has been developed allowing the analysis of any HNet. This tool has been used for the control strategies proposed for type B (taken into account fit-and-forget static settings) and C (considering adaptive settings). Focusing on type B, a holistic analysis of four different schemes: *reference control*, *power factor control*, *local voltage control* and *remote voltage control* has been provided. Note that those schemes can be gathered in two distinct groups: those control schemes that maintain a certain power factor and voltage control. For each control scheme fixed static parameters are obtained thanks to the AC-multi-period OPF. From this analysis it can be surmised that the best option is a voltage control where wind farms control a remote bus. Otherwise, of the localized control schemes that do not require telemetry, *power factor control* has a better performance representing a key result. In fact, the Spanish proposals (P.O. 7.5) encourage the *local voltage control* which has been seen is not the best option.

Contrarily, for type C HNets, a central controller distributes settings that depend on the operational and external conditions. This central controller has been developed following the guidelines of well-known TNet hierarchical voltage control schemes and more specifically in their secondary loop. Nonetheless, several modifications have been done in accordance with the HNet characteristics and the nature of distributed generation such as its variability. Firstly, it should be emphasized that wind farms' reactive power set-points instead of voltage ones, have been considered. Those set-points are evaluated for minimizing the pilot voltage bus deviation taking into account also reactive margins maximization. For that purpose the tertiary loop, which commonly plays an important role in reactive power management has been avoided, obtaining a fast response.

Moreover, for obtaining a smooth response avoiding unncesary tap changes, a first-order lag (with a sample time much smaller than1 s) has been incorporated. For avoiding instabilities or oscillatory performance and reducing communication requirements the control variable increments have been evaluated with respect to the initial values obtaining a proportional response and not an integral one as is commonly done in traditional TNet schemes. Nonetheless, the integral response is never reached if reactive power margins are also considered. Finally, concerning OLTC transformers a supervised decentralized operation has been suggested to guarantee fast and optimal operation.

7.2.5. OFFLINE TUNING OF DYNAMIC SETTINGS

Any control scheme design should also consider the dynamic coordination of wind farms and cascade OLTC transformers. In that sense this thesis proposes an offline method to tune some relevant dynamic settings to be applied to the voltage control of Type B and C. These settings are wind farms' controller time constants and for OLTC

transformers their time delay and dead band. This last setting is not commonly used with coordination purpose although there is not any barrier that impedes its use as has been proposed in this thesis.

For that purpose two well-known metaheuristic algorithms (Genetic algorithm and MOPSO) have been used. Concerning type B, the dynamic analysis reinforces the previous statement (see subsection 7.2.4) showing how in the event of implementing a *local voltage control* scheme, to avoid oscillation, very slow controller action is necessary. Finally, it should be noted that a demanding voltage control such as the *remote* one increases the number of tap changes significantly. Concerning type C, the same method has been employed focusing this time only on the MOPSO algorithm. The results obtained have been expanded, clustering the Pareto front obtaining different dynamic settings patterns.

7.3. PUBLICATIONS

This section gathers the publications derived from this thesis, 6 journals (all of them already published) and 1 conference publications.

Journal publications

E. Sáiz-Marín, E. Lobato, "Optimal voltage control by wind farms in distribution networks using regression techniques", *Przeglad Elektrotechniczny*. vol. 88, no. 01a, pp. 117-121, Enero 2012. CIRC: **A**

E. Sáiz-Marín, E. Lobato, I. Egido, "Optimal voltage control by wind farms using data mining techniques", *IET Renewable Power Generation*. vol. 8, no. 2, pp. 141-150, Marzo 2014. [Online: Septiembre 2013] CIRC: **EX**

E. Sáiz-Marín, E. Lobato, I. Egido, "Local hosting capacity increase by means of wind farm voltage control provision", *IEEE Transactions on Power Systems*. vol. 29, no. 4, pp. 1731-1738, Julio 2014. [Online: Enero 2014] CIRC: **EX**

E. Sáiz-Marín, E. Lobato, I. Egido, L. Rouco, "Economic assessment of voltage and reactive power control provision by wind farms", *Wind Energy*. [Online: Marzo 2014] CIRC: **EX**

E. Sáiz-Marín, E. Lobato, I. Egido, C. Gómez-Sánchez, "Voltage control assessment of wind energy harvesting networks", *IET Renewable Power Generation*. vol. 8, no. 8, pp. 915-924, Noviembre 2014. [Online: Junio 2014] CIRC: **EX**

E. Sáiz-Marín, P. Cuffe, A. Keane, E. Lobato, I. Egido, "Offline Tuning of Dynamic Settings Considering an Online Central Controller ", accepted for its publication *IET Renewable Power Generation* CIRC: **EX**

Conference publications

E. Sáiz-Marín, E. Lobato, I. Egido, L. Rouco, "Power losses minimization within Spanish wind farms evacuation networks", 2013 IEEE Power and Energy Society General

Meeting - IEEE PES 2013. ISBN: 978-1-4799-1301-5, Vancouver, Canadá, 21-25 Julio 2013

7.4. FUTURE RESEARCH

Despite the huge literature available concerning voltage control, further research should be carried out. The main areas in which further research can be made are: (a) expand the results to other systems, e.g., DNets, isolated systems or smart grid (b) integration of type C control strategy into the TNet hierarchical control, (c) experimental validation of the control schemes proposed and (d) definition of a proper regulation framework and grid codes. Each of these specific topics are briefly expanded in the subsequent subsections.

7.4.1. REPLICABILITY AND SCALABILITY

The results presented in this thesis can be expanded to other systems such as microgrids, smart grid or DNets where reactive power management is essential. In those cases, as has been done for a HNet, centralized and decentralized control schemes can be suggested considering also different control strategies whose selection may be done in accordance with the three relevant indexes here proposed: PQ chart, power losses and voltage margins. In addition, in these systems the FACTs and STORAGE devices may play an important role and thus, their incorporation in any control strategy is crucial.

7.4.2. HNET INTEGRATION INTO A TNET HIERARCHICAL VOLTAGE CONTROL

At the end, those HNet plants should be coordinated within the whole TNet. This fact can be done in two different manners as has been already stated within the thesis. On one hand, the TSO can directly give a set-point. On the other hand, the HNet can be integrated in a TNet hierarchical control scheme and hence automatically receive set-points from its higher loop (secondary voltage control loop). As a result, the required information that the TSO needs for providing the set-points must be defined.

7.4.3. EXPERIMENTAL VALIDATION OF THE CONTROL SCHEMES PROPOSED

This thesis has provided tangible simulation results, which as has been emphasized in the document, will not differ significantly from more realistic approaches such as hardware-on-the-loop. However, its real implementation should be studied in detail analyzing all practical issues that can arise which may be translated into control adjustments and improvements.

7.4.4. REGULATIONS AND GRID CODE PROPOSAL

Finally, this thesis has provided an important know-how of voltage control which could be used in the design of regulation measures or grid codes.

REFERENCES

[Abdelkader, et al. 2009]
Abdelkader, S.M. and Flynn, D., 2009. Graphical determination of network limits for wind power integration, IET Generation, Transmission & Distribution, vol. 3, no. 9, pp. 841-849.

[Ackermann. 2005]
Ackermann, T., 2005. Wind Power in Power System. NJ, USA: John Wiley & Sons, Ldt http://www.windpowerinpowersystems.info/.

[AEMO. 2013]
AEMO, 2013. Wind turbine plant capabilities report. 2013 Wind integration Studies

[Al Kaabi, et al. 2014]
Al Kaabi, S.S., Zeineldin, H.H. and Khadkikar, V., 2014. Planning Active Distribution Networks Considering Multi-DG Configurations, IEEE Transactions on Power Systems, vol. 29, no. 2, pp. 785-793.

[Alnaser, et al. 2015]
Alnaser, S.W. and Ochoa, L.F., 2015. Advanced Network Management Systems: A Risk-Based AC OPF Approach, IEEE Transactions on Power Systems, vol. 30, no. 1, pp. 409-418.

[Alnaser, et al. 2013]
Alnaser, S.W. and Ochoa, L.F., 2013, Distribution network management system: An AC OPF approach, IEEE Power and Energy Society General Meeting (PES).

[Alobeidli, et al. 2014]
Alobeidli, K. and El Moursi, M.S., 2014. Novel coordinated secondary voltage control strategy for efficient utilisation of distributed generations, IET Renewable Power Generation, vol. 8, no. 5, pp. 569-579.

[Alonso. 2001]
Alonso, J., 2001. Phd dissertation: Algoritmo de optimización para el control secundario de tensiones y potencia reactiva en sistemas de energía electrica. Universidad Pontificia Comillas

[Arcidiacono, et al. 1977]
V. Arcidiacono, S. Corsi, A. Garzillo, M. Mocenigo, 1977. Studies on area voltage and reactive power control at ENEL. CIGRE, report 32-77-6,

[Arlaban, et al. 2012]
Arlaban, T., Peiró, J., Lorenzo, P., Alonso,Ó., Rivas,R., Ortiz,D. and Quiñonez-Varela,G. , 2012, Voltage control by multiple wind power plants: field test results, General meeting CIGRE. Paris.

[Azpiri, et al. 2012]
Azpiri, I., Linares, M. and Juberías, G., 2012. TWENTIES project, Deliverable 3.3: Facilities at local and EMS system level.

[Azpiri, et al. 2013]
Azpiri, I., Combarros, C., Pérez, J.C., Veguillas, R., López, M., Lorenzo, M., Linares, M., Egido, I., Lobato, E. and Sáiz-Marín, E., 2013. TWENTIES project. DEMO 1. Test results, with their technical impact and validation, regarding the secondary frequency control demonstration & voltage control demonstration.

[Barbarossa, et al. 2007]
Barbarossa, S. and Scutari, G., 2007. Decentralized Maximum-Likelihood Estimation for Sensor Networks Composed of Nonlinearly Coupled Dynamical Systems, IEEE Transactions on Signal Processing, vol. 55, no. 7, pp. 3456-3470.

[Barros, et al. 2012]
Barros, R.C., Basgalupp, M.P., De Carvalho, A.C P L F. and Freitas, A.A., 2012. A Survey of Evolutionary Algorithms for Decision-Tree Induction, IEEE Transactions on Systems, Man, and Cybernetics, Part C: Applications and Reviews, vol. 42, no. 3, pp. 291-312.

[Bellman. 1957]
Bellman, R.E., 1957. Dynamic Programming. Princeton: NJ: Priceton Univ. Press.

[Berizzi, et al. 2012]
Berizzi, A., Bovo, C., Ilea, V., Merlo, M., Miotti, A.and Zanellini, F., 2012, Decentralized Reactive Power Control of Wind Power Plants. IEEE International Energy Conference and Exhibition (ENERGYCON).

[Bertsekas. 2005]
Bertsekas, D., 2005, Dynamic Programming and Suboptimal Control: From ADP to MPC, 44th IEEE Conference on Decision and Control, European Control Conference. CDC-ECC

[Bignucolo, et al. 2009]
Bignucolo, F., Caldon, R. and Sacco, A., 2009, A novel market based Distribution System controller for active distribution networks, Proceedings of the 44th International Universities Power Engineering Conference (UPEC).

[Biserica, et al. 2011]
Biserica, M., Berseneff, B., Besanger, Y. and Kieny, C., 2011, Upgraded coordinated voltage control for distribution systems, IEEE PowerTech.

[Blanchon. 1972]
G. Blanchon, 1972. A new aspect of studies of reactive enery and voltage. Proceedings of 4th PSCC

[Boamba, et al. 2013]
Boamba, C.-., Mirea,C. and Eremia,M. , 2013, Wind power plant hierarchical control systems: Dynamic operation in the Romanian transmission grid, 8th International Symposium on Advanced Topics in Electrical Engineering (ATEE).

[Bolognani, et al. 2013]
Bolognani, S. and Zampieri, S., 2013. A Distributed Control Strategy for Reactive Power Compensation in Smart Microgrids, IEEE Transactions on Automatic Control, vol. 58, no. 11, pp. 2818-2833.

[Borghetti. 2012]
Borghetti, A., 2012. A Mixed-Integer Linear Programming Approach for the Computation of the Minimum-Losses Radial Configuration of Electrical Distribution Networks, IEEE Transactions on Power Systems, vol. 27, no. 3, pp. 1264-1273.

[Bresesti, et al. 2007]
Bresesti, P., Kling, W.L., Hendriks, R.L. and Vailati, R., 2007. HVDC Connection of Offshore Wind Farms to the Transmission System, IEEE Transactions on Energy Conversion, vol. 22, no. 1, pp. 37-43.

[Calderaro, et al. 2014]
Calderaro, V., Conio, G., Galdi, V., Massa, G. and Piccolo, A., 2014. Optimal Decentralized Voltage Control for Distribution Systems With Inverter-Based Distributed Generators, IEEE Transactions on Power Systems, vol. 29, no. 1, pp. 230-241.

[Caldon, et al. 2013]
Caldon, R., Coppa, M., Sgarbossa, R. and Turri,R. , 2013. A simplified algorithm for OLTC control in active distribution MV networks, AEIT Annual Conference.

[Capitanescu, et al. 2014]
Capitanescu, F., Bilibin, I. and Romero Ramos, E., 2014. A Comprehensive Centralized Approach for Voltage Constraints Management in Active Distribution Grid, IEEE Transactions on Power Systems, vol. 29, no. 2, pp. 933-942.

[Celli, et al. 2005]
Celli, G., Ghiani, E., Mocci, S. and Pilo, F., 2005. A multiobjective evolutionary algorithm for the sizing and siting of distributed generation, IEEE Transactions on Power Systems, vol. 20, no. 2, pp. 750-757.

[Chiodo, et al. 1992]
Chiodo, E., Losi, A., Mongelluzzo, R. and Rossi, F., 1992. Capability chart for electrical power systems, IEE Proceedings C Generation, Transmission and Distribution, vol. 139, no. 1, pp. 71-75.

[Chun-xia Dou, et al. 2013]
Chun-xia Dou and Bin Liu, 2013. Multi-Agent Based Hierarchical Hybrid Control for Smart Microgrid, IEEE Transactions on Smart Grid, vol. 4, no. 2, pp. 771-778.

[CIGRE. 2014]
CIGRE, 2014, Paris, biennial session.

[Coello, et al. 2002]
Coello, C.A. and Lechuga, M.S., 2002, MOPSO: a proposal for multiple objective particle swarm optimization, Congress on Evolutionary Computation.

[Corsi, et al. 2010]
Corsi, S., De Villiers, F. and Vajeth, R., 2010. Secondary Voltage Regulation applied to the South Africa transmission grid, IEEE Power and Energy Society General Meeting.

[Corsi, et al. 2004a]
Corsi, S., Pozzi, M., Sabelli, C. and Serrani, A., 2004a. The coordinated automatic voltage control of the Italian transmission Grid-part I: reasons of the choice and overview of the consolidated hierarchical system, IEEE Transactions on Power Systems, vol. 19, no. 4, pp. 1723-1732.

[Corsi, et al. 2004b]
Corsi, S., Pozzi, M., Sforna, M. and Dell'Olio, G., 2004b. The coordinated automatic voltage control of the Italian transmission Grid-part II: control apparatuses and field performance of the consolidated hierarchical system, IEEE Transactions on Power Systems, vol. 19, no. 4, pp. 1733-1741.

[Cuffe, et al. 2014a]
Cuffe, P. and Keane, A., 2014a. Voltage Responsive Distribution Networks: Comparing Autonomous and Centralized Solutions, IEEE Transactions on Power Systems, vol. PP, no. 99, pp.1-9.

[Cuffe, et al. 2014b]
Cuffe, P., Smith, P. and Keane, A., 2014b. Capability Chart for Distributed Reactive Power Resources, IEEE Transactions on Power Systems, vol. 29, no. 1, pp. 15-22.

[Cuffe, et al. 2014c]
Cuffe, P., Smith, P. and Keane, A., 2014c. Capability Chart for Distributed Reactive Power Resources, IEEE Transactions on Power Systems, vol. 29, no. 1, pp. 15-22.

[Cuffe, et al. 2012a]
Cuffe, P., Smith, P. and Keane, A., 2012a. Transmission System Impact of Wind Energy Harvesting Networks, IEEE Transactions on Sustainable Energy, vol. 3, no. 4, pp. 643-651.

[Cuffe, et al. 2012b]
Cuffe, P., Smith, P. and Keane, A., 2012b. Transmission System Impact of Wind Energy Harvesting Networks, IEEE Transactions on Sustainable Energy, vol. 3, no. 4, pp. 643-651.

[de la Fuente. 1997]
de la Fuente, J.I., 1997. PhD dissertation: Configuración del control jerárquico de tensiones en un sistema de energía eléctrica. Universidad Pontificia Comillas

[Deb, et al. 2007]
Deb, K., Rao, U.B. and Karthik, S., 2007, Dynamic multi-objective optimization and decision-making using modified NSGA-II: a case study on hydro-thermal power schedulingProceedings of International Conference on Evolutionary Multi-criterion Optimization. Matsushima, Japan.

[Deb, et al. 2002]
Deb, K., Pratap, A., Agarwal, S. and Meyarivan, T., 2002. A fast and elitist multiobjective genetic algorithm: NSGA-II, IEEE Transactions on Evolutionary Computation, vol. 6, no. 2, pp. 182-197.

[Delfino, et al. 2010]
Delfino, F., Procopio, R., Rossi, M. and Ronda, G., 2010. Integration of large-size photovoltaic systems into the distribution grids: a p-q chart approach to assess reactive support capability, IET Renewable Power Generation, vol. 4, no. 4, pp. 329-340.

[DeVore. 2004]
DeVore, J.L., 2004. Probability and Stadistics for Engineering and the Sciences. 6th ed.Duxbury pressThomson-Brooks/Cole.

[Di Fazio, et al. 2013]
Di Fazio, A.R., Fusco, G. and Russo, M., 2013. Decentralized Control of Distributed Generation for Voltage Profile Optimization in Smart Feeders, IEEE Transactions on Smart Grid, vol. 4, no. 3, pp. 1586-1596.

[Domínguez. 2013]
Domínguez, M., 2013. PhD dissertation: Conducción eficiente de trenes metropolitanos con ATO. Universidad Pontificia Comillas

[EirGrid. 2014]
EirGrid, 2014. DS3: Voltage Control Workstream (2013 -2015). http://www.eirgrid.com/media/DS3_Voltage_Control_Workstream_Plan_2013_(January%202013).pdf

[EirGrid. 2011]
EirGrid, 2011. EirGrid Grid Code, Version 4.0 http://www.eirgrid.com/media/Grid%20Code%20Version%204.pdf

[Eirgrid, et al. 2013]
Eirgrid and SONI, 2013. DS3: Voltage control workstream. 2013 update. http://www.eirgrid.com/media/DS3_Voltage_Control_Workstream_Plan_2013_(January%202013).pdf

[Eirgrid, et al. 2012]
Eirgrid and SONI, 2012. Voltage control. DS3 Advisory council discussion paper http://www.eirgrid.com/media/DS3%20Advisory%20Council%20Discussion%20Document%20on%20Voltage%20Control.pdf

[Energinet. 2010]
Energinet, 2010. Technical regulation 3.2.5 for wind power plants with a power output greater than 11 kW. https://www.energinet.dk/SiteCollectionDocuments/Engelske%20dokumenter/El/55986-10_v1_Grid%20Code%203%202%205_v%204%201-30%20%20September%202010.pdf

[Engelhardt, et al. 2011]
Engelhardt, S., Erlich, I., Feltes, C., Kretschmann, J. and Shewarega, F., 2011. Reactive Power Capability of Wind Turbines Based on Doubly Fed Induction Generators, IEEE Transactions on Energy Conversion, vol. 26, no. 1, pp. 364-372.

[ENTSO-E. 2013]
ENTSO-E, 2013. Network Code for Requirements for Grid Connection Applicable to all Generators.http://networkcodes.entsoe.eu/wp-content/uploads/2013/08/130308_Final_Version_NC_RfG1.pdf

[ENTSO-E. 2012]
ENTSO-E, 2012. ENTSO-E Draft Network Code for Requirements for Grid Connection applicable to all Generators. https://www.entsoe.eu/fileadmin/user_upload/_library/consultations/Network_Code_RfG/120124_Network_Code_for_Requirements_forGrid_Connection_applicable_to_all_Generators.pdf

[e-on. 2006]
e-on, N., GmbH, 2006. Grid Code. High and extra high voltage. https://www.avacon.de/cps/rde/xbcr/avacon/NAR_englisch.pdf

[Erlich, et al. 2011]
Erlich, I., Nakawiro, W. and Martinez, M., 2011, Optimal dispatch of reactive sources in wind farms IEEE Power and Energy Society General Meeting.

[Etherden, et al. 2011]
Etherden, N., Bollem, M. H. J., 2011, Increasing the Hosting Capacity of Distribution Neworks by Curtailment of Renewable Energy Resources IEEE PowerTech

[EWEA. 2012]
EWEA., 2012. Wind in power, 2011 European statistics. http://www.ewea.org/fileadmin/files/library/publications/statistics/Wind_in_power_2011_European_statistics.pdf.

[Falahi, et al. 2013]
Falahi, M., Butler-Purry, K. and Ehsani, M., 2013. Dynamic Reactive Power Control of Islanded Microgrids, IEEE Transactions on Power Systems, vol. 28, no. 4, pp. 3649-3657.

[Farag, et al. 2013]
Farag, H.E., El-Saadany, E.F. and Seethapathy,R., 2013, A multi-agent voltage and reactive power control for multiple feeders with distributed generation, IEEE Power and Energy Society General Meeting (PES).

[Farhangi. 2010]
Farhangi, H., 2010. The path of the smart grid, IEEE Power and Energy Magazine , vol. 8, no. 1, pp. 18-28.

[Fei-Yue Wang, et al. 2009]
Fei-Yue Wang, Huaguang Zhang and Derong Liu, 2009. Adaptive Dynamic Programming: An Introduction, IEEE Computational Intelligence Magazine, vol. 4, no. 2, pp. 39-47.

[FP7, 2015]
European commision seventh framework. Research and Innovation http://ec.europa.eu/research/fp7/index_en.cfm

[Frias. 2008]
Frias, P., 2008. PhD dissertation: A regulatory model proposal for voltage control in electric power systems. Universidad Pontificia Comillas

[Furong Li, et al. 2005]
Furong Li, Pilgrim, J.D., Dabeedin, C., Chebbo, A. and Aggarwal, R.K., 2005. Genetic algorithms for optimal reactive power compensation on the national grid system, IEEE Transactions on Power Systems, vol. 20, no. 1, pp. 493-500.

[Gamesa. 2013]
Gamesa, 2013. 2.0 - 2.5 MW technological evolution. http://www.gamesacorp.com/recursos/doc/productos-servicios/aerogeneradores/catalogo-g9x-20-mw-eng.pdf

[Gao, et al. 2011]
Gao, C. and Redfern, M.A., 2011. Advanced Voltage Control Strategy for On-Load Tap-Changer Transformers with Distributed Generations, Proceedings of 46th International Universities' Power Engineering Conference (UPEC).

[García-González, et al. 2010]
García-González, J., Mata, J.L. and Veguillas, R., 2010, Improving the integration of renewable sources in the European electricity networks, IEEE Power and Energy Society General Meeting.

[Gargiulo, et al. 2002]
Gargiulo, G., Mangoni, V. and Russo, M., 2002. Capability charts for combined cycle power plants, IEE Proceedings Generation, Transmission and Distribution, vol. 149, no. 4, pp. 407-415.

[GE. 2010]
GE, 2010. 2.5 MW wind turbine series. http://pdf.directindustry.com/pdf/ge-wind-turbines/25-mw-wind-turbine/34152-169490.html

[Global Wind Energy Council. 2013]
Global Wind Energy Council, 2013. Global Wind Energy Report. http://www.gwec.net/publications/global-wind-report-2/global-wind-report-2013/

[Hamzeh, et al. 2013]
Hamzeh, M., Mokhtari, H. and Karimi, H., 2013. A decentralized self-adjusting control strategy for reactive power management in an islanded multi-bus MV microgrid, Canadian Journal of Electrical and Computer Engineering, , vol. 36, no. 1, pp. 18-25.

[Hashemi, et al. 2011]
Hashemi, Z. and Mardaneh, M., 2011, Improvement in the performance of cascaded tap changers using a fuzzy rule-based scheme, 6th IEEE Conference on Industrial Electronics and Applications (ICIEA).

[Holland. 1992]
Holland, J.H., 1992. Adaptation in natural and artificial systems. The MIT press.

[Hu, et al. 2014]
Hu, W., CHEN, Z., Bak-Jensen, B. and Hu, Y., 2014. Fuzzy adaptive particle swarm optimisation for power loss minimisation in distribution systems using optimal load response, IET Generation, Transmission & Distribution, vol. 8, no. 1, pp. 1-10.

[Janssens. 1993]
Janssens, N., 1993, Tertiary and secondary voltage control for the Belgian HV system, IEE Colloquium on International Practices in Reactive Power Control.

[Keane, et al. 2012]
Keane, A., Cuffe, P., Diskin, E., Brooks, D., Harrington, P., Hearne, T., Rylander, M. and Fallon, T., 2012. Evaluation of Advanced Operation and Control of Distributed Wind Farms to Support Efficiency and Reliability, IEEE Transactions on Sustainable Energy, vol. 3, no. 4, pp. 735-742.

[Keane, et al. 2013]
Keane, A., Ochoa, L.F., Borges, C.L.T., Ault, G.W., Alarcon-Rodriguez, A.D., Currie, R., Pilo, F., Dent, C. and Harrison, G.P., 2013. State-of-the-Art Techniques and Challenges Ahead for Distributed Generation Planning and Optimization, IEEE Transactions on Power Systems, vol. 28, no. 2, pp. 1493-1502.

[Keane, et al. 2011]
Keane, A., Ochoa, L.F., Vittal, E., Dent, C.J. and Harrison, G.P., 2011. Enhanced Utilization of Voltage Control Resources With Distributed Generation, IEEE Transactions on Power Systems, vol. 26, no. 1, pp. 252-260.

[Keane, et al. 2007]
Keane, A. and O'Malley, M., 2007. Optimal Utilization of Distribution Networks for Energy Harvesting, IEEE Transactions on Power Systems, vol. 22, no. 1, pp. 467-475.

[Kennedy, et al. 1995]
Kennedy, J. and Eberhart, R., 1995, Particle swarm optimization, Proceedings of IEEE International Conference on Neural Networks.

[Konopinski, et al. 2009]
Konopinski, R.J., Vijayan, P. and Ajjarapu, V., 2009. Extended Reactive Capability of DFIG Wind Parks for Enhanced System Performance, IEEE Transactions on Power Systems, vol. 24, no. 3, pp. 1346-1355.

[Kulmala, et al. 2007]
Kulmala, A., Maki, K., Repo, S. and Jarventausta,P., 2007, Active Voltage Level Management of Distribution Networks with Distributed Generation using On Load Tap Changing Transformers, IEEE PowerTech.

[Kulmala, et al. 2014]
Kulmala, A., Repo, S. and Järventausta, P., 2014. Coordinated Voltage Control in Distribution Networks Including Several Distributed Energy Resources, Smart Grid, IEEE Transactions on, vol. 5, no. 4, pp. 2010-2020.

[Kulmala, et al. 2012]
Kulmala, A., Mutanen,A., Koto,A., Repo,S. and Jarventausta,P., 2012, Demonstrating coordinated voltage control in a real distribution network, 3rd IEEE International Conference and Exhibition on Innovative Smart Grid Technologies (ISGT Europe).

[Kundur. 1994]
Kundur, P., 1994. Power System Stability and Control. Palo Alto, California: McGraw-Hill.

[Lechuga. 2006]
Lechuga, M.S., 2006. Multi-Objective Optimisation using Sharing in Swarm Optimisation Algorithms.

[Lefebvre, et al. 2000]
Lefebvre, H., Fragnier, D., Boussion, J.Y., Mallet, P. and Bulot,M. , 2000, Secondary coordinated voltage control system: feedback of EDF, IEEE Power Engineering Society Summer Meeting.

[Lewis. 1992]
Lewis, F.L., 1992. Applied Optimal Control and Estimation. Upper Saddle River: NJ: Prentice-Hall.

[Lewis, et al. 1995]
Lewis, F.L. and V. Syrmos, L., 1995. Optimal Control. New York: NY: Wiley.

[Li, et al. 2010]
Li, L. and Zhang, X., 2010, Study of data mining algorithm based on decision tree, International Conference on Computer Design and Applications (ICCDA).

[Liew, et al. 2002]
Liew, S.N. and Strbac, G., 2002. Maximising penetration of wind generation in existing distribution networks, IEE Proceedings Generation, Transmission and Distribution, vol. 149, no. 3, pp. 256-262.

[Loia, et al. 2013]
Loia, V., Vaccaro, A. and Vaisakh, K., 2013. A Self-Organizing Architecture Based on Cooperative Fuzzy Agents for Smart Grid Voltage Control, IEEE Transactions on Industrial Informatics, vol. 9, no. 3, pp. 1415-1422.

[Losi, et al. 1998]
Losi, A., Mangoni, V. and Russo, M., 1998. Optimal exploitation of generator-transformer units, IEEE Transactions on Energy Conversion, , vol. 13, no. 1, pp. 90-95.

[Losi, et al. 1996]
Losi, A., Russo, M., Verde, P. and Menniti, D., 1996, Capability chart for generator-transformer units, 8th Mediterranean Electrotechnical Conference MELECON.

[Madureira, et al. 2009]
Madureira, A.G. and Pecas Lopes, J.A., 2009. Coordinated voltage support in distribution networks with distributed generation and microgrids, IET Renewable Power Generation, vol. 3, no. 4, pp. 439-454.

[Martinez, et al. 2011]
Martinez, M.I., Tapia, G., Susperregui, A. and Camblong, H., 2011. DFIG Power Generation Capability and Feasibility Regions Under Unbalanced Grid Voltage Conditions, IEEE Transactions on Energy Conversion, vol. 26, no. 4, pp. 1051-1062.

[Masters. 2002]
Masters, C.L., 2002. Voltage rise: the big issue when connecting embedded generation to long 11 kV overhead lines, Power Engineering Journal, vol. 16, no. 1, pp. 5-12.

[Bollen, et al. 2011]
Math H.J Bollen, Fainan Hassan., 2011. Integration of Distributed Generation in the Power System. New Jersey, USA: John Willey & Sons Inc Hoboken.

[McArthur, et al. 2007]
McArthur, S.D.J., Davidson, E.M., Catterson, V.M., Dimeas, A.L., Hatziargyriou, N.D., Ponci, F. and Funabashi, T., 2007. Multi-Agent Systems for Power Engineering Applications—Part I: Concepts, Approaches, and Technical Challenges, IEEE Transactions on Power Systems, vol. 22, no. 4, pp. 1743-1752.

[Meegahapola, et al. 2012]
Meegahapola, L.G., Vittal,E., Keane,A. and Flynn,D. , 2012,Voltage security constrained reactive power optimization incorporating wind generation, IEEE International Conference on Power System Technology (POWERCON).

[Ministério da economia, da inovação e do desenvolviento. 2010]
Ministério da economia, da inovação e do desenvolviento, 2010. Portaria n.º 596/201030 de Julho 2010.

[Moradzadeh, et al. 2013]
Moradzadeh, M., Boel, R. and Vandevelde, L., 2013. Voltage Coordination in Multi-Area Power Systems via Distributed Model Predictive Control, IEEE Transactions on Power Systems, vol. 28, no. 1, pp. 513-521.

[Muttaqi, et al. 2013]
Muttaqi, K.M., Le,A.D.T., Negnevitsky, M. and Ledwich,G., 2013, A coordinated voltage control approach for coordination of OLTC, voltage regulator and DG to regulate voltage in a distribution feeder, IEEE Industry Applications Society Annual Meeting.

[Nakawiro. 2014]
Nakawiro, W., 2014, Predictive voltage control for a distribution network with renewable energy sources, International Electrical Engineering Congress (iEECON).

[Nasri, et al. 2012]
Nasri, M., Farhangi, H., Palizban, A. and Moallem, M. , 2012, Multi-agent control system for real-time adaptive VVO/CVR in Smart Substation, IEEE Electrical Power and Energy Conference (EPEC).

[Ochoa, et al. 2010]
Ochoa, L.F., Dent, C.J. and Harrison, G.P., 2010. Distribution Network Capacity Assessment: Variable DG and Active Networks, IEEE Transactions on Power Systems, vol. 25, no. 1, pp. 87-95.

[Ochoa, et al. 2011]
Ochoa, L.F. and Harrison, G.P., 2011. Minimizing Energy Losses: Optimal Accommodation and Smart Operation of Renewable Distributed Generation, IEEE Transactions on Power Systems, vol. 26, no. 1, pp. 198-205.

[Ochoa, et al. 2010]
Ochoa, L.F. and Harrison, G.P., 2010, Using AC Optimal Power Flow for DG planning and optimisation, IEEE Power and Energy Society General Meeting.

[Ochoa, et al. 2011]
Ochoa, L.F., Keane, A. and Harrison, G.P., 2011. Minimizing the Reactive Support for Distributed Generation: Enhanced Passive Operation and Smart Distribution Networks, Power Systems, IEEE Transactions on, vol. 26, no. 4, pp. 2134-2142.

[Ozturk, et al. 2009]
Ozturk, A. and Dosoglu, K., 2009, Investigation of the control voltage and reactive power in wind farm load bus by statcom and SVC, International Conference on Electrical and Electronics Engineering, ELECO.

[Pagola. 1993]
Pagola, L., 1993. Apuntes de Control Digital. UPCO-ICAI-ETS de ingenieros industriales.

[Pappala, et al. 2010]
Pappala, V.S., Nakawiro, W and Erlich, I., 2010, Predictive optimal control of wind farm reactive sources, IEEE Transmission and Distribution Conference and Exposition.

[Paul, et al. 1987]
Paul, J.P., Leost, J.Y. and Tesseron, J., 1987. Survey of the Secondary Voltage Control in France: Present Realization and Investigations, IEEE Transactions on Power Systems, vol. 2, no. 2, pp. 505-511.

[Pilo, et al. 2011]
Pilo, F., Pisano, G. and Soma, G.G., 2011. Optimal Coordination of Energy Resources With a Two-Stage Online Active Management, IEEE Transactions on Industrial Electronics, vol. 58, no. 10, pp. 4526-4537.

[Piret, et al. 1992]
Piret, J.P., Antoine, J.P., Stubbe, M., Janssens, N. and Delince, J.M., 1992. The Study of a Centralised Voltage Control Method Applicable to the Belgian System.

[Quinlan. 1993]
Quinlan, R., 1993. C4.5: Programs for Machine Learning. San Mateo, CA: Morgan Kaufmann.

[Quinlan. 1986]
Quinlan, R., 1986. Induction of Decision Trees. Machine Learning.

[Ranamuka, et al. 2014]
Ranamuka, D., Agalgaonkar, A. and Muttaqi, K.M., 2014. Online Voltage Control in Distribution Systems With Multiple Voltage Regulating Devices, IEEE Transactions on Sustainable Energy, vol. 5, no. 2, pp. 617-628.

[Raquel, et al. 2005]
Raquel, C.R. and Naval, P.C., 2005, An effective use of crowding distance in multiobjective particle swarm optimization, Proceedings of the 2005 conference on Genetic and evolutionary computation, 2005 Washington DC, USA. ACM, 257-264.

[REE. 1998]
REE, 1998. P.O.1.1: Criterios de funcionamiento y seguridad para la operación del sistema eléctrico.

[REE. 2005]
REE, 2005. P.O. 13.1: Criterios de desarrollo de la red de transporte," Art 3.1.7. Only available in Spanish

[REE. 2010]
REE, 2010a. P.O. 12.2: Instalaciones conectadas a la red de transporte y equipo generador: requisitos mínimos de diseño, equipamiento, funcionamiento, puesta en servicio y seguridad. Only available in Spanish

[REE. 2011]
REE, 2011. P.O. 7.5: Servicio complementario de control de tensión en el sistema eléctrico español aplicable al régimen especial (borrador). Only available in Spanish

[Robertson, et al. 2012]
Robertson, J., Harrison, G.P. and Wallace, A.R., 2012, A pseudo-real time distribution network simulator for analysis of coordinated ANM control strategies, CIRED Workshop on Integration of Renewables into the Distribution Grid.

[Rouco, et al. 2013]
Rouco L, Sáiz-Marín E., (Iberdrola supervisión: Pérez-Campion J.C.,) 2013 Comparación de la contribución de la generacion síncrona y no síncrona a la estabilidad del sistema.

[Rueda-Medina, et al. 2013]
Rueda-Medina, A. and Padilha-Feltrin, A., 2013. Distributed Generators as Providers of Reactive Power Support — A Market Approach, IEEE Transactions on Power Systems, vol. 28, no. 1, pp. 490-502.

[Ruggeri, et al.2008]
F. Ruggeri, R. Kenett and F. Faltin. 2008. Classification and Regression Tree Methods, In: Encyclopedia of Statics in Quality and ReliabilityWiley, pp. 315-323http://www.stat.wisc.edu/~loh/treeprogs/guide/eqr.pdf.

[Sáiz-Marín, et al.2014]
Saiz-Marin, E., Lobato, E. and Egido, I., 2014b. Local Hosting Capacity Increase by Means of Wind Farm Voltage Control Provision, IEEE Transactions on Power Systems, vol. 29, no. 4, pp. 1731-1738.

[Sansawatt, et al. 2012]
Sansawatt, T., Ochoa, L.F. and Harrison, G.P., 2012. Smart Decentralized Control of DG for Voltage and Thermal Constraint Management, IEEE Transactions on Power Systems, vol. 27, no. 3, pp. 1637-1645.

[Sansawatt, et al. 2011]
Sansawatt, T., Ochoa, L.F. and Harrison, G.P., 2011, Operational windows for decentralized control of renewable DG: Techno-economic trade-offs, 2nd IEEE International Conference and Exhibition on Innovative Smart Grid Technologies (ISGT Europe).

[Sansawatt, et al. 2010]
Sansawatt, T., Ochoa, L.F. and Harrison, G.P., 2010, Integrating distributed generation using decentralised voltage regulation, IEEE Power and Energy Society General Meeting.

[Siano, et al. 2010]
Siano, P., Chen, P., Chen, Z. and Piccolo, A., 2010. Evaluating maximum wind energy exploitation in active distribution networks, IET Generation, Transmission & Distribution, vol. 4, no. 5, pp. 598-608.

[Siemens 2015]
Siemens, 2015 PSS\E http://w3.siemens.com/smartgrid/global/en/products-systems-solutions/software-solutions/planning-data-management-software/planning-simulation/pages/pss-e.aspx.

[Singh, et al. 2010]
Singh, S.N., Østergaard, J. and Singh, B., 2010, Reactive power capability of unified DFIG for wind power generation, IEEE Power and Energy Society General Meeting.

[Smith, et al. 2010]
Smith, P., Cuffe, P., Grimes, S. and Hearne,T., 2010, Ireland's approach for the connection of large amounts of renewable generation, IEEE Power and Energy Society General Meeting.

[Spanish government. 2004]
Ministerio de Industria, Turismo y Comercio, 2004. Royal decree 436/2004. https://www.boe.es/diario_boe/txt.php?id=BOE-A-2004-5562.

[Spanish government. 2007]
Ministerio de Industria, Turismo y Comercio, 2007. Royal decree 661/2007. http://www.boe.es/boe/dias/2007/05/26/pdfs/A22846-22886.pdf Only available in Spanish

[Spanish government. 2011]
Ministerio de Industria, Turismo y Comercio, 2011. Planificación de los sectores de electricidad y gas, 2012-2020. Desarrollo de las redes de transporte. http://www.minetur.gob.es/energia/es-ES/Novedades/Documents/PlanificacionElectricidadGas_2012_2020.pdf

[Spanish government. 2010]
Ministerio de Industria, Turismo y Comercio, 2010. Royal decree 1565/2010 http://www.boe.es/boe/dias/2010/11/23/pdfs/BOE-A-2010-17976.pdf http://www.omel.es/files/correccion_r.d_1565-2010_de_19_de_noviembre_10-03-2011.pdf. Only available in Spanish.

[Strang. 1988]
Strang, G., 1988. Linear algebra and its applications. 3rd ed.Harcourt Brace Jovanovich, Inc.

[Sulligoi, et al. 2011]
Sulligoi, G., Chiandone, M. and Arcidiacono, V., 2011, NewSART automatic voltage and reactive power regulator for secondary voltage regulation: Design and application, IEEE Power and Energy Society General Meeting.

[Tan, et al. 2005]
Tan, P., Steinbach, M. and Kumar, V., 2005. Introduction to data mining. Reading. MA, USA: Adison-Wesley.

[Taranto, et al. 2000]
Taranto, G.N., Martins, N., Falcao, D.M., Martins, A.C.B. and Dos Santos,M.G., 2000, Benefits of applying secondary voltage control schemes to the Brazilian system, IEEE Power Engineering Society Summer Meeting.

[Timofeev. 2004]
Timofeev, R., 2004. MPhil: Classification and regression trees (CART). Theory and Application.

[TWENTIES. 2013]
TWENTIES., 2013. European project funded by 7th framework. http://www.twenties-project.eu/node/1.

[Vaccaro, et al. 2011]
Vaccaro, A., Velotto, G. and Zobaa, A.F., 2011. A Decentralized and Cooperative Architecture for Optimal Voltage Regulation in Smart Grids, IEEE Transactions on Industrial Electronics, vol. 58, no. 10, pp. 4593-4602.

[Valverde, et al. 2014]
Valverde, G. and Orozco, J.J., 2014, Reactive power limits in distributed generators from generic capability curves, IEEE Power and Energy Society General Meeting.

[Valverde, et al. 2013]
Valverde, G. and Van Cutsem, T., 2013. Model Predictive Control of Voltages in Active Distribution Networks, IEEE Transactions on Smart Grid, vol. 4, no. 4, pp. 2152-2161.

[Van Cutsem, et al. 1998]
Van Cutsem, T. and Vournas, C., 1998. Voltage stability of electric power systems. Boston, USA: Kluwer Academic Publishers.

[Venayagamoorthy, et al. 2012]
Venayagamoorthy, G.K., Rohrig, K. and Erlich, I., 2012. One Step Ahead: Short-Term Wind Power Forecasting and Intelligent Predictive Control Based on Data Analytics, IEEE Power and Energy Magazine, vol. 10, no. 5, pp. 70-78.

[Vialas, et al. 1988]
Vialas, C. and Paul, J.P., 1988. Trends in Automatic Regional Voltage Control of the French EHV Power System: The Effect on Communication Requirements.

[Vovos, et al. 2007]
Vovos, P.N., Kiprakis, A., Wallace, A. and Harrison, G.P., 2007. Centralized and Distributed Voltage Control: Impact on Distributed Generation Penetration, IEEE Transactions on Power Systems, vol. 22, no. 1, pp. 476-483.

[Wehenkel. 1997]
Wehenkel, L., 1997. Automatic Learning Techniques in Power Systems. Boston, MA, USA: Kluwer.

[Wei Zhang, et al. 2014]
Wei Zhang, Wenxin Liu, Xin Wang, Liming Liu and Ferrese, F., 2014. Distributed Multiple Agent System Based Online Optimal Reactive Power Control for Smart Grids, IEEE Transactions on Smart Grid, vol. 5, no. 5, pp. 2421-2431.

[Werbos. 1977]
Werbos, P.J., 1977. Advanced forecasting method for global crisis warning and models of intelligence, General Syst. vol. 22, pp. 25-38.

[Wilson. 1975]
Wilson, E.O., 1975. Sociobiology: The new synthesis, vol. Belknap Press, Cambridge, MA.

[Windham. 1982]
Windham, M.P., 1982. Cluster Validity for the Fuzzy c-Means Clustering Algorithrm, IEEE Transactions on Pattern Analysis and Machine Intelligence, vol. PAMI-4, no. 4, pp. 357-363.

[Wooldridge. 1996]
Wooldridge, M., 1996, What agents aren't: a discussion paper, IEE Colloquium on Intelligent Agents and Their Applications.

[Xiangyu Zhang, et al. 2010]
Xiangyu Zhang, Heming Li and Yi Wang., 2010, Control of DFIG-based wind farms for power network frequency support, International Conference on Power System Technology (POWERCON).

[Xiaohu Liu, et al. 2012]
Xiaohu Liu, Aichhorn, A., Liming Liu and Hui Li, 2012. Coordinated Control of Distributed Energy Storage System With Tap Changer Transformers for Voltage Rise Mitigation Under High Photovoltaic Penetration, IEEE Transactions on Smart Grid, vol. 3, no. 2, pp. 897-906.

[Yang. 2008]
Yang, X.S., 2008. Nature - Inspired Metaheuristic Algorithm. Luniver Press.

[Yanhua Liu, et al. 2011]
Yanhua Liu, Xu Zhang, Dongmei Zhao and Min Ma. , 2011, Research on the Wind Farm Reactive Power Compensation Capacity and Control Target, Asia-Pacific Power and Energy Engineering Conference (APPEEC).

[Ye Li, et al. 2010]
Ye Li, Nair, N.C. and Sing-Kiong Nguang. , 2010, Improved coordinated control of On-load Tap Changers, 20th Australasian Universities Power Engineering Conference (AUPEC).

[Yorino, et al. 2014]

Yorino, N., Zoka, Y., Watanabe, M.and Kurushima, T., 2014. An Optimal Autonomous Decentralized Control Method for Voltage Control Devices by Using a Multi-Agent System, IEEE Transactions on Power Systems, vol. PP, no. 99, pp. 1-91.

[Young-Jin Kim, et al. 2013]

Young-Jin Kim, Seon-Ju Ahn, Pyeong-Ik Hwang, Gi-Chan Pyo and Seung-Il Moon, 2013. Coordinated Control of a DG and Voltage Control Devices Using a Dynamic Programming Algorithm, IEEE Transactions on Power Systems, vol. 28, no. 1, pp. 42-51.

[Yu, et al. 2010]

Yu, Z., Haghighat, F., Fung, B.C.M. and Yoshino, H., 2010. A decision tree method for building energy demand modeling, Energy & Buildings vol. 42, pp. 1637-1646.

[Zechun Hu, et al. 2012]

Zechun Hu and Furong Li, 2012. Cost-Benefit Analyses of Active Distribution Network Management, Part I: Annual Benefit Analysis, IEEE Transactions on Smart Grid, vol. 3, no. 3, pp. 1067-1074.

[Zhao, et al. 2005]

Zhao, B., Guo, C.X. and Cao, Y.J., 2005. A multiagent-based particle swarm optimization approach for optimal reactive power dispatch, IEEE Transactions on Power Systems, vol. 20, no. 2, pp. 1070-1078.

[Zwe-Lee Gaing. 2003]

Zwe-Lee Gaing, 2003. Particle swarm optimization to solving the economic dispatch considering the generator constraints, IEEE Transactions on Power Systems, vol. 18, no. 3, pp. 1187-1195.

APPENDIX A
TEST NETWORKS EVALUATED

Eight different HNets have been used throughout this thesis for showing the adequacy of different voltage control schemes depending on their characteristics. Two of them have been evaluated in more detail in Chapter 3. In this appendix their characteristics and one-line diagrams are provided.

The first HNet analyzed is a radial one containing short feeders. This network contains 11 wind farms and a solar thermal plant which maintains a unity power factor in Chapter 3. Nonetheless, subsequent chapters will assume that this plant provides also reactive power/voltage control. The installed active power of all wind farms and the solar thermal plant within HNet1 is presented in Table A-1. The one-line diagram of this network is depicted in Figure A-1 in which the solar plant is depicted with dotted lines.

Table A-1. Installed active power of each wind farm within HNet1

	Wind farms											
	1	2	3	4	5	6	7	8	9	10	11	Solar plant
Power (MW)	24	20	50	28	12	16	26	50	50	50	50	100

The second HNet has 13 wind farms. This network is partially meshed and representative of long lines. The total installed power of each wind farm in HNet2 is presented in Table A-2 and its one-line diagram is depicted in Figure A-2.

Table A-2. Installed active power of each wind farm within HNet2

Wind farms	1	2	3	4	5	6	7	8	9	10	11	12	13
Power (MW)	16	30	38	18	48	12	30	32	25	35	40	40	150

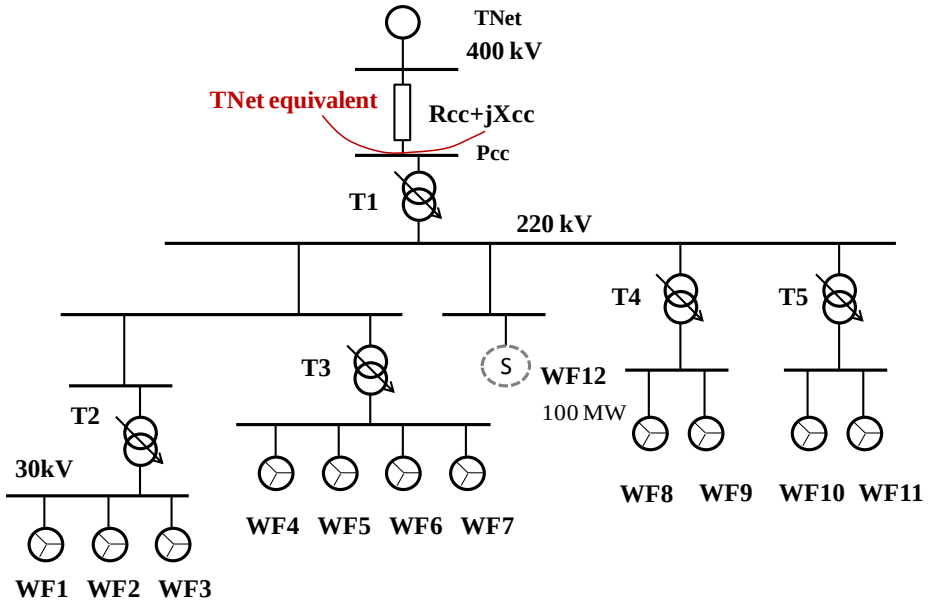

Figure A-1 First wind energy HNet evaluated (HNet1)

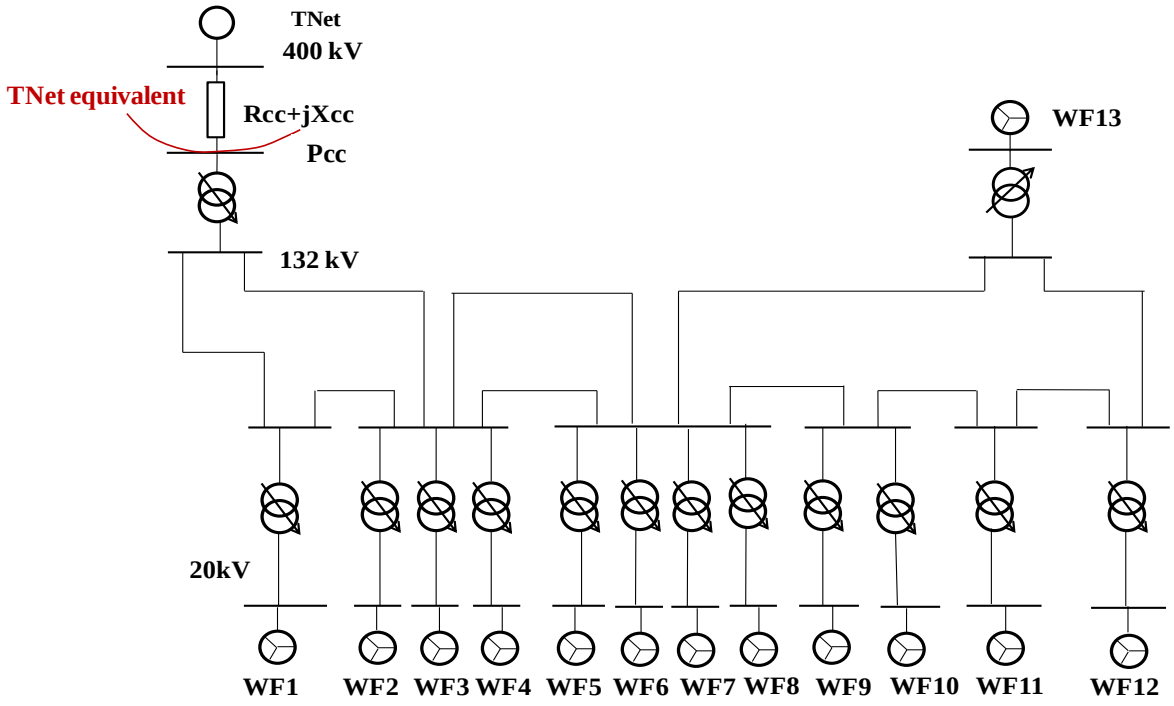

Figure A-2 Second wind energy HNet evaluated (HNet2).

In both networks, TNet is represented with the Thevenin equivalent (R_{Thev}+jX_{Thev}), where X_{Thev} is the inverse of the short-circuit power assuming ($Z_{Thev} \approx X_{Thev}$) and R_{Thev} is evaluated in accordance with the X/R ratio. Within this thesis the mean values (year 2010) of these magnitudes for the real networks are used. On one hand, the mean yearly

short-circuit power is 5065 MVA for HNet1 and 8033MVA for HNet2. On the other hand, the mean yearly X/R ratio is 11.4 for HNet1 and 11.2 for HNet2.

Wind farm capabilities have been defined in accordance with the proposal P.O. 7.5 [REE 2011] which demands more controllability. In this proposal the reactive power constraints are defined with the PQ chart next depicted in Figure A-3. As can be seen, those requirements lineally increase from 0 to 20% of total installed active power neglecting the lagging effect of discharging lines. Once that this active power level is reached, constant limits (30%) are considered, which are reduced for the lagging component when the wind farm is highly loaded. In addition, the QV chart is also provided in Figure A-4 where the Spanish and the ENTSO-E charts are compared. Focusing on the Spanish grid code (first subplot), a lineal relationship between Q and V has been established. Nonetheless, other relationship more demanding could be established always that not exceed the ENTSO-E inner envelope [ENTSO-E 2013]. Based on that, this thesis has considered that wind farms have reactive power capabilities in all voltage range 0.95-1.05 p.u.

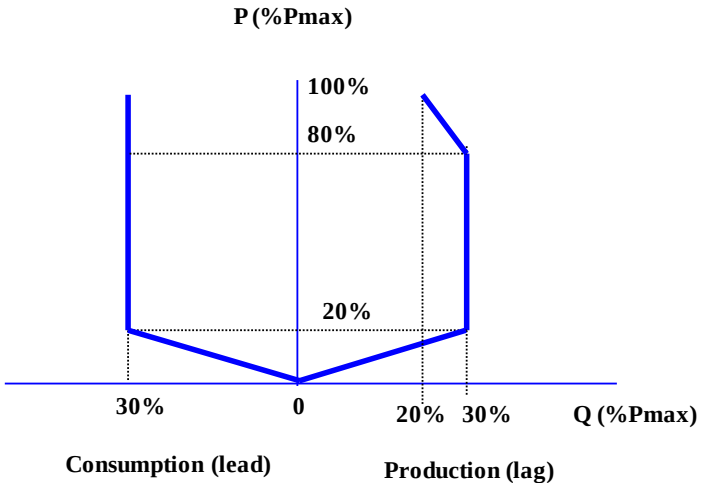

Figure A-3 PQ chart at wind farms connection bus [REE 2011]

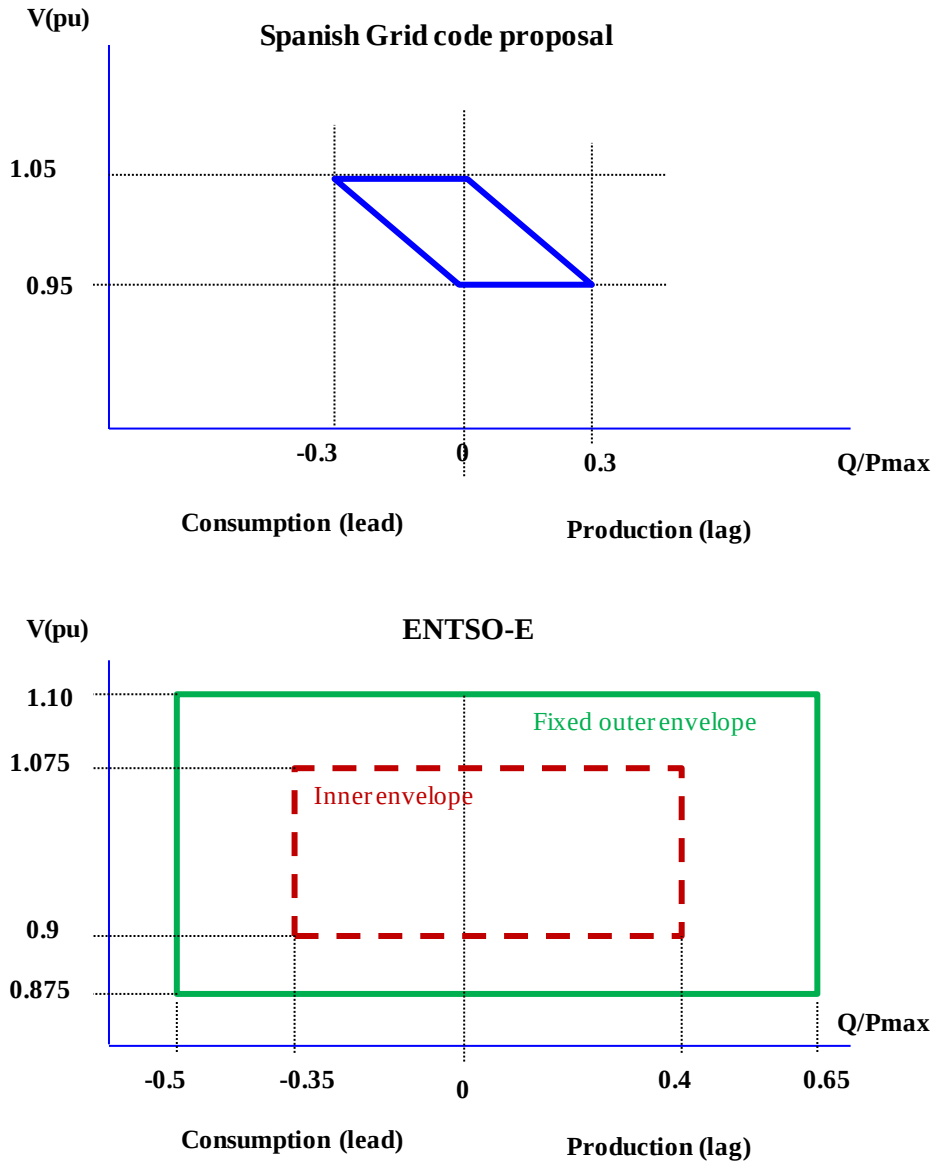

Figure A-4 QVchart at wind farms connection bus [REE 2011, ENTSO-E 2013]

APPENDIX B

QV RELATIONSHIP AND LOCAL HOSTING CAPACITY

This appendix presents the QV relationship outlining the important role of the X/R ratio, parameter that affects the possible rise or decrease of voltages when active power is increased. Moreover, how the local hosting capacity can be increased thanks to voltage control provision is discussed considering simplified models. Note that the proper area analysis is included in Chapter 3.

B.1 VOLTAGE RISE EFFECT

From the transmission network perspective, voltage drop (which could be the origin of voltage collapse) is the most risky situation. However, [Masters 2002] states that in distribution network the voltage rise is a major issue which appears before. This different behaviour is due to the X/R ratio. On one hand, transmission network typically presents high X/R ratio, which means that are inductive networks. On the other hand, distribution network are more characterised for having low X/R meaning that are network with a high resistive component. HNets, which are the focus of this thesis, resembles distribution networks presenting also a high resistive component. This section addressed this issue which is complemented with examples in the next section and is ended with a mathematical demonstration. The first network model evaluated depicted in Figure B-1,

is a very simplified one. As can be seen the aggregate model of the HNet is connected to TNet through its thevenin equivalent (voltage source and thevenin impedance).

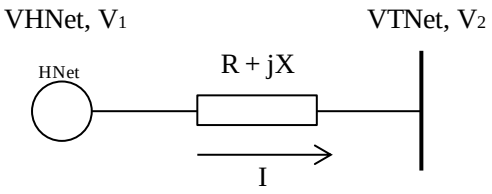

Figure B-1 Simplified network model of both HNet and TNet

Taking into account this model a graphical analysis of the R impact has been done which later is expanded with examples and mathematically demonstrated. In case (a), only a reactance is considered. Hence, V_1 (HNet voltage) is perpendicular to jXI and V_2 corresponds to the circle diagonal. This fact means that always V_2 (TNet voltage) will be higher than V_1. In the event of considering V_2 constant, V_1 is allocated always in the circumference. On the contrary, in case (b), a resistance has been added. In this situation V_1 is out of the circle, meaning that depending on the size of this component V_2 will be higher or lower than V_1

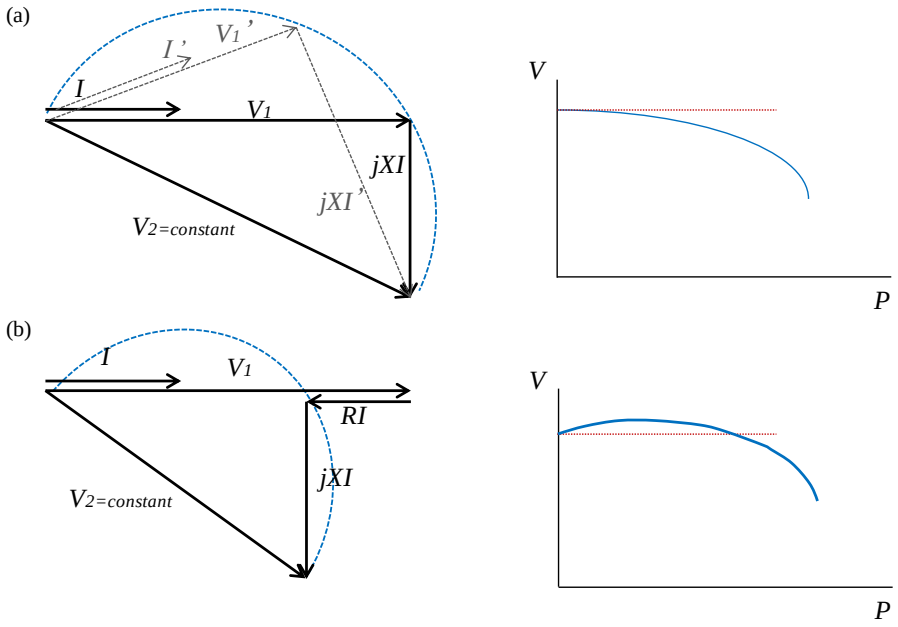

Figure B-2 Graphical analysis of the R impact

B.2 LOCAL HOSTING CAPACITY

Using the simplified model of both TNet and HNet (as was outlined in the previous subsection), this section explains how steady-state voltage boundaries may limit wind hosting capacity and how the use of wind farms' reactive power capabilities delays the

appearance of this type of constraints. Considering steady-state bus voltage constraints, Figure B-3 shows an example of the increase in local hosting capacity that can be gained with the provision of voltage control. In this figure, the SCC is fixed to 4000 MVA (which is a representative low value and thus, an unfavourable one) and an initial voltage of V_{TNet}=1.00 p.u is used. The PV curves have been obtained for a low (2) and a considerably high (30) X/R ratio in two situations. The first situation, assumes that wind farms maintain a fixed power factor equal to one whereas the second situation takes into account the HNet reactive power capabilities to maintain an adequate voltage profile.

The PQ chart of the HNet in this simplified model is represented by a linear function of the hosting capacity, obtained extrapolating the wind turbines capabilities as shows Figure B-4. In this figure three PQ charts are depicted, for 1 wind turbine, 2 wind turbines and for 3 wind turbines assuming a typical wind turbine of 2MW (with reactive power capabilities of ±0.65MVAR), in order to show how reactive power capabilities increase with the addition of wind power installation capacity. In addition, a continuous thick line indicates the reactive capability in case of taking into account that the wind active power penetration increment means an increment in the installed capacity. This hypothesis, which corresponds with the most unfavourable situation, will be used throughout the appendix.

When the X/R ratio is small, the rise in voltage is significant and the production of wind power could be limited due to over-voltages (voltages over 1.05 p.u.) as can be seen in Figure B-3. In case of providing voltage control, the rise in voltage decreases significantly and the hosting capacity limit resulting from overvoltage disappears. As a result, the hosting capacity increases significantly. When the ratio is large, the hosting capacity is limited because of voltage under the admissible value (0.95 p.u.). In this case, thanks to the voltage control provision, the hosting capacity is increased. Nevertheless, the hosting capacity increment is significantly lower when the limitation on the hosting capacity is caused by voltages under the limit value than when it is caused by overvoltage, as can be observed in Figure B-3. In addition, reactive power capabilities might not be sufficient to maintain V_{TNet} at a fixed value as can be seen in the first subplot of Figure B-3 between 0 and 1000 MW. In that period as can be contrasted in Figure B-5 the maximum reactive power is delivered.

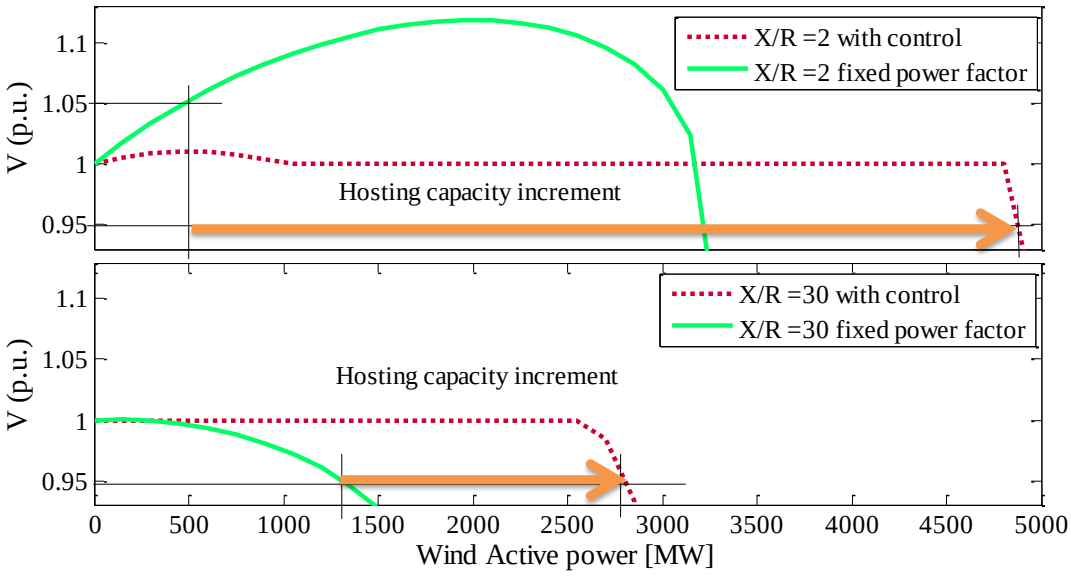

Figure B-3 Voltage for two different X/R ratios (SCC=4000 MVA, VTNet=1.00 p.u.) in two situations

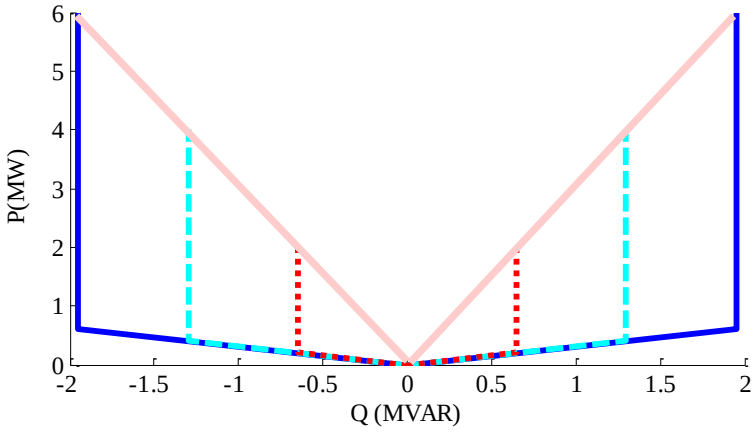

Figure B-4 Wind turbines extrapolated PQ chart

In Figure B-5 (first subplot), the reactive power delivered by the wind farm if it provides voltage control is presented for the two cases analyzed above (X/R = 2 and X/R = 30). For a low X/R ratio the wind farm consumes reactive power in order to mitigate the voltage rise effect (between 0 and 3500MW). For a high X/R ratio, the wind farm always generates reactive power, reaching the reactive capability limit above 2500 MW. Thus, the hosting capacity increment that could be obtained thanks to the provision of voltage control is lower than for a low ratio (see Figure B-3). The second subplot within Figure B-5 presents the reactive power that must be provided by the rest of the system. Note that the difference in the quantity of the reactive power provided by the rest of the system with and without control is equal to the reactive power provided by wind farms (in the event of providing this control) plus the difference of reactive power losses.

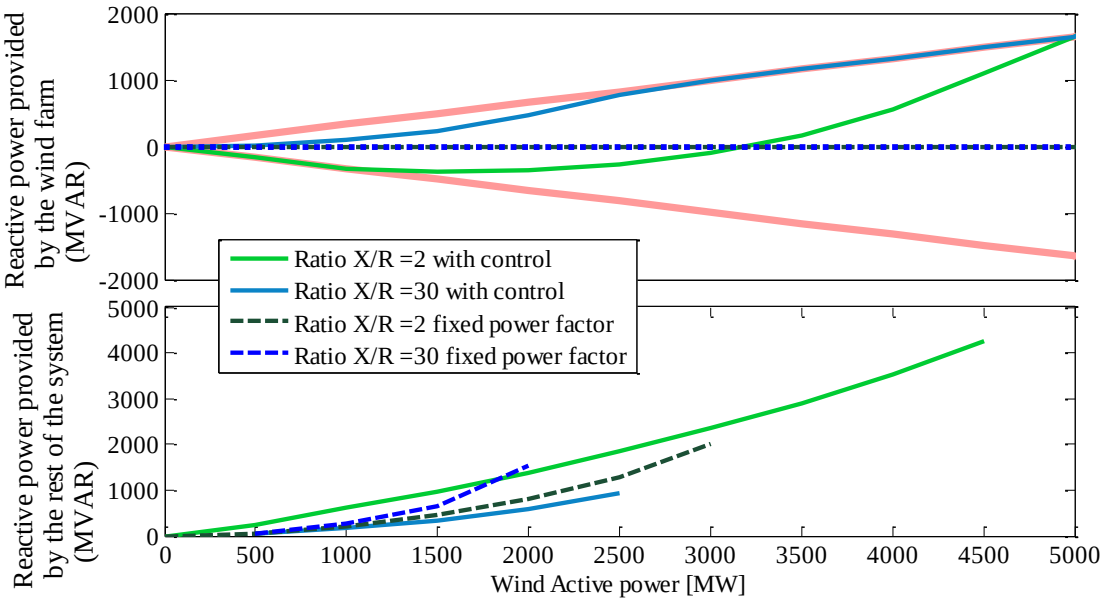

Figure B-5 Reactive power for two different ratios (SCC=4000 MVA, VTNet=1.00 p.u.) in two situations

For evaluating the short-circuit power (SCC) influence in the voltage rise effect, Figure B-6 is presented. In this figure the reactive power and the voltage are depicted for several SCC maintaining the ratio X/R fixed to 2. It could be appreciated how the maximum values of the voltage are the same for all different short-circuit powers analyzed. Hence, the voltage rise limit depends on the X/R ratio whereas the SCC imposed where this limit is reached. The mathematical demonstration of this fact is provided for the simplified model in the last section of this appendix.

In Figure B-7 the same curves as in Figure B-3 are presented. Nevertheless, in this figure the ratio has been fixed (X/R = 6) and two different values of V_{TNet} have been evaluated (1.00 p.u. and 1.04 p.u.). In this figure it can be seen that if the initial value of V_{TNet} is high and wind farms do not provide voltage control, the hosting capacity could be promptly limited due to overvoltage.

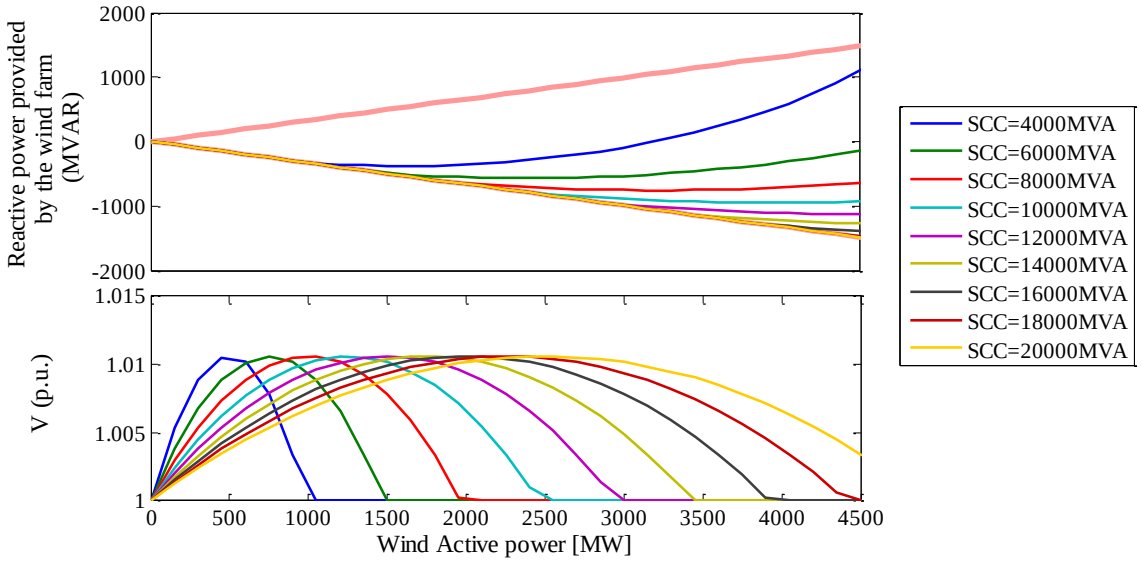

Figure B-6 Reactive power and voltage for a ratio equal to 2 and different SCC when the wind farm provides voltage control

However, if wind farms provide voltage control, the hosting capacity is limited, because of voltage under the admissible value (0.95 p.u.), leading to a substantial hosting capacity increment of 3200 MW. For the initial value of V_{TNet} = 1.00 p.u., the hosting capacity is limited because of voltage under the admissible value in both situations (with and without voltage control). Contrarily when V_{TNet} is equal to 1.04 p.u. the hosting capacity is limited becase of overvoltage in the event that reactive power support is not paid.

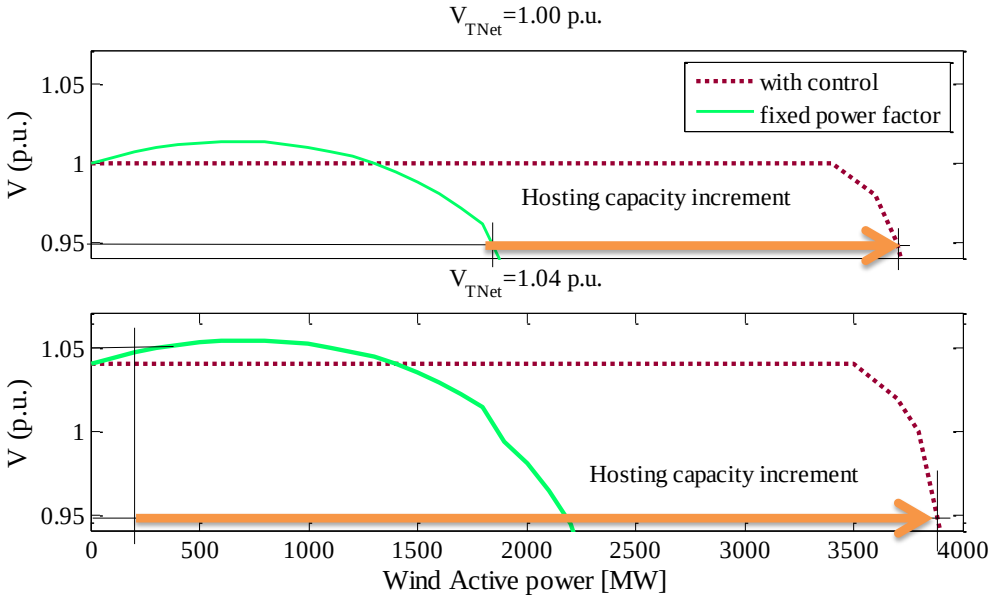

Figure B-7 Voltage for two different VTNet (1.00 p.u. and 1.04 p.u.) maintaining the SCC and the X/R ratio at a fixed value (SCC=4000 MVA X/R=6)

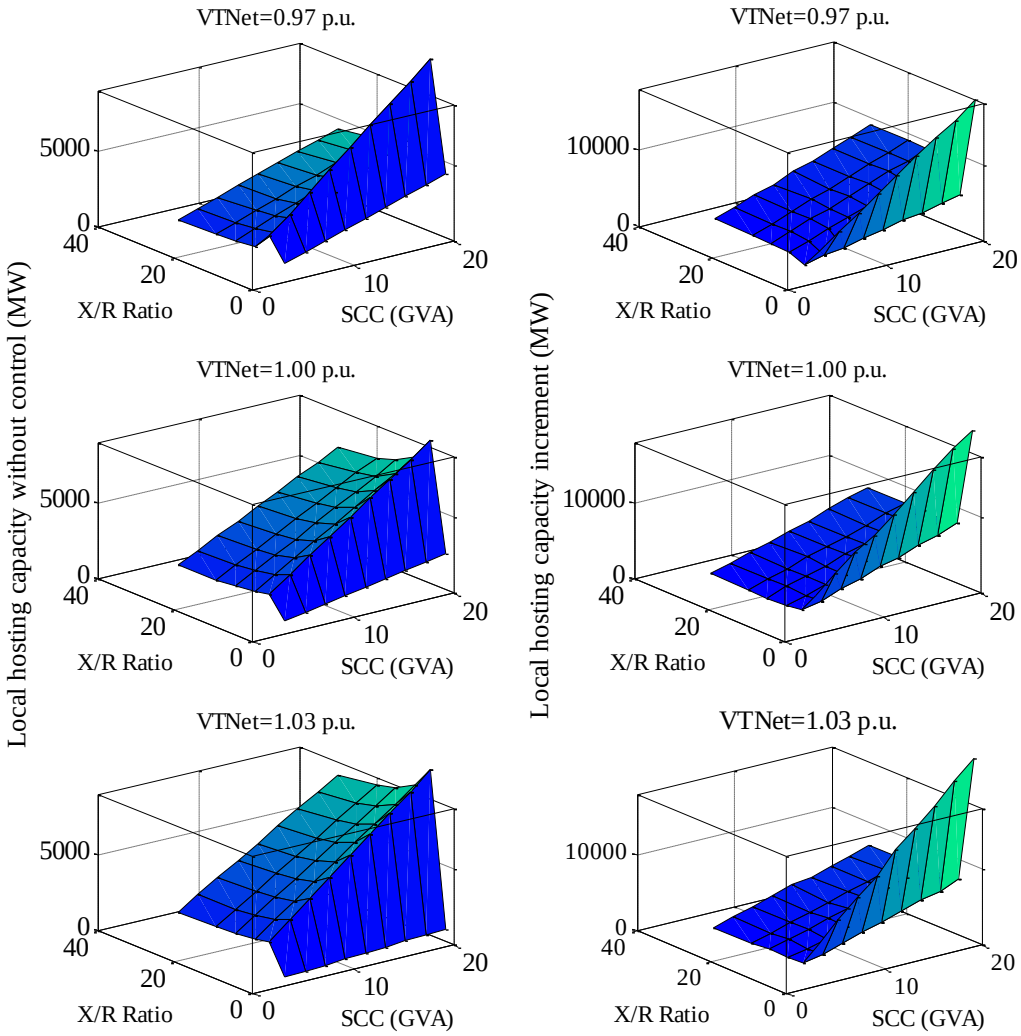

Figure B-8 Summary of the hosting capacity limit without control and the increment of the hosting capacity thanks to the voltage control provision

These results are very valuable for both wind farm owners and system operators, indicating the wind farm capability of removing steady-state bus voltage limitations and enhancing the flexibility of the system. Having evaluated different situations in detail, Figure B-8 plotted the wind power limitation without providing voltage control and the increment achieved thanks to the voltage control provision for three different values of V_{TNet}. For most values (V_{TNet}, SCC) steady-state voltage limitations appear for a hosting capacity higher than 2000 MW which, although they are theoretical limits, they are not realistic according to the Spanish power system in which, it is not possible to install more than 2000 MW in a single bus [REE 2005]. Since this thesis has paid an especial attention to the Spanish power system, the value of 2000MW has been selected as the maximum potential value of realistic hosting capacity; otherwise the limitation is not effective. However, before reaching this value, the hosting capacity could be limited because of transmission capacity constraints as has been clearly seen in Chapter 3. In all cases a considerable increment in hosting capacity can be achieved, being very significant for low X/R ratio.

B.3 SPANISH LOCAL CAPACITY EVALUATION

In order to analyze how relevant the unfavourable cases are, a statistical analysis of the Spanish system using data from year 2010 has been carried out. In Figure B-9 the histogram of the mean, maximum and minimum SCC and X/R ratios in all 400kV buses within the Spanish power system are presented. The same information is provided in Figure B-10 for 220 kV buses. Concerning this last voltage level, most of the buses have a mean SCC between 3000 MVA and 6000 MVA and the X/R ratio is between 6 and 10. With respect to the 400 kV buses, most of them have a mean SCC between 7000 MVA and 13000 MVA and the X/R ratio is between 10 and 14.

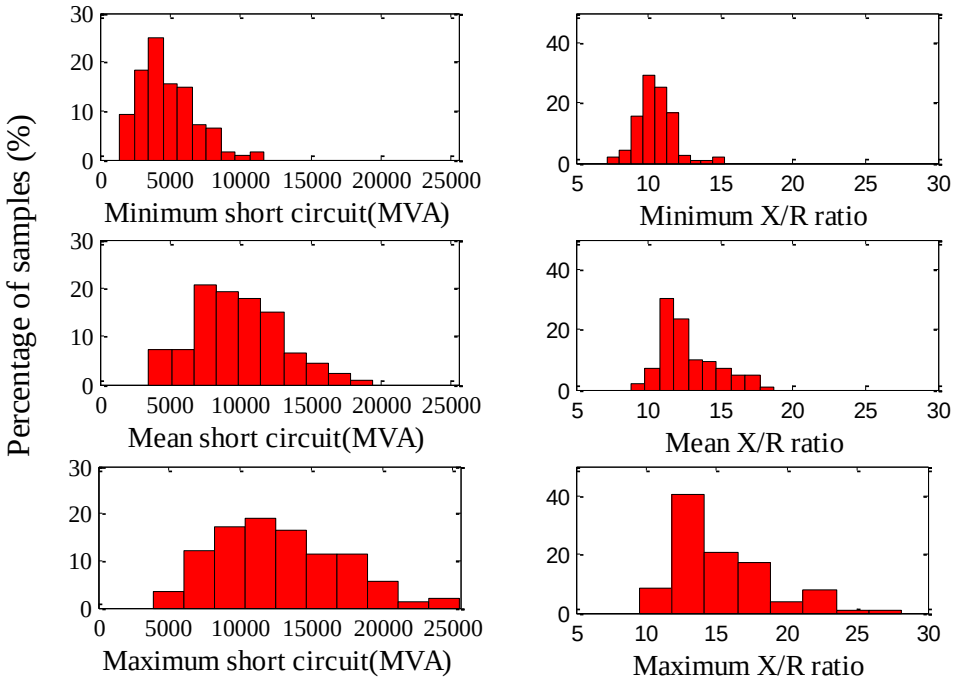

Figure B-9 Statistical data of SCC and X/R ratio 400 kV buses within the Spanish system (year 2010)

This information is numerically summarized in Table B-1for the mean and also the minimum distributions of X/R ratio and SCC. In all cases, the cumulative distribution is evaluated in order to obtain the values that correspond to the percentiles 25% (low), 50% (mean) and 75% (high).

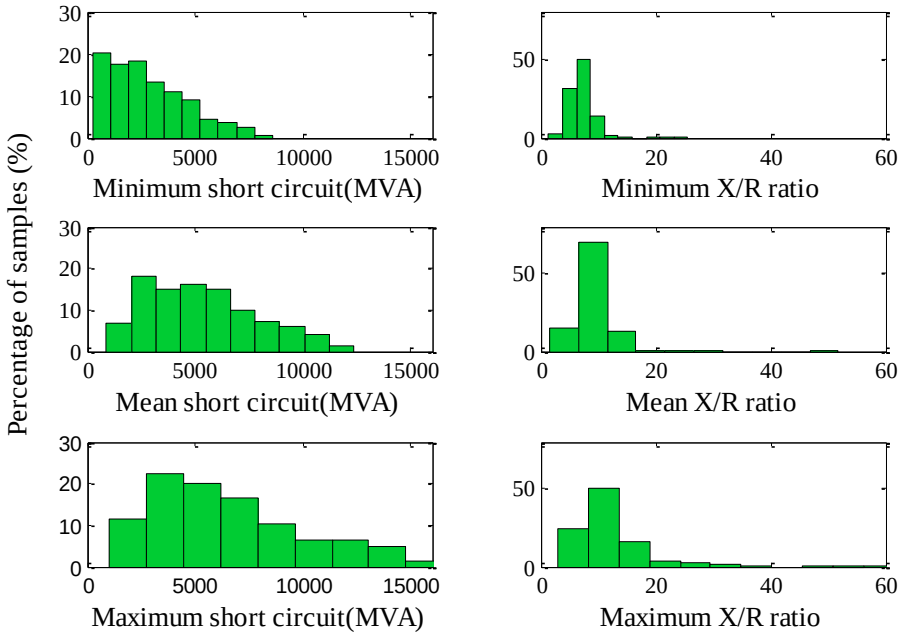

Figure B-10 Statistical data of SCC and X/R ratio 220kV buses within the Spanish system (year 2010)

Table B-1. Spanish TNet statistical data

		X/R ratio		SCC (MVA)	
		Mean	Minimum	Mean	Minimum
220 kV	High	10	9	7015	3853
	Mean	9	7	5136	2495
	Low	8	5.5	4000	1439
400 kV	High	14	11.5	11742	6106
	Mean	12	10.5	9669	4762
	Low	11	9.5	7595	3419

Using the mean values of X/R ratio and SCC, Table B-2 presents the limitations of hosting capacity imposed by steady-state voltage constraints if the wind farm does not provide voltage control for each combination of values.

As explained in the previous section, the value of 2000MW is considered as the maximum potential value of realistic hosting capacity. Evaluating the results provided in this table (considering mean values), it can be concluded that the hosting capacity will not be limited because of steady-state voltage constraints. In these cases the hosting capacity could be limited due to other reasons such as system capacity, dynamic performance, frequency control or transmission capacity constraints. However, the system operator should consider not only mean values, but also minimum values. Next, Table B-3 presents the hosting capacity limitations without voltage control, for the minimum values of X/R ratio and SCC. For these values the hosting capacity is limited in a greater number of cases. Nevertheless, for most TNet buses, using the reactive power available from the HNet doubled the permissible hosting capacities surpassing the 2000MW limitation imposed by the Spanish grid code.

Table B-2. Summary of wind power limitations (MW) considering mean

			Low V_{TNet} 0.97 p.u.	Nominal V_{TNet} 1.00 p.u.	High V_{TNet} 1.03 p.u.
220 kV buses	High X/R ratio	High SCC	2063	2776	3339
		Mean SCC	**1481**	2009	2391
		Low SCC	**1152**	**1545**	**1843**
	Mean X/R ratio	High SCC	2204	2926	3479
		Mean SCC	**1580**	2103	2500
		Low SCC	**1232**	**1639**	**1929**
	Low X/R ratio	High SCC	2496	3184	3685
		Mean SCC	**1793**	2284	2621
		Low SCC	**1395**	**1782**	2007
400 kV buses	High X/R ratio	High SCC	3064	4315	5488
		Mean SCC	2529	3561	4525
		Low SCC	**1973**	2777	3527
	Mean X/R ratio	High SCC	3230	4465	5385
		Mean SCC	2665	3684	4447
		Low SCC	2080	2874	3470
	Low X/R ratio	High SCC	3338	4561	5237
		Mean SCC	2754	3764	4317
		Low SCC	2148	2935	3364

Table B-3. Summary of wind power limitations (MW) considering minimum values

			Low V_{TNet} 0.97 p.u.	Nominal V_{TNet} 1.00 p.u.	High V_{TNet} 1.03 p.u.
220 kV buses	High X/R ratio	High SCC	**1192**	**1578**	**1877**
		Mean SCC	**767**	**1018**	**1213**
		Low SCC	**442**	**587**	**688**
	Mean X/R ratio	High SCC	**1350**	**1717**	2007
		Mean SCC	**867**	**1104**	**1292**
		Low SCC	**491**	**630**	**750**
	Low X/R ratio	High SCC	**1545**	**1974**	2167
		Mean SCC	**993**	**1267**	**1393**
		Low SCC	**569**	**732**	**788**
400 kV buses	High X/R ratio	High SCC	**1699**	2458	2818
		Mean SCC	**1327**	**1919**	2199
		Low SCC	**950**	**1378**	**1578**
	Mean X/R ratio	High SCC	**1761**	2393	2871
		Mean SCC	**1375**	**1865**	2243
		Low SCC	**985**	**1343**	**1609**
	Low X/R ratio	High SCC	**1836**	2336	2933
		Mean SCC	**1432**	**1824**	2289
		Low SCC	**1030**	**1309**	**1649**

In buses affected with low SCC, steady-state voltage limits justified the legislation changes, in which TSOs are imposing wind farms voltage control (Spain [REE 2011], Denmark, [Energinet 2010] and Ireland [Eirgrid et al. 2012, Eirgrid et al. 2013]). In

addition, voltage control is also justified because the dynamic and stability performance of the power system is improved. Further evidence to support the need for legislation for TSOs is provided in Chapter 3 where the importance of the local nature of reactive power is seen.

This simplified model can be enriched taking into account the real HNet PQ chart as was done in Chapter 3, computed maximizing the reactive power delivered and absorbed. Considering that real PQ chart the local hosting capacity limits have been updated, identifying that moving from idealized to realistic PQ charts tends to reduce the hosting capacity by about 30% as can be derived from Table B-4. Nevertheless, there still are significant increments in the hosting capacity due to the voltage control provision.

Table B-4. Hosting capacity increment comparison

		SCC (MVA)								
		4000	6000	8000	10000	12000	14000	16000	18000	20000
		Hosting capacity increment using ideal PQ chart								
X/R Ratio	2	4325	6588	8852	10316	12578	14842	17105	19368	21132
	6	1616	2162	3213	3768	4819	5370	6425	6978	8032
	10	1410	2114	2819	3524	4726	5430	6137	6841	7546
	15	1356	2381	3057	3732	4756	5432	6111	7136	7813
	20	1424	2133	2845	3903	4614	5323	6036	7096	7807
	30	1491	2232	2978	3720	4463	5207	6301	7046	7790
		Hosting capacity increment using real PQ chart								
	2	2957	4314	5983	7030	9001	10083	11131	13348	14346
	6	204	371	526	685	834	961	1096	1238	1381
	10	207	347	487	626	765	896	1018	1145	1273
	15	195	357	466	585	719	841	957	1083	1208
	20	200	334	445	581	689	808	933	1043	1166
	30	214	307	441	547	667	781	892	1010	1119

Finally, in order to analyze the accuracy of the simplified model, the wind power limitations with an ideal control scheme and assuming a fixed power factor equal to one were also obtained using the full model of the Spanish power system. In this case, the hosting capacity was increased in one bus and proportionally reduced in the rest of the generating buses of the whole Spanish system in accordance with their reactive power reserves, until bus voltages reached their maximum limits. The results obtained from the full model are compared with those obtained with the simplified model (the actual SCC, X/R ratio and V_{TNet} for each bus are interpolated, taking into account the regression line that approximates the simplified results). Figure B-11 shows how the results obtained with the simplified model of both TNet and HNet are quite similar to the results obtained with the full model in most of the cases. However, when SCC increases, the accuracy of the simplified model diminishes.

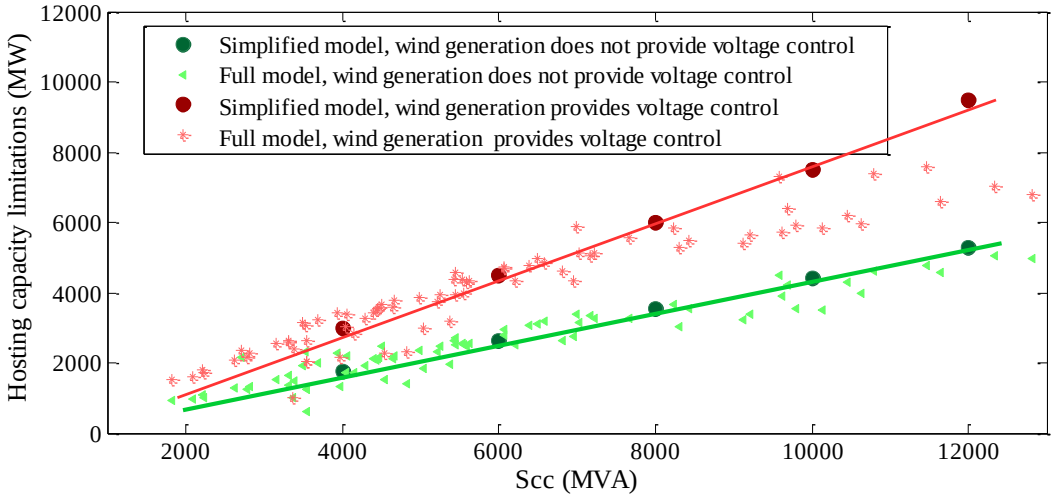

Figure B-11 Comparison of simplified and detailed models of TNet

The Spanish power system is very meshed guaranteeing that the operation is quite linear and far away from voltage collapse for actual values of demand. Thus, the simplified model gives a good indication of local hosting capacities imposed by steady-state voltage limits.

B.4 MATHEMATICAL DEMONSTRATION

In Figure B-6 the reactive power and the voltage are depicted for several short-circuit powers maintaining the ratio X/R fixed to 2. In this figure it can be appreciated how the maximum values of the voltages are the same for all the different short-circuit powers analyzed. The mathematical demonstration of this fact is next presented in this section.

In this simplified model, V_2 is the voltage of V_{TNet} and V_1 is the voltage of the bus where the wind farm is connected as can be shown in Figure B-1. The voltage that has been fixed is V_1 and V_2 is computed. The reason of this consideration is that if V_1 is fixed the current can be easily obtained and the relation V_2/V_1 is the same independently of the voltage considered.

$$V_2 = V_1 - I(R + jX) \qquad I = \frac{P - jQ}{V_1}$$

$$V_2 = V_1 - \frac{P - jQ}{V_1}(R + jX) \qquad \text{B-1}$$

$$V_2 = V_1 - \frac{PR + QX}{V_1} - j\frac{PX - QR}{V_1}$$

In order to determine the maximum value of the voltage, it is first necessary to determine where the maximum is achieved. Thus the derivative of V_2 with respect to P must be calculated. Because the maximums of V_2 and V_2^2 are located at the same P values, the derivative of V_2^2 with respect P is calculated due to the fact that it is easy to compute.

In addition, the maximum always is achieved when the wind farm is consuming the maximum reactive power ($Q=-0.33\cdot P$).

$$V_2^2 = \left\{V_1 - \frac{PR - 0.33PX}{V_1}\right\}^2 + \left\{\frac{0.33PR + PX}{V_1}\right\}^2$$

$$\frac{dV_2^2}{dP} = 2\left\{V_1 - \frac{PR - 0.33PX}{V_1}\right\}\left(-\frac{R}{V_1} + \frac{0.33X}{V_1}\right) + 2\left\{\frac{0.33PR + PX}{V_1}\right\}\left(\frac{0.33R}{V_1} + \frac{X}{V_1}\right) = 0$$

$$If\ V_1 = 1$$

$$\frac{dV_2^2}{dP} = (-R + 0.33X)(1 - PR + 0.33PX) + (0.33PR + PX)(0.33R + X) = 0 \qquad \text{B-2}$$

$$P = \frac{R - 0.33X}{1.11R^2 + 1.11X^2}$$

$$If Ratio\frac{x}{r} = 2$$

$$P = \frac{R - 0.33\cdot 2\,R}{1.11R^2 + 1.11\cdot(2R)^2} = \frac{0.0612}{R}$$

Replacing *P*, the maximum value of V_2 is computed.

$$V_2^2 = \left\{V_1 - \frac{PR - 0.33PX}{V_1}\right\}^2 + \left\{\frac{0.33PR + PX}{V_1}\right\}^2$$

$$If\ V_1 = 1$$

$$V_2^2 = 1 + (PR)^2 + (0.33PX)^2 - 2PR0.33PX - 2(PR - 0.33PX) + (0.33PR)^2 + (PX)^2 + 2PR0.33PX$$

$$V_2^2 = 1 + \left(\frac{0.0612}{R}R\right)^2 + \left(0.33\frac{0.0612}{R}2R\right)^2 - 2\left(\frac{0.0612}{R}R - 0.33\frac{0.0612}{R}2R\right)^2 + \left(0.33\frac{0.0612}{R}R\right)^2 + \left(\frac{0.0612}{R}2R\right)^2 \qquad \text{B-3}$$

It can be appreciated that this value is constant and independently on the short-circuit power $V_2 = 0.9895$

In this analysis the voltage that has been fixed is $V_2 = V_{TNet} = 1.00$ p.u. As a result, V_1 can be computed as:

$$V_2 = \frac{1}{0.9895} = 1.0106$$

It can be observed that this value corresponds to the maximum value obtained in Figure B-6

APPENDIX C

SENSITIVITY MATRIXES

For implementing an optimal voltage control scheme in real time, the sensitivity vectors are required (vector calculated using the linear model of the power system). This appendix presents the HNet model used in this thesis and the assumptions considered in order to compute the sensitivity matrix.

C.1 HNET LINEAL MODEL

Any power system can be modelled with the linear power flow equations next presented. In order to simplify its formulation the different derivative terms are named (H, N, M and L) where ΔP vector dimention is equal to the number of generator (g) plus the number of loads (l) i.e., $(n_g+n_l)\ x\ 1$ whereas ΔQ vector dimention is $n_l\ x\ 1$

$$\begin{pmatrix} \Delta\overline{\mathbf{P}} \\ \Delta\overline{\mathbf{Q}} \end{pmatrix} = \begin{pmatrix} \dfrac{\partial\overline{\mathbf{P}}}{\partial\overline{\boldsymbol{\theta}}} & \mathbf{V}\dfrac{\partial\overline{\mathbf{P}}}{\partial\overline{\mathbf{V}}} \\ \dfrac{\partial\overline{\mathbf{Q}}}{\partial\overline{\boldsymbol{\theta}}} & \mathbf{V}\dfrac{\partial\overline{\mathbf{Q}}}{\partial\overline{\mathbf{V}}} \end{pmatrix} \begin{pmatrix} \Delta\overline{\boldsymbol{\theta}} \\ \Delta\overline{\mathbf{V}}/\mathbf{V} \end{pmatrix} = \begin{pmatrix} \mathbf{H} & \mathbf{N} \\ \mathbf{M} & \mathbf{L} \end{pmatrix} \begin{pmatrix} \Delta\overline{\boldsymbol{\theta}} \\ \Delta\overline{\mathbf{V}}/\mathbf{V} \end{pmatrix} \tag{C-1}$$

$$\begin{bmatrix} H_{gg} & H_{gl} & N_{gg} & N_{gl} \\ H_{lg} & H_{ll} & N_{lg} & N_{ll} \\ M_{gg} & M_{gl} & L_{gg} & L_{gl} \\ M_{lg} & M_{ll} & L_{lg} & L_{ll} \end{bmatrix} \cdot \begin{bmatrix} \Delta\theta_g \\ \Delta\theta_l \\ \Delta V_g \\ \Delta V_l \end{bmatrix} = \begin{bmatrix} \Delta P_g \\ \Delta P_l \\ \Delta Q_g \\ \Delta Q_l \end{bmatrix} \tag{C-2}$$

Next, the different terms are enumerated:

IF i=j

$$\begin{aligned} H_{ii} &= \frac{\partial P_i}{\partial \theta_i} = \frac{\partial}{\partial \theta_i}\left(V_i \sum_{j=1}^{n} V_j \left(G_{ij}\cos\theta_{ij} + B_{ij} sen\,\theta_{ij} \right) \right) = -Q_i - V_i^2 B_{ii} \\ N_{ii} &= V_i \frac{\partial P_i}{\partial V_i} = V_i \frac{\partial}{\partial V_i}\left(V_i \sum_{j=1}^{n} V_j \left(G_{ij}\cos\theta_{ij} + B_{ij} sen\,\theta_{ij} \right) \right) = P_i + V_i^2 G_{ii} \\ M_{ii} &= \frac{\partial Q_i}{\partial \theta_i} = \frac{\partial}{\partial \theta_i}\left(V_i \sum_{j=1}^{n} V_j \left(G_{ij} sen\,\theta_{ij} - B_{ij}\cos\theta_{ij} \right) \right) = P_i - V_i^2 G_{ii} \\ L_{ii} &= V_i \frac{\partial Q_i}{\partial V_i} = V_i \frac{\partial}{\partial V_i}\left(V_i \sum_{j=1}^{n} V_j \left(G_{ij} sen\,\theta_{ij} - B_{ij}\cos\theta_{ij} \right) \right) = Q_i - V_i^2 B_{ii} \end{aligned} \tag{C-3}$$

IF i ≠ j

$$\begin{aligned} H_{ij} &= \frac{\partial P_i}{\partial \theta_j} = \frac{\partial}{\partial \theta_j}\left(V_i V_j \left(G_{ij}\cos\theta_{ij} + B_{ij} sen\,\theta_{ij} \right) \right) = V_i V_j \left(G_{ij} sen\,\theta_{ij} - B_{ij}\cos\theta_{ij} \right) \\ N_{ij} &= V_j \frac{\partial P_i}{\partial V_j} = V_j \frac{\partial}{\partial V_j}\left(V_i V_j \left(G_{ij}\cos\theta_{ij} + B_{ij} sen\,\theta_{ij} \right) \right) = V_i V_j \left(G_{ij}\cos\theta_{ij} + B_{ij} sen\,\theta_{ij} \right) \\ M_{ij} &= \frac{\partial Q_i}{\partial \theta_j} = \frac{\partial}{\partial \theta_j}\left(V_i V_j \left(G_{ij} sen\,\theta_{ij} - B_{ij}\cos\theta_{ij} \right) \right) = -V_i V_j \left(G_{ij}\cos\theta_{ij} + B_{ij} sen\,\theta_{ij} \right) = -N_{ij} \\ L_{ij} &= V_j \frac{\partial Q_i}{\partial V_j} = V_j \frac{\partial}{\partial V_j}\left(V_i V_j \left(G_{ij} sen\,\theta_{ij} - B_{ij}\cos\theta_{ij} \right) \right) = V_i V_j \left(G_{ij} sen\,\theta_{ij} - B_{ij}\cos\theta_{ij} \right) = H_{ij} \end{aligned} \tag{C-4}$$

Considering this formulation, it can be derived that the voltage deviation is affected by both reactive and active power (see next formula).

$$\begin{bmatrix} S_{gg} & S_{gl} \\ S_{lg} & S_{lg} \end{bmatrix} \begin{bmatrix} \Delta V_g \\ \Delta V_l \end{bmatrix} = \begin{bmatrix} \Delta Q_g \\ \Delta Q_l \end{bmatrix} - \begin{bmatrix} T_{gg} & T_{gl} \\ T_{lg} & T_{lg} \end{bmatrix} \begin{bmatrix} \Delta P_g \\ \Delta P_l \end{bmatrix} \tag{C-5}$$

Due to the P-V relationship is not significant for typical X/R ratios when the system is far away voltage collapse as has been seen in the previous appendix, an assumption widely used is that the P-θ and Q-V relationship are decoupled. Hence, the voltage deviation is assumed directly proportionally to the reactive deviation $S\,\Delta V = \Delta Q$. This thesis considers a semi-decoupled approach as was also adopted in [de la Fuente 1997]. This means that although the active power deviation effect is depreciated, the active power flows are considered when S is evaluated as is next shown.

$$\begin{bmatrix} S_{gg} & S_{gl} \\ S_{lg} & S_{ll} \end{bmatrix} = \begin{bmatrix} L_{gg} & L_{gl} \\ L_{lg} & L_{ll} \end{bmatrix} - \begin{bmatrix} T_{gg} & T_{gl} \\ T_{lg} & T_{ll} \end{bmatrix} \begin{bmatrix} N_{gg} & N_{gl} \\ N_{lg} & N_{ll} \end{bmatrix}$$

$$\begin{bmatrix} T_{gg} & T_{gl} \\ T_{lg} & T_{ll} \end{bmatrix} = \begin{bmatrix} J_{gg} & J_{gl} \\ J_{lg} & J_{ll} \end{bmatrix} \begin{bmatrix} H_{gg} & H_{gl} \\ H_{lg} & H_{ll} \end{bmatrix}^{-1} \tag{C-6}$$

C.2 SENSITIVITY MATRIX USED

Recalling section 6.3, the HNet control determines the set-point of each wind farm in order to fulfil the required voltage set-point at the pilot bus. Hence, the sensitivity matrix that relates both magnitudes is used.

$$\begin{bmatrix} S_{gg} & S_{gl} \\ S_{lg} & S_{lg} \end{bmatrix} \begin{bmatrix} \Delta V_g \\ \Delta V_l \end{bmatrix} = \begin{bmatrix} \Delta Q_g \\ \Delta Q_l \end{bmatrix} \tag{C-7}$$

Assuming the general case in which there are both PQ and PV buses the next relation is obtaining

$$S_{lg}\,\Delta V_g + S_{ll}\,\Delta V_l = \Delta Q_l \;\rightarrow\; \Delta V_l = {S_{ll}}^{-1}\Delta Q_l - {S_{ll}}^{-1} S_{lg} \Delta V_g \tag{C-8}$$

It can be appreciated that the voltage deviation of the load buses (being the pilot bus one of them) depends on the reactive power injections at the PQ buses and the deviation on the voltage set-points of the generators (PV buses). In the HNets evaluated no demands are located. Consequently, the set-points received by wind farms impose the type of bus that should be considered, PV or PQ. In this thesis both, voltage and reactive power set-points have been analyzed being the latter the one selected owing to the reasons

explained in Chapter 6. Nonetheless, next the sensitivity matrixes in both cases are outlined.

$$\mathrm{M}_{\text{sensitivity PV}} = -{S_{ll}}^{-1} S_{lg} \;\; ; \;\; \mathrm{M}_{\text{sensitivity PQ}} = -{S_{ll}}^{-1} \tag{C-9}$$

Finally, in order to just considered the voltage deviation at the pilot bus *C* matrix is added, indicating which load bus is considered a pilot bus. In this matrix the number of rows corresponds to the number of pilot buses (in the particular case of a HNet just one hence a vector is obtained) whereas the columns correspond to all load buses ($n_p \times n_l$). Thus, all terms of the matrix are cero except the ones in which the pilot and load buses coincides.

$$\Delta V_p = C \; \mathrm{M}_{\text{sensitivity PQ}} \, \Delta Q_l \tag{C-10}$$

Hence the following notation has been used throughout the thesis $vS_{pc} = C \; \mathrm{M}_{\text{sensitivity PQ}}$

When a significant voltage deviation of the pilot bus is seen the voltage set-points of the OLTC transformers are updated. Thus theirs sensitivity matrixes are required $\Delta V_p = S_{ct} \, \Delta \mathrm{V}_{\mathrm{ct}}$ .Where S_{ct} is calculated as follows, taking into account that a tap position change means a voltage increase/decrease (TV%) of 1%.

$$S_{ct} = \left(\frac{\partial Q}{\partial V}\right)^{-1} \cdot \frac{\partial Q}{\partial t} \cdot \mathrm{TV\%} \tag{C-11}$$

APPENDIX D

SIMULATORS

In order to study the dynamic performance of any control scheme a simulator is required. In that respect two bespoke tools have been developed in the context of this thesis. The first one, which is employed throughout Chapters 5 and 6, simulates the performance of the whole HNet considering an aggregate model of each wind farm. The second one focuses on a specific wind farm, being used for evaluating the limitations of it providing this service, results that are later explained in Appendix I.

D.1 HNET SIMULATOR

The simulator, whose structure is presented in Figure D-1, is composed of the following components: a model of the network, a power flow solver, and a dynamic voltage control model. In addition, it should be emphasized that any control scheme rely on some specific settings (e.g., voltage/reactive power set-points, droop ...) which can be fixed (see Chapter 5) or adaptive (see Chapter 6). In the first case, those values are computed offline with an AC multi-period OPF. In the second case a central controller computes online those values. In that sense, an optimization problem is solved by quadratic programming every period. Finally, some input data (transmission bus voltage, and wind farm active power time evolution patterns) are required.

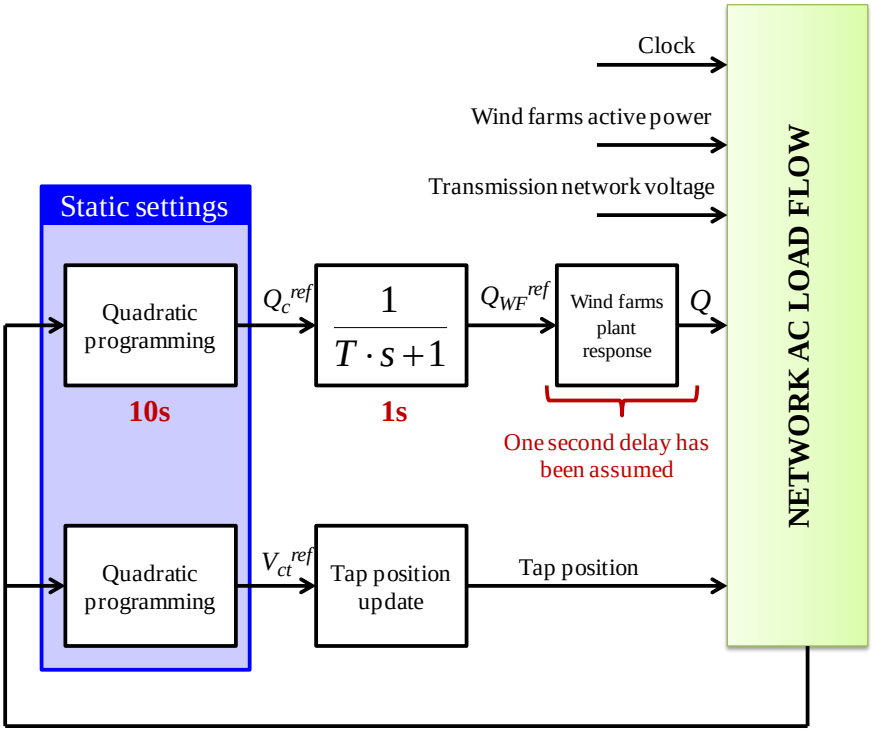

Figure D-1 Simulator used for evaluating the performance of each control

The response of that central controller or directly the fixed settings (considering also the first order lag and the tap changes perform after a certain time delay and dead band) is applied to the network load flow model, which is resolved every second. This general sample time has been fixed to one as the wind farms historic power is also available at that granularity. Hence, the controller set-points (voltages or reactive power) can be compared with the real measurement, representing the error signals to be compensated. However, the voltage controllers require communications which are not continuously available. Hence, the sample time for voltage controllers should be defined. Recalling Chapter 2, the HNet voltage control could be considered as the secondary control loop of a typical TNet hierarchical control, where the sample time commonly is ten seconds [de la Fuente 1997]. During this ten second interval the control actions (tap position and reactive power operating points) are fixed, being therefore discrete variables.

In this hierarchical control scheme the plant and primary control loops correspond to wind farms and wind turbines control loops respectively. Both, wind farms and wind turbines controllers have not been considered within the simulator assuming ideal response; the wind farm reactive power dynamic is modelled as a one second delay. Simplification made in accordance with the current status of some relevant grid codes [ENTSO-E 2012] which demands that the 90% of the reactive power should be provided before one second. In addition, this assumption was validated by the results provided in [Azpiri et al. 2013]. In that document the internal wind farm control (which has been avoided) was proved showing how fast can it be. This fact, jointly with the sample time considered by the central controller (which is significantly higher than the possible communication delays), make no necessary the consideration of more realistic approaches such as hardware-in-the-loop [Xiaohu Liu et al. 2012].

D.2 WIND FARM SPECIFIC SIMULATOR

In Figure D-2 the specific wind farm simulator (taking into account its internal grid) is presented outlining the data received from the HNet control loop. One one hand, the OLTC transformer voltage set-point. On the other hand, the wind farm reactive power set-point. This last set-point should be distributed among all wind turbines. For this task many control schemes can be considered: a simple proportional control, control rules or solving an optimization problem. However the design of this control scheme is not the purpose of the thesis and hence, a simple proportional control has been assumed.

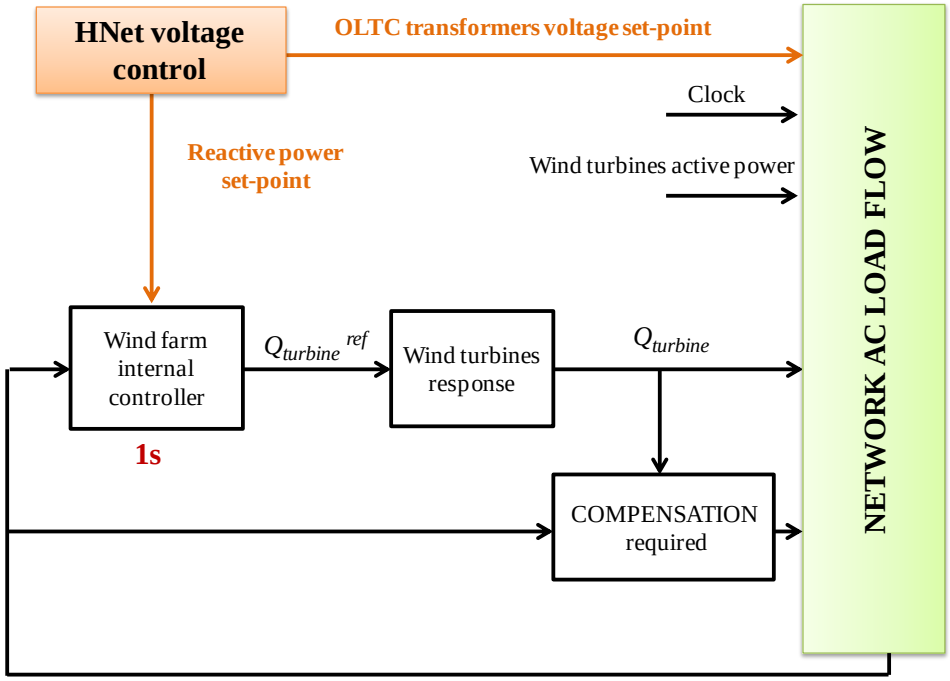

Figure D-2 Internal wind farm simulator

Subsequently, the wind turbines response should be evaluated taking into account the reactive power limitations principally imposed by the QV chart. This chart highly depends on the wind turbine technology. In this thesis a sensible assumption has been made, the maximum reactive power is available within steady-state limits (0.95 – 1.05 p.u.) and then is linearly decreased until 0.9 or 1.1. Nonetheless, note that current technology already expand the boundaries here proposed. In the event that wind turbines are not able to fulfil the wind farm reactive power requirement a compensation element should be added.

The sample time considered for the whole simulator is one second assuming instantaneous wind turbine response.

APPENDIX E

WIND FARMS SCENARIOS

In the thesis different wind farm scenearios have been considered e.g., totally random or considering the same active power level of utilization. These scenarios are accuarate enough for computing limits or evaluating the most unfavourable situations. However, a more realistic approach is demanded in those applications that highly rely on active power scenarios such as the AC multi-period OPF. In this case more sophisticated scenarios considering also their occurrence probability are required. In addition, for the dynamic analyses carried out in Chapters 5 and 6, temporal evolution patterns are required. This appendix explains both cases. Subsection E.1 evaluates the correlation between wind farms considering real data. This result is employed for creating the multi-period scenarios employed in Chapters 5. Subsequently, subsection E.2 presents the temporal dimension required for dynamic studies.

E.1 CORRELATION WIND FARM DATA

For creating active power scenarios it is essential to know the correlation between the wind farms within the HNet. For this purpose the measure of the active power of two wind farms has been recorded for one week every ten seconds. These data have been interpolated, considering one second sample, for performing an adequate correlation. In Figure E-1 the difference between both wind farms level of utilization is presented showing that the difference of most data bins is within ±0.2 p.u.

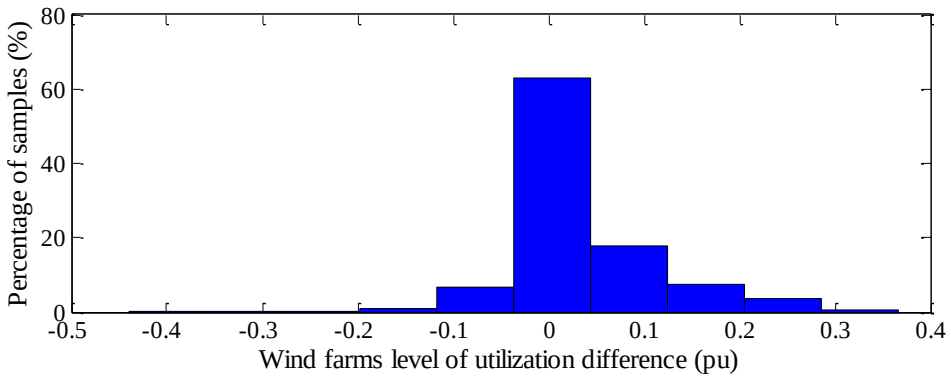

Figure E-1 Wind farms distribution function.

Consequently, the multi-scenario optimization considered that for a global level of utilization of the whole HNet wind farms could deviate ±0.2 p.u. in accordance with a uniform distribution for the sake of simplicity. Each one of these scenarios should be weighted within the objective function. In that respect, their occurrence probability is essential. For clarifying this process Figure E-2 has been included. For a certain global level of utilization, wind farms could present different individual level of utilization. In the event of a 0.4 global level of utilization, the specific wind farm level of utilization can be between 0.2 and 0.6 as is depicted in this figure. It must be noted that two different scenarios of the same global level of utilization do not produce the same total active power as were depicted in Figure 5-4 for explanatory purposes owing to the different wind farms' rate powers. In addition each scenario has a weight depending on its frequency.

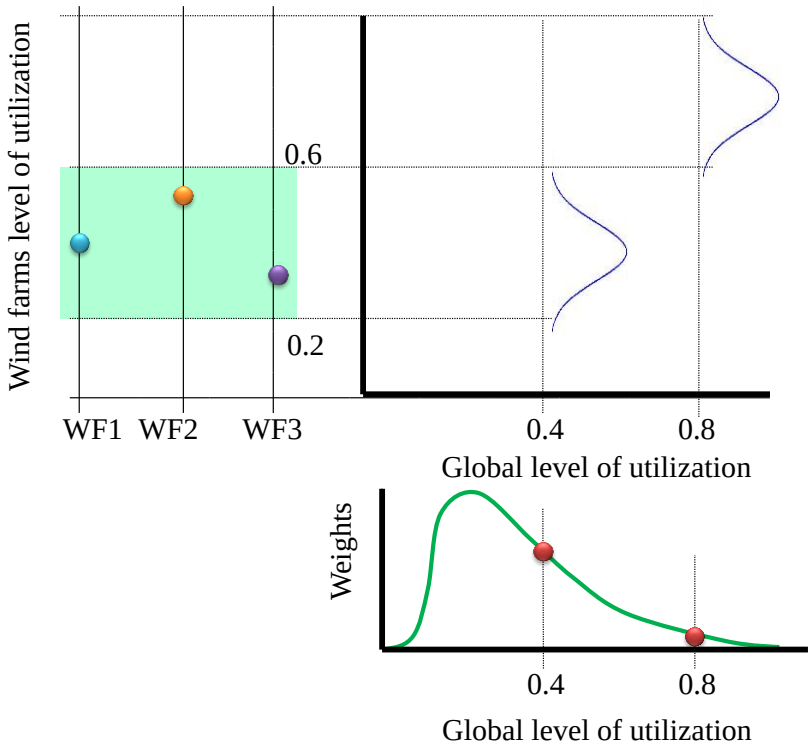

Figure E-2 Process of creating scenarios

This figure depicts the specific weight for the 0.4 and 0.8 global level of utilization scenarios based on an annual distribution function. As can be seen, a significant higher weigh is assigned for the 0.4 global scenario because its occurrence probability is higher. In this thesis the same weights used for performing [Cuffe et al. 2014a] were adopted due to the lack of accurate data. In order to extrapolate these data to the network evaluated, the relationship between the active power and the weights is derived, obtaining a distribution function as is depicted in Figure E-2. Then, the total power is computed and a certain weight is assigned interpolating in the distribution function obtained based on [Cuffe et al. 2014a] data. In total, 300 active power scenarios have been evaluated, scenarios that can be spitted in 11 global level of utilization scenarios.

E.2 WIND FARMS TIME EVOLUTION PATTERNS

Whereas for the steady-state analysis just the active power correlation among the different wind farms was needed, in the dynamic analysis its time evolution is also required. Thus, the evaluation of wind farm time evolution patterns is demanded. For carrying out this previous analysis real data of the active power of two wind farms is used as was already done for the steady-state analysis. For classifying these data a cluster analysis has been carried out. Hence, the data are categorized in different subsets or clusters which are supposed to share some common characteristics, and also differ from the others clusters, being the fuzzy c-means [Windham 1982] the algorithm selected.

Within this study, two approaches were followed. In the first one, the active power level was the main driver. In the second approach the active power profiles were normalized ($\frac{x-x_{min}}{x_{max}-x_{min}}$) and hence, the classification is performed in accordance with theirs shapes. Moreover, for the first assessment the two wind farms data have been used without considering any correlation aspect, i.e., all profiles have been considered separately. For the second assessment, the data of the two wind farms have been considered jointly, hence the active time evolution correlation between the two of them can be also seen.

Figure E-3 depicts the clusters obtained depending on the active power level considering the first approach. As can be seen, three clusters have been identified. Each one has been depicted with a different colour. For each cluster its centre has been outlined (dark blue line). However, wind farm variability is not appropriately caught and hence cannot be used as a pattern.

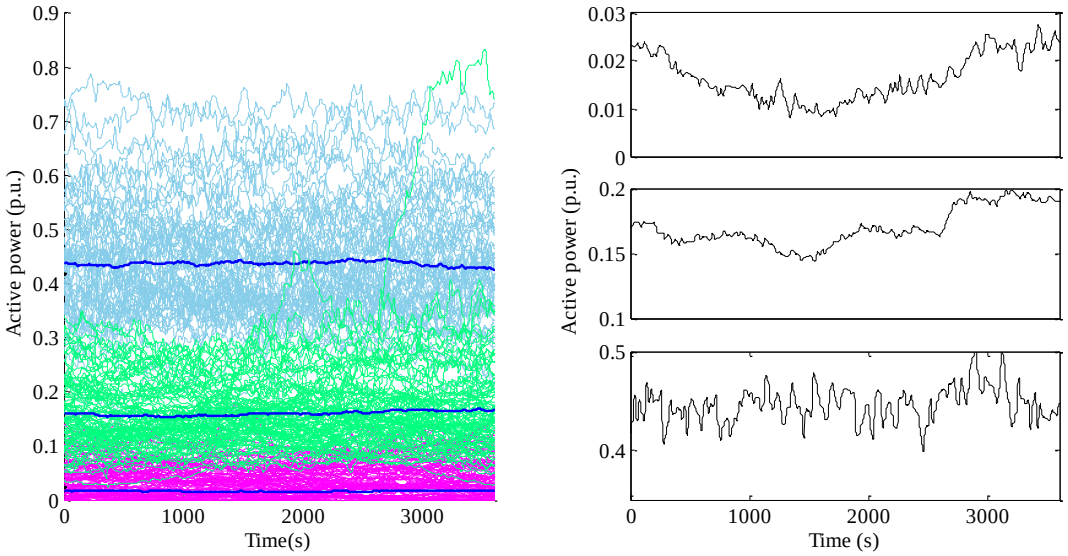

Figure E-3 Active power profile categorization

One possibility for avoiding this drawback is the selection of the most representative pattern within the cluster, measure provided by the fuzzy c-means algorithms. In Figure E-3, those patterns, one for each cluster have been also included, which as can be seen correspond to the nearest ones to the centres. In this thesis, the most unfavourable situation from the voltage perspective, i.e., the highest load scenario is evaluated. Note that for the same set-point, the voltage deviation at Pcc increases when the load also increases demanding more reactive power. Thus the active power profile has been selected among the cluster with the highest active power level. Moreover, instead of considering the most relevant pattern the one with the highest difference to the centre of the cluster is selected guarantying a high load. Next, Figure E-4 presents the final pattern selected, which has a significant short-term variability reinforcing the unfavourable situation selected.

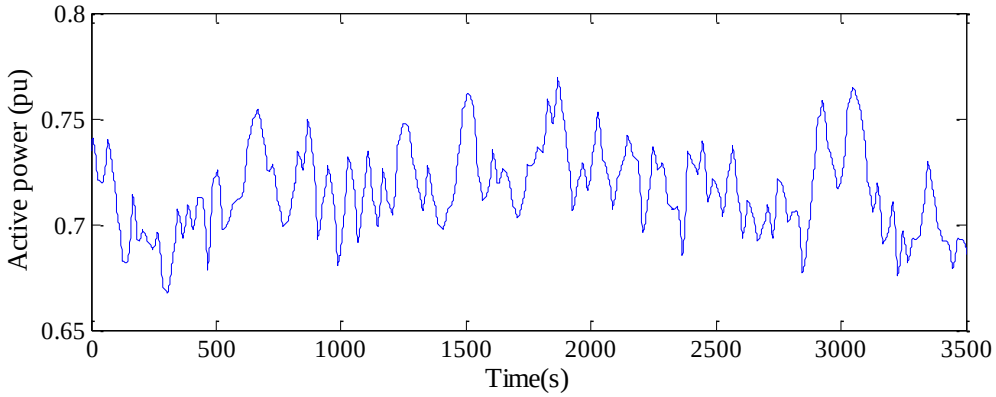

Figure E-4 Active power profile selected

Subsequently, how to extrapolate the pattern selected to the other wind farms within the HNet must be addressed. In that sense, the second approach, i.e., the classification is performed in accordance with theirs shapes, was carried out. Figure E-5 depicts the

centres of the shape clusters, each wind farm with a different colour. As can be seen four different behaviours can be identified. In the first one, it is appreciated how both wind farms have a similar performance although each wind farm has its own variability. Thus, this cluster has been named *constant*. The next two clusters correspond to a decreasing and increasing performance presenting a significant long-term variability. Nonetheless, for the dynamic settings tuning process the main concern is the short-term variability due to that could be the origin of unnecessary tap changes. The last one corresponds to an oscillatory performance among wind farms. Because this thesis focuses on the most unfavorable scenario, in which the network is more loaded during all the period studied, the *constant* approach is selected keeping the short-term variability (see Figure E-4). Consequently, the wind farms' patterns have been built around the active profile depicted in Figure E-4 assuming a constant shape.

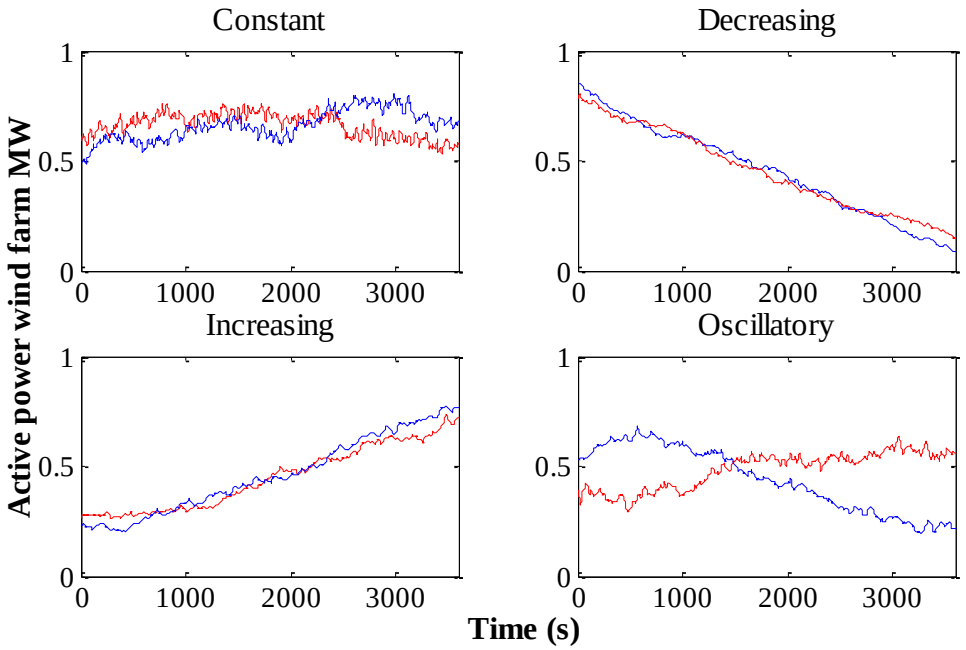

Figure E-5 Shape clusters

APPENDIX F

METAHEURISC ALGORITHMS

Recently methauristic algorithms have gain relevance, being used in innumerable problems. One reason behind their suscess is that they are easily integrated with simulations [Domínguez 2013] as is required in this thesis. Among the metaheuristic algorithms different approaches have been used: heuristic search, simulated annealing, swarm intelligence and evolutionary algorithm [Yang 2008]. Although any of these approaches could be used, this thesis has focused on the last two ones; specifically, in the genetic and the particle swarm algorithms in its multiple version (MOPSO) which are explained respectively in sections F.1 and F.2.

F.1 GENETIC ALGORITHM

This algorithm was first proposed by [Holland 1992] and subsequently several proposals (NSGA-II [Deb et al. 2002] and DNSGA-II [Deb, et al. 2007]) have been made to cope with multi-objective problems and environmental changes. Nonetheless, those extensions have not considered within the thesis.

The idea behind this algorithm takes inspiration from the evolution of the species: the strongest individuals are those who survive. Thus, an initial population evolves with each iteration (generation) until the optimal solution is achieved. The population is formed by M individuals. Typically the number of individuals is determined by trial- and-error methods. In addition, the initial population is randomly created. Each individual is

formed by chromosomes corresponding to the variables to be obtained. In order to measure the "strentgh" of each individual, the objective function, also named fitness in this context, must be evaluated. This evaluation must be performed in all iterations (generations) for every individual in the population. In each generation the evolutionary process is as follows: (a) selection of M individuals that go to the matting pool, (b) crossover of couples of individuals of the matting pool, (c) mutation of individuals with the intention of exploring new areas trying not to become stuck at a local optimum.

The idea of the selection in a genetic algorithm is that the best individuals have more possibilities to be selected. In this analysis the best individual is always selected into the matting pool, and the rest (M-1) are selected according to the roulette wheel. For constructing the roulette wheel, firstly, the probability of each individual is calculated in accordance with the following formula:

$$P_i = \frac{1/F_i^2}{\sum_1^n 1/F_j^2} \tag{F-1}$$

where P_i is the probability of i individual and F_i is the fitness of that individual. The square of the fitness is considered for prioritizing the selection of the best individuals. Once that the probabilities are calculated they are sorted and the cumulative probability is obtained. Then (M-1) random numbers are generated and the (M-1) individuals are selected. The idea of the crossover is generating individuals that are similar to their parents. First, two parents are determined randomly from the selected population. Another number is then generated randomly and if it is less or equal than the crossover probability, the parents are crossed obtaining two sons. The two sons are obtained according to the following formulas:

$$\begin{aligned} X_{iSon1} &= 0.5X_{iParent1} + 0.5X_{iParent2} \\ X_{iSon2} &= 0.8X_{iParent1} + 0.2X_{iParent2} \end{aligned} \tag{F-2}$$

where X_i corresponds to chromosome i of the individual. That process is repeated until the whole population is replaced.

The mutation is done for introducing new "genetic material". First, one individual is chosen randomly from the resulting crossed population within the iteration. A random number is generated and if this number is lower or equal than the mutation probability the individual is mutated. The chromosome of the individual to be mutated is chosen with another random number between zero and the number of chromosomes N. In this analysis a linear decreasing mutation probability within each iteration is employed to enhance the performance of the genetic algorithm. This process must be repeated the necessary number of generations for achieving convergence. The optimal generation in which the algorithm should be interrupted is the one that corresponds to the bend point of the evolution of the mean fitness. This point is known "a posteriori". Hence, the number of

generations should be large enough for guarantying that this point has been reached, in this first example 100 generations have been considered.

F.2 MOPSO

Among the different multi-objective algorithms, the MOPSO [Coello, et al. 2002, Lechuga 2006] has been proven as a reliable option as identified in [Domínguez 2013]. This algorithm is an extension of the traditional PSO [Kennedy, et al. 1995], which took the inspiration from the collective behaviour of animals (e.g., fish shoals or bird flocks). This collective behaviour has been studied by biologists [Wilson 1975] suggesting that there are social sharing of information among swarms. This fact means that the individual members take advantage of its own and also global (shoal, flock) experience during the search of food. This hypothesis, as the authors recognized in [Kennedy, et al. 1995], was fundamental for the development of PSO.

Focusing on the algorithm itself a swarm of particles moves within the search space memorizing which is the best value of the objective function that they have found, both from the individual and global perspective. These values are used as a reference and will conduct the search. In order to see graphically how this algorithm works, Figure F-1 depicts the behaviour of one particle (with two components) located in $x_i(t)$ base on its known best experience (*pbest*) and the global best (*gbest*) assuming that the position is equal to the objective for facilitating its interpretation.

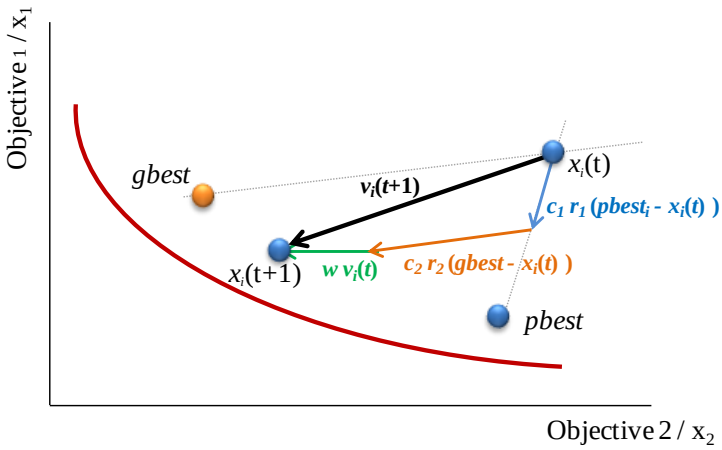

Figure F-1 Behaviour of one particle base on its known best experience

Note that normally $x_i(t)$ have more than two dimensions (e.g., dynamic settings) and the objectives are obtained after simulated a specific position performance, consequently objectives and position differ. The new position of this particle $x_i(t+1)$ is equal to its current position plus the velocity vector $(x_i(t) + v_i(t))$, vector that is built in accordance with its current velocity and the distance of this particle to its *pbest* and *gbest* as is next presented:

$$v_i(t+1) = w\, v_i(t) + c_1\, r_1\, (pbest_i - x_i(t)) + c_2\, r_2\, (gbest - x_i(t)) \qquad \text{F3}$$

Where c_1 and c_2 are positive constants (both fixed to one in this case) that indicate the maximum influence of *pbest* and *gbest* respectively, r_1 and r_2 are random numbers between 0 and 1 and w is the inertial weigh. This last parameter has a similar function as the mutation parameter of the genetic algorithm (which recalling previous section its function is "exploring new areas") and consequently is treated in a similar way. A high inertial weight is good for a global search whereas a low inertial weight is more adequate for a local one. Consequently, firstly a high weight is desired for obtaining the whole Pareto frontier which should be decreased with the iterations. In this thesis an initial value of 0.9 has been considered which has been linearly decreased with the iteration until 0.2 as suggested [Domínguez 2013].

Taking into account this equation, it can be easily surmised that the evaluation of *pbest* and *gbest* is a key issue in this algorithm. On one hand, each particle updates its *pbest*. If the new particle position provides better results in all objectives the current *pbest* is a dominated solution and hence is substituted as it is outlined in Figure F-2.

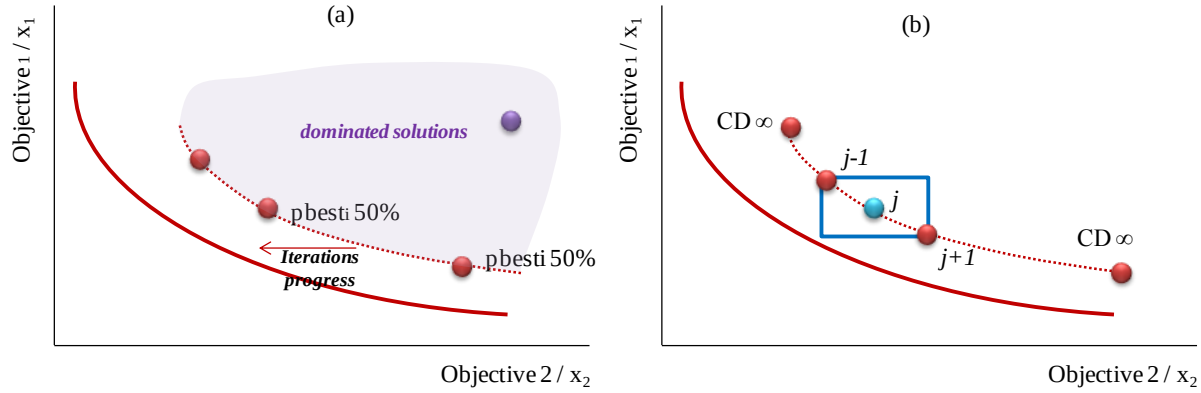

Figure F-2 Evolution of wind farms control time constant of the reactive power control of wind farms (Local and remote voltage control)

However, what happens if the new particle position only provides better results in one objective? In this situation the probability of replacing the *pbest* typically depends on the number of objectives (50% for 2 objectives, 33,33% for 3 objectives and so on). In these cases a random number is created and if it is higher than the probability defined *pbest* is replaced by $x_i(t+1)$.

On the other hand, *gbest* is selected among all non-dominated solutions. Note that the number of non-dominated solutions varies with the iterations. In the event of just considering one random particle from this file the algorithm works. However, the Pareto set obtained may not be uniform. Thus, the crowing distant (CD) concept was also incorporated [Raquel, et al. 2005]. In this case two more parameters are needed, *Top select* (6%) and *Top select probability* (98%) values selected in accordance with [Domínguez 2013]. Firstly, all non-dominated solutions are sorted in accordance with

CD [Deb et al. 2002], which provides an estimation of the density of the solutions surrounding a particular one. Focusing on a specific particle *j*, the cuboid formed when the nearest neighbours (*j*+1 and *j*-1) are considered as vertices, is evaluated (see in Figure F-2, subplot (b)). For guarantying a uniform Pareto frontier, an extremely large CD is assigned to those extreme solutions, i.e., solution in which one of the objective is minimum (in a minimization problem such the one under study). Then the elite, which correspond to the best *Top* solutions *select* (the 6% with higher crowing distance) is constituted. Finally, one individual is selected with *Top select probability* (98%) among the elite and with just a 2% probability among the others non-dominated solutions.

APPENDIX G

DETAIL COMPARISON AMONG CONTROL SCHEMES

In Chapter 5 the possibility of employing fit-and-forget settings is discussed for four different control schemes, *reference*, *power factor*, *local voltage*, and *remote voltage control*. From the steady-state analysis the best one is the *remote voltage control* scheme. Consequently, for no bothering and distracting the reader only this scheme has been expanded in the dynamic analysis in that chapter. Nonetheless, this appendix presents the results for the other schemes being structured as follows. Firstly, the control scheme performance is evaluated in section G.1. Subsequently, dynamic settings tendency, obtained with the genetic algorithm, is addressed in section G.2. In addition, the improvements obtained with respect to the sensible current practice (downward transformer time delay 20-40s higher than the upward one) are elucidated. Finally, in section G.3 both solutions (initial and the one obtained with the genetic algorithm) are located within the search space visualizing the margin for improvement.

G.1 CONTROL SCHEME PERFORMANCE

The dynamic performance is depicted in Figure G-1, Figure G-2 and Figure G-3 for the *reference*, *power factor* and *local voltage control* schemes respectively. In all cases,

transmission voltage step excursions of +/- 3% and the active power pattern selected (see Appendix E), have been considered.

All the figures previously enumerated have three subplots. In the first subplot, voltages at various buses are depicted in light blue. The voltage at the common coupling bus is presented in red, and the voltage of the transmission network is presented with a wide dark blue line. The second subplot presents the reactive power delivered by all wind farms. Where the reactive power provided by WF12 is presented in a different colour for outlining that the limits depicted in this subplot correspond to this specific wind farm. Finally, in the last subplot the winding ratio (i.e., tap setting) of the five transformers within the HNet is presented.

Focusing on the *reference control* scheme (see Figure G-1) it can be seen that the reactive power delivered by every wind farm is zero, as the power factor of all wind farms is one. As a result, a considerable voltage deviation between TNet voltage and the voltage at the common coupling bus is seen. In this control scheme, only the OLTC transformers are in charge of the voltage regulation function. Thus, a significant number of tap changes are seen after each transmission network voltage step.

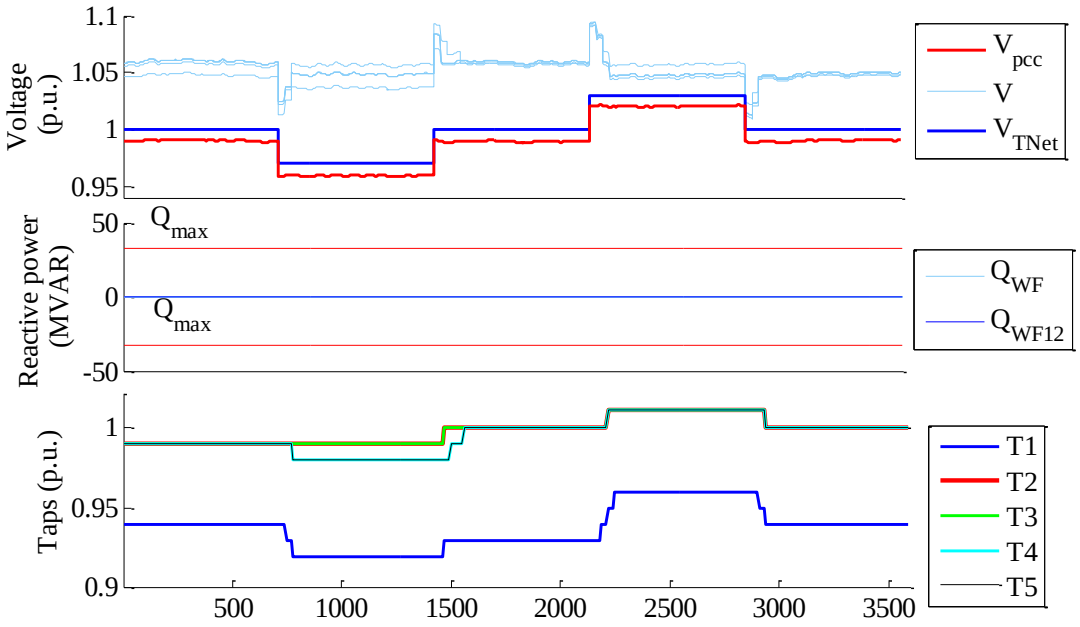

Figure G-1 Reference control scheme dynamic performance

In the *power factor control* scheme (see Figure G-2) the wind farms provide a certain amount of reactive power in accordance with the optimal power factor obtained in the steady-state assessment. Thanks to this provision the voltage deviation is compensated. In addition, it can be seen how the OLTC transformers control strategy can be maintained without obtaining any oscillatory performance. Moreover, it should be emphasized that tap changes can appear when steady-state is already achieved for certain dynamic setting values. These tap changes are originated because steady-state is reached near to the dead

band limit which may be surpassed owing to the active power variability which also implies reactive power variability.

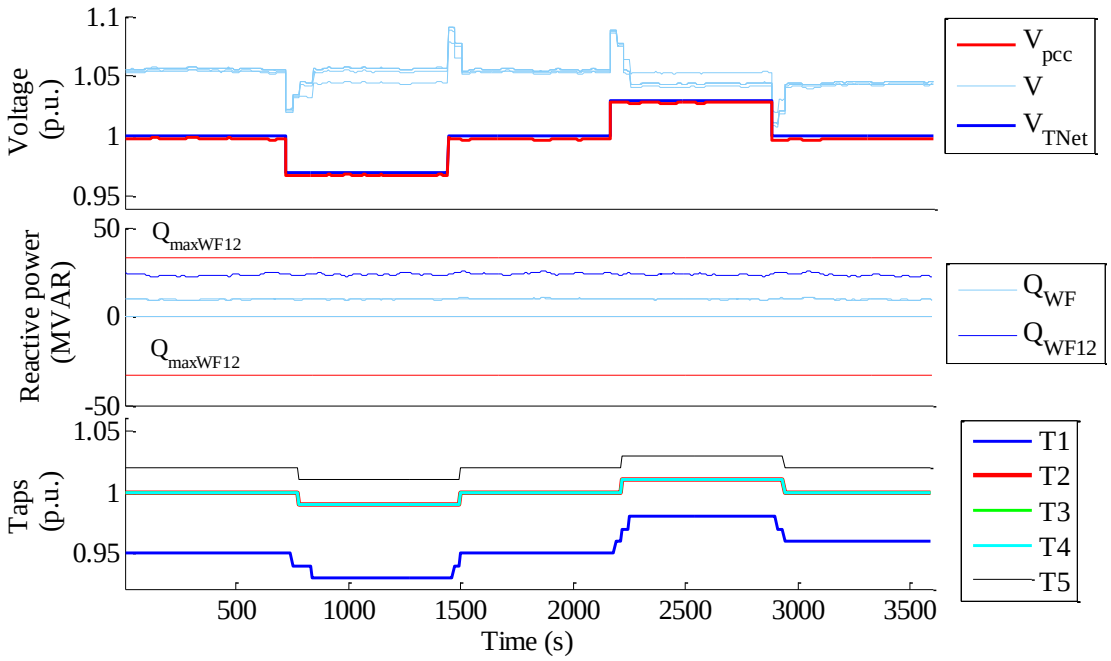

Figure G-2 Power factor control scheme dynamic performance

The *local voltage control* scheme is next presented in Figure G-3, showing how oscillations appear as several devices control the same bus. These oscillations are caused by the small droop value resulted from the AC multi-period OPF, drawback that can be solved limiting its minimum value. Nonetheless this means deteriorate its steady-state performance. Consequently, an adequate trade-off must be found. In the event of implementing this control scheme, when a voltage excursion appears wind farms inject a large amount of reactive power due to the steady-state objective function (minimizing the voltage set-point deviation) used for determining the droop. This fact may incur in a higher voltage variation than the desired. Hence, in the next control action wind farms consume reactive power. These oscillations can be also mitigated increasing wind farm controller dead band. However, this setting has not been considered in the optimization process because usually is a TSO requirement (see [REE 2010a]) which cannot be employed for coordination purposes. In fact, the value considered within the TWENTIES project was adopted, which was doubled for the *local voltage control* after identified the oscillations. Thus, the possibility of slowing the control actions by increasing wind farms' time constants (first-order lag included within the central controller) is discussed. These problematic oscillations further undermine the attractiveness of *local control* mode, which objective function computation (see Table 5-2) was worse than more readily-implementable *power factor control* schemes.

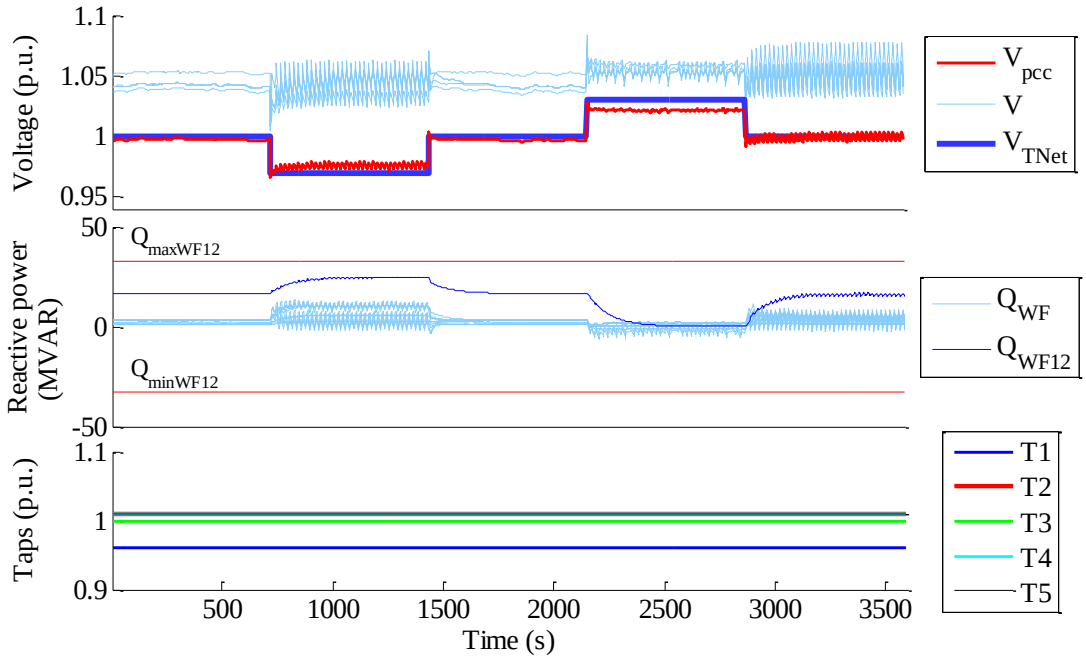

Figure G-3 Local voltage control scheme dynamic performance

In order to better understand the nature of the aforementioned oscillations and how they can be damped changing the droop or wind farms' time constants Figure G-4 and Figure G-5 are presented respectively. In both cases, the initial droops are the ones previously calculated in the steady-state assessment and a time constant of 40 seconds have been assumed for all wind farm controllers.

Figure G-4 is related to the droop impact, where in addition to the initial simulation two additional ones have been added in which droops have been doubled successively. Regarding this initial simulation, if all droops are doubled a better dynamic performance is appreciated although not all oscillations have been eliminated; fact that is reached when droops are doubled again. Nonetheless, these actions are not free implying a worst performance from the steady-state perspective. This drawback is more significant in those periods where the transmission voltage differ from its nominal one reducing the reactive power support provided.

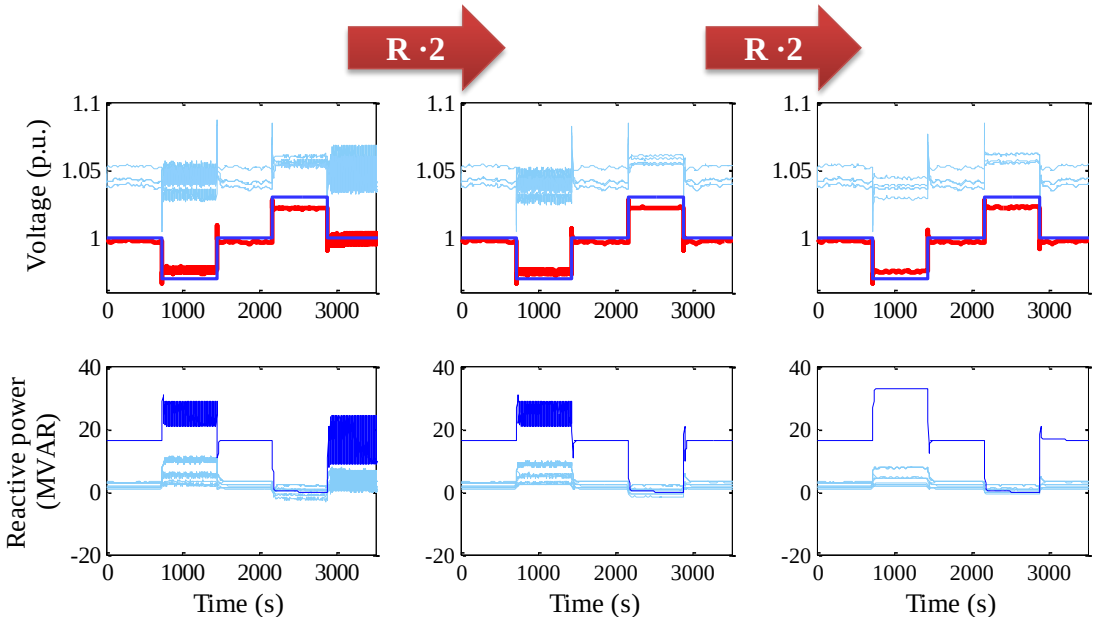

Figure G-4 Impact of the proportional slope on the dynamic performance

Similar conclusions can be derived from Figure G-5 where instead of increasing the droops, the wind farms' controller time constants are doubled successively. Hence, in this case the oscillations are mitigated considering slower wind farms' reactive power response. Contrary to the previous example the same steady-state is reached, representing the option selected within this thesis. Nonetheless, an unpredictable response can be obtained as can be seen in the last subplot for WF12 around 1000s. Thus, these constants, which no necessary are the same for all wind farms, should be optimally determined.

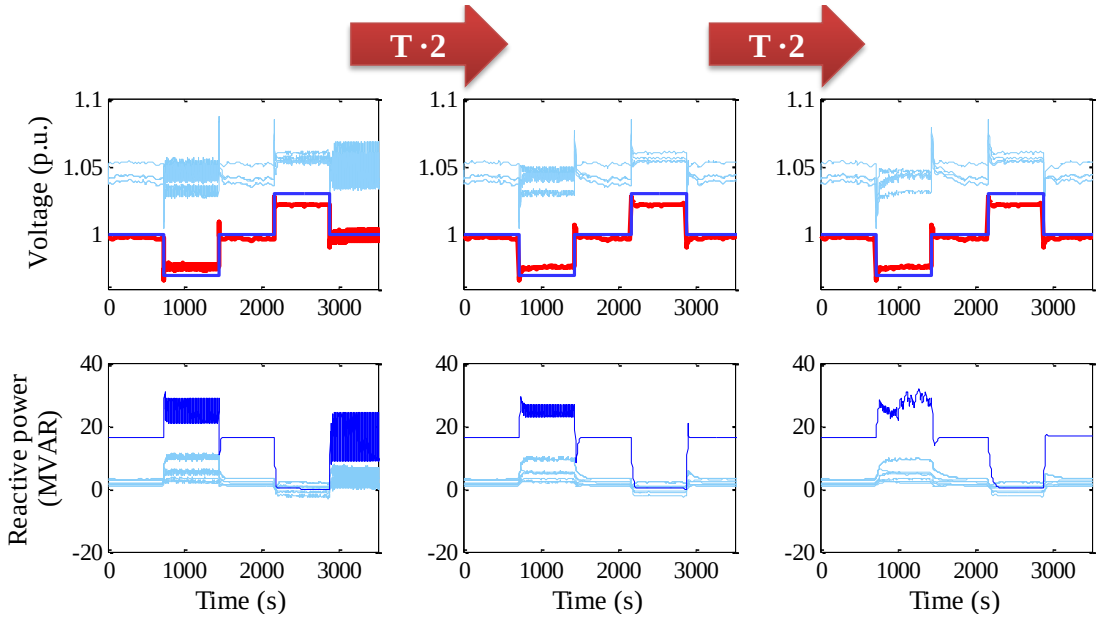

Figure G-5 Impact of wind farms' time constants

G.2 DYNAMIC SETTINGS TUNING

Recalling Chapter 5, several objectives should be considered in the optimization process for appropriately tuning the dynamic settings. Table G-1 reminds these objectives, indicating the relevant ones for each control scheme. Moreover, the dynamic settings evaluated in each control scheme are also outlined.

Table G-1. Objective to be minimized and dynamic settings to be tuned

	Objectives				**Transformers**		**Wind farms**
	Tap changes	**Transformers voltage**	**Voltage breaches**	**Oscillations**	**Time delay**	**Dead band**	**Time constant**
Reference control	X	X	X	–	X	X	–
Power factor control	X	X	X	–	X	X	–
Local voltage control	–	–	–	X	–	–	X
Remote voltage control	X	X	X	–	X	X	X

G.2.1. GENETIC ALGORITHM PENALTY FACTORS SELECTED

In the event of a simple genetic algorithm the trade-off among objectives should be determined in advance. For assessing their impact the *reference control* scheme has been first evaluated considering just one of the objectives. In other words, all weight factors are zero expect the one corresponding to the objective evaluated. Figure G-6 shows the tendency (corresponding to the mean values along the generations) of the time delay and dead band of all the transformers within HNet2. It should be emphasized that the population spread diminishes with the algorithm generations. Thus, the mean and optimal settings are quite similar at the end of the process. For understanding the tendencies obtained it should be recalled that the network analyzed is HNet2 (see Figure A-2). Thus, T1 is the bulk transformers (400/220kV) whereas (T2 to T5) correspond to wind farms transformers (220/30kV).

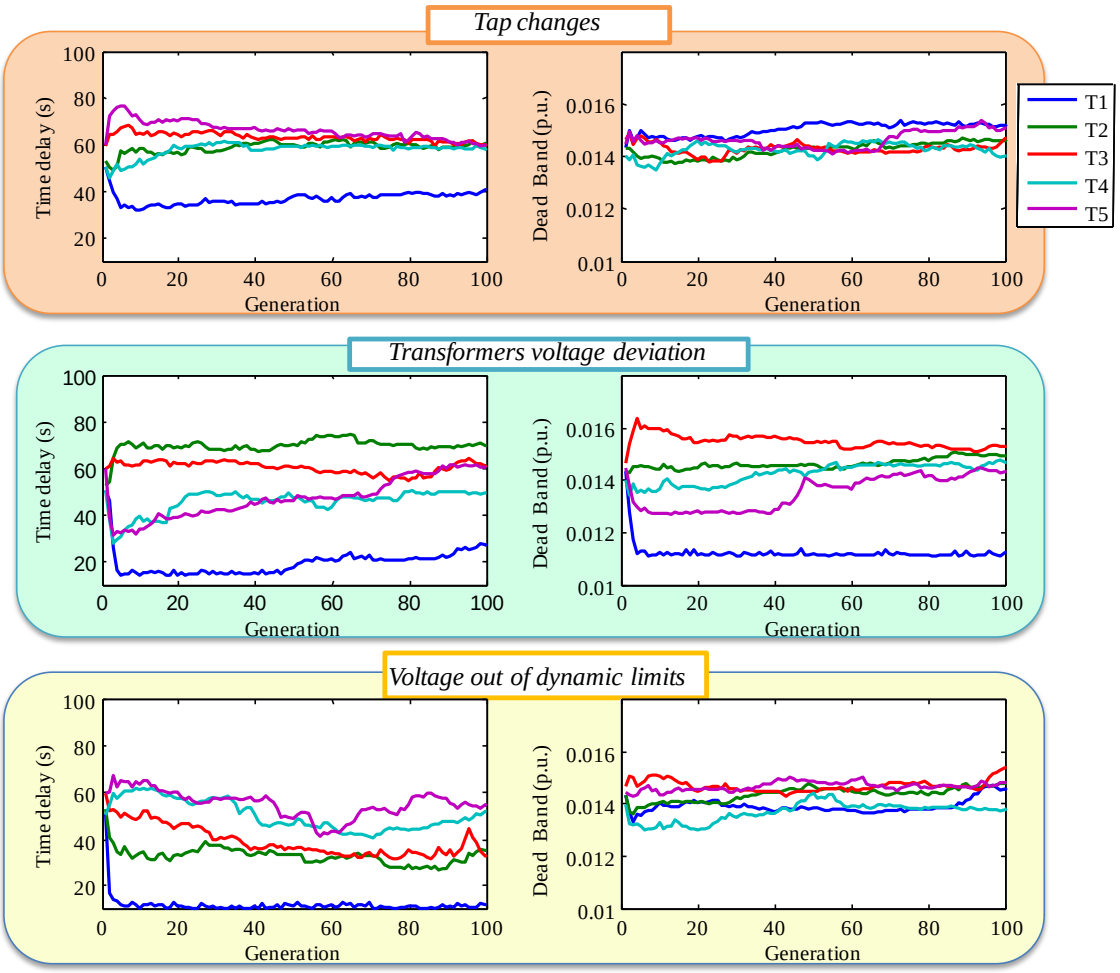

Figure G-6 Time delay and dead band for the reference control in the event that just one term of the objective function is minimized

The dead band tendency is really flat (i.e., all transformers have a similar dead band, which do not evolve with the generations) except when the voltage deviation term is optimized. This fact is due to the impact of the dead band on the other terms/objectives (tap changes, and voltage out of dynamic limits) is negligible in this control scheme compared to the time delay impact. Thus, for a correct evaluation of the dead band a significant weight of the transformer voltage deviations term is demanded. In the event of just optimizing this term it can be seen how T1 dead band should be lower than the dead band of the other transformers. Focusing on the time delay, the same conclusion can be obtained for all terms optimized; T1 should act fastest than the downstream transformers, changing the specific values depending on the term optimized. It can be seen that if the time in which voltages are out of dynamic limits is minimized, T1 should act as quick as possible. However, the other transformers should have a higher time delay for avoiding unnecessary tap changes. If the voltage deviation is minimized T1 time delay increased up to 20 seconds and up to 40-70 seconds for the other transformers. Finally, if tap changes are minimized T1 time delay increased up to 40 seconds whereas the downstream transformers time delay is 60 seconds. This value decreases when voltage breaches are considered. Table G-2 gathers the different fitness terms or objectives in the

event of optimizing one of these objectives. Note that the appearance of decimals is because mean values are evaluated.

Table G-2. Terms evaluated depending on the optimized term

		Tap changes (O1)	**voltage deviation of the set-point (O2)**	**voltages outside the dynamic limits (O3)**
Objective optimized	O1	19.82	0.098	6.50
	O2	20.87	0.085	8.06
	O3	25.60	0.104	3.33
	O1+50*O2+O3	20.81	0.086	5.76

In addition, the weight factors finally selected in order to obtain an adequate trade-off among the objectives has been included (W1=1, W2=50, W3=1). These weight factors are also used for the *power factor control* scheme whereas for the *remote voltage control* scheme a higher value has been assigned to the tap changes. This decision has been done owing to the dramatically increase of tap changes in this control scheme.

Changing the penalty factors the Pareto set can be obtained helping its selection. Nonetheless, this process is very time consuming. Consequently, a multi-objective algorithm, more suitable for evaluating the non-dominated solutions, has also been developed and will be compared with these results in section G. 3.

G.2.2. DYNAMIC SETTINGS TENDENCY, GENETIC ALGORITHM RESULTS

For all control schemes the fitness and dynamic settings evolution are next presented comparing the results among schemes. In Figure G-7 the fitness evolution (which has been normalized, i.e., $\frac{F-F_{min}}{F_{max}-F_{min}}$for comparison purposes) is depicted. As can be seen the genetic algorithm has a prompt convergence in all cases evaluated obtaining the fastest convergence for the *local voltage control* scheme in which the OLTC transformers are not involved and thus only wind farms' controller time constants (one for each wind farm) are optimized. Note that despite the *remote voltage control* scheme has more variables to be selected a faster convergence than for the *reference* or *power factor control* schemes has been obtained. This fact is because the population has been increased up to 150 individuals increasing also the search space.

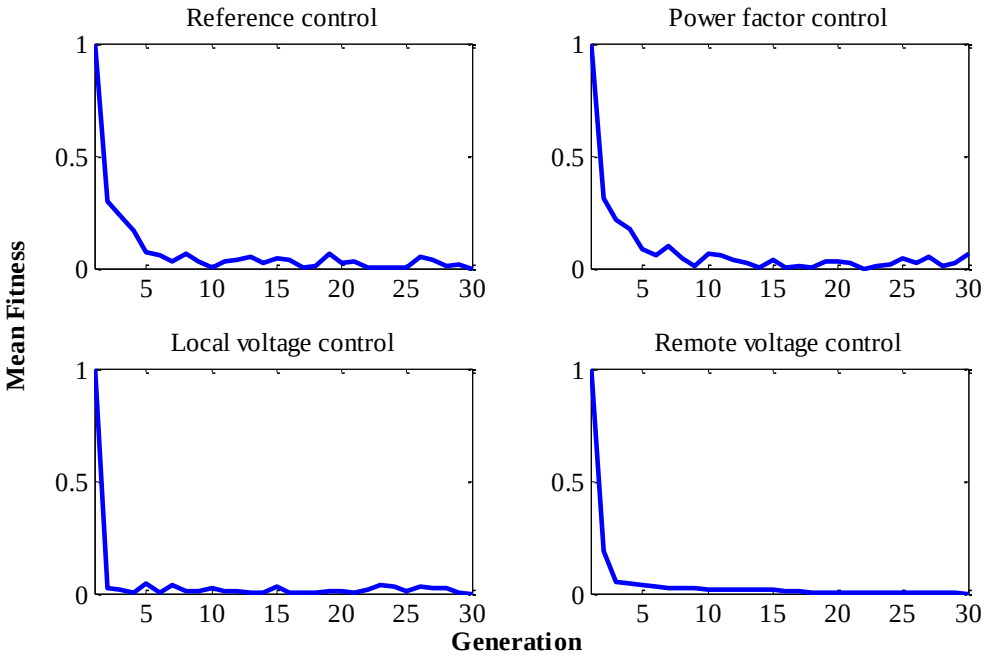

Figure G-7 Fitness evolution for different controls evaluated

In Figure G-8 transformers time delays are presented for all control schemes expect the *local voltage control* scheme. In all of them, T1 (presented in red and dotted lines) has a lower time delay than the rest of the transformers, as was expected. In fact it reaches the minimum value defined, 10 second. In addition, when the *remote voltage control* scheme is incorporated these time delays are decreased significantly to reduce the time in which voltages are out of dynamic limits. Moreover, analyzing this figure jointly with Figure G-7 it can be seen than a similar fitness can be achieved for different time delays.

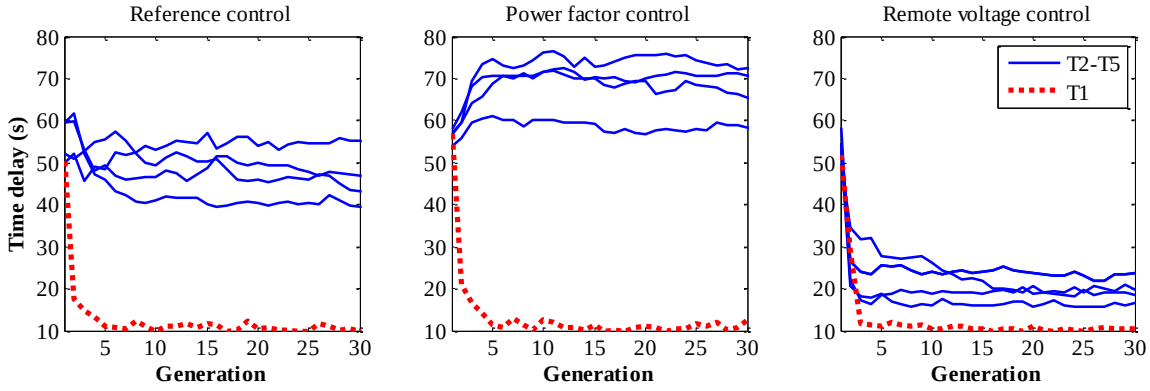

Figure G-8 Transformers time delay for the different controls evaluated

In Figure G-9 the transformers dead band for the *reference*, the *power factor* and the *remote voltage control* schemes are presented over each generation. It can be seen that T1 (also presented in red and dotted lines) has a slightly lower dead band in all cases. Nonetheless, in the event of a *power factor control* scheme all values are increased for avoiding unnecessary tap changes related with the active power variability.

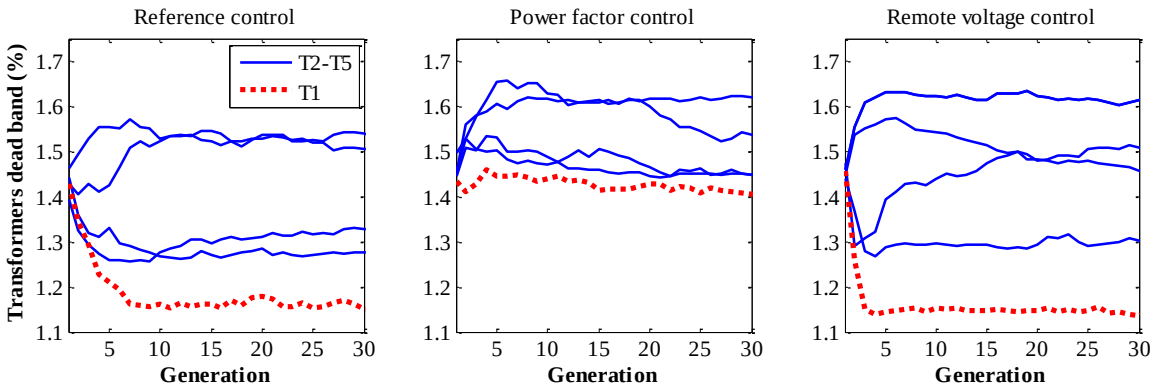

Figure G-9 Transformers dead band (Transformer and Power factor control)

The evolution of wind farms' controller time constants is shown in Figure G-10. Concerning the *remote voltage control* scheme it can be noted a wide spread (between 25 and 85 seconds) being WF12 (presented in red and dotted line) the fastest wind farm corresponding to the nearest one to the TNet. This can be observed also for the *local voltage control* scheme. Nonetheless, a slower response for all wind farms is demanded in this scheme for avoiding oscillations.

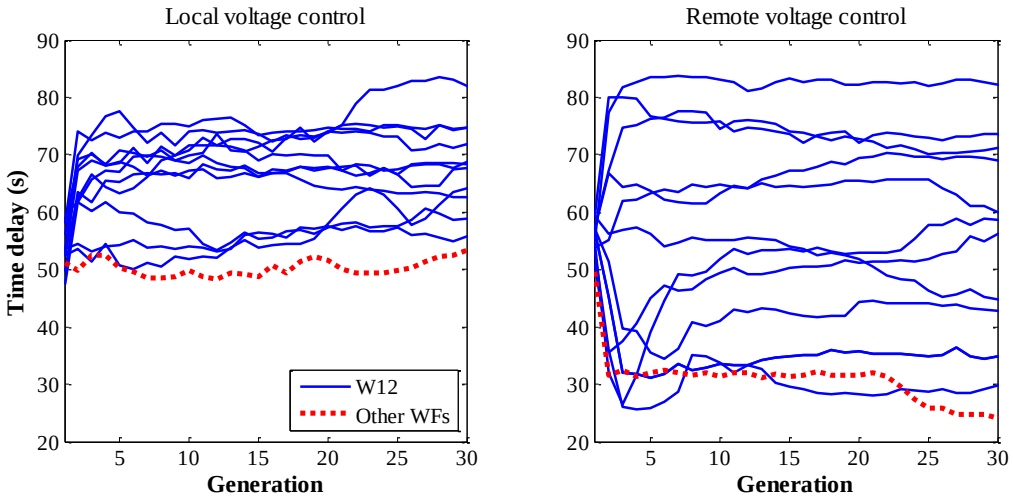

Figure G-10 Evolution of wind farms control time constant of the reactive power control of wind farms (Local and remote voltage control)

G.2.3. TUNED VS INITIAL DYNAMIC SETTINGS

In order to clearly see the improvements obtained tuning the dynamic settings Figure G-11, Figure G-12, Figure G-13 and Figure 5-13 are provided for the *reference*, *power factor*, and *local voltage* schemes respectively (*remote voltage control* is presented in Chapter 5). In all these figures the control scheme performance with the tuned settings (the mean dynamic settings obtained with the genetic algorithm) is compared with an initial sensible set selected based on [Van Cutsem, et al. 1998]. This book suggest 20s for the EHV/HV transformer (in our case 400kV/220kV) and 50s for HV/MV transformers (in our case 220/30kV). Moreover, a dead band of 1.35% for all

transformers and a time constant of 65s for all wind farm controllers have been considered.

In the first subplot of all figures, the voltage of one bus where a wind farm is connected and hence, is more vulnerable to reactive power changes is depicted. In addition, V_{TNet} has been included showing where a fast action of the OLTC transformers is essential for mitigating voltage breaches. Then depending on the control scheme one or two other subplots have been added where the most relevant magnitudes are included. On one hand, in those schemes where the reactive power is fixed, i.e., *reference* and *power factor* schemes the transformer ratio has been included. On the other hand, in the event of a *local voltage control* scheme the reactive power, which is the driver of the control has been added. All these magnitudes do not correspond to the same bus. Hence, a transformer tap movement may not correspond to a voltage variation. In all cases it can be concluded that the control performance can be widely improved tuning adequately the dynamic settings. Indeed, in the most unfavourable case 4 tap movements[14] are avoided in 1 hour, reducing also voltage breaches and transformer voltage deviations.

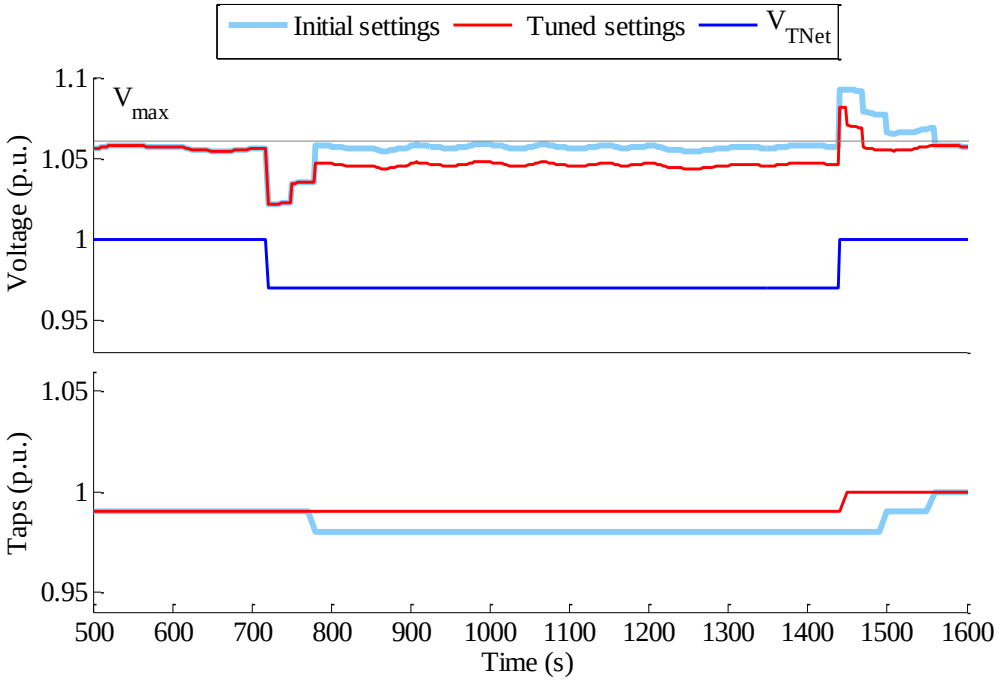

Figure G-11 Reference control scheme. Initial settings vs final settings

[14] In accordance with [Erlich, et al. 2011] each tap movement is valorated in 10c€

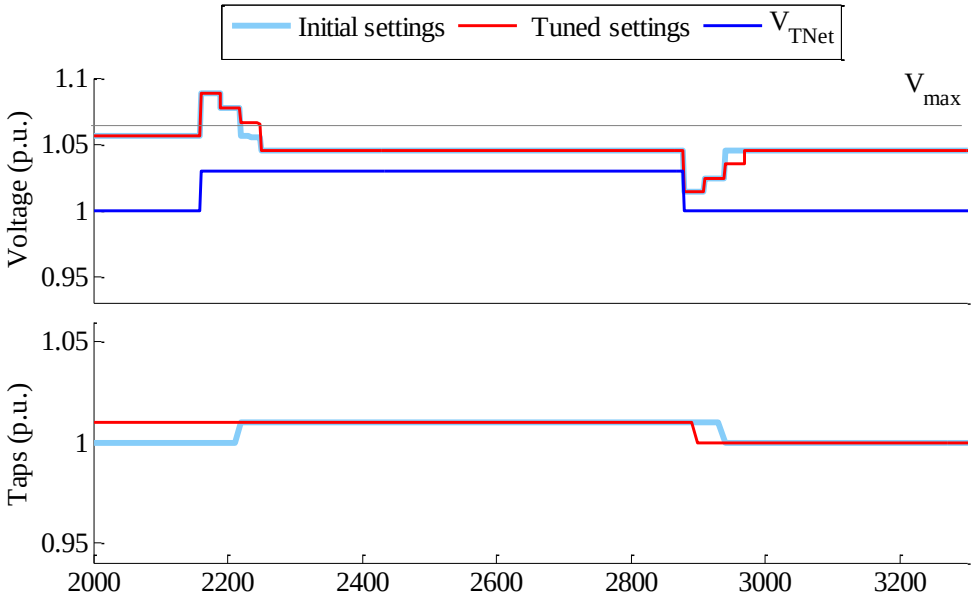

Figure G-12 Power factor control scheme. Initial settings vs final settings

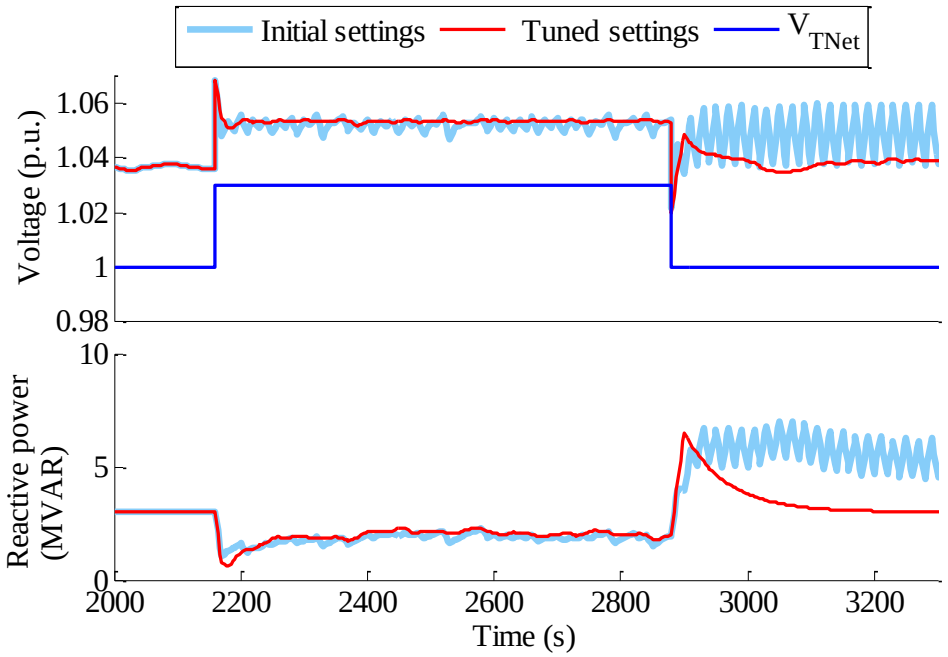

Figure G-13 Local voltage control scheme. Initial settings vs final settings

Finally, all control schemes, considering the tuned settings, have been jointly depicted in Figure G-14. From this figure, it can be derived that the *remote voltage control* scheme presents an opposite behaviour compared to the *reference* and *power factor control* schemes from the voltage point of view (see t=2200s). In addition, highly increases the tap changes as has been seen throughout the chapter. In the middle it can be seen the

local voltage control scheme where the voltage breaches are not relevant due to the reactive power support is very limited undermining the adequacy of this scheme.

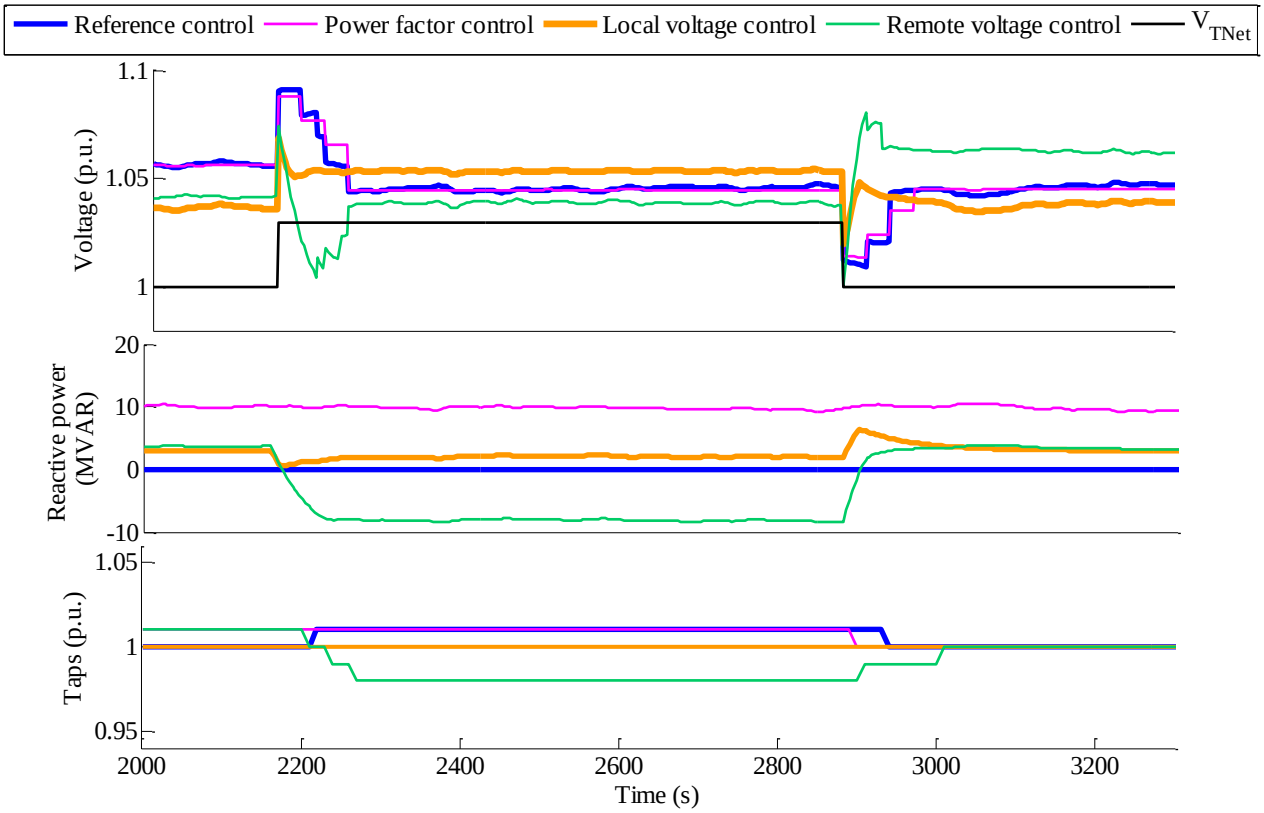

Figure G-14 Tuned schemes comparison

G.3. MARGIN VISUALIZATION

Both dynamic setting sets, initial and tuned, are located within the search space and compared with the Pareto frontier identified with the MOPSO algorithm. Figure G-15 (for the *reference control* scheme), Figure G-16 (for the *power factor control* scheme) and Figure G-17 for the (*remote voltage control* scheme) depict the first three terms of the fitness function (tap changes, transformers voltage deviation and voltages out of limits) in pairs. Note that the oscillation term is not included because only appears in the *local control*.

In all schemes the current practice is not senseless. However there are margin for the improvement as was presented in the previous subsection (in the worst-case 4 unnecesary tap changes are avoided in one hour). Moreover, the Pareto frontier provides useful information for defining the trade-off among objectives.

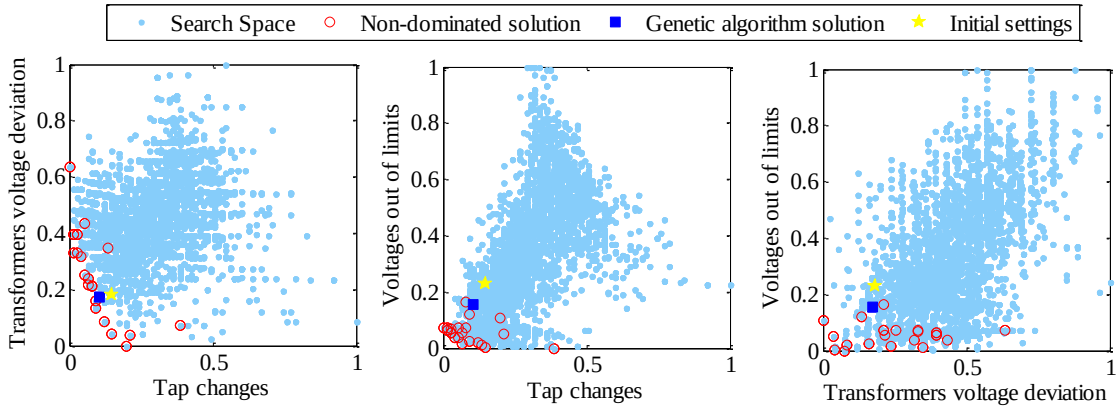

Figure G-15 Algorithm comparison. Reference control

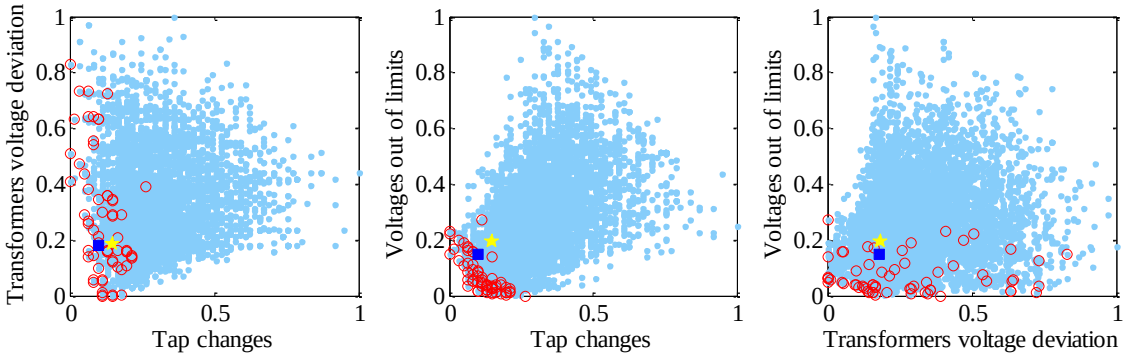

Figure G-16 Algorithm comparison. Power factor control

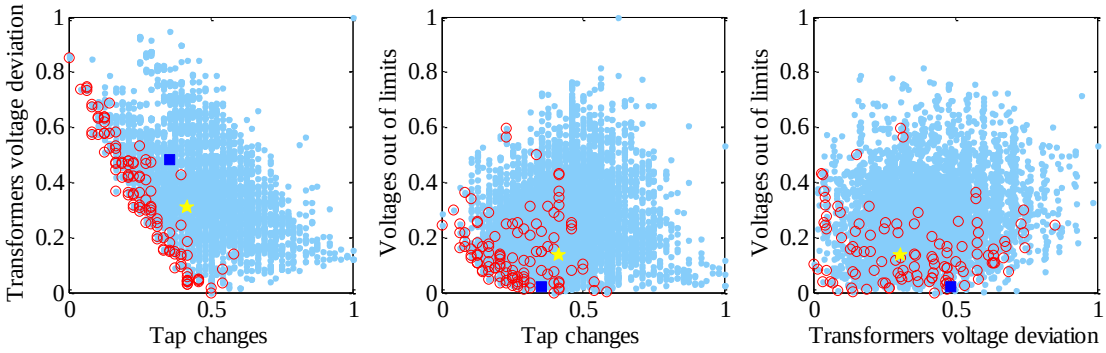

Figure G-17 Algorithm comparison. Remote voltage control

APPENDIX H

NECESSITY OF ADAPTIVE SETTINGS AND ADEQUACY OF THE CONTROL SCHEMES PROPOSED

Two different approaches have been explained throughout the thesis: fit-and-forget (Chapter 5) and adaptive (Chapter 6) settings. The former eschews online computation avoiding communication. Nonetheless, for a pro-active strategy this approach is not enough as is discussed in section H.1. In order to implement this strategy, several control schemes have been proposed, especially in transmission network. The adequacy of those schemes and the comparison with the central controller presented in this thesis are explained in section H.2.

H.1. NECCESITY OF ADAPTING THE SETTINGS IN REAL TIME OPERATION

Due to considering the same settings for all wind production scenarios the performance of the control is eroded compared to the possibility of taking into account the optimal settings in each scenario. This fact was clearly stated in Chapter 3 where it was seen how a droop depending on active power scenarios was needed in order to take advantage of the maximum PQ chart.

In the event of considering a pro-active voltage control strategy (i.e., the whole HNet resembles a conventional plant which could be integrated in the TNet hierarchical control) a rapid response to $V_{setpoint}$ changes is demanded. This fact represents a key difference with respect to the approach presented in Chapter 5. In that approach the aim of all control schemes evaluated were just minimize the HNet impact on TNet. Hence, a single $V_{setpoint}$ equal to the most probable V_{TNet} was assigned. Nonetheless, V_{TNet} disturbances were considered for coordinating all devices involved by means of the dynamic settings. In those periods, reactive power support was provided especially in the *remote voltage control* scheme. Nonetheless, its provision could differ from the optimal one as is going to be explained.

For analyzing how the objective function value of the AC multi-period OPF used in Chapter 5 and the settings obtained vary for $V_{setpoint}$ changes, three different values (0.97, 1.00 and 1.03 p.u.) have been considered, assuming a constant value of the transmission network voltage equal to 1.00 p.u.. In this case it is expected that static settings change considerably. This fact happens when $V_{setpoint}$ is lower than V_{TNet} as can be seen in Table H-1 and Table H-2. However, if $V_{setpoint}$ is equal to V_{TNet} the reactive consumption of the whole harvesting network is not compensated for all wind production scenarios. Hence, the voltage at the common coupling bus differs from $V_{setpoint}$. Any increase of $V_{setpoint}$ only changes the value of the objective function.

In the event of a *remote voltage control* scheme there are infeasibilities when $V_{setpoint}$ differs from $V_{TNet.}$ The reason of these infeasibilities is that large droop values are demanded in order to be feasible in all scenarios. However, the approximation employed for linearizing the droop avoiding the discontinuities caused by the machine capabilities limits [Cuffe et al. 2014a], is not adequate enough for extremely large or small droops. Consequently, a higher voltage set-point does not change the static settings. On the contrary, for a set-point lower than V_{TNet} the reactive consumption can be increased significantly especially for the *power factor control* scheme, meaning that the voltage at the common coupling bus can be reduced as is desired. However, although its performance is increased, having fixed settings notably erodes the controls capabilities.

Table H-1. Optimal settings for different values of $V_{setpoint}$ for reference and power factor control

		Transformers control			**Power factor control**		
		V=388 kV	**V=400 kV**	**V=412 kV**	**V=388 kV**	**V=400 kV**	**V=412 kV**
		Voltage Setting			**Voltage Setting**		
TRANSFORMER	T1	**0.950**	**1.048**	**1.048**	**1.049**	**1.046**	**1.046**
	T2	**0.950**	**1.050**	**1.050**	**1.050**	**1.050**	**1.050**
	T3	**0.950**	**1.050**	**1.050**	**1.050**	**1.050**	**1.050**
	T4	**0.950**	**1.050**	**1.050**	**1.050**	**1.050**	**1.050**
	T5	**0.950**	**1.050**	**1.050**	**1.050**	**1.050**	**1.050**
		Power factor			**Power factor**		
WIND FARMS	WF 1-3	**1.00**	**1.00**	**1.00**	**1 (-)**	**1 (+)**	**1 (+)**
	WF 4-7	**1.00**	**1.00**	**1.00**	**0,99 (-)**	**1 (+)**	**1 (+)**
	WF 8-9	**1.00**	**1.00**	**1.00**	**0,97 (-)**	**0,97 (+)**	**0,97 (+)**
	WF 10-11	**1.00**	**1.00**	**1.00**	**1 (-)**	**1 (+)**	**1 (+)**
	WF 12	**1.00**	**1.00**	**1.00**	**1 (-)**	**0,95 (+)**	**0,95 (+)**
OBJECTIVE FUNCTION		**29209.91**	**2429.50**	**59955.23**	**23995.55**	**305.36**	**43873.76**

Table H-2. Optimal settings for different values of Vsetpoint for local and remote voltage control

		Local voltage control						Remote voltage control			
		$V_{setpoint}$ = 0.97 p.u.		$V_{setpoint}$ = 1 p.u.		$V_{setpoint}$ = 1.03 p.u.		$V_{setpoint}$ = 0.97	$V_{setpoint}$ = 1 p.u.		$V_{setpoint}$ = 1.03
		Ratio						Approximation not reliable	Voltage Setting		Approximation not reliable
OLTC	T1	1.018		0.955		0.955			1.042		
	T2	0.936		1.007		1.007			31.50		
	T3	0.936		1.002		1.002			31.50		
	T4	0.936		1.008		1.008			31.50		
	T5	0.936		1.006		1.006			31.50		
		Voltage Setting	Droop	Voltage Setting	Droop	Voltage Setting	Droop		Voltage Setting	Droop	
WIND FARMS	WF 1-3	1.011	2.39	1.050	2.39	1.050	2.39		Vset-point	2.39	
	WF 4-7	1.010	3.17	1.050	2.39	1.050	2.74			2.39	
	WF 8-9	1.009	2.91	1.050	2.91	1.050	2.91			2.91	
	WF 10-11	1.013	2.91	1.050	2.91	1.050	2.91			2.91	
	WF12	0.955	1.04	1.046	1.00	1.046	1.00			1.00	
OBJECTIVE FUNCTION		17366.36		343.57		39063.22			5.23		

Those schemes have been also compared with the central controller (adaptive settings approach) from a dynamic perspective. In that sense the objectives evaluated for tuning the dynamic settings have been adressed. These objectives are transformers voltage deviation, voltages out of limits and tap changes. These objectives have been minimized in all cases thanks to a MOPSO algorithm. The results are summarised in Figure H-1 where the non-dominated solutions of the central controller are depicted jointly with the ones obtained for the *reference* and *remote voltage control* schemes. The latter, recalling Chapter 5, presents a similar performance than the central controller. The *reference control* scheme is only included as a reference as its name indicated. However in this control scheme the wind farm do not provide any reactive power support. As was expected the central controller also increases the tap changes with respect to the *reference* and *power factor control* (not included in this figure) schemes. Nonetheless, for many non-dominated solutions the central controller presents less tap changes than the *remote voltage control*. Fact due to OLTC transformers voltage set-points change in accordance with the central controller. Moreover, a decrement of the spread of the voltage out of limits objective is seen owing to the dead band incorporation in the central controller constraints.

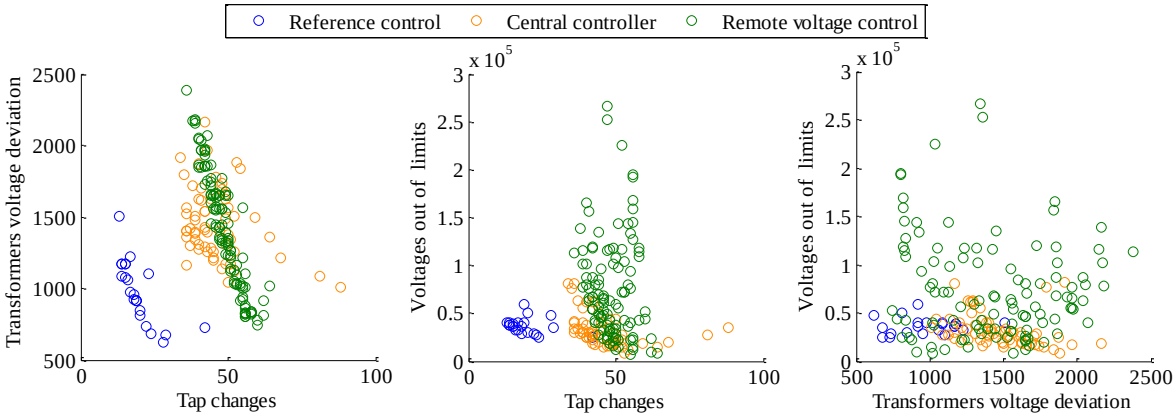

Figure H-1 Search space of reference control (Chapter 5), remote voltage control (Chapter 6) and central controller

H.2. TNET VOLTAGE CONTROL ADEQUACY

The participation of wind generation in the voltage control should not change its philosophy. Nonetheless, the characteristics of this technology, which are related with the generation itself (such as its variability) and the nature of the networks where it is located, should be taken into account. Concerning the last fact, it should be reminded that a common scheme in the HNet is that several wind farms of different owners share the HNet connection point, in which also the OLTC transformer plays an important role. Hence, some considerations on the control should be performed.

Recalling section 2.3, in which some already implemented TNet hierarchical control schemes were explained, in order to fulfil the voltage set-point of the pilot bus, individual voltage set-points were given to the plants. In the case under study, these plants correspond to wind farms and the pilot bus to the HNet common coupling point (*Pcc*). Thus, giving a voltage set-point to each one considering an integral control is not an option due to the possible hunting[15] effect. This fact leaves two alternatives. On one hand, providing reactive power set-points, on the other hand, still considering a voltage set-point including another loop for coordinating the wind farms connected in the same bus. Both alternatives present advantages and disadvantages. On one hand, controlling the reactive power and not the voltage increases the interactions risk among generators [de la Fuente 1997], it should be noted that the PV buses absorb the reactive power perturbations avoiding dynamic couplings. On the other hand, the addition of a new loop makes the control slower. This thesis has focused on the first alternative once confirmed the no appearance of interactions after tuning the central controller parameters.

Moreover, in these networks there are cascade transformers. Those devices were traditionally evaluated in the tertiary loop. However, in HNets a more rapid actuation is required. In that sense, the tertiary loop is avoided proposing a decentralized operation of the OLTC transformers supervised by the central controller explained in the subsequent section.

[15] One wind farms may produce the maximum whereas other consumes the maximum reactive power and the TNet voltage remains equal.

Table H-3. Secondary voltage control formulation

	CSVC	J.I. de la Fuente 1997	J. Alonso 2001	Proposal
Objective function	$\begin{Bmatrix} w \cdot \left\| \alpha \cdot \left(V_p^{ref} - V_p(k) \right) - S_{pc} \cdot \Delta V_c(k) \right\|^2 + \\ w_q \cdot \left\| \alpha \cdot \left(Q_c^{ref} - Q_c(k) \right) - A_{cc} \cdot \Delta V_c(k) \right\|^2 + \\ w_g \cdot \left\| \alpha \cdot \left(V_c^{ref} - V_c(k) \right) - \Delta V_c(k) \right\|^2 \end{Bmatrix}$	$\begin{Bmatrix} \left\| \alpha \cdot \left(V_p^{ref} - V_p(k) \right) - S_{pc} \cdot \Delta {V_c}^{ref}(k) \right\|^2 + \\ w_q \cdot \left\| \alpha \cdot \left([Q_c^{ref} + S \cdot d(k)] - Q_c(k) \right) - A_{cc} \cdot \Delta {V_c}^{ref}(k) \right\|^2 \end{Bmatrix}$	$\Delta T_{losses}(k) + w_q \cdot \Delta T_{Qmargins}(k)$	$\left\| \gamma \cdot \left({V_p}^{ref} - V_p(k) \right) - v S_{pc}(k) \left(\Delta {Q_c}^{ref}(k) \right) \right\|^2 + W \Delta T_{Qmargins}(k)$
Constraints	$V_c^{min} \le V_c(k) + \Delta V_c(k) \le V_c^{max}$ $V_s^{min} \le V_s(k) + S_{sc} \cdot \Delta V_c(k) \le V_s^{max}$ $a \cdot \left(Q_c(k) + A_{cc} \cdot \Delta V_c(k) \right) + b \cdot \Delta V_c(k) \le c$	$-\Delta V_c^{min} \le \Delta {V_c}^{ref}(k) \le -\Delta V_c^{max}$ $V_c^{min} \le V_c(k) + \Delta {V_c}^{ref}(k) \le V_c^{max}$ $Q_c^{min} \le Q_c(k) + A_{cc} \cdot \Delta {V_c}^{ref}(k) \le Q_c^{max}$ $-1 \le d(k) \le 1$ $V_s^{min} \le V_s(k) + S_{sc} \cdot \Delta {V_c}^{ref}(k) \le V_s^{max}$	$V_p(k) + \Delta V_p(k) \le V_p^{max}$ $V_c^{min} \le V_c(k) + \Delta {V_c}^{ref}(k) \le V_c^{max}$ $Q_c^{min} \le Q_c(k) + A_{cc} \cdot \Delta {V_c}^{ref}(k) \le Q_c^{max}$	${Q_c}^{min} - Q_0 \le \Delta {Q_c}^{ref}(k) \le {Q_c}^{max} - Q_0$
Input require	${V_p}^{ref}, Q_c^{ref}, V_c^{ref}$	${V_p}^{ref}, Q_c^{ref}$	V_p^{max}	${V_p}^{ref}$
Output	$\Delta V_c(k)$	$\Delta {V_c}^{ref}(k),\ d(k)$	$\Delta {V_c}^{ref}(k)$	$\Delta {Q_c}^{ref}(k)$
Tertiary loop	In charge of evaluating: • Optimal voltage profile • Reactive power management	In charge of evaluating: • Reactive power management	Can be avoided	Can be avoided
Time constant	Imposed by α	Imposed by α	Imposed by α Note that ${V_c}^{ref}(k+1) =$ ${V_c}^{ref}(k) + \boldsymbol{\alpha}\, \Delta {V_c}^{ref}(k)$	Imposed by the first order lag included
Sample time	10 seconds	10 seconds	10 seconds	• 10 seconds (optimization process) • 1 seconds

APPENDIX I

OLTC TRANSFORMERS STRATEGY FOR MAXIMIZING THE REACTIVE POWER DELIVERED BY WIND FARMS

Throughout the thesis it has been assumed that wind farms fulfil the requirements presented in P.O. 7.5 (recall PQ chart Appendix A). Thus, all assessments have focused on the HNet without taken into consideration the internal wind farm infrastructure. However, as it is outlined in [Arlaban, et al. 2012] not all current wind farms fulfil these requirements without adding additional devices. In those cases, the OLTC transformers can be used for minimizing the size of the reactive compensation element added. This appendix intimates this alternative strategy using real data of one wind farm (internal infrastructure and active power profiles). This consideration does not change the methodologies explained trough the thesis affecting only to the voltage limits considered in those buses where the OLTC transformers are located.

Wind turbines' reactive power capabilities depend on the voltage and hence, on where each turbine is located within the feeder. In Figure I-1 this fact is outlined. As can be seen, if wind turbines absorb reactive power, voltages decrease along the feeder whereas the opposite effect is seen when wind turbines inject reactive power. These decrements or increments could mean that a certain wind turbine surpassed the limits and hence the reactive power is limited (recall PQV chart). Consequently, the initial feeder voltage (imposed by the 20 – 30kV/132 -220kV OLTC transformers) plays an important role.

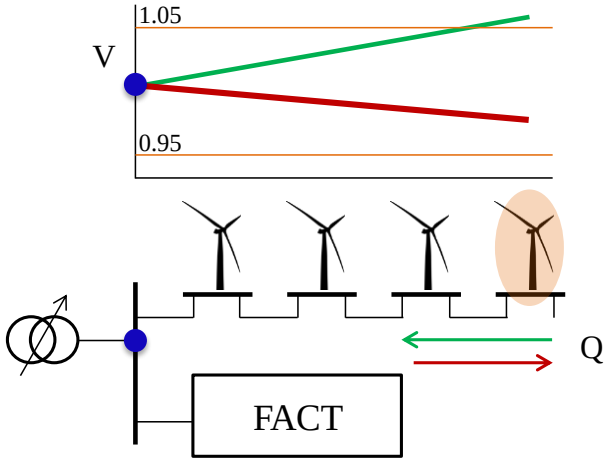

Figure I-1 wind farm grid voltage impact (simplified model)

This effect has been measured for a real wind farm considering also real active power data. For that purpose, the maximum wind farm reactive power set-point (absorb/inject) has been considered, which is proportionally distributed among wind turbines. The difference between the first and last wind turbine of a specific feeder is presented in Figure I-2 assuming a constant OLTC transformer voltage set-point equal to 1.02 p.u.. In this figure two subplots can be seen. In the first one, the reactive power provided and its respective set-point is depicted for both wind turbines. In the second one the voltage at those buses are depicted. As can be seen, those voltages surpassed 1.05 p.u. value above the reactive power is limited (a zoom of that area is provided). Thus, the reactive power provided differs from their set-points.

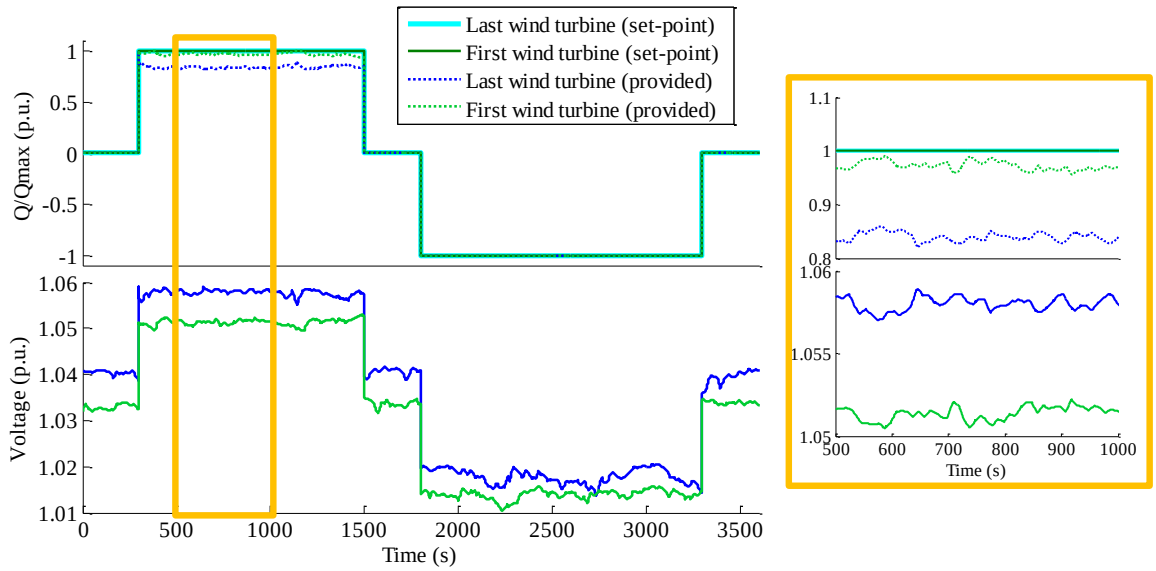

Figure I-2 Reactive power depending on the wind turbine feeder location

This simulation is repeated for several OLTC transformer voltage set-points (0.9 p.u. – 1.1p.u.) computing the maximum reactive compensation and the oscillations that arise which are calculated as follows:

$$\sum_{t=t_{oss}}^{t=t_{fss}} abs(Q_{\mathrm{FACT}}(t) - meanQ_{\mathrm{FACT}}) \qquad \text{(D-1)}$$

Those results are summarized in Figure I-3 where each point corresponds to a whole simulation as the one presented in Figure I-2. As can be appreciated in this figure no VAr compensation is requerid when the OLTC transformer voltage set-point is between [0.975-1 p.u.]. Nonetheless, the VAr compensation increases under/above this margin. In addition it is important to note the appearance of oscillations which dramatically increase for voltages under 0.925 p.u. and above 1.05 p.u..

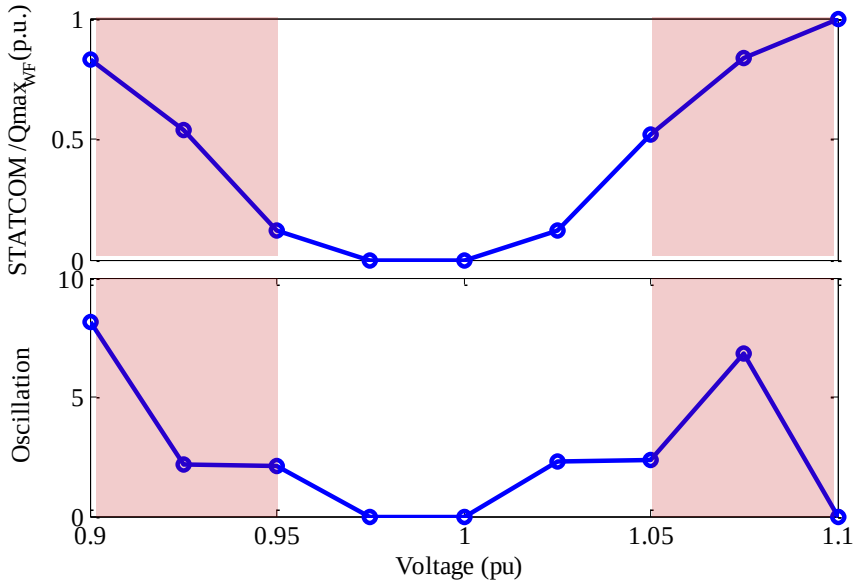

Figure I-3 Impact of changing OLTC transformers voltage set-point